Fine Sediment Infill Reduction in Offshore Dredged Approach Channel

MSc. Thesis

B.J.M. van Velzen

Technische Universiteit Delft

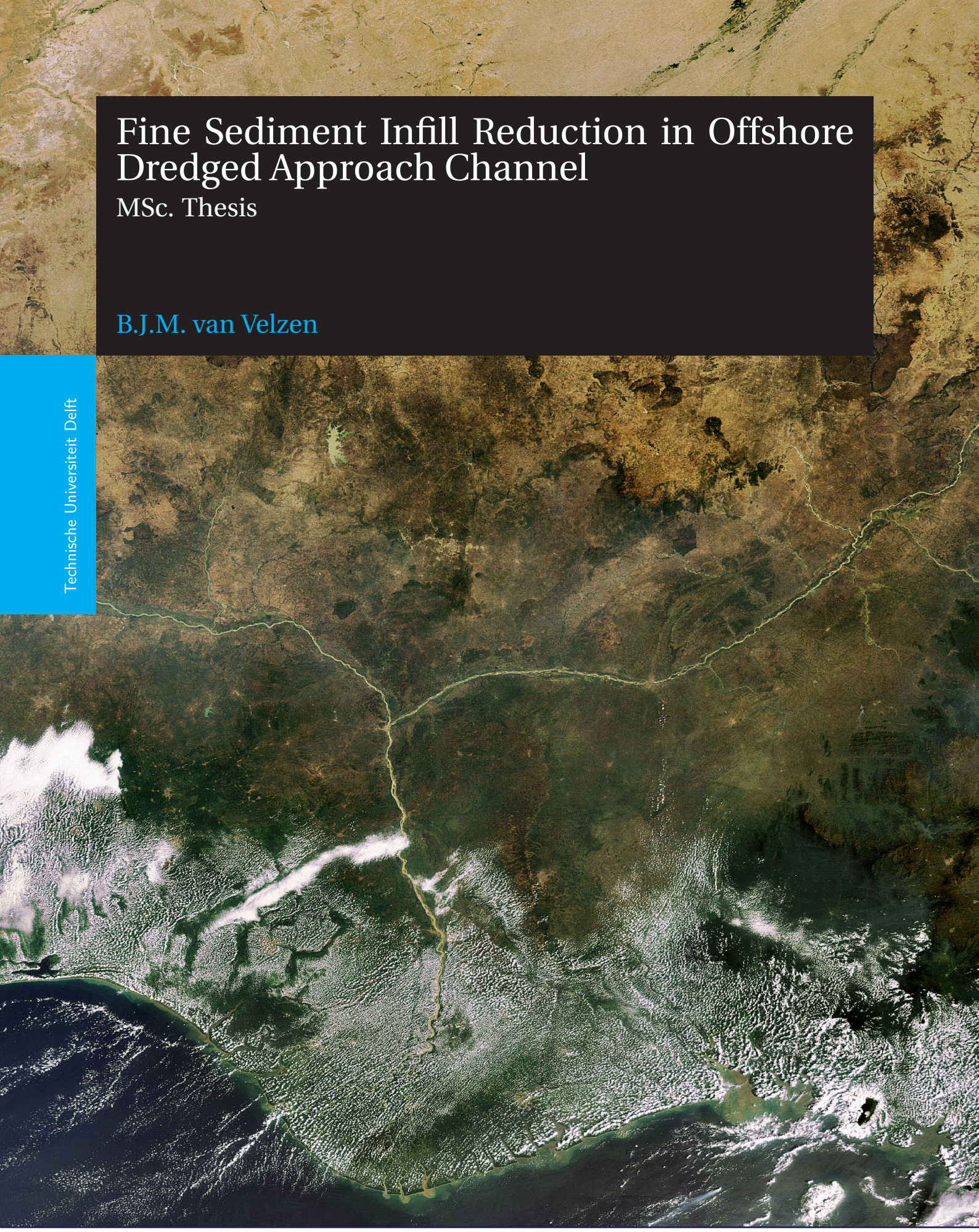

TU Delft Delft University of Technology

Boskalis

Challenge the future

Fine Sediment Infill Reduction in Offshore Dredged Approach Channel

MSc. Thesis

by

B.J.M. van Velzen

in partial fulfillment of the requirements for the degree of

Master of Science
in Civil Engineering

at the Delft University of Technology,
to be defended publicly on Friday July 4, 2014 at 4:00 PM

Student number:	1378740	
Project duration:	September 2, 2013 – July 4, 2014	
Supervisor:	Prof. dr. ir. J. C. Winterwerp	TU Delft/Deltares
Thesis committee:	Ir. A. P. Luijendijk,	TU Delft/Deltares
	Ir. J. van Overeem,	TU Delft/Arcadis
	Dr. ir. W. Jacobs,	Royal Boskalis Westminster
	Ir. D. C. Rijks,	Royal Boskalis Westminster

This thesis is confidential and cannot be made public until July 4, 2016.

TU Delft Delft University of Technology Boskalis hydronamic

"Why we are on this particular mission, we'll never know..."

CAPT. JIMMY WILDER, INDEPENDENCE DAY (1996)

Cover image:
Niger Delta Satellite image from Envisat's Medium Resolution Imaging Spectrometer (MERIS) instrument on 12 December 2007.
http://www.redorbit.com/images/pic/18257/the-niger-delta/#fhWeTGH6BW7GoiZy.99

PREFACE

This document is the report of my MSc. Thesis which is the concluding phase of my Civil Engineering Master's degree in the field of Hydraulic Engineering at Delft University of Technology.

When I obtained the subject of my thesis at Boskalis, the project was said to have a high potential of actual realization. A few months later, when I started with my thesis the actual execution of the project, unfortunately, became uncertain. I used earlier performed studies on this subject by research companies to obtain a first interpretation and understanding of the problem. The amount of work already done on this problem was overwhelming and I had to dig deep into new theoretical subjects in order to be able to understand the processes involved as well as identify the most relevant findings from earlier research.

I would like to thank my supervisors from Delft University of Technology and Boskalis, Han Winterwerp, Arjen Luijendijk, Jan van Overeem, Walter Jacobs and Daan Rijks for their help, support and patience during the writing of my thesis. When searching to find a correct approach with which to continue my research, Walter gave sharp comments and directions on how to move on. For the Delft3D modeling, Arjen helped me out a lot when I was struggling with the model, particularly when he found out the software version I was using appeared to be corrupt.

Special thanks go to my family, my girlfriend and close friends who supported me while working on my thesis. Without their help during moments of struggle I would not have been able to finish my thesis the way I did.

During the writing of my thesis I have learned a lot, I developed myself on a personal level as well as on a professional level. The limited amount of data resulted in significant uncertainty of the different sediment transport processes. I tried to figure out a way to avoid these uncertainties instead of continue and accept them at first. Later I realized uncertainties will always be present and should be taken into account properly during the process, instead of letting them slow me down by trying to resolve all uncertainties initially.

B.J.M. van Velzen
Delft, June 2014

ABSTRACT

An offshore terminal is proposed to be constructed in the Niger Delta. Dredging works for this project consist of an approach channel (approximately 250 m wide and 9 km long) and harbor basin (approximately 1 km wide and 1 km long) to a depth of -14 m LAT allowing ships to reach the terminal. The project area is located close to an estuary in a muddy coastal environment with a persistent swell wave climate. High transport rates of fine sediment are expected to cause infill of undesirably high quantities with respect to maintenance dredging costs. Additionally, down-time for maintenance dredging is caused by shipping traffic in the approach channel. In this thesis the sediment transport processes in the project area are analyzed and mitigation measures for reducing fine sediment infill of the dredged channel are proposed and considered for this specific case and for similar cases in general.

An analysis of the local environment based on measured data and reference literature is conducted in order to gain understanding of the hydrodynamic and morphologic system. The local environment is subject to strong seasonal variations in wave heights, wind speeds, residual current velocities as well as varying discharges of water and sediment by the estuary. Significant wave heights during the wet season are typically 1.5 m with a peak period of 13 s. The capacity of the waves to erode sediment in the coastal zone is larger than the capacity of the flow to keep the sediments suspended. This causes sediment induced buoyancy effects to take place.

Two main sediment transport mechanisms are found to be responsible for the expected infill. A persistent residual flow is present that carries suspended sediment in the coastal zone in Westward direction towards the proposed channel, and episodic high sediment transport rates from the estuary are expected to cause infill peaks in the proposed channel. Sediment originated from the estuary could cause infill directly by interception of suspended sediment in the channel as well as indirectly in the form of fluid mud.

Fluid mud events were observed during measurement campaigns in the area between the estuary and the approach channel. Little information is available on these events and the expected infill by this mechanism is highly uncertain. Accumulating sediment that is deposited outside the estuary is expected to be mobilized during extreme wave events creating a mobile fluid mud layer.

Sediment fluxes from the estuary were analyzed by the use of a 3D numerical sediment transport model (Delft3D). From the model results it is concluded that the amount of infill expected from the estuary is relatively low compared to infill expected from the residual sediment transport.

Additionally, from the numerical model it was found that stratification effects as a result of salinity differences partly drive the residual current, and are therefore of significant influence on the local sediment transport. In earlier studies it was concluded that a large scale ocean current is responsible for the residual current in the project area.

A list of potential effective measures for similar projects as this specific case is proposed. From an analysis of these measures it is concluded that no single solution is able to reduce sediment transport towards a dredged channel on a long term. Due to the complexity of fine sediment transport and varying conditions each case requires individual consideration. In the design phase of these kind of projects it should be taken into account that the configuration and location of a channel determines the sediment infill for a large part. Measures that require the use of fixed structures are generally costly and not practical in such muddy deltaïc environments due to the weak subsoil and availability of rock. The large size and complexity of these systems make it difficult to change the sediment transport patterns significantly, therefore the focus should be on the channel configuration to minimize trapping of sediment and to optimize maintenance dredging efficiency.

For the specific case, three mitigation measures for reducing infill by the residual transport were suggested to reduce sediment infill from an initial evaluation of the list of proposed measures:

- Channel bed slope;
- Redirect Estuary plume;
- Sediment trap.

A downward sloping channel bed was proposed to achieve a self-cleansing channel by transporting the mud infill in offshore direction under the influence of gravity. Due to the gentle surrounding bed slope and resulting maximum slope of the channel bed, the effectiveness of this solution is expected to be low. Additional analyses with a fluid mud flow model should be carried out to further investigate the potential of this measure.

A reduction of the stratification induced residual current was proposed to be achieved by redirecting the fresh water discharge from the Estuary away from the project area. The effect of a dredged channel in the ebb tidal bar of 400 m wide to a depth of approximately 8 m LAT was considered by the use of the Delft3D model. The model showed that the residual current did not decrease by a dredged channel in the ebb tidal bar of these dimensions. Therefore this solution is not expected to reduce infill in the proposed channel by the residual transport. A larger channel might be effective in reducing the sediment transport rates, however this should be further analyzed and may result in unrealistically high required dredging volumes.

The sediment trap was analyzed using a 2-DV trapping model, set up with the Delft3D software package. The model incorporates sediment induced buoyancy effects to represent the correct sediment concentration profile. The reduction of erosion due to damping of wave action by a thin fluid mud layer on the bed does not take place in the model. Different consolidation behaviors of the sediment are modeled in order to obtain a range for the trapping efficiency. The (main) approach channel is expected to have a trapping efficiency in the order of 45 - 100 %. The initial trapping efficiency of a sediment trap of 25 m wide and 5 m deep parallel to the channel is estimated between 20 - 55 %. A trap of these dimensions is expected to be filled in 1 - 3 months during the peak wet season for a density of 300 kg/m^3. If sediment infill has taken place, the trapping efficiency of the trap is most probably reduced and during high infill rates the consolidation rate is not expected to be able to keep up with the amount of infill. Therefore the sediment trap should either be maintained more frequently or the geometry should be adjusted to have higher capacity and trapping efficiency after initial infill. The down-time due to shipping was estimated to be 30 % of the year. The sediment trap can be maintained during this time, therefore more time is available to dredge the same amount of material.

Additional data would improve the accuracy of this study and allows for further calibration of the Delft3D model. However, due to the high seasonally and annually variability of the system, the large amount of required data is expected to be costly to obtain. The accuracy of this study can be improved by taking a probabilistic approach or conducting a sensitivity analysis of the calculations.

Further research in the optimum use of a nautical depth in the approach channel is recommended. It is thought that the trapping efficiency in the approach channel is reduced for low sediment concentrations in the channel already. The presence of these low sediment concentrations are the result of the expected low consolidation rate, which is hypothesized to be partially induced by wave action.

CONTENTS

List of Figures

List of Tables

NOMENCLATURE

Symbol	Unit	Description
c	kg/m^3	Suspended sediment concentration
C	m$^{0.5}$/s	Chezy roughness coefficient
C	kg/m^3	Depth averaged sediment concentration
c'	kg/m^3	turbulent fluctuation in sediment concentration
c_D	-	Constant relating mixing length
c_m	kg/m^3	Sediment concentration of fluid mud layer
C_M	kg/m^3	Solids concentration
c'_μ	-	Constant in Kolmogorov Prandtl's eddy viscosity formulation
c_{res}	kg/m^3	Sediment concentration of residual transport
c_s	kg/m^3	Mass concentration of suspended sediment
C_s	kg/m^3	Saturation concentration
c_{soil}	kg/m^3	Reference density for hindered settling
$\overline{c}$	kg/m^3	Time averaged sediment concentration
d	m	Thickness of fluid mud layer
d	m	Mean water depth
d_j	m	Jet diameter
d_m	m	Fluid mud layer thickness
d_{50}	m	Mean sediment particle size
D_f	-	Wave dissipation factor
D_H^{back}	m^2/s	background horizontal eddy diffusivity
D_H^{back}	m^2/s	background vertical eddy diffusivity
E	kg/m^2/s	Erosion rate
ECS	-	Earlier Confidential Studies
F_m	kg/m/s	Sediment flux by fluid mud layer
F_{res}	kg/m/s	Sediment flux of residual transport
f_w	-	Friction factor
F_x	N	Unbalance of horizontal Reynolds stresses
g	kgm/s^2	Gravitational acceleration
h	m	Water depth
h_0	m/s	Water depth outside dredged channel
h_1	m/s	Water depth inside dredged channel
h_{chan}	m	Channel depth
H_s	m	Significant wave height
h_{seabed}	m	Local water depth
H_{rms}	m	Root-mean-square wave height
HAT	m	Highest Astronomical Tide
k	m^2/s^2	Turbulent kinetic energy
LAT	m	Lowest Astronomical Tide
LL	%	Liquid limit
M_e	kg/m^2/s	Erosion parameter
M_x	Nm	External sources of momentum such as wave stresses
MHWN	-	Mean High Water Neap
MHWS	-	Mean High Water Spring
MLWN	-	Mean Low Water Neap
MLWS	-	Mean Low Water Spring
MSL	-	Mean Sea Level
P	N/m^2	Hydrostatic pressure

Symbol	Unit	Description
PI	%	Plasticity index
PL	%	Plastic limit
P_x	N/m^2	Horizontal pressure gradient
$q_{in/out}$	1/s	Local source or sink per unit
$\hat{Q}_{tide}$	m3/s	Tidal discharge amplitude
Q_{res}	m^3/s	Residual discharge
Re_w	-	Wave Reynolds number
Ri_f	-	Flux Richardson number
$Ri_{f,cr}$	-	Critical flux richardson number
t	s	Time
T	s	Period
$T_{flood/ebb}$	s	Tidal ebb/flood period
$T_{m,set}$	s	Mean settling period
T_p	s	Peak period
u	m/s	Horizontal flow velocity
u'	m/s	Turbulent horizontal velocity
u_*	m/s	Shear velocity
u_0	m/s	Flow velocity outside dredged channel
$u_{0,j}$	m/s	Jet discharge velocity
u_1	m/s	Flow velocity inside dredged channel
$u_{1,e}$	m/s	Equilibrium flow velocity in channel
u_m	m/s	Flow velocity of fluid mud layer
u_{orb}	m/s	Wave orbital velocity
u_{tide}	m/s	Depth averaged tidal flow velocity in shore parallel direction
u_w	N/m^2	Wave averaged pore pressure
u_{res}	m/s	Residual flow velocity
u_{tide}	m/s	Tidal velocity amplitude
U_w	m/s	Bottom orbital velocity amplitude
w	m/s	Vertical flow velocity
W	m	Width
w'	m/s	Turbulent vertical velocity
w_s	m/s	Effective settling velocity
W_s	m/s	Constant or characteristic settling velocity
$ws,0$	m/s	Defined mean settling velocity
$w_{s,50}$	m/s	Mean settling velocity
$w_{s,c}$	m/s	Settling velocity of coast sediment fraction
$w_{s,r}$	m/s	Settling velocity of river sediment fraction
x	m	Horizontal coordinate
x_{dis}	m	Displacement in shore parallel direction
X_m	m	Maximum extent of constant stress contour in x-direction
y	m	Horizontal coordinate
Y_m	m	Maximum extent of constant stress contour in y-direction
z	m	Vertical coordinate
z	m	Water depth
z_0	m	Roughness length
z_{max}	m	Maximum water depth for settling

Greek letters

Symbol	Unit	Description
$\alpha_{0,f}$	°	Flow approach angle wrt. Channel axis
$\alpha_{0,w}$	°	Wave angle wrt channel axis
$\alpha_{1,f}$	°	Flow angle in channel wrt. Channel axis
β	-	Rouse number
β	-	slope angle
δ	-	Relative density between solids and water
ε	m^2/s^2	Turbulent energy dissipation
$\varepsilon_{T,z}$	m^2/s	Vertical turbulent eddy diffusivity
ζ	m	Water level variation
$\hat{\zeta}$	m	Tidal water level amplitude
κ	-	Von Karman constant
λ_a	m/s	Flow adaptation length
ρ	kg/m^3	Density of water
ρ_b	kg/m^3	Bulk density
ρ_m	kg/m^3	Density of water-sediment mixture
ρ_s	kg/m^3	Specific density solids
ρ_w	kg/m^3	Density of water
σ	N/m^2	Wave-averaged effective normal stress
σ_h	N/m^2	Hydrostatic pressure
σ_T	-	Prandt-Schmidt number relating eddy diffusivity and eddy viscosity
τ	N/m^2	Shear stress
τ_b	N/m^2	Maximum bed shear stres generated by waves
$\tau_{c,c}$	N/m^2	Critical shear stress for erosion of coast sediment fraction
$\tau_{c,r}$	N/m^2	Critical shear stress for erosion of river sediment fraction
τ_d	N/m^2	Critical bed shear stress for deposition
τ_e	N/m^2	Critical bed shear stress for erosion
$\overline{\tau}_w$	N/m^2	Maximum instantaneous bed shear stress by waves
υ	m^2/s	Kinematic viscosity
υ	m^2/s	Vertical eddy viscosity
υ_H^{back}	m^2/s	Background horizontal eddy viscosity
υ_V^{back}	m^2/s	Background vertical eddy viscosity
ϕ	deg	Phase difference water level and flow velocity
ω	-	Wave angular frequency
ω	m/s	Vertical velocity relative to the moving z-plane

1

INTRODUCTION

This document is the MSc. thesis of Bart van Velzen for the Master program Hydraulic Engineering of the TU Delft. The Msc. thesis is carried out at the company of Boskalis. The subject of the MSc. thesis originates from a project preparation process Boskalis is involved in. The project takes place in the Niger delta in Nigeria, where an offshore terminal is planned to be constructed. This report focuses on the reduction of sediment infill in the dredged approach channel and harbor basin. Figure 1.1 shows the project location.

1.1. PROJECT DESCRIPTION

The terminal is to be located adjacent to the Estuary, which is supplied by fresh water by the River, a branch of the Niger River. The initial dredging activities consist of the construction of the harbor basin of approximately 1×1 km^2 and the approach channel of approximately 9 km long and 250 m wide both to a depth of -14 m LAT.

The dredged harbor basin and approach channel are expected to be subject to large quantities of sediment infill. For the design of the approach channel and harbor basin the sediment infill rates during and after construction are assessed. During previous studies conducted by Lanier Wallingford International (LWI) and Earth Sciences and Surveying international (EGSi) it was concluded that large amounts (order of magnitude: 10 million m^3/year (LWI, 2012b)) of fine sediment are transported into the proposed dredged area, for a large part on a seasonal basis. As the Estuary (re-)supplies significant amounts of sediment to the coastal system, the seasonal discharge variations of the Estuary due to the wet season cause a large fluctuation in sediment supply over the year according to these studies.

During the wet season high sediment concentration events have been observed that might be able to

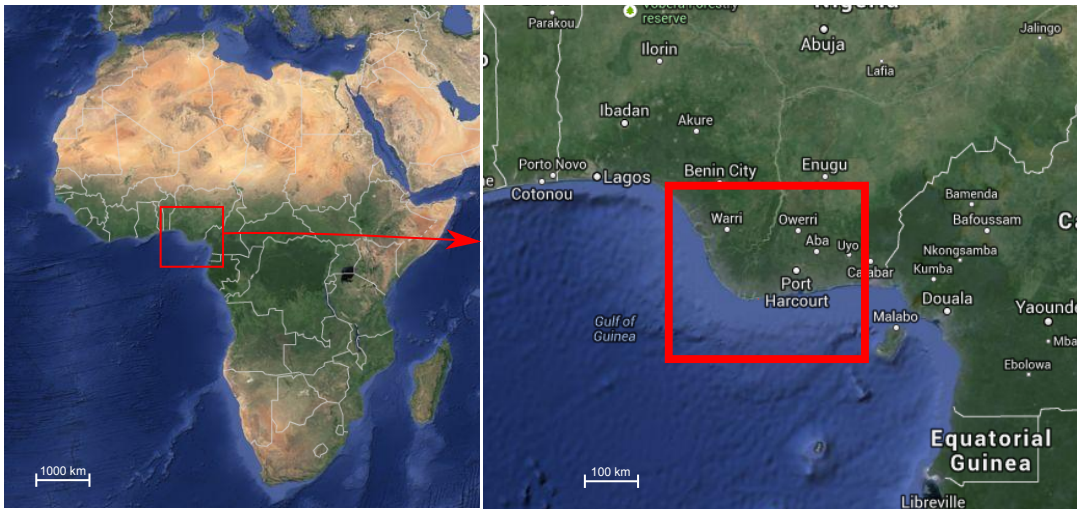

Figure 1.1: Project location Google

cause high infill rates in the dredged area in relatively short periods of time. Together with general Westward sediment transport consisting, again, of mostly fine sediments, extensive maintenance dredging activities are required in order to uphold the navigational depth in the approach channel and harbor basin. Figure 1.2 shows a schematization of the sediment transport patterns in the vicinity of the project site as identified during previous research (LWI, 2012b). Sand transport is mostly restricted to the ebb tidal bar and the shoreline. Mud transport however, takes place in the area of the proposed terminal and is originated from both the Estuary and a near-bed residual transport.

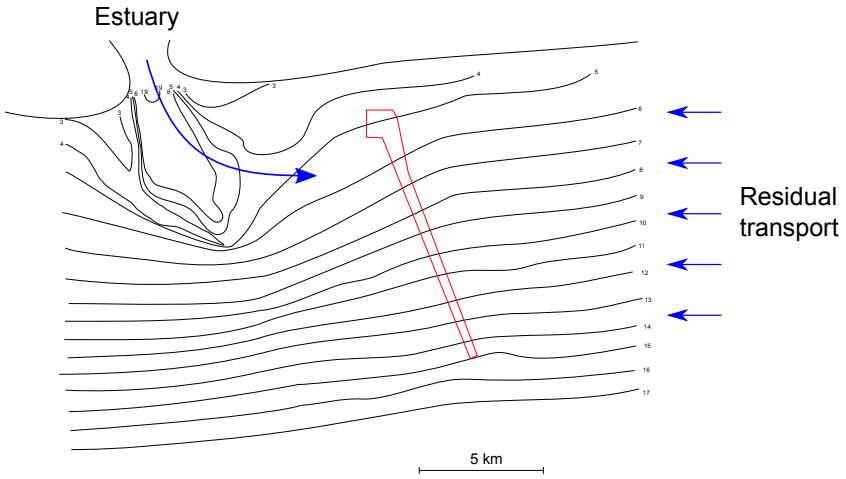

Figure 1.2: Sediment infill processes identified by LWI

The two processes that are responsible for the sediment infill as identified by LWI are:

1. Episodic discharge of the Estuary;
2. Interception of fine material in coastal zone.

The high sediment transport rates in the project area have initiated the consideration of alternative measurements to the rapid infill apart from executing maintenance dredging activities in the harbor basin and approach channel only. A contributing factor to this are the safety rules, which do not allow dredging vessels to be present in the approach channel or harbor basin while other vessels are moving.

1.2. PROBLEM DEFINITION

Resulting from the afore mentioned project description, the following problem definition is formed:

Problem definition:
Sediment infill rates of the harbor basin and approach channel are expected to be high due to complicated processes and may require significant maintenance dredging, further it is difficult to assess the effectiveness of mitigation measures.

Research question:

Which smart measures can be taken to mitigate the scale of infill in order to make the specific project as well as similar projects more cost effective?

1.3. OBJECTIVES

The objectives of this thesis are divided into one main objective and multiple sub-objectives.

Main objective:

Gain insight in complex processes that determine sediment infill in the proposed approach channel both qualitatively and quantitatively, then find (soft) mitigation measures to reduce sediment infill.

Sub-objectives:

1. Describe local (physical) processes that drive sediment transport to gain insight in dominant processes. This is done using available literature;
2. Investigate dominant sediment transport processes both qualitatively and quantitatively;
3. Find and assess possible mitigation measures to select effective solutions;
4. Establish a detailed model with which the in objective 3 generated solutions can be assessed;
5. Elaborate the best solution and identify the most important parameters that determine the effectiveness for the specific case and similar circumstances in general.

1.3.1. ASSUMPTIONS AND HOLDS

The following list of assumptions and holds is used for the specific case:

- The location of the harbor basin and approach channel is given. As the current location has been considered extensively in previous studies.
- The bed surface properties of the project area are assumed to be constant in shore parallel direction, except for the ebb-tidal delta.
- The possible effects of the trestle that connects the onshore facilities to the offshore terminal on the sediment transport is not taken into account.
- Only fine sediment transport is considered, infill rates due to sand are therefore not included in this research.
- The quantitative effects on sedimentation in the harbor basin by the breakwater at the terminal is not taken into account.

1.4. CONTENTS OF THESIS

First a review of literature will be done to describe the local system in Chapter 2. Earlier studies have been conducted for this project to find sediment transport and infill rates of the dredged areas. Dominant sediment transport processes are identified and further analyzed in Chapter 3. A 3D sediment transport model (Delft3D) is used to analyze the local system in more detail and investigate the relative importance of the main morphological processes. After the dominant processes are analyzed in detail, mitigation measures are proposed and considered in general and for the project specifically in Chapter 4. In Chapter 5 the measures that were found to be effective to mitigate sediment infill in the previous chapter are assessed using the Delft3D model as well as a separately established 2-DV trapping efficiency model. Finally conclusions and recommendations are presented in Chapter 6.

2

System Description

This chapter presents the system description for the project site based on available literature and previous researches. The system description gives a detailed view on the processes that are of influence on sediment transport in and around the project area. This analysis is required to provide input for the analyses in subsequent chapters. Earlier research on the local system for the design of the offshore terminal have been conducted by LWI and EGSi. Results of measurement campaigns are used as a basis for this system analysis. Hydrodynamic and sediment transport modeling was conducted by LWI and EGSi as well, of which the results are summarized in a separate section.

First the site location is described. Secondly the hydrodynamic characteristics are presented. Thirdly the morphological characteristics are discussed, consisting of sediment properties, dominant morphological processes. Furthermore, a summary of previously conducted research on sediment infill is presented. Finally a concluding overview of the local system is shown.

2.1. Site location

As was stated in Chapter 1, the project site is located in the Niger Delta area in Nigeria. The proposed channel will be located 2 km offshore at approximately 8 km East of the Estuary entrance, as shown in Figure 2.1.

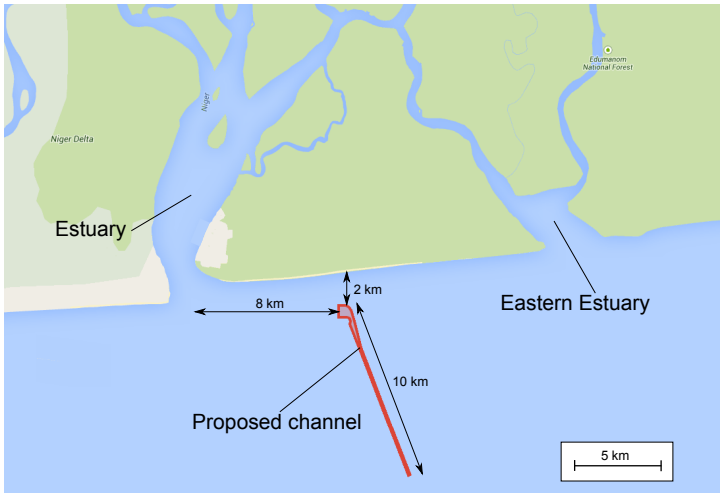

Figure 2.1: Site location (Google)

2.1.1. Geology

Two suites of sediment build up the current Nigerian Continental shelf. The older deposition originates from the Pleistocene and early Holocene period. This deposit consists of mainly well sorted, coarse quartz sand with locally shell and foraminiferal debris, “glauconite”, fecal pellets and silt or clay. Around the shelf break

at the flanks of the delta this suite of sediment is exposed. In the shallower depths along the delta coast this suite covers larger areas, eg. at the nose of the Delta. Between the exposed areas and in the coastal regions of the sub-aerial delta the older sands are covered by a thick layer of younger sediments. At some places the older sands are formed in broad bars roughly parallel to the existing coastline which indicates that the older sands used to form beaches and barrier island formations which are currently submerged due to relative sea level rise (Allen and Wells, 1962).

The sands of the beaches, coastal shoals, and river mouth bars develop into laminated sandy and then silty clays a few miles seaward, and eventually into fine clays on the deep shelf and continental slope. The younger sediment suite reaches a maximum thickness of around 45 m. It covers most of the area of the shelf, as well as extending down the continental slope as an apron. The younger sediments are deposited during the most recent expansion of the Niger Delta (Allen and Wells, 1962), see Figure 2.2.

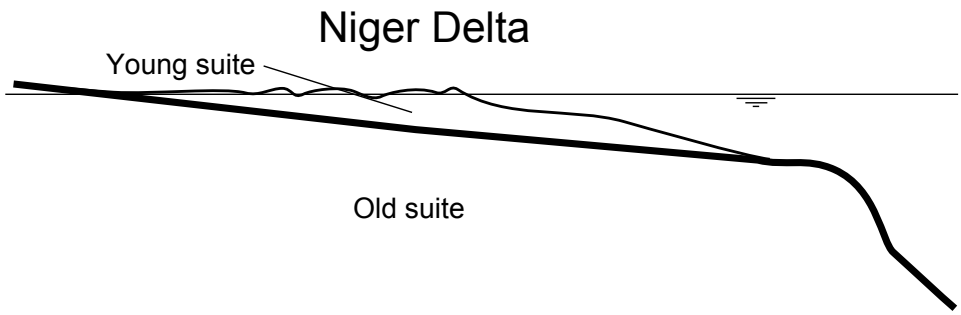

Figure 2.2: Niger Delta deposit (young suite) on continental shelf (old suite), after Allen and Wells (1962)

2.1.2. COAST CHARACTERIZATION

The characterization of the coast is divided in large scale and small scale. The large scale coast characterization presents the properties of the entire Niger Delta coastline, and the small scale coast characterization describes the local coast at the project location.

LARGE SCALE

The Nigerian coast can be divided in multiple zones with typical characteristics, these zones are shown in Figure 2.3. The largest part of the Nigerian coast is represented by the Arcuate Delta, which is also where the project area is located. It stretches for 284 km and is formed by 16 main river mouths/tidal inlets that divide the coastline into barrier islands. Intertidal beach faces are typically around 50 m with beach slopes of $1:15-1:20$. The beaches consist mostly of fine to medium grained well sorted sand (Sexton and Murday, 1994).

The overall morphology varies along the Arcuate Delta coast, this is determined by the sediment supply and the physical processes active on a given subdelta. The Niger Delta experiences cyclic sedimentation as periods of regression are followed by periods of transgression. 80 % of the fresh water discharge from the Niger Delta flows into the ocean on the Western side according to NEDECO (1961). The Western side of the delta is therefore currently most fluvially active, whereas the Eastern side of the Arcuate Delta is experiencing an erosional phase since the 1980's, according to Sexton and Murday (1994). The change in fresh water supply from one part of the delta to another by a change in upstream river configuration causes the varying sedimentation and erosional behavior of the coastline. The Western side of the delta, often consists of river dominated subdeltas while on the Eastern side of the delta distinct ebb tidal deltas are predominantly found.

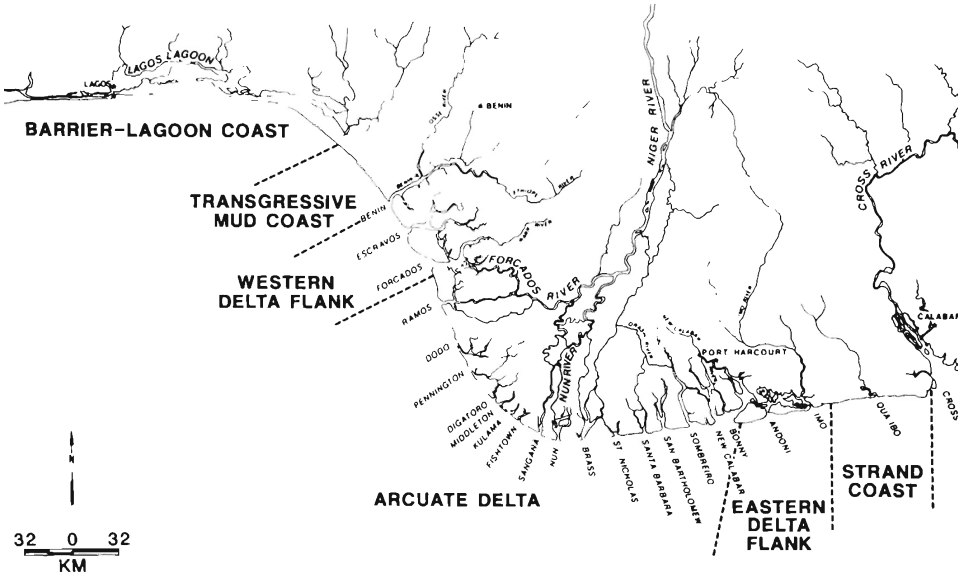

Figure 2.3: Nigerian coastal zones (Sexton and Murday, 1994)

The large scale bathymetry is characterized as a delta coast which is formed by deposits from the river system. The continental shelf along the Nigerian coast is relatively short with a distance of 50 - 65 km offshore towards the shelf edge, this can be seen in Figure 2.4. No submarine canyons that could potentially function as a sediment sink are present in the proximity of the project location.

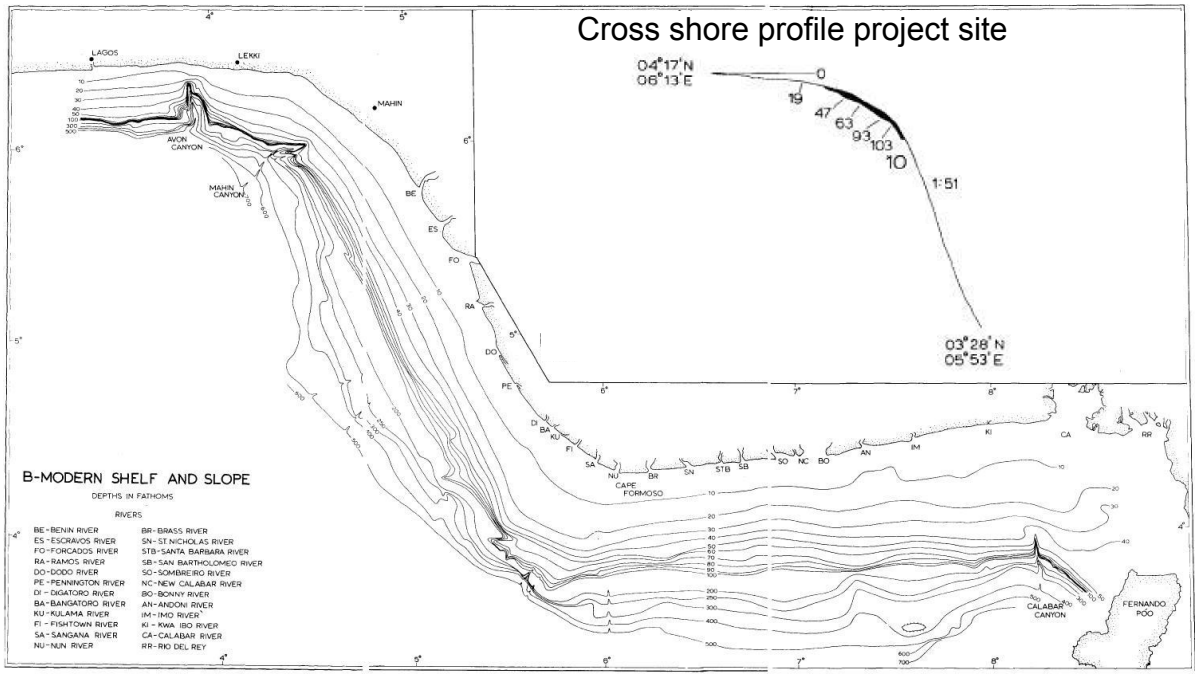

Figure 2.4: Niger Delta large scale bathymetry (Allen, 1964)

Figure 2.5 shows the dominant sediment transport and wave directions. It can be seen that in the project area the sediment transport direction is Eastward due to the South-West originated offshore waves.

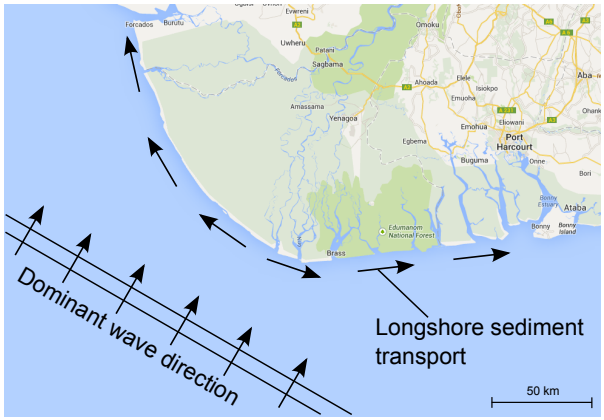

Figure 2.5: Niger Delta large scale sediment transport pattern (Google),after Sexton and Murday (1994)

SMALL SCALE

In the project area, the coastline is formed by a wide sandy intertidal zone. Behind this zone a channel system is present that drains the marshes of the low lying hinterland. Along the coast the depth contours are generally straight and parallel with a relatively uniform slope of 1:1000, except for the area around the Estuary ebb tidal delta. At the Estuary entrance the morphology is relatively complex, with a sandy ebb tidal delta bar connecting the Western to the Eastern coastlines. Due to the longshore sediment transport directed towards the East the ebb tidal bar is curved towards the East. Sediments grade from sand on the (near)shore to mud outside the bar. This ebb tidal bar extends the sand deposits further offshore than the adjacent stretches of coast (LWI, 2012b). Due to the curvature of the ebb tidal bar, the discharge from the Estuary is directed towards the East, in the direction of the project area. The direct influence of a smaller Estuary on the Eastern side of the project area is expected to be insignificant compared to the main project Estuary, due to the similar configuration and larger distance to the project area.

Alternating phases of erosion and accretion along the coastline cause a dynamic morphological character. Sand transport across the ebb tidal bar does not always match the down drift transport rates along the coast in the project area, this causes fluctuations in sedimentation and erosion rates. Satellite images from 2004 to 2011 have been analyzed to examine recent trends in erosion by LWI. The shoreline along the onshore facilities of the project experiences average erosion rates of 3 - 5 m/year. However, more eastward of the onshore facilities accretion takes place. An oscillating sedimentation and erosion pattern is observed (LWI, 2012b). Figure 2.6 shows the local bathymetry, constructed from multiple bathymetric measurements carried out for the project during earlier studies by LWI.

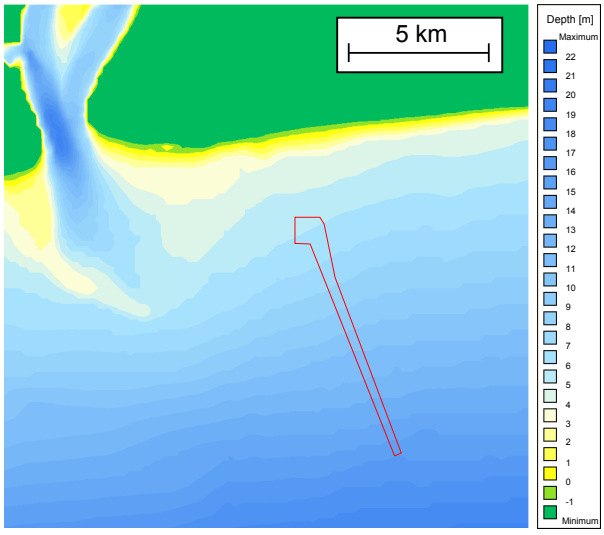

Figure 2.6: Local bathymetry

2.2. ESTUARY

The Estuary is described by its discharge and sediment separately in the following paragraphs.

2.2.1. DISCHARGE

The Estuary is one of the larger estuaries of the Niger Delta coast. Fresh water is supplied to the Estuary by the River, which is a branch of the Niger River. The Niger River mean discharge is approximately 6,000 m^3/s, and 8% Of the Niger discharge is estimated to flow into the River by NEDECO (1961). This gives a mean fresh water discharge of 480 m^3/s. However, strong seasonal differences in river discharge occur, Figure 2.7 shows the Niger River discharge distribution over the year.

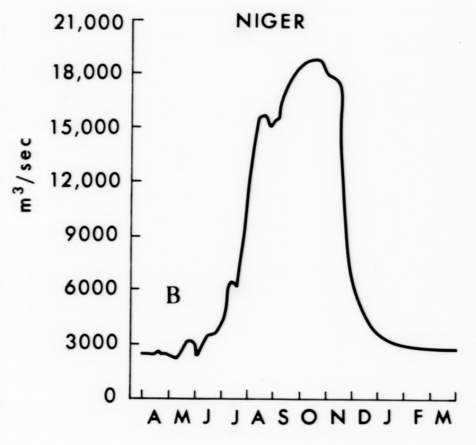

Figure 2.7: Niger River discharge distribution over the year, after Louisiana State University

The period of high river discharge is called the fluvial wet season and extends from August to November. The fluvial wet season does however, not completely coincide with the local meteorological wet season with high precipitation rates that extends from April to October. River discharge rates can reach a factor 10 during the wet season compared to dry season discharge values (Fugro, 2006). The River discharge fluctuates between 180 - 1,800 m^3/s (LWI, 2012b).

Discharge values in the Estuary mouth have been measured by LWI by taking transects from the Eastern to the Western banks with ADCP measurement devices. Simultaneously, sediment concentrations have been measured, which will be discussed in the next section. Discharge values at the Estuary entrance are significantly larger than the fresh water discharge from the River. Figure 2.8 shows discharge measurements at different moments in the Estuary entrance. It is clear that ebb tidal discharges are larger than flood tidal discharges, particularly during the wet season. The maximum observed ebb tidal discharge is 37,000 m^3/s and flood tidal discharge 23,500 m^3/s. The measurements were not carried out over full tidal cycles which makes it difficult to see the difference in duration between the ebb and flood tide. It is noted that the difference in ebb and flood discharge is significantly larger than the fresh water supply from the River. It is unclear why the ebb tidal discharge is significantly larger, and should be studied in future research.

The flow velocities in the Estuary entrance depend strongly on the tidal amplitude. During spring tides the peak depth averaged flow velocity can reach 2 m/s on the ebb tide, whereas on the flood tide the flow velocity is typically half the ebb velocity. During neap tides the flow velocities in the Estuary entrance are approximately half the spring tide velocities, with 1 m/s during the ebb tide and 0.5 m/s during the flood tide.

SALINITY

Salinity differences in the Estuary could cause stratification and associated additional flows. Particularly in the case of well mixed estuaries, horizontal stratification causes estuarine circulation, this mechanism is indicated in Figure 2.9. As the fresh water discharge is relatively low compared to the total discharge of the Estuary (1:20-50), the Estuary is classified as weakly stratified to well-mixed (Fischer et al., 1979). Salinity profiles have been taken in the Estuary mouth during the measurement campaigns by LWI, from these profiles it is shown that a region of strong gradients in salinity is occasionally present. Mostly a continuous stratification profile occurs with relatively constant salinity in the bottom layer. This suggests that the saline water in the deep

entrance of the Estuary is not pushed out during the ebb tide. During spring tides the salinity in the bottom region changes more significantly. Figure 2.10 shows salinity measurements in the Estuary entrance.

During the wet season the mean salinity is around 15 - 20 ppt whereas during the dry season the mean salinity is typically between 25 - 30 ppt. During spring tides the bottom salinity varies more strongly than during neap tides.

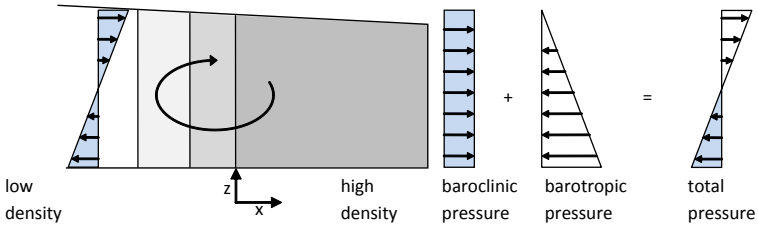

Figure 2.9: Concept of estuarine circulation (Pietrzak, 2013)

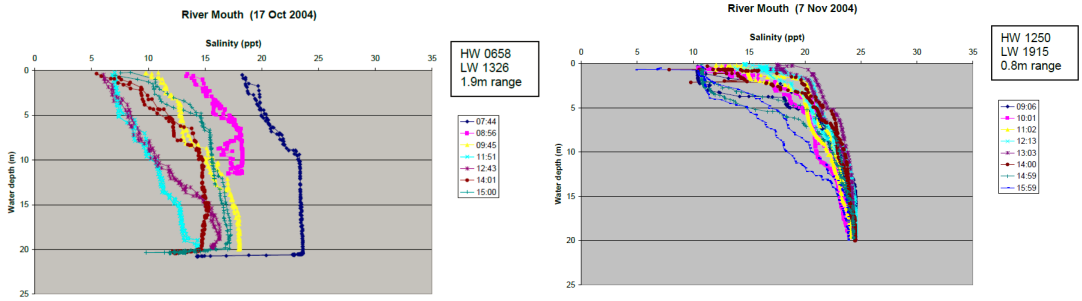

(a) Measured salinity profile Estuary entrance during (wet) spring tide

(b) Measured salinity profile Estuary entrance during (wet) neap tide

Figure 2.10: Salinity profiles Estuary entrance (LWI, 2012b)

Estuarine Turbidity Maximum At the landward side of the salt intrusion limit in an estuary an estuarine turbidity maximum (ETM) typically forms. During flood flow, significant turbulence causes mixing of sediments over the entire water column, this turbulence induces the breakdown of mud flocs. During high water slack (HWS) sediment flocculates due to lower turbulence and increased salinity, rapid settling occurs as a result of the low turbulence. During the start of the ebb tide a stratified concentration profile is present with fluid mud on the bed, which is able to sustain because of stable floc sizes (Winterwerp and van Kesteren, 2004). During flood tide the sediment is mixed over the water column again by the higher bed shear stresses.

The breakup and breakdown of mud flocs is an important mechanism for the ETM, during flood tide the higher shear stresses at the bottom break down mud flocs and makes the particles easier to suspend. At HWS flocculation takes place again and the sediment settles towards the bed. Figure 2.11 shows a schematization of the ETM at the salt intrusion limit.

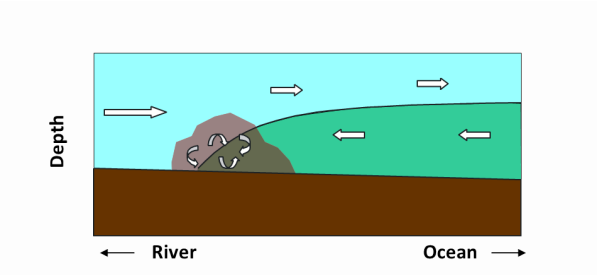

Figure 2.11: Estuarine turbidity maximum at salt intrusion limit (University of Washington, 2011)

As was shown by the salinity measurements by LWI (see also Section 2.2) the salinity in the lower part of the Estuary entrance remains quite stable during normal tidal discharges. However, during extreme discharge events the salinity was shown to reduce significantly. This suggests that the high sediment concentrations associated with the ETM might be pushed out of the Estuary during these high ebb flow rates.

2.2.2. SEDIMENT

The mean annual sediment discharge of the Niger River is around $4 * 10^{10}$ kg/yr (dry solid) (Milliman et al., 1995) of which 80 % is silt and clay (Bakker, 2009). This would lead to a mean sediment supply of around $3.2 * 10^9$ kg/year from the River (8 %). The mean sediment load of the River would then be around 0.21 kg/m^3 or 210 mg/l, which is comparable to other larger rivers in the world, however in the lower range, see Table 2.1.

Table 2.1: Large river discharges and sediment loads, (Milliman et al., 1995) and (Louisiana State University). The values are from relatively old data, therefore the current sediment and discharge values might be different. The values are used for qualitative comparison.

	Amazon	**Orinoco**	**Ganges**	**Yangtze**	**Mississippi**	**Mekong**	**Congo**	**Niger**
Discharge $[10^9 m^3/yr]$	6300	1100	970	920	490	470	1200	190
Sediment load $[10^9 kg/yr]$	1200	150	1050	480	210	160	430	40
Mean sed. conc. $[kg/m^3]$	0.19	0.14	1.08	0.52	0.43	0.34	0.36	0.21

The Estuary is described as muddy by the Admiralty Chart 1321, and according to soil penetration tests conducted by Fugro (2006), the top soil of the inner part of the Estuary consists of a few meters of soft clay.

Figure 2.12 shows the sediment plume from the Estuary from a satellite image. A clear sediment plume is visible in the image, here it can be seen that the extent of the sediment plume does not cover the complete coastal area around the project site. It is noted that the tidal phase and amplitude associated with the satellite image are not known.

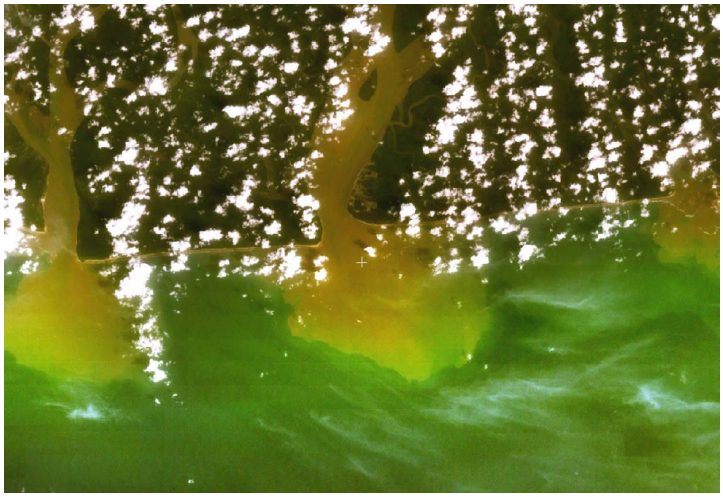

Figure 2.12: Satellite image of project area, with clear sediment plume from adjacent estuaries, taken in January (dry season) EGSi (2006)

Sediment concentrations in the Estuary entrance have been measured by LWI (2012b) using ADCP devices. Figure 2.13 shows depth averaged sediment concentrations as presented by LWI over a tidal cycle (some lines show combined data from multiple cycles). It can be seen that particularly during two measured spring tides during the wet season (yellow and purple line) sediment concentrations are significantly larger than the other measurements. The peak depth averaged concentrations reach up to 1,200 mg/l during the ebb tide. The sediment concentrations are lower during the flood tide than during the ebb tide, which suggests that significant sediment is supplied to the coastal area during these (large) wet spring tides. It is also noted that the sediment concentrations can be well above the mean sediment concentration of the Niger River.

The month November is identified as a transition season between the wet and dry season by LWI. The dark blue line represents a spring tide during the transition season and shows higher concentrations during the

flood tide than during the ebb tide, this is in contrast to the higher sediment concentrations during the ebb tide by the large spring tides in the wet season. The other measurements typically show increasing sediment concentrations during the flood tide as well. Higher concentrations during the flood tide could indicate a net import of sediment during these tidal cycles into the Estuary.

Additionally LWI measured sediment concentrations upstream of the Estuary mouth and observed a near bed layer of higher suspended concentrations, this could suggest the estuarine turbidity maximum is located quite close to the Estuary entrance.

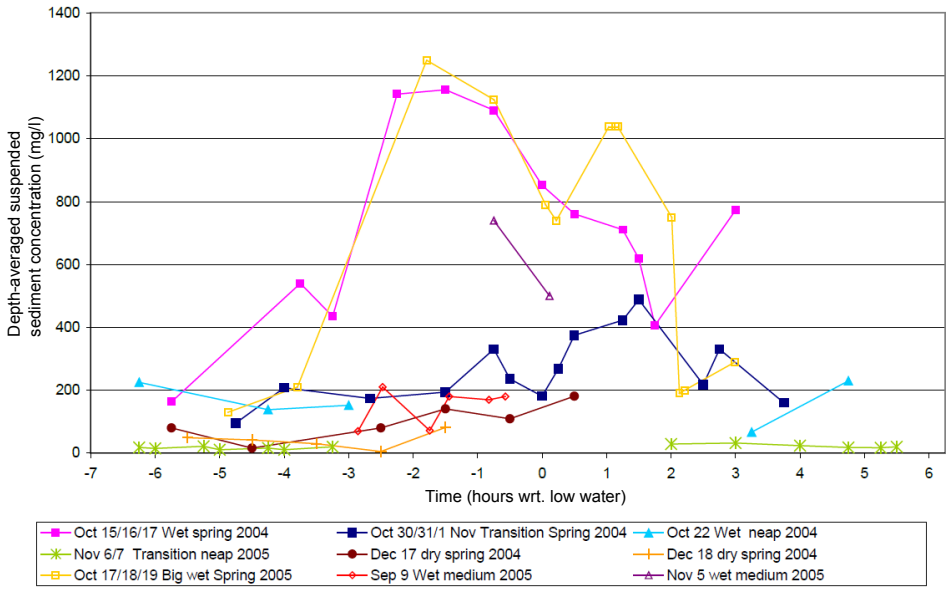

Figure 2.13: Estuary entrance sediment concentrations (LWI, 2012b)

From the sediment concentration measurements it is concluded that highly variable sediment concentrations occur in the Estuary mouth depending on tidal discharges and season.

2.3. HYDRODYNAMIC SITE CHARACTERIZATION

The hydrodynamic characteristics are considered in this section. The area is located in the tropics and experiences a distinct wet and dry season as is described earlier in this chapter. The local meteorological wet season takes place from approximately April-October and the dry season from November-March. The hydrodynamic conditions vary strongly in accordance with the seasons as is elaborated in the following paragraphs.

The hydrodynamic characteristics follow from measurement results presented by LWI (2006b). A number of (fixed) measurement locations have been used during the measurement campaigns, the most important ones are shown in Figure 2.14. The measurements include sediment concentrations, flow velocities, salinity profiles and wave heights. Not all measurements were conducted at each of the locations.

2.3.1. TIDAL FORCING

Here the tidal forcing in the project area is described. First the measured water level variation is treated, followed by a description of the tidal propagation in the project area.

WATER LEVEL VARIATION

The tide in the project area has a semi-diurnal character with two inequalities, the tidal range is typically between 1 – 2 m during neap and spring tides respectively. A tide gauge was deployed for a year long to measure the water levels in the Estuary entrance by LWI. Figure 2.15 shows the tidal record from the tide gauge. It is noted that the mean water level surface has a small seasonal variation, during October and November the mean sea level is around 0.1 m higher and 0.1 m lower during June and July LWI (2012b). The standard tidal levels with respect to mean sea level are presented in Table 2.2.

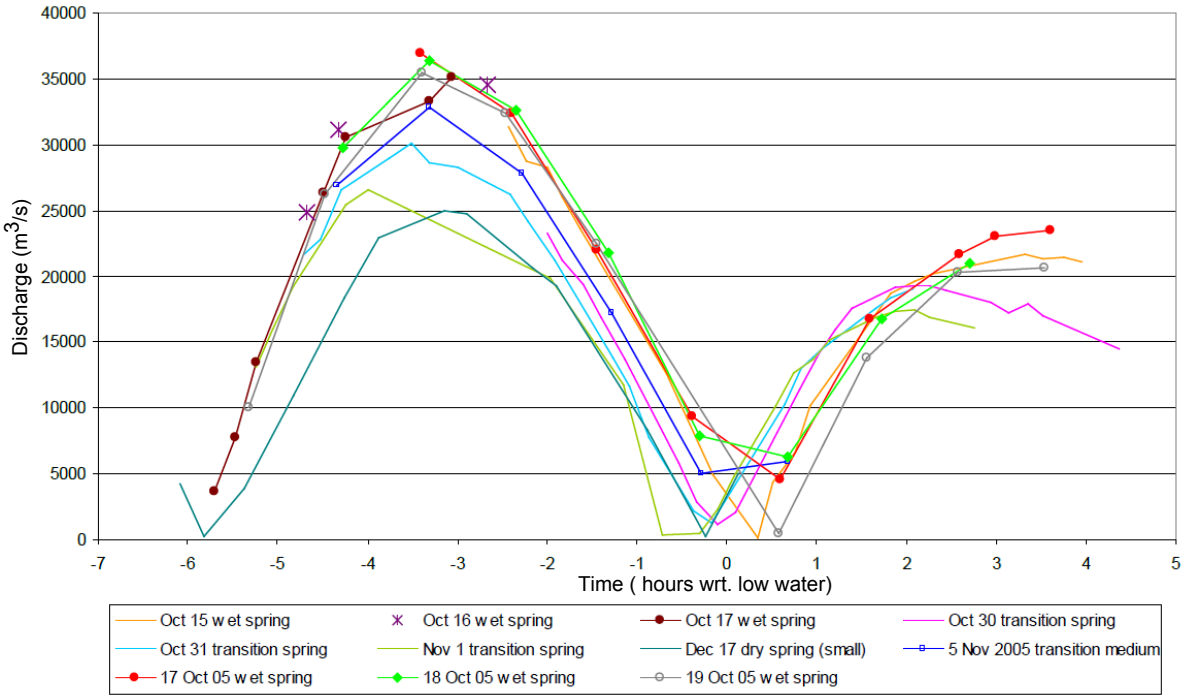

Figure 2.8: Estuary discharge (vertical axis) against time in hours to low water (horizontal axis), measured during various tidal levels and seasons (LWI, 2012b)

Figure 2.14: Fixed measurement locations, colors indicate measurement campaigns: yellow (2002-2003) and orange (2004-2005)

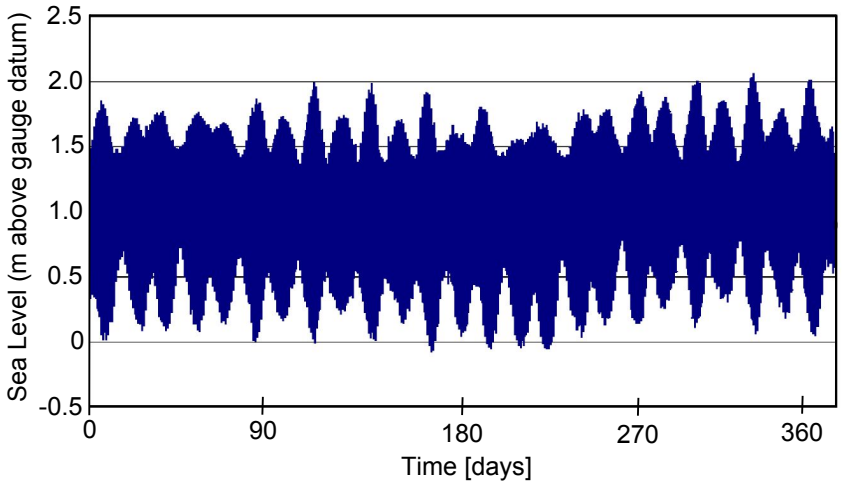

Figure 2.15: Tidal record taken at Estuary with number of measurement days on horizontal axis and meter above gauge datum on vertical axis (LWI, 2012b)

Table 2.2: Standard tidal levels with respect to mean sea level (MSL) (LWI, 2012b)

Location	HAT [m]	MHWS [m]	MHWN [m]	MSL [m]	MLWN [m]	MLWS [m]	LAT [m]
Estuary entrance	1.06	0.70	0.35	0.00	-0.36	-0.85	-1.19

The larger harmonic amplitudes derived from the tidal record are shown in Table 2.3.

Table 2.3: Larger harmonic amplitudes from tide gauge data LWI (2012b)

Constituent	Amplitude [m]
K1	0.150
N2	0.111
M2	0.535
S2	0.190

TIDAL PROPAGATION

The tidal wave is generated in the South Atlantic Ocean and travels Northwards along the West African coast. Along the Southern stretch of the Niger Delta the tidal wave in the deep oceans travels from East to West. The tide in the deeper ocean travels with high propagation speed due to the large depths, on the continental shelf the tidal propagation is significantly slower because of the smaller water depths. This causes a phase difference in the water level variation at the coast and in the deep ocean (Houwman and Hoekstra, 1998). As the continental shelf along the Niger Delta is relatively short (50 – 65 km) the gradients in water level are large, cross shore tidal currents occur as a result of this. The tidal currents on the continental shelf are North-South directed as a result of the large difference in tidal propagation speed between the shelf and the deep ocean.

2.3.2. CURRENT PROFILE

The current profile in the project area is quite complex due to a combination of tidal currents, wind driven currents and stratification.

TIDAL CURRENTS

Tidal currents along the Niger Delta were examined by Allen (1965). According to his paper the maximum tidal currents in the project area are in the order of magnitude of 20 – 40 cm/s. The Estuary is expected to influence the tidal currents in the area of the proposed channel to a large extent. The tidal currents closer to the Estuary would be directed more obliquely towards the entrance compared to offshore North-South

directed tidal currents. From ADCP measurement results it is observed that the tidal flow direction at the project location is North-West during flood tide and South-East during ebb tide. The depth averaged flow velocities are similar to the values found by Allen. The North-South flow character of the tide is clearly shown in the measured record from Figure 2.16.

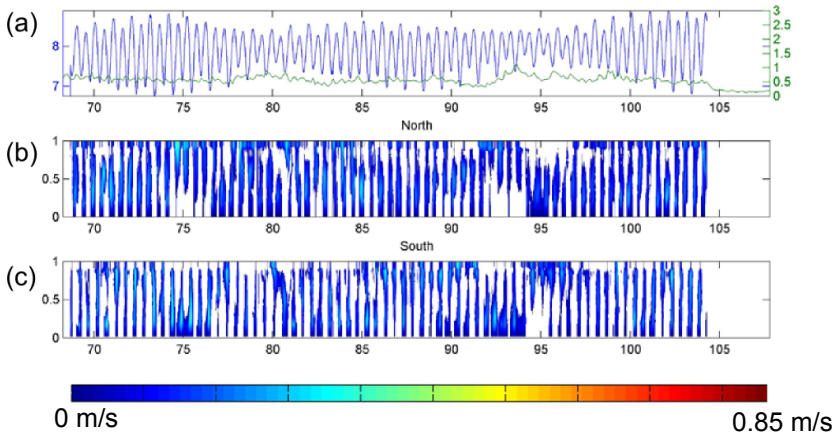

Figure 2.16: Time record of (a) tidal amplitudes(blue) and wave heights (green), (b) flow in Northern direction over normalized depth, (c) flow in Southern direction over normalized depth (LWI, 2012b)

STRATIFICATION

The velocity measurements show significant differences in flow profile between the top and bottom part of the water column. Figure 2.17 shows a tide-averaged current rose at measurement location P2 for the vertically averaged flow over the top and bottom half of the water column. In the figure it is clearly shown that the bottom layer experiences net flow in West/North-West direction and the top layer experiences a net flow in Eastern direction.

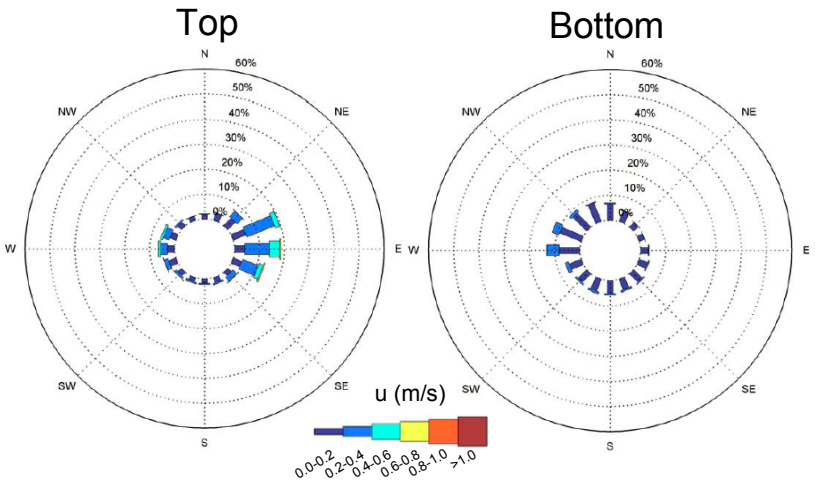

Figure 2.17: Current roses for top and bottom layer at measurement location P2. A net flow in North/North-West direction in the bottom layer and a net flow in the top layer in Eastern direction are shown. The data is from combined fortnightly measurements conducted at different moments throughout the year. (LWI, 2012b)

The following sections treat the flow driving factors that are responsible for the vertically stratified flow profile at the project location.

WIND DRIVEN CURRENTS

Wind patterns in the project area were measured by a land-based meteorological station at the project site. The predominant wind direction is very consistent over the year from South-Western direction. Wind speeds

show a seasonal trend in this area, during the wet season wind speeds are larger than during the dry season. Typical daily average wind speeds during the dry season are below 3.5 m/s and during the wet season up to 5 m/s. The flow velocities in the surface waters are strongly influenced by the wind speed, as can be observed in Figure 2.18. The bottom layer is less effected by wind induced currents.

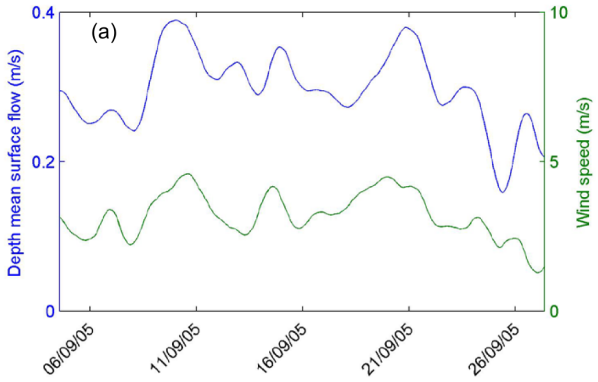

Figure 2.18: Wind speed vs depth mean surface flow measured in September 2005 LWI (2012b)

OCEAN CURRENTS

According to LWI (2012b) and Bakker (2009), large scale ocean currents play an important role in the bottom flow profile around the Niger Delta. The large scale ocean currents around the Niger Delta are relatively complex. The dominant factors of these currents are the Eastward Guinea Current on the surface and the Westward Guinea Counter Current that flows underneath the Guinea Current. The Guinea Current is a relatively shallow flow, that extends from the surface to a depth of about 15 m near the coast, and to around 25 m offshore. In areas where the water depth is less than 40 m the Guinea Current is in contact with the sea bed (Allen, 1965). A thermocline at 40 m depth separates an upper warm water body and a lower cold water body. The upper water body is affected by the Guinea Current, and the lower water body by the Guinea Counter Current. Figure 2.19 shows a simulation of the large scale ocean currents in the area of the Niger Delta during the Northern summer and winter. It can be seen that the flow velocities in the vicinity of the Niger Delta are lower during (Northern) winter than during summer months.

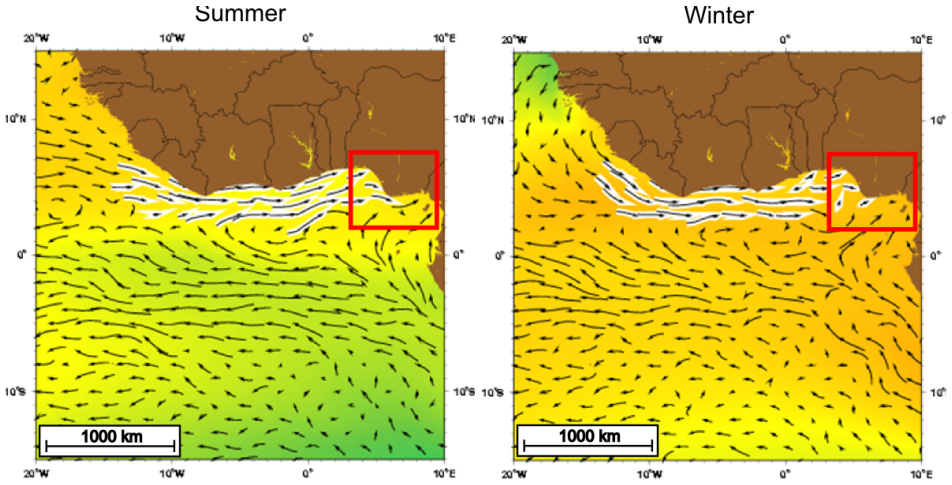

Figure 2.19: Guinea current in Northern summer (Jul/Aug/Sep) (left) and winter (Jan/Feb/Mar) (Right), arrow length indicates velocity magnitude (University of Miami). It is shown that the guinea current is stronger during summer than during winter months.

The Guinea Current velocity varies between 0.2−0.6 m/s with highest velocities during the Northern summer as the North Equatorial Counter current that feeds the Guinea Current is largest in this period as well. The higher velocity in summer can be explained by higher wind speeds during this time of the year. Coastal

upwelling occurs during summer, which causes the thermocline to shift upwards to 20 - 30 m depth, with an upper limit of 12 - 15 m depth according to Rider (2004). This could cause the Guinea Counter Current to flow along the bottom in more shallow regions.

In measurements taken by LWI a persistent Westward undercurrent is observed along the bottom, the measurement data were used to construct a schematization, shown in Figure 2.20. According to LWI and Bakker (2009) the large scale ocean currents are responsible for the Westward undercurrent along the Niger Delta. As the interface between the Eastward directed surface current and the Westward directed undercurrent is represented by the thermocline at a depth of approximately 40 m, it is doubted that in the project area the Westward near bed current is caused by large scale ocean currents because of the limited depths at the project site (max 15 m LAT).

The Westward undercurrent could be caused by horizontal stratification as a result of salinity differences as well, this is treated in the next section.

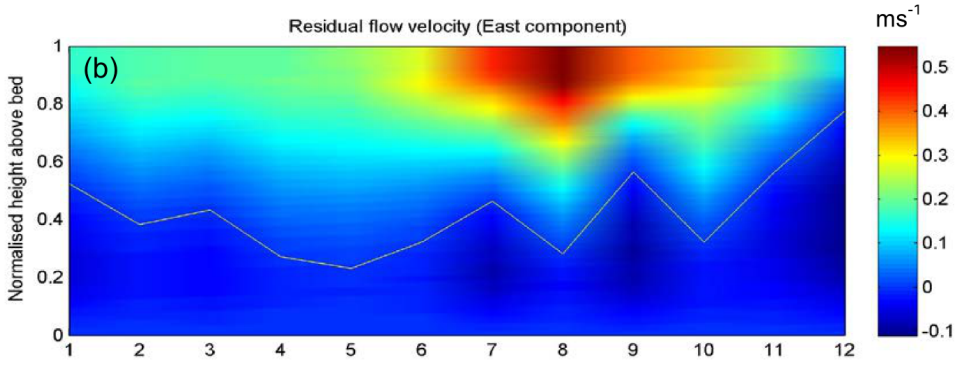

Figure 2.20: Current velocity over normalized depth throughout the year (LWI, 2012b). The separation in flow direction is indicated by the white line.

STRATIFICATION

Fresh water river run-off generates density differences in the area around the Estuary entrance. Salinity induced stratification could play a significant role in the hydrodynamic properties in the area.

Salinity profiles have been measured by LWI during the wet season, the vertical salinity profile does not show a particular region with sharp gradients in salinity in most of the measurements. Only in some measurements during small tidal amplitudes, a sharp gradient in salinity is observed. This is expected to be caused during low discharges when less mixing takes place. Most measurements show linear increasing salinity profiles from the bottom to higher parts of the water column with often increasing gradients in the upper part of the water column. Typical bottom salinity is 30 ppt and surface salinity is 20 ppt. The (mixed) vertical salinity profile suggests horizontal gradients in salinity to be present. Figure 2.21 shows salinity profiles for a wet spring and neap tide in the project area. Compared to the salinity profiles at the Estuary mouth, a difference of around 10 ppt is found between the Estuary entrance and the project area.

Horizontal salinity gradients in shore parallel direction could cause near bed flows in the direction of the Estuary. A net flow velocity in this direction is measured by LWI at the project location, however no measurements were conducted on the Western side of the Estuary to verify whether the stratification by the Estuary causes the residual current. This hypothesis is further elaborated in Chapter 3. Because of the seasonal variation in the fresh water run-off, salinity profiles change over the year, probably causing varying stratification effects.

2.3.3. WAVES

Waves in the project area consist of three types, swell waves, wind sea waves and low frequency waves. The most dominant wave type is swell waves, as these have the largest contribution to the energy spectrum (LWI, 2006b) because of the high frequency of occurrence and relatively large wave heights. Wind sea waves occur as well, however due to the relatively low probability of high wind speeds these waves tend to be less frequent and lower (< 1 m) than swell waves. Low frequency ($T > 25$ s) wave heights show a strong correlation to swell wave heights and are generally between $0.1 - 0.2$ m.

Significant wave heights (H_s) in the project area are typically around $1 - 1.5$ m with a peak period of $12 -$

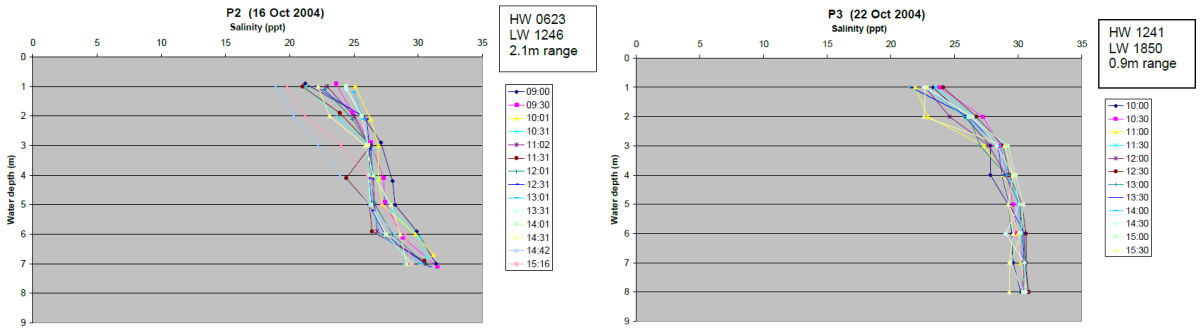

(a) Measured salinity profile at measurement location P2 during (wet) spring tide

(b) Measured salinity profile at measurement location P2 during (wet) neap tide

Figure 2.21: Salinity profiles in project area (LWI, 2012b)

13 s, the direction is predominantly South to South-South-West. The wave heights show a strong seasonal variation, higher waves are present in the summer season. Figure 2.22 shows significant wave heights with occurrence percentages per month. During the Northern hemisphere summer period (or local wet season), waves with $H_s > 1$ m are almost constantly present. During the dry season wave heights are clearly lower.

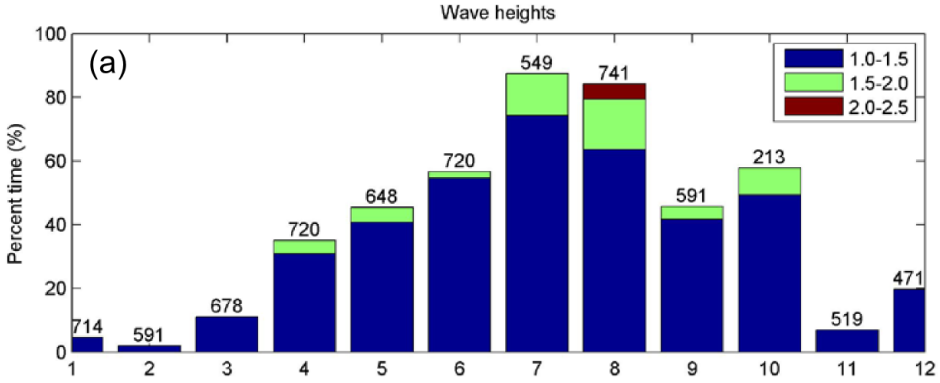

Figure 2.22: Significant wave height distribution per month (LWI, 2012b), the numbers above the bars indicate the number of samples used for the bars.

Two wave related processes are of most interest with respect to sediment transport:

- wave driven currents;
- wave induced bottom shear stresses.

Wave driven currents are able to transport suspended sediment along the coast. The wave driven currents are mostly felt close to the shore, as breaking waves drive these currents.

Wave orbital velocities are responsible for wave induced bottom shear stresses. The maximum wave orbital velocities along the Niger Delta were examined by Allen (1965), the maximum orbital velocities in the project area are > 50 cm/s. Wave orbital motions are particularly important for the mobilization of bed material.

2.4. MORPHOLOGICAL SITE CHARACTERIZATION

This section discusses the morphological characteristics of the project area based on available literature. First the sources and sinks of sediment are discussed.

2.4.1. SEDIMENT SOURCES AND SINKS

As is described in Section 2.2.2 sediment is supplied to the coastal system by the Niger River. The process of sediment supply by the Niger River has been present for centuries and a thick layer of fine material has built up around the entire Niger Delta (Allen, 1965). Submarine canyons function as sediment sinks along the Niger Delta, however, none of these canyons are located close to the project area (Bakker, 2009).

A local source of sediment is considered to be the Estuary, supplying sediment to the coastal system. The Estuary could be sediment importing due to estuarine circulation effects and therefore it is not directly known whether the Estuary is importing sediment or exporting sediment on a net basis.

Sediment residence time As was stated in Section 2.3.2, horizontal density gradients due to the fresh water supply from the Niger River along the entire delta coast probably cause near bed currents in shoreward direction. This effect could reduce the gravity induced sediment transport in offshore direction and thereby increase the residence time of suspended sediment in the coastal area. This is similar to the effect of the Rhine fresh water discharge on fine sediment transport in the North Sea along the Dutch coast (Winterwerp, 2014).

2.4.2. SEDIMENT CHARACTERISTICS

The beaches along the coast of the project area consist of sand, in offshore direction the sediment becomes finer. In the higher energy areas where wave breaking occurs fine sediments are not able to settle and will therefore only be deposited in calmer waters.

The sediments in the project area were investigated by Fugro (2006), LWI (2012b) and EGSi (2006). Multiple grab samples and cores have been collected and analyzed to describe the sediment characteristics.

No information is available on the settling velocity of sediment in the vicinity of the project location. However, in the MSc. Thesis of Bakker (2009) there were suggestions that very low settling velocities occur in the Niger Delta. The project of that particular study is located in a different part of the Niger Delta (Barrier-lagoon coast Figure 2.3) and according to Porrenga (1966), the Montmorillonite content in that region is higher than the considered area of this study. Montmorillonite is known for low flocculation rates and could therefore be of significant influence on the settling velocity. The potential low settling velocity is not further treated in this study.

Soil samples are taken just outside the Estuary entrance in offshore direction and from there towards the project area. The bar in front of the river mouth is clearly represented in the results. In front of the bar the water depth is large (13 m) and becomes smaller closer towards the bar (7 m). The top soil of the deeper parts have relatively coarse sediment, consisting mostly of fine to coarse sand. Towards the bar the material gets finer, where the sediment consists of silty fine to medium sand. Beyond the bar the sediment becomes even finer, as just off the bar the sediment consists of sandy silt and closer to the project area the sediment becomes sandy silty clay. Fine sediment cannot accumulate in the Estuary entrance because of high current velocities.

Figure 2.23 shows the soil composition of the dredged area. The soil consists predominantly of soft clay, with an exception at the shallowest parts where the top layer consists of fine sand.

Core samples have been taken at the project location and examined by Fugro. Most of these samples investigated deeper soil layers for the foundation of the breakwater. The samples taken closest to the bed surface were at 0.5 m below the bed. These were taken at a local water depth of 8.0 m and 8.4 m LAT. Table 2.4 shows the soil compositions of the samples. Based on this data an estimate of the mean sediment particle size is made, $d_{50} \approx 0.012$ mm. The fraction of fines (< 0.06 mm) is around 70 % for both samples. Figure 2.24 shows a ternary diagram for the soil samples. The clay-silt ratio is around 1:2.

The plasticity index PI is determined by the plastic limit PL and the liquid limit LL of the soil. These parameters are determined for the soil at the same locations as used above (Boskalis, 2012a). The plasticity index and liquid limits are treated in Appendix A. The samples show to be in the range of inorganic clays with low plasticity in the upper soil layer (0 - 2 m) and increasing plasticity with increasing depth.

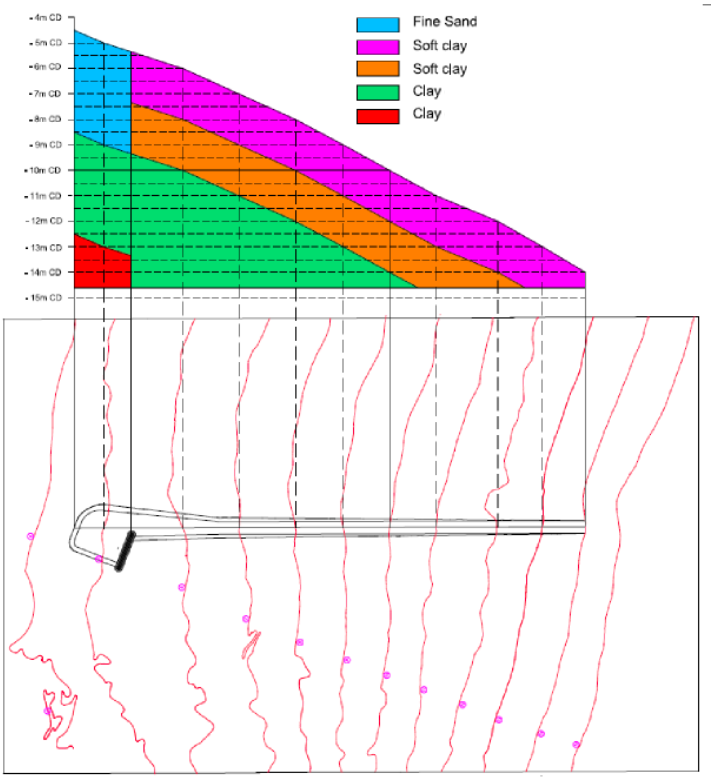

Figure 2.23: Soil characteristics of dredged area (Boskalis, 2012a)

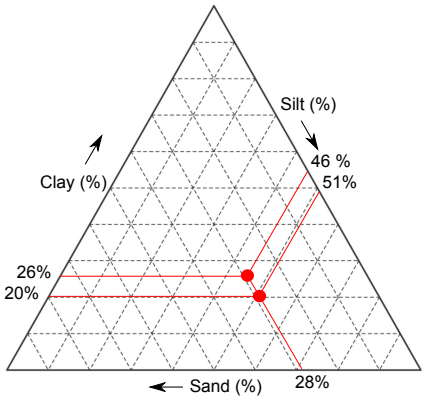

Figure 2.24: Ternary diagram of soil samples

Table 2.4: Soil composition at 8.0 m (maneuvering area) and 8.4 m depth (breakwater)

Soil fraction	Maneuvering area	Breakwater
<0.002 mm	20 %	26 %
0.002-0.06 mm	51 %	46 %
0.06-0.2 mm	23 %	24 %
0.2-0.6 mm	5 %	4 %

CRITICAL BED SHEAR STRESS

Multiple relations are found in literature to estimate the critical bed shear stress for erosion (τ_e [N/m^2]) of cohesive sediments, however all of these relations are highly empirical (Winterwerp and van Kesteren, 2004).

A critical bed shear stress for deposition($\tau_{c,d}$) is often used as well, which gives a maximum bed shear stress that allows for sedimentation (Manning et al.). This value is practical in use for modeling, however in reality simultaneous deposition and erosion occurs (Winterwerp and van Kesteren, 2004). The calculation for the critical bed shear stress is given in Appendix A.

The critical bed shear stresses depend on the rate of consolidation of the clay sample, as the bulk density increases over time due to consolidation and the same will be valid for the plasticity index. Sediment that has just been deposited has a lower density and will therefore be eroded more easily. The critical bed shear stress for consolidated and unconsolidated bed material are found separately.

The critical bed shear stress for erosion of the consolidated bed is estimated around 2 N/m^2. For unconsolidated deposits the bed shear stress is estimated to be around 0.5 N/m^2.

WAVE INDUCED BED SHEAR STRESS

The maximum shear stress that is generated by waves (τ_b) is used to determine which area is subject to erosion for the local wave climate. Using wave data from LWI (LWI, 2012b) and Boskalis, typical wave heights with associated periods for the project area are determined. A distinction is made between wind waves and swell waves. The calculation of wave induced shear stresses is given in Appendix A.

Figure 2.25 shows the results for the bed shear stress induced by the characteristic swell waves. Some lines are not smooth due to a transition between smooth turbulent and laminar behavior of the wave induced current. The critical bed shear stress for erosion of consolidated bed (τ_b = 2 N/m^2) and unconsolidated deposits (τ_b = 0.5 N/m^2) are shown as dashed lines in the graphs.

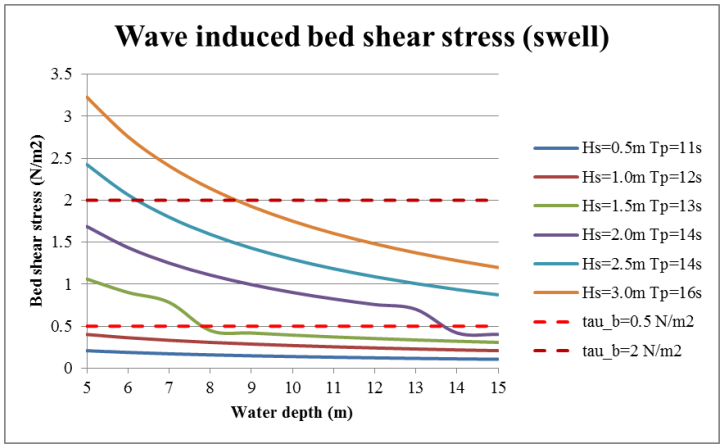

Figure 2.25: Characteristic swell wave induced bed shear stress

The graphs show that only large swell waves are capable of eroding consolidated bed material, and solely in the shallower regions of the coastal zone. Wind waves are not capable of eroding the consolidated bed material as the bed shear stresses do not exceed 2 N/m^2 . Unconsolidated deposits are eroded relatively easily by swell waves, above H_s = 1.5 m freshly deposited sediments are eroded for depths smaller than 10 m. It was shown in Section 2.3 that particularly in the wet season wave heights are practically constant higher than 1 m. This would suggest that the weaker subsoil is continuously mobilized by waves.

2.4.3. SEDIMENT CONCENTRATION PROFILE

Sediment concentration profiles in the area of the dredged channel were measured using OBS devices at different depths by LWI. The OBS sensors were subject to biofouling during the measurements and only a small part of the data was useful. Limited data is available from the sediment concentration profile measurements for this thesis. Figures 2.26 and Figures 2.27 show data from the OBS measurements. The figures show wave heights, and sediment concentrations at 20 cm and 40 cm above the bed. It can be seen that the sediment concentrations strongly depend on the wave heights and react rather quickly to a change in wave conditions. This indicates that sediment brought in suspension by waves does not stay suspended for long periods. The sediment concentrations in the two figures do not show significant variation over spring-neap cycles compared to the variation due to wave heights. For fine sediment with low settling velocities it is commonly expected that the sediment concentration varies over longer periods. However here it is not shown to be the

case. In Chapter 2.4.3 the phenomenon of sediment induced buoyancy effects is explained, which causes sediment concentration profiles with high concentrations near the bed while sediment concentrations higher in the water column are negligible.

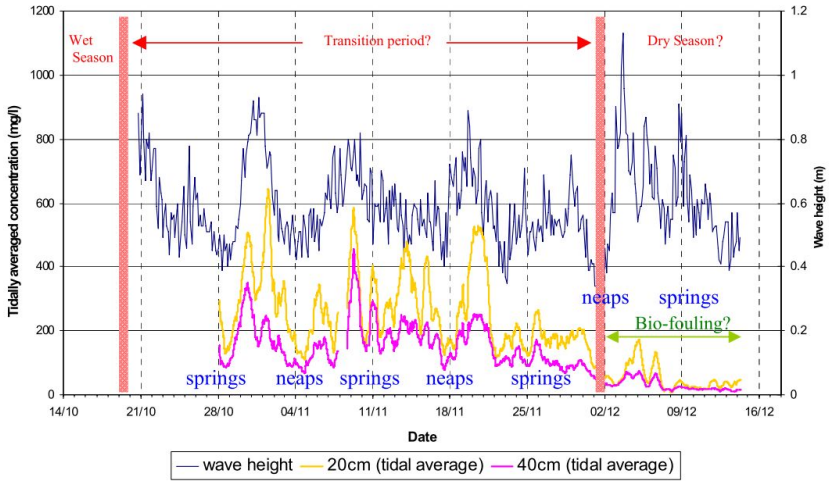

Figure 2.26: Tidally averaged suspended sediment concentration and wave height (LWI, 2012b) at measurement location P2

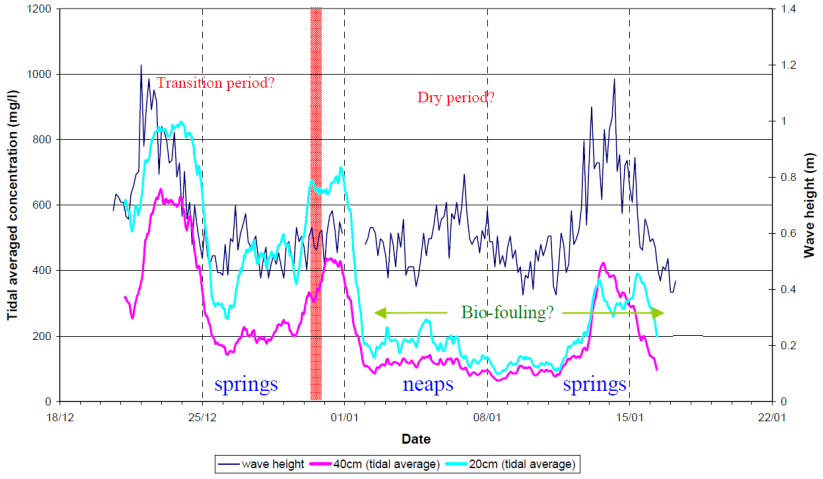

Figure 2.27: Tidally averaged suspended sediment concentration and wave height (LWI, 2012b) at measurement location F

From the given figures it is concluded that the wave heights are important for the sediment concentrations in the lower parts of the water column.

The OBS devices were able to measure sediment concentrations up to around $1-2$ g/l. If sediment concentrations are higher the measurement devices become saturated and an increase in sediment concentration gives lower output values from the OBS devices. It was shown that during a high wave event ($H_s \approx 2.5$ m) the sediment concentration exceeded the maximum measurable turbidity.

Figure 2.28 shows a typical sediment concentration profile at location P2. It is shown that sediment concentrations are highest in the lowest meter of the water column (LWI, 2012b).

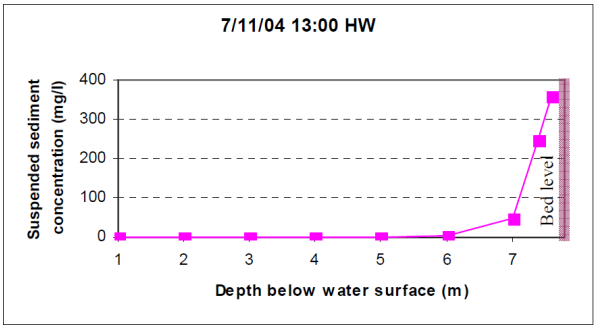

Figure 2.28: Typical sediment concentration at measurement location P2 (LWI, 2012b)

Monthly averaged sediment concentrations for the bottom meter of the water column are shown in Table 2.5. The wet season is characterized by the higher sediment concentrations, in accordance with the larger wave heights in this period.

Table 2.5: Monthly average sediment concentrations in the bottom meter of the water column, values with '*' are linearly interpolated between adjacent values (LWI, 2012b)

Months	Sediment concentration [g/l]
Jan	0.17
Feb	0.10
Mar	0.25
Apr	0.49*
May	0.73
Jun	0.97*
Jul	1.22*
Aug	1.46
Sep	1.62
Oct	1.52
Nov	0.23
Dec	0.30

ROUSE PROFILE

The sediment concentration profile for cohesive sediments are different than for non-cohesive sediments. The equilibrium concentration does not occur in the way it does for sand in the case of cohesive sediments (Winterwerp and van Kesteren, 2004). Because settling velocities for mud suspensions are much lower than for sand, a more uniform concentration profile over the water depth is usually present. Mud suspensions commonly show slow changes due to changes in the flow or wave pattern.

The Rouse profile for fine sediment gives a suspended sediment concentration profile from the balance between the settling flux and turbulent mixing flux of sediment, for equilibrium conditions. Based on the assumption of a logarithmic velocity profile (hence a parabolic diffusivity profile). The turbulent mixing of sediment can be determined by the instantaneous sediment flux in vertical direction. This is given by the following equation (Winterwerp and van Kesteren, 2004):

$$W_s c = -\varepsilon_z * \frac{\partial \overline{c}}{\partial z} = -\frac{\kappa u_*}{\sigma_T} z(1 - \frac{z}{h}) \frac{dc}{dz} \tag{2.1}$$

With W_s = mean settling velocity [m/s], c = suspended sediment concentration [kg/m^3], ε_z = vertical turbulent eddy diffusivity [m^2/s], $\frac{\partial \overline{c}}{\partial z}$ = vertical gradient in sediment concentration [kg/m^2], κ = Von Kárman constant $\approx$ 0.41 [-], u_* = shear velocity [m/s], σ_T = Prandtl-Schmidt number = 0.7 [-], h = water depth [m].

The Rouse number is given by:

$$\beta = \frac{\sigma_T W_s}{\kappa * u_*} \tag{2.2}$$

The sediment concentration profile over the water depth is then given by:

$$c = \overline{c} \frac{sin(\pi\beta)}{\pi\beta} \left(\frac{1 - z/h}{z/h} \right)^{\beta} \tag{2.3}$$

With: $\overline{c}$ = depth averaged sediment concentration [kg/m^3].

Figure 2.29 gives sediment concentration profiles for different Rouse numbers. A high Rouse number represents relatively low shear velocity to settling velocity and represents sediment concentrations typically found for sand. Low Rouse numbers represent relatively high shear velocity to settling velocity, this is typically found for fine sediments.

Based on the Rouse profile a vertically mixed sediment concentration profile would be expected in the project area. As the energetic wave climate causes high shear velocities and the fine sediment causes low settling velocities. However, the measured concentration profiles showed high concentrations near the bed and almost no suspended sediment higher in the water column. This is caused by sediment induced buoyancy effects, which is discussed in the next section.

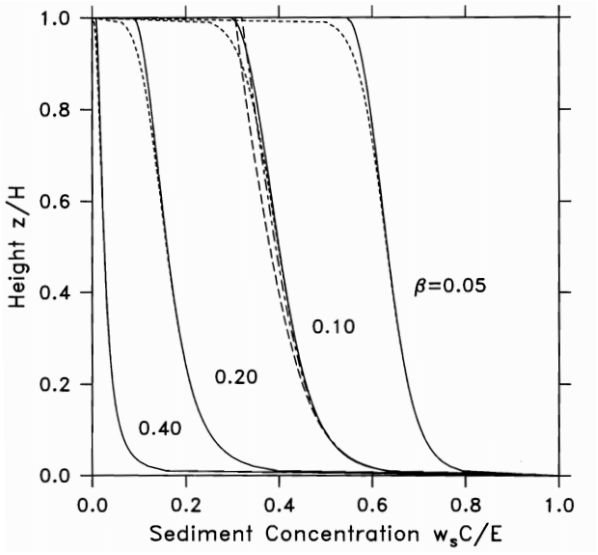

Figure 2.29: Suspended sediment concentration profiles for different values of β, on the x-axis a dimensionless sediment concentration is given in $w_s C/E$, where w_s = settling velocity [m/s], C = sediment concentration [kg/m^3] and E = erosion rate [kg/m^2/s] (Mofjeld and Lavelle, 1988)

SEDIMENT INDUCED BUOYANCY EFFECTS

In the previous section it was stated that a 'regular' sediment concentration for fine sediment does not apply in the considered area. Sediment is concentrated close to the bed instead of mixed over the entire water column, what might be expected for fine sediment. A collapse of the sediment concentration profile may be caused by sediment induced buoyancy effects.

Sediment suspended in the water column can cause a collapse in the concentration profile once the capacity of the flow to keep the particles in suspension is lower than the required capacity to keep the sediment suspended. Sediment starts to settle as a result of this and a fluid mud layer is formed on the bed due to hindered settling of mud particles. This fluid mud layer damps turbulence in the entire water column. The reduced turbulence implies a reduction in the sediment carrying capacity, resulting in a self-reinforcing mechanism (Winterwerp and van Kesteren, 2004).

The flux Richardson number (Ri_f) is defined as the ratio of the buoyancy destruction and production. Once Ri_f reaches a certain critical value ($Ri_{f,cr}$) a collapse of the turbulent field occurs. The flux Richardson number is given by, (Winterwerp, 2005):

$$Ri_f = -\frac{\Delta g \overline{w'c'}}{\rho_m \overline{u'w'} \delta u / \delta z} \tag{2.4}$$

With: u = horizontal velocity [m/s], z = water depth [m], u' = turbulent fluctuation in x-velocity [m/s], w' = turbulent fluctuation in z-velocity [m/s], c' = turbulent fluctuation in sediment concentration [kg/m^3], $\overline{w'c'}$ and $\overline{u'c'}$ = turbulent fluctuations in vertical and horizontal sediment flux respectively, Δ = relative excess sediment density [-], ρ_m = density of water-sediment suspension [kg/m^3].

For specific flow conditions a 'saturation concentration' (C_s) exists for which the critical flux Richardson number is met. Once the depth averaged sediment concentration exceeds C_s the sediment concentration profile collapses and a two layered fluid system is generated with fluid mud being the lower one.

In order to assess the possibility of a collapse in the sediment concentration profile in the project area a relation for the saturation concentration, C_s [kg/m^3], is used from Winterwerp and van Kesteren (2004):

$$C_s = 0.023 \frac{U^3}{W_s} \tag{2.5}$$

With U = depth averaged flow velocity [m/s], h= local water depth [m] and W_s= settling velocity [m/s]. The saturation concentration is calculated for variating settling velocities (0.1 mm/s < W_s < 1 mm/s) as no measured values are available. Figure 2.30 shows the saturation concentration for various settling velocities, depths and flow velocities.

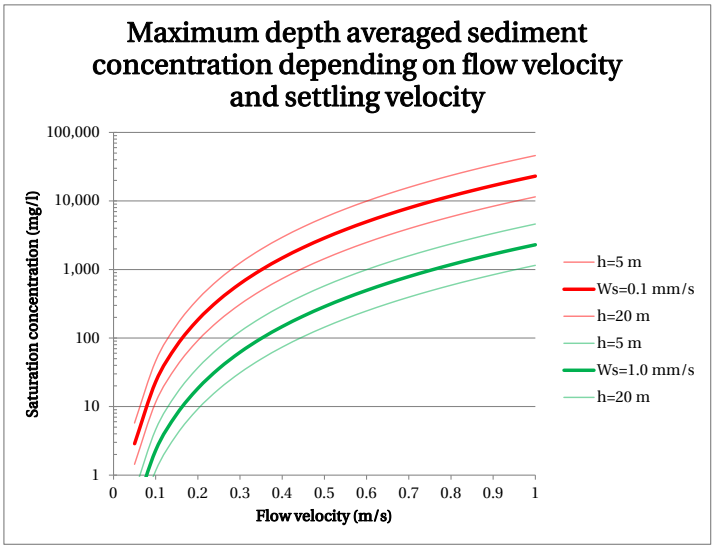

Figure 2.30: Saturation concentration (C_s) for W_s = 0.1 mm/s (red) and W_s = 1 mm/s (green),the solid lines represent h=10 m, the thin lines represent 5 m (top) and 20 m (bottom) water depth, after Bakker (2009)

From Figure 2.30 it is concluded that the low flow velocities in the project area in the range of 0−0.4 m/s are not capable of keeping sediment suspended for concentrations above 1,000 mg/l and a collapse of the sediment concentration profile would occur. This mechanism is held responsible for the sediment concentration profiles that show typically no sediment in the upper part of the water column and high concentrations near the seabed.

The energetic wave conditions cause a larger capacity to erode sediment from the bed than the available capacity to keep sediment suspended by the flow velocities.

The measured sediment concentration profiles showed sediment suspended in the bottom meter with average concentrations of 1 g/l. According to Figure 2.30 a collapse in the sediment concentration profile should occur for the low flow velocities as measured in the bottom region of the water column as well. A reason for the suspended sediment concentration that is not collapsed could be the settling velocity of the sediment. In the MSc. Thesis of Bakker (2009) it was suggested that very low settling velocities of the sediment were present as is discussed before. It is expected that the turbulence by wave action is not entirely damped

and some vertical mixing still occurs in the bottom part of the water column, keeping sediment suspended in the bottom meter.

High concentration events During the measurement campaigns sediment concentrations were found in excess of the common observed concentrations (in the order of 1 g/l). A few grab samples show sediment concentrations in the range of 30 – 60 g/l, however not found at the location of the dredged area, but (1 km) closer to the Estuary entrance. According to LWI (2012b) these high concentrations are caused by rapid settling of sediment supplied by the Estuary or from wave fluidization of bed material. In Section 3.3 the formation mechanisms of fluid mud are further treated.

2.4.4. SEDIMENT TRANSPORT MECHANISMS

Following from the analysis of the Estuary and coastal hydrodynamic and morphologic regimes. Two main sediment transport mechanisms are identified for causing infill in the dredged channel, in accordance with analyses from LWI:

1. Sediment (re-)supplied by the Estuary;
2. Residual Westerly near bed current transporting wave eroded material.

Sediment (re-)supplied by the Estuary As was shown in Section 2.2.2 sediment concentrations tend to vary strongly as a result of fluctuating tidal discharges through the Estuary entrance. It is expected that sediment discharged by the Estuary is able to reach the dredged channel in suspension if tidal currents are strong enough to keep the sediment suspended. However, due to the complex nature of the hydrodynamic regime it is unknown which proportion of sediment is able to be transported far enough to cause sedimentation of the dredged channel. Stratification effects could cause significant impact on the sediment transport in the Estuary area. 3D sediment transport modeling should be performed in order to describe the morphologic behavior around the Estuary in more detail.

The formation of a high concentrated layer as was found by LWI, is thought to be (potentially) generated by rapid settling of high concentrations from the Estuary. Additionally, wave fluidization of sediment depositions outside the ebb tidal bar is suggested as a second mechanism for the formation of high concentration layers. The formation and behavior of high concentration layers is further elaborated in Chapter 3.

Residual Westerly near bed current The sediment concentration measurements show that wave action is of significant influence on the sediment concentration. The residual flow in Western direction caused by either stratification due to fresh water outflow of the Estuary or the Guinea undercurrent transports the suspended sediments towards the dredged area and could thereby cause significant infill. In Chapter 3 the sediment flux by this mechanism is estimated using data from the measurements by LWI.

2.5. EARLIER INFILL STUDIES

Earlier findings from research done by LWI and EGSi to determine the sediment infill are summarized in this section. A more extensive review of the earlier infill studies is provided in Appendix B. A trial pit experiment was conducted to estimate the infill rates and consolidation behavior of the mud infill. The results of this experiment are found in the confidential appendix and is not publicly available.

2.5.1. SEDIMENT TRANSPORT MODELING

In order to estimate the infill of the dredged area, multiple modeling assessments have been undertaken by LWI and EGSi. In 2003, 2004, 2005 and 2006 hydrodynamic and sediment transport models were executed. The earlier models were done with a different layout of the offshore terminal as the design was changed to reduce the offshore pipeline length.

The "Dredging and Offshore Sand Winning Databook" (LWI, 2012b) presents the final infill calculation results. As all available measurement data was used in the latest model calculations these are assumed to be the most accurate for the current project layout. However, for the infill due to fluid mud the results from fluid mud transport modeling was extrapolated from a previous channel configuration. The calculated total annual infill rate is highly variable and a wide probability range is given by LWI, see Table 2.6. The best estimate of the total annual infill is 10 M m^3 per year.

A distribution of the infill over the dredged area was made by LWI as well, the maneuvering area and the first 2 kilometers of the approach channel have the largest infill rates due to the Estuary discharge. The remaining part of the approach channel experiences almost exclusively infill from Westward sediment transport. An overview of the sediment infill distribution is given in Figure 2.31.

It was concluded that 70 % of the annual infill occurs during August - November, as a result of larger Estuary discharges as well as a combination of higher waves and stronger bottom currents. The other 30 % occurs during the rest of the year.

Table 2.6: Annual sediment infill with probability intervals (LWI, 2012b)

Volume (M m^3)		
P10	P50	P90
5	10	15

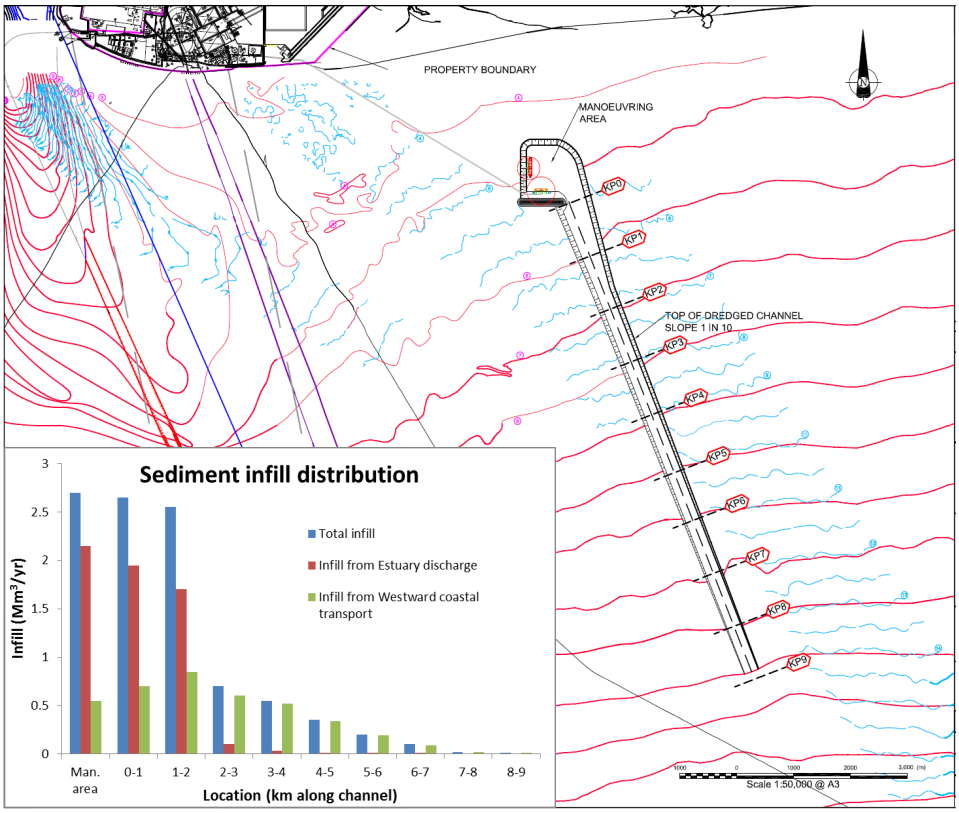

Figure 2.31: Infill sources of harbor basin and approach channel (LWI, 2012b)

2.6. CONCLUSION

This chapter achieves the first sub-objective by describing the local system. The chapter forms a basis for the understanding of the processes that are of influence on the infill of the dredged channel. The system description is divided into its hydrodynamic characteristics and its morphological characteristics.

2.6.1. HYDRODYNAMIC CHARACTERIZATION

The hydrodynamic characterization shows that the project area is located in a complex hydrodynamic system. The Estuary influences the local coastal system to a large extend. Fresh water discharge through the Estuary entrance cause stratification and varying tidal velocities in the project area. The Estuary is classified as mixed and estuarine circulation is expected to take place as a result of the horizontal stratification.

A strong seasonal variation in currents, wind and waves is observed. A distinction is made between the local meteorological wet season that extends from May to October and the Estuary fluvial wet season from August to November.

Figure 2.32 shows a schematic overview of the hydrodynamic processes. The most important processes that determine the hydrodynamic system and their variability are shown in the list below:

1. Bathymetry;

   The project area is located in the Niger Delta, the large scale bathymetry is characterized by a short continental shelf of around 50 - 65 km. The slope of the seabed in the area of the dredged channel is gentle with a typical slope of 1:1000, indicating fine sediment. The depth contours are generally parallel to the coast, except for the ebb tidal bar at the Estuary entrance.

2. Tidal forcing [spring/neap];

   As a result of the narrow continental shelf, the tidal currents are North/South directed along the Southern Niger Delta coast. The tidal ranges in the project area vary between approximately 1-2 m during neap and spring cycles respectively. Due to the Estuary tidal discharge, flow velocities are larger in the vicinity of the Estuary entrance. The dredged channel is located in an area where the influence of the Estuary is present, depth average tidal currents are estimated to be around $0.15 - 0.3$ m/s from measurement data.

3. Current profile [wet/dry];

   A complex 3D current profile is observed. Residual flow velocities in the top part of the water column are oppositely directed to the near bed flow. This is thought to be caused by stratification, large scale ocean currents and wind induced currents. Residual surface currents are predominantly directed in Eastward direction and bottom flows are generally Westward. A seasonal variation for wind induced currents is observed as wind speeds are lower during the dry season (< 3.5 m/s) and larger during the wet season (< 5 m/s). The bottom residual flow velocity in Westward direction is expected to be important for sediment transport, and is generally in the order of 0.05 m/s.

   The cross shore horizontal gradients in stratification are expected to cause bottom currents in shoreward direction. The bottom current is particularly important for the residence time of sediments in the coastal system.

4. Waves [wet/dry].

   A typical swell wave climate is present with a very strong seasonal variation but consistent South to South-South-West direction. Waves are commonly higher during the wet season (mean $H_s \approx 1.5$ m) than during the dry season ($H_s < 1$ m). Wave induced shear stresses are important for the sediment transport as the fine sediments in the near-shore area are easily eroded. Wave induced longshore currents in Eastward direction are important for transport of sand along the coast, which is not further considered in this report.

5. Estuary [wet/dry, spring/neap];

   The Estuary discharge depends on the tide and river discharge rates. Peak ebb discharges reach up to $37,000$ m^3/s with associated flow velocities in the river mouth up to 2.5 m/s. Peak flood discharges tend to be lower than ebb discharges and have been observed up to $25,000$ m^3/s. The River freshwater discharge fluctuates strongly over the year, however only limited data is available on the freshwater

discharge. The fresh water discharge is around 8 % of the total Niger River discharge and therefore estimated to vary between 180 m^3/s and 1,800 m^3/s.

Figure 2.32 shows a schematic overview of the hydrodynamic system

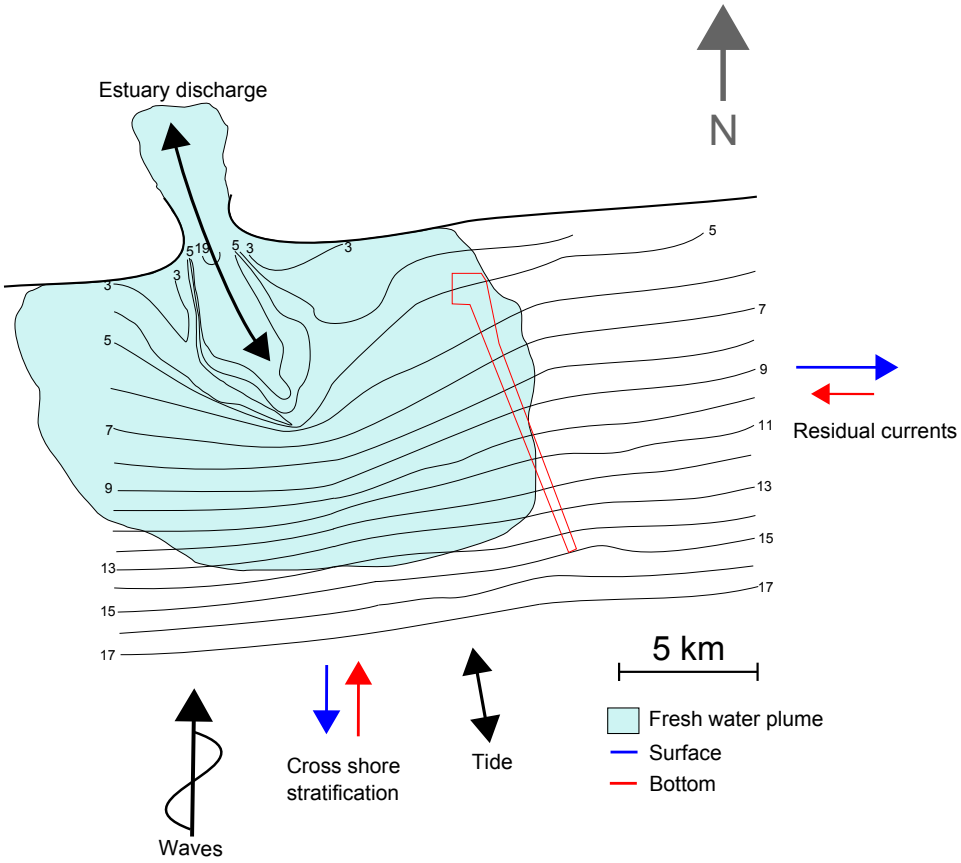

Figure 2.32: Overview of dominant hydrodynamic processes, red arrows show bottom currents, blue arrows show surface currents

2.6.2. MORPHOLOGICAL CHARACTERIZATION

The morphological site characterization consists of the sediment properties, sinks and sources and sediment transport processes. Figure 2.33 shows an overview of the morphologic site characterization. The most important characteristics of the morphological system are listed below:

1. Sediment properties

   The consolidated seabed offshore of around 5.5 m LAT consists of mud, whereas the ebb tidal bar, shallower areas and the shoreline consist of sandy material.

2. Residual transport of fine sediment;

   The Westward undercurrent in the coastal region transports wave eroded suspended fine sediments in Westward direction. Sediment is concentrated in the bottom meter of the water column as a result of sediment induced buoyancy effects. During the wet season higher waves cause increased sediment concentrations. The higher concentrations in combination with stronger residual currents cause sediment transport rates to be significantly larger during the wet season.

3. Estuary sediment supply/resupply;

   Sediment from the River enters the Estuary and is then supplied to the coastal system. Due to the tidal fluctuating flows in the Estuary, sediment re-enters the Estuary during flood tides. Therefore no continuous supply of sediment from the Estuary takes place. Sediment is eroded by waves in the coastal zone as well and transported to the Estuary by stratification induced currents.

Sediment concentrations in the Estuary entrance fluctuate with tidal flows and show typically high concentrations during wet spring tides. Under average tidal amplitudes, the Estuary is expected to import sediment, whereas during spring tides the Estuary is expected to export large amounts of sediment.

4. Fluid mud;

   Fluid mud was observed in the area between the ebb tidal bar and the proposed channel. Infill from fluid mud could be significant if it is able to reach the proposed channel. The frequency and magnitude of occurrence of the fluid mud layer is uncertain due to limited data. In the next chapter this will be further discussed.

5. Cross shore transport due to stratification circulation;

   Due to the cross-shore stratification driven shoreward bottom current, sediment is kept longer in the coastal area (long residence time). This effect is expected to be more pronounced during the wet season as a result of larger gradients in salinity.

6. Longshore transport of sand along coast and tidal bar.

   Due to the South to South-South-West originated waves, the wave driven longshore transport of sand is Easterly. Sand is transported from the Western coast along the ebb tidal bar and eventually reaches the Eastern coast.

Figure 2.33 shows a schematic overview of the morphologic characteristics of the considered system.

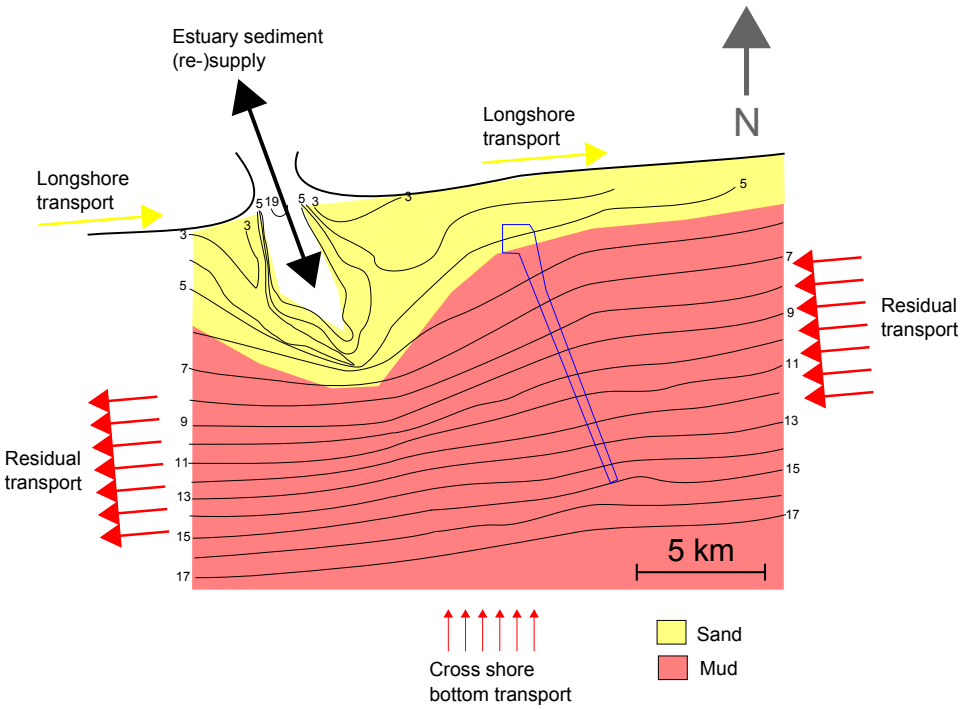

Figure 2.33: Overview of dominant morphologic processes

Chapter 3 discusses the dominant morphological processes in more detail. Available literature as well as numerical sediment transport modeling are used to obtain qualitative and quantitative sediment transport rates to asses the relative importance of the different morphological processes.

3

ANALYSIS OF DOMINANT MORPHOLOGICAL PROCESSES

In this chapter the dominant morphological processes are analyzed. The analysis provides a detailed overview of the main sediment transport fluxes in the coastal system, based on earlier studies by LWI and numerical modeling with the Delft3D software package. This chapter aims to achieve sub-objective 2 by providing qualitative and quantitative estimates on the sediment transport processes.

The two main morphological processes that were identified in Chapter 2 are the residual Westward sediment transport and Estuary sediment (re-)supply. Three transport modes are considered from these two main morphological processes.

- Saturated sediment concentration conditions cause relatively high concentrations near the bed, that are transported by residual near bed currents;
- Suspended sediment in sub-saturated conditions are transported to the proposed channel by Estuary tidal discharge;
- Fluid mud formed in the coastal area flows under the influence of tidal currents and gravity towards the proposed channel.

First the residual Westward transport of sediment is quantified using measured data and earlier findings. Secondly, the Estuary sediment supply is analyzed using Delft3D model software. Thirdly, the formation of fluid mud in the coastal system is discussed.

This chapter should provide information on the main sediment infill mechanism, such that solutions can be established to limit the sediment infill.

3.1. RESIDUAL TRANSPORT

The residual transport of sediment is considered as one of the main sediment fluxes in the project area. It is found in Chapter 2 that (fine) sediment transport in the coastal area is directed towards the West (LWI, 2012b). In earlier studies by LWI it was assumed that the large scale ocean current is responsible for the residual transport, this will be treated in more detail in Section 3.2.2. Seasonally varying wave heights and flow velocities are found that cause the residual transport to be larger during the wet season.

Two approaches are applied to estimate the sediment supply by the Westerly residual near-bed current. The first approach uses sediment fluxes calculated by LWI, whereas the second approach uses measured sediment concentrations and flow velocities directly. Both approaches assume that all sediment transported in Westward direction is intercepted by the channel. Therefore all Eastward transport is assumed to be originated from the Estuary and is not considered in these calculations.

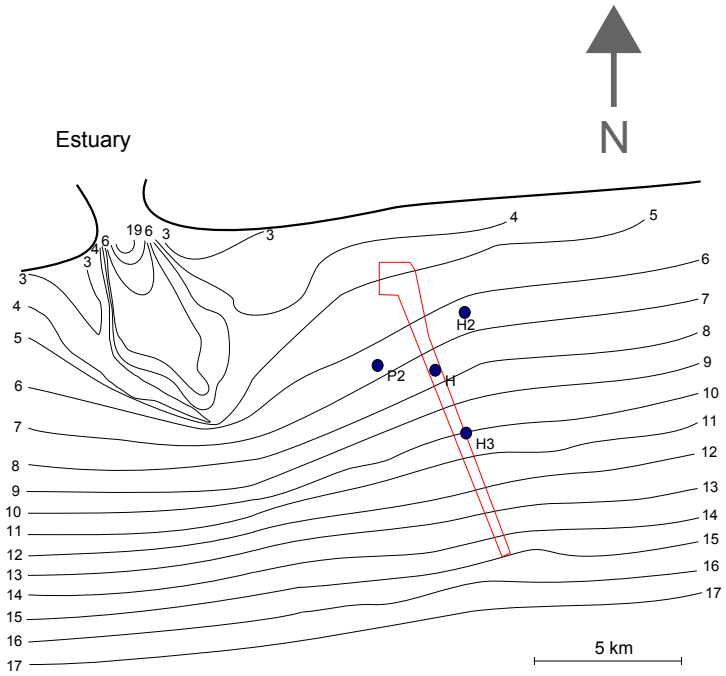

Figure 3.1: Residual transport and measurement locations used for flux calculations (LWI, 2012b)

3.1.1. FIRST APPROACH

Sediment fluxes were determined by LWI by integrating the flow velocities and associated OBS derived suspended sediment concentrations over the bottom meter as shown in Section 2.4. The measurement locations for the sediment fluxes are P2, H, H2 and H3 shown in Figure 3.1. LWI assumed that the fluxes measured at the different locations apply for the whole area occupied by the approach channel and maneuvering area. The sediment infill in the dredged channel is assumed to be equal to the gross transport from the East. Thus, a 100 % trapping efficiency of the channel is assumed.

The gross monthly average sediment fluxes are shown in Table 3.1. For April, June and July no data is available, these values are found by linear interpolation between the adjacent values. The sediment supply caused by Westward residual transport is calculated by multiplying the sediment flux [kg/m/day] by the total North-South distance of the channel, approximately 9,000 m. The annual sediment supply is calculated from the fluxes in Table 3.1 by multiplying the mean daily flux by 365 days, resulting in a gross sediment flux in Westward direction of around $2 * 10^9$ kg/year.

Table 3.1: Monthly averaged gross Western flux in kg/m/day, values with '*' are linearly interpolated between adjacent values LWI (2012b)

Month	Western flux [kg/m/day]
Jan	73
Feb	43
Mar	83
Apr	387*
May	691
Jun	973*
Jul	1254*
Aug	1536
Sep	894
Oct	581
Nov	147
Dec	147

LWI combined Western, Northern and Southern fluxes to estimate the total infill of the approach channel

and maneuvering area. The amount of infill determined by LWI based on all the sediment fluxes is $4 * 10^6$ m^3/year with a density of 400 kg/m^3, hence $1.6 * 10^9$ kg/year. A reduction of sediment infill due to wave sheltering caused by the construction of the dredged works and breakwater is estimated to reduce the amount of infill by $3 * 10^6$ m^3/year or $1.2 * 10^9$ kg/year (LWI, 2012b). This would suggest that almost half the measured flux will reach the dredged channel due to the wave sheltering effect. No calculations are provided to determine the wave sheltering effect by LWI and therefore it is assumed that this is a rough estimate. A second approach is used to come up with another estimate for the total Westward residual sediment flux based on measured concentrations and flow velocities.

3.1.2. SECOND APPROACH

This approach uses the monthly averaged sediment concentrations measured by LWI that were used to calculate the fluxes in the first approach directly. The concentrations are combined with velocity measurements taken from the same locations and averaged per meteorological season. Only data of Westward directed flow is used and the data is taken representative for the entire channel length.

Table 3.2 shows the measured average concentrations per month and the measured flow velocities in the bottom half of the water column, averaged per season.

Table 3.2: Monthly average sediment concentrations in the bottom meter (C) and mean residual flow velocities in the bottom half of the water column (u), values with '*' are linearly interpolated between adjacent values (LWI, 2012b)

Months	C [kg/m^3]	u [m/s]
Jan	0.17	0.03
Feb	0.10	0.03
Mar	0.25	0.03
Apr	0.49*	0.03
May	0.73	0.08
Jun	0.97*	0.08
Jul	1.22*	0.08
Aug	1.46	0.08
Sep	1.62	0.08
Oct	1.52	0.08
Nov	0.23	0.08
Dec	0.30	0.03

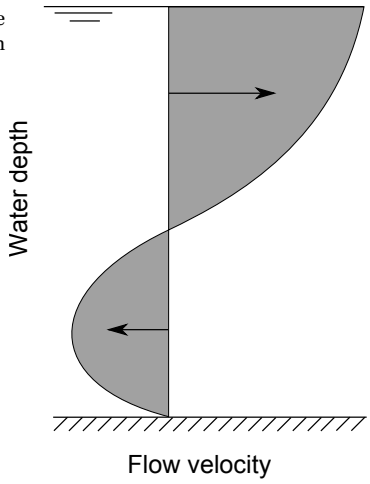

Figure 3.2: Schematized vertical velocity profile

The sediment concentrations represent mean values over the bottom meter of the water column whereas the flow velocity measurements are averaged values over the bottom half of the water column. The flow velocities in the bottom meter are probably lower than the average flow velocity over the bottom half of the water column as a flow profile as shown in Figure 3.2 is expected. The velocity in the bottom meter of the water column is taken as 50 % of the average flow velocity in the bottom half of the water column. Table 3.3 shows the results of this approach. Combining the fluxes for each month a sediment supply of $7.80 * 10^9$ kg/year is found. This estimation is thus larger than the calculated supply with approach 1, but within the same order of magnitude.

Daily fluxes show large differences between the dry and wet season. Daily fluxes in the wet season can go up to 5,000 kg/m/day. This would lead to total infill rates of 100,000 m^3/day on average during three wet season months. This is a significantly larger amount than the estimates by LWI. During high wave events the concentrations might be higher than the monthly averaged and daily fluxes can then be even significantly larger.

Table 3.3: Monthly mean sediment concentration (C) and residual current (u) in bottom meter and resulting Westward sediment flux

Month	C [kg/m^3]	u [m/s]	Flux [kg/m/day]
Jan	0.17	0.015	218
Feb	0.10	0.015	129
Mar	0.25	0.015	330
Apr	0.49	0.015	635
May	0.73	0.04	2506
Jun	0.97	0.04	3357
Jul	1.22	0.04	4207
Aug	1.46	0.04	5057
Sep	1.62	0.04	5609
Oct	1.52	0.04	5236
Nov	0.23	0.04	806
Dec	0.30	0.015	392

3.1.3. DISCUSSION

Two approaches were applied to find sediment fluxes based on data from LWI, the first approach used the sediment fluxes already calculated by LWI whereas the second approach used measured sediment concentrations and flow velocities directly. The first approach resulted in a sediment supply of roughly $2 * 10^9$ kg/year compared to roughly $8 * 10^9$ kg/year by the second approach. LWI estimated significantly lower sediment transport as a result of the wave reduction by the proposed channel. This effect is not taken into account in this study, as the existing flux from the residual current is compared to the existing flux from the Estuary. In the second approach it was assumed that the Westward residual flow is constant at half the flow velocity measured in the bottom meter, which might not be the case as not all velocity measurements showed the Westward residual current. The total flux from the residual transport is estimated to be around $4 * 10^9$ kg/year, which is equivalent to approximately 10 million m^3 (for a density of 400 kg/m^3).

A strong seasonal difference is observed, the wet season accounts for 90 % of the total flux due to the higher waves and higher residual flow velocities. It is expected that sediment concentrations are higher in the near-shore zone and lower in the offshore zone due to the difference in wave induced bed shear stress. If the ocean current is the driving factor for the Westward current it is expected to be stronger in deeper water, however this is not shown clearly in the measurements.

Daily mean fluxes in the peak wet season months (August, September and October) are estimated around 2,500 kg/m/day and during the dry season the mean fluxes are around 10% of this. Daily maximum fluxes can be significantly larger than the mean values during extreme wave events. The limited amount of measurements result in uncertainty of the calculated fluxes, and therefore the values are a rough estimation. Because the sediment concentrations are found to be highest in the bottom meter a trapping efficiency of the channel of 100 % is found plausible. The infill during the wet season would be around 0.75 m per month for a density of 400 kg/m^3.

3.2. DELFT3D MODELING

This section treats the numerical modeling of the local hydrodynamics and sediment transports using the Delft3D software package. The main goal is to simulate the sediment transport from the Estuary in order to assess the relative contribution of the Estuary on the infill of the dredged channel. Additionally the effect of stratification on the flow profile and the residual transport are analyzed.

3.2.1. MODEL SET-UP

A model is set-up with the process-based Delft3D sediment transport model software. The main processes that are incorporated in the model are hydrodynamic forcing, salinity and sediment transport. As is discussed in Chapter 1, non-cohesive sediment is not taken into account in this research. The detailed model set-up is given in Appendix C.

DOMAIN AND GRID

The model domain extends for around 40 km in shore parallel direction, with the Estuary entrance just West of the center of the model. The offshore model domain extends roughly 25 km to the 30 m depth contour

and the inland model domain extends to roughly 30 km inland. Due to the expected importance of salinity, the model is set-up in 3D. 10 computational layers are used in the vertical, with higher resolution near the bed (layer 1 = top layer and layer 10 = bottom layer). Figure 3.3 shows the model grid and bathymetry, the dredged channel is not present in the bathymetry as the model is used to understand the existing behavior of the area and would require a finer computational grid to model sediment infill of the channel. Additional storage areas are introduced to the model grid to increase the tidal prism to represent the discharges through the Estuary mouth more accurately.

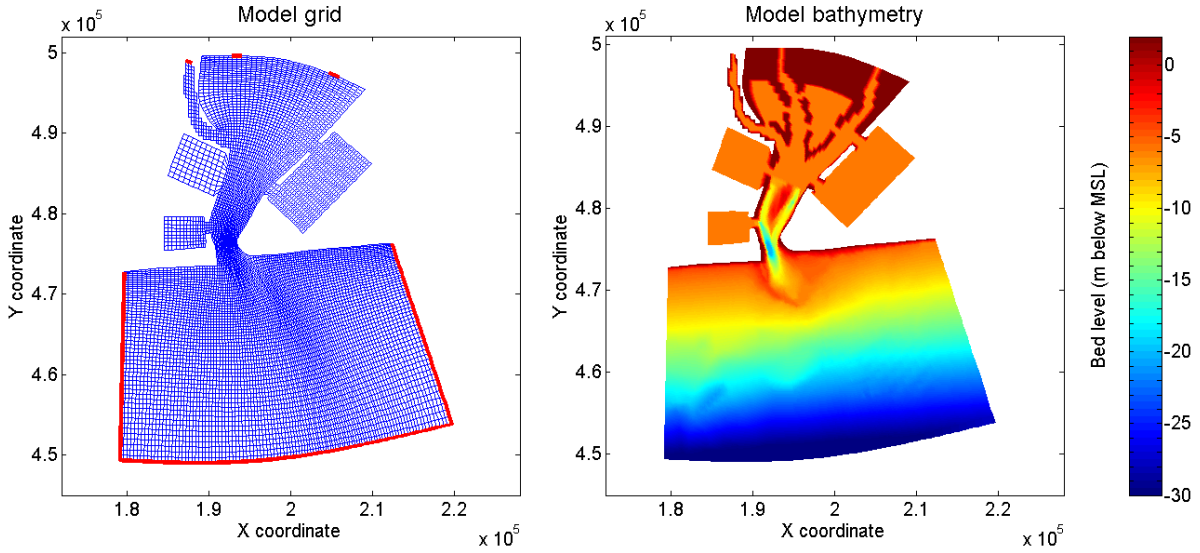

Figure 3.3: Model grid with open boundaries (left) and model bathymetry (right)

BOUNDARY CONDITIONS

The offshore (coast parallel) boundary condition consists of tidal water levels. These are obtained from the TOPEX/POSEIDON global tide model. The cross-shore boundaries consist of Neumann water level conditions. The inland boundaries are the fresh water inflow from the three branches of the River entering the Estuary. The fresh water inflow during the dry season is taken as 600 m^3/s and during the wet season 1,800 m^3/s. These values were used in the model studies by LWI (2006a) as well.

SEDIMENT AND MORPHOLOGY

The inner Estuary bed in the model consists of a layer of cohesive sediment which is brought in suspension by to the tidal flows in the Estuary. In the Estuary entrance no sediment is applied on the bed as this part consists of sandy material which is not considered in this report Fugro (2006). The sediment fraction of the river bed has a constant settling velocity of $W_{s,r} = 0.2$ mm/s and a critical shear stress for erosion $\tau_{c,r} = 0.3$ N/m^2.

Another sediment fraction is applied in the coastal region, as sediment in saline water is expected to show different behavior than sediment from the Estuary. The coastal sediment fraction has a higher settling velocity due to flocculation ($W_{s,c} = 0.75$ mm/s) and a higher critical shear stress for erosion ($\tau_{c,c} = 0.5$ N/m^2).

3.2.2. HYDRODYNAMIC MODEL RESULTS

The model output for the hydrodynamic forcing are treated in this section. Only the relevant results are shown, the more detailed output is found in Appendix C.

TIDAL FORCING

The modeled water levels in the Estuary entrance over a three month period are shown in Figure 3.4. The tidal ranges show to be within the same range as the long term tidal record taken by LWI shown in Figure 2.15.

The flow velocities with respect to water levels in the Delft3D model show a typical standing wave pattern. There are no measurements on water levels and associated velocities or discharges to verify the phase difference between the two.

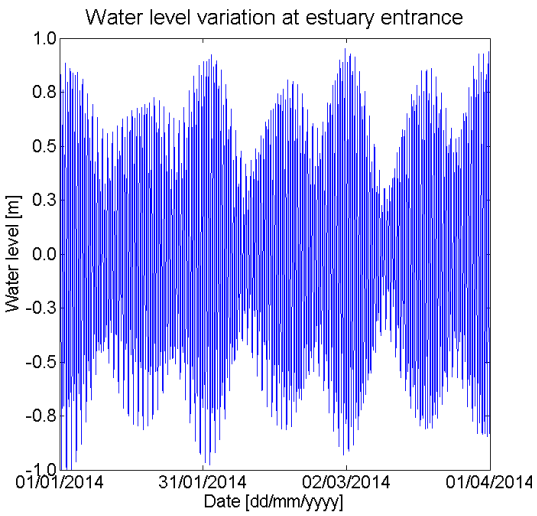

Figure 3.4: Tidal water level variation in Estuary entrance from Delft3D model

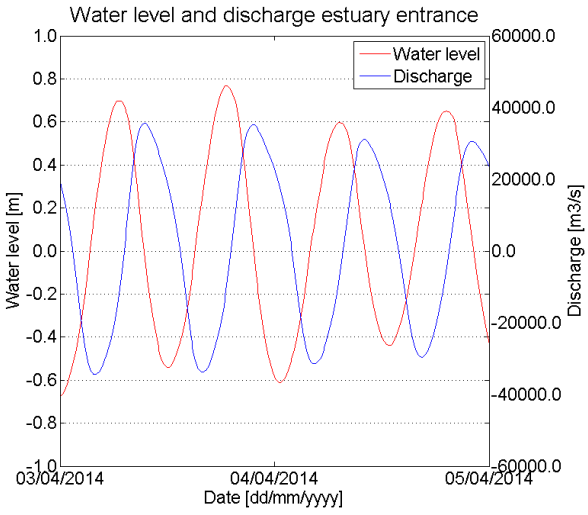

Figure 3.5: Tidal water level variation (red) and discharge (blue) in Estuary entrance from Delft3D model.

In the measurements it was shown that flood tidal discharges were lower than ebb tidal discharges, however it is unknown what causes this effect as the difference is significantly larger than the River fresh water discharge. In the Delft3D model the difference in tidal discharges through the Estuary entrance are smaller than measured, and therefore the flood tidal discharge rates are somewhat overestimated in the Delft3D model.

The depth averaged maximum eb and flood flow field in the area of the Estuary entrance and the dredged channel for a mean tidal range is shown in Figure 3.6. The flow velocities are highest in the area of the Estuary entrance and decrease strongly behind the ebb tidal bar.

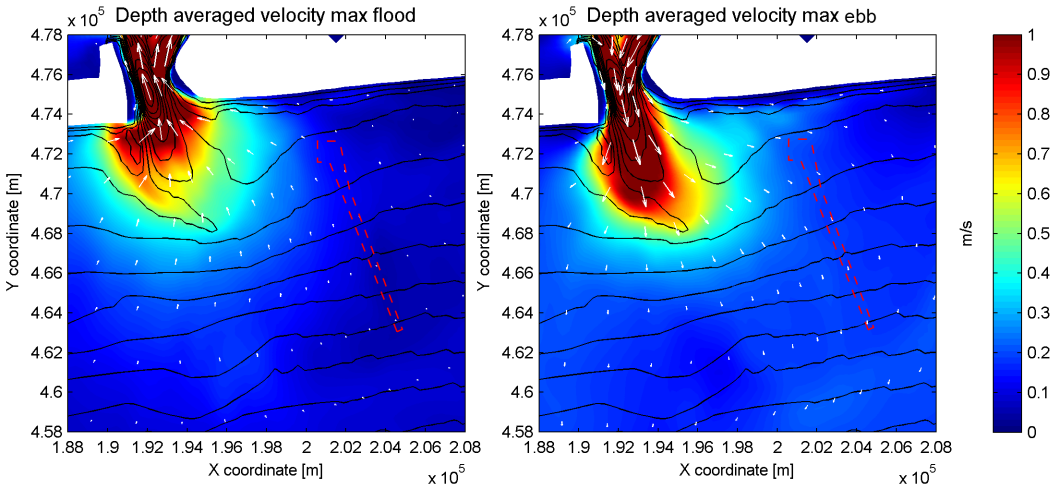

Figure 3.6: Depth averaged velocity pattern at max ebb and max flood discharge during a mean tide, with indicated dredged channel. Flow velocities around the Estuary entrance exceed 1 m/s.

CURRENT ELLIPSES

Tide-averaged current ellipses from the Delft3D model in the area of the proposed channel are shown in Figure 3.7, fresh water discharge from the Estuary is included in the model results used for these figures. The black lines show the depth averaged ellipses and the colored lines the ellipses for different layers in the water column taken from a single tidal cycle during a mean tide in the wet season. The depth averaged velocities show relatively neat ellipses, whereas the separate layers show a more irregular pattern. A highly complex flow field is present with large differences over the vertical. The current ellipses show that closer to the shore the velocities are directed more towards the Estuary and therefore the flow becomes more shore parallel. The offshore flow velocities are smaller in magnitude and show a more cross shore profile, as these are less influenced by the Estuary discharge. Depth averaged flow velocities at the channel are directed parallel to the channel.

The near-bottom layer (green) ellipse is tilted counter-clockwise compared to the depth averaged ellipse. The flow velocities in this layer are therefore directed more shore-parallel. A residual flow in North-Westward direction is found in the bottom layer, whereas the top layer shows constant positive X-directed flow velocities and hence an Eastward residual current.

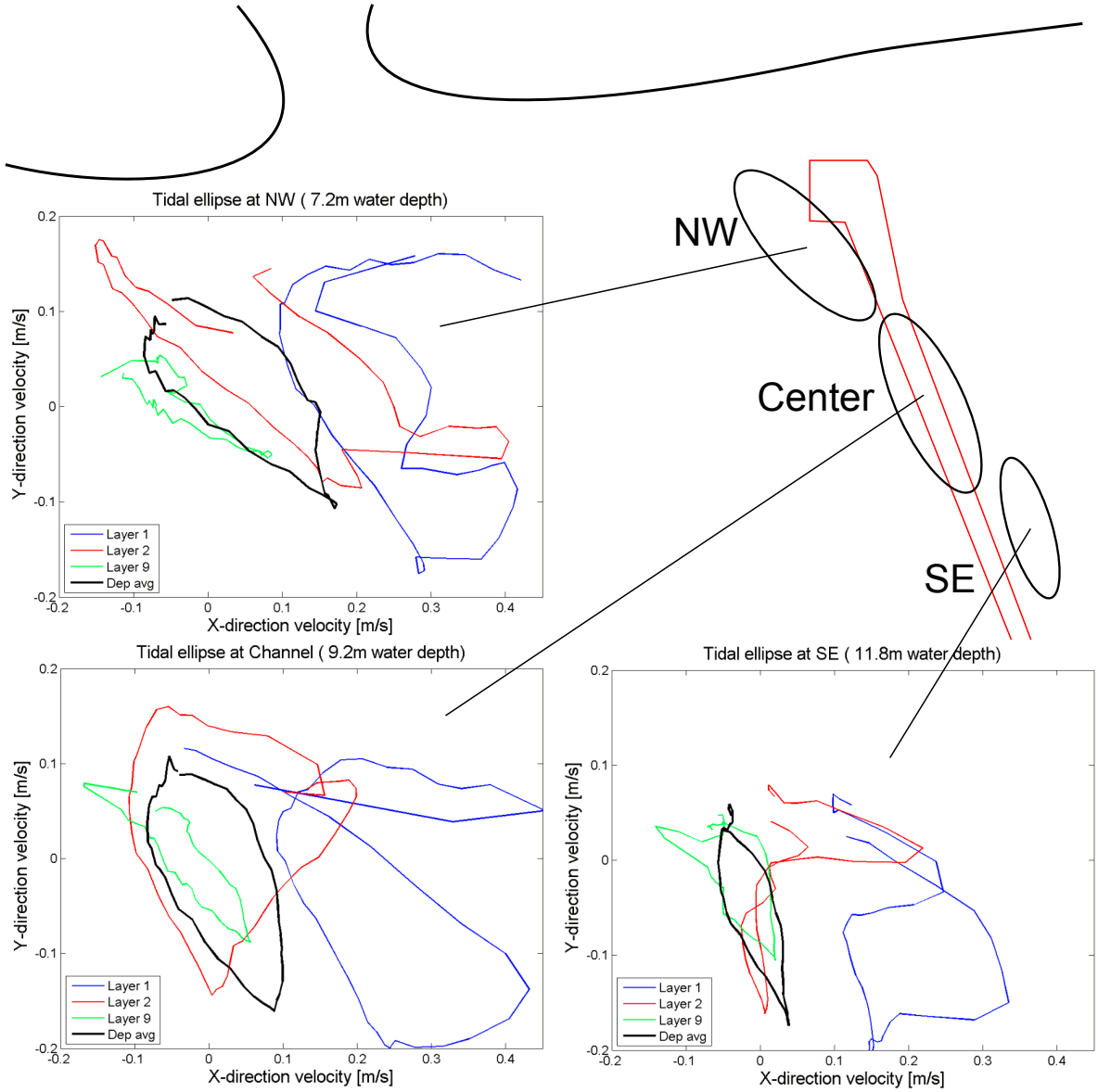

Figure 3.7: Tide-averaged current ellipses at different locations in the dredged channel area: black = depth averaged, blue = layer 1 (water surface), red = layer 2 and green = layer 9 (near-bed)

FLOW VELOCITY PROFILE

Figure 3.8 shows the flow velocity in Westward direction with accompanying water level for the channel center. Flow velocities in the top part of the water column show a net flow in Eastward direction. In the bottom part of the water column, the flow is directed in Westward direction. This flow direction change between the upper and bottom part of the water column was measured by LWI as well.

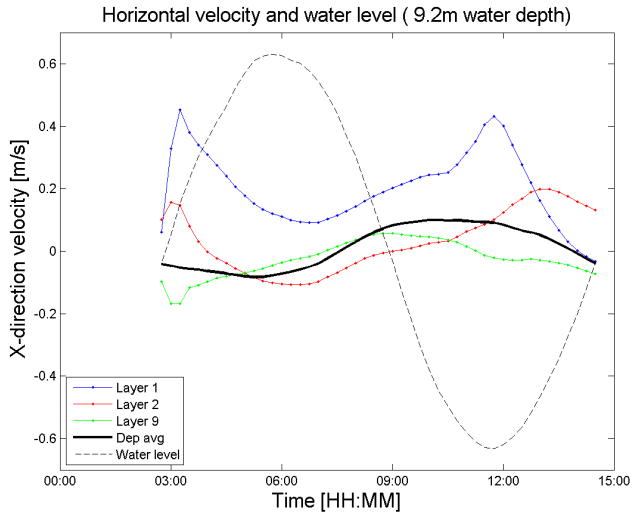

Figure 3.8: Center channel water level (dashed line) and flow velocity in x-direction: black = depth averaged, blue = layer 1 (water surface), red = layer 2 and green = layer 9 (near-bed). Positive x-direction is Eastward.

The tide averaged flow velocities over the water depth in ebb direction are shown in Figure 3.9. These are taken at the same locations as the tide-averaged current ellipses of Figure 3.7. Opposite directed net flow velocities in the upper and bottom parts of the water column are shown. The flow direction seems to change at around half the water depth. The residual Westward current is not incorporated in the model as a separate boundary condition, therefore it is interesting to see that a near bed residual flow occurs nevertheless. This would suggest that stratification is (at least partly) responsible for the measured Westward residual current in the project area. The order of magnitude of the near bed residual current is similar to the measured flows of several cm/s.

LWI concluded that the measured residual flow is driven by the large scale (geostrophic) ocean currents. However, from the Delft3D model results it is found that the measured residual flow could also be driven by stratification effects. Current measurements were only conducted by LWI on the Eastern side of the ebb tidal bar, therefore it is not verified whether the Westward residual current persists further along the coast in Westward direction. It is plausible that the residual currents are (partly) caused by stratification.

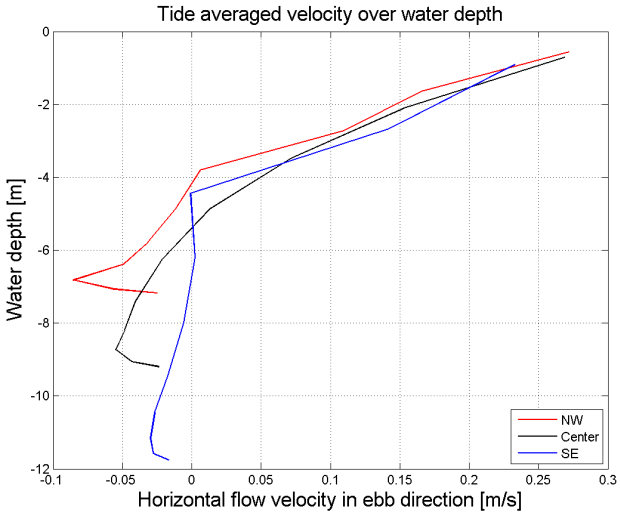

Figure 3.9: Tide averaged velocity at same locations as figure above.

SALINITY

The salinity in the project area fluctuates due to tidal discharges and seasonally varying fresh water supply. During the dry season, when fresh water discharge is low, the salt intrusion limit in the Estuary and River is located more inland than during the wet season when the fresh water supply is significantly larger. Figure 3.11 shows the salinity profile from the Delft3D model along a transect from 15 km upstream the Estuary to 5 km outside the ebb tidal bar at low water, shown in Figure 3.10. During spring tides, the salinity profiles are shown to be the most vertically mixed whereas during lower tidal ranges the horizontal mixing is reduced and a more vertically stratified profile occurs.

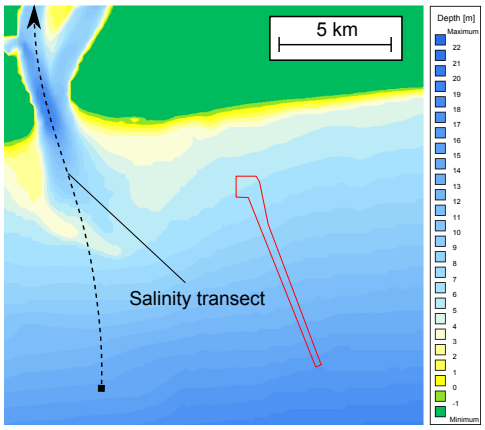

Figure 3.10: Salinity transect used in figure 3.11

An estuarine turbidity maximum (ETM) is typically formed around the salt intrusion limit (Park et al., 2008), therefore the ETM is expected to be located further inland during the dry season. During the wet season the salt intrusion limit will be located closer to the Estuary entrance. During high discharge events it is plausible that the ETM reaches the Estuary entrance and cause high sediment concentrations in the Estuary entrance.

Sediment in the estuarine turbidity maximum is commonly mixed during the flood tide due to the higher shear stresses at the bed as a result of the salt water intrusion from below. It is expected that sediment in the turbidity maximum region is mixed by ebb tidal flows during high discharge events as well, similar to the vertical mixed profile of the salinity. Whereas normally, ebb tidal currents might not be strong enough to mix the sediment in the turbidity maximum region over the entire water column. As the estuarine turbidity maxi-

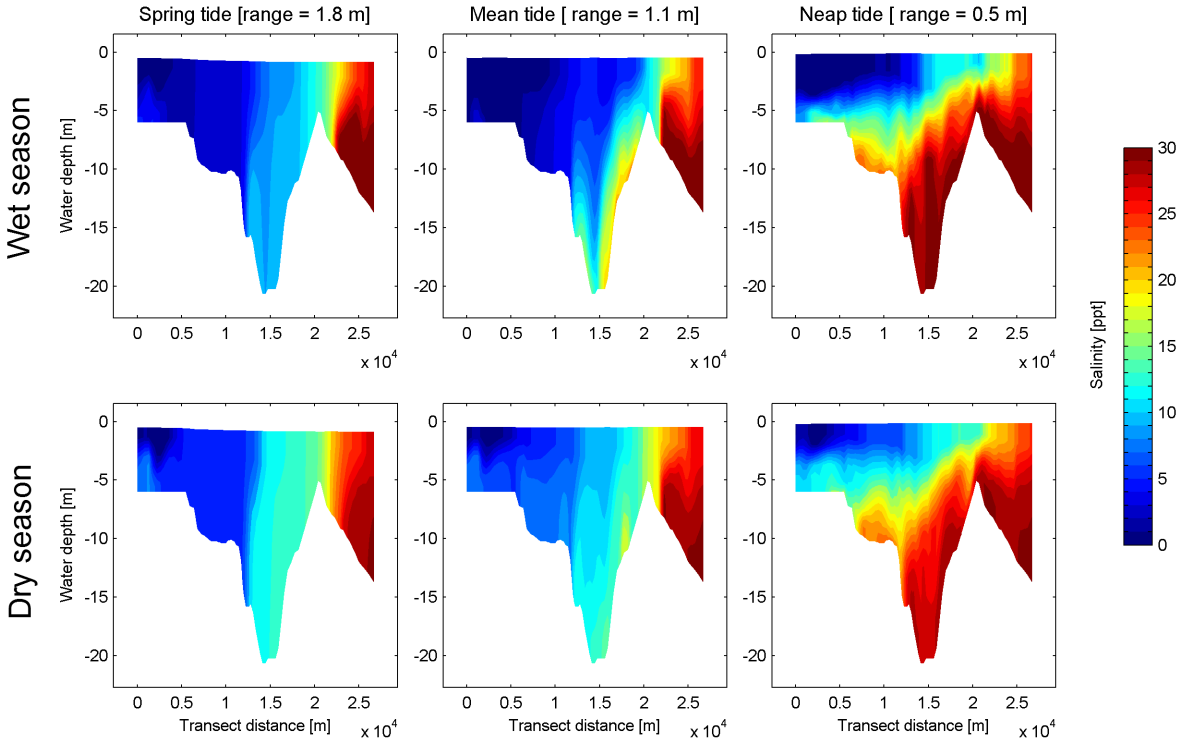

Figure 3.11: Salinity transects at low water slack through Estuary entrance for spring(left), mean(middle) and neap(right) tides during the wet(top row) and dry season (bottom row)

mum is probably located closer to the Estuary mouth in the wet season, this would explain the high sediment concentrations observed in the Estuary entrance during wet spring tides as were shown in the measurements (see section 2.2.2).

3.2.3. MORPHOLOGIC MODEL RESULTS

The morphologic model results are separately discussed for the coastal sediment fraction and the Estuary sediment fraction respectively. The main focus of the model is the simulation of the Estuary transports, therefore this part is treated more extensively.

COASTAL SEDIMENT CONCENTRATIONS

Sediment eroded by waves in the coastal area showed to be concentrated in the bottom meter of the water column by the field measurements (see Section 2.4.3). Average measured concentrations in this bottom meter are 1.5 g/l during the wet season and 0.25 g/l on average in the dry season. This effect is expected to be caused predominantly by the difference in wave heights. Sediment induced buoyancy effects cause the sediment to be concentrated near the bed. In the Delft3D model the effect of sediment on the fluid density is enabled, which allows for buoyancy destruction.

The coastal area is occupied by a separate sediment fraction with different properties than the estuarine sediments, as is discussed in Section 3.2.1. Figure 3.12 shows the sediment concentration profiles at different locations at max flood flow during a wet spring tide with wave heights of H_s = 1.5 m. The sediment concentration profiles in the region of the proposed channel have reached an equilibrium in erosion and sedimentation. The concentration profiles show similar shapes as the measured profiles, which indicates that buoyancy destruction occurs. It is shown however, that sediment concentrations reach higher than the bottom meter and are lower than the measured values of > 1 g/l.

It is expected that the difference in sediment concentration in the model and measurements is caused by the configuration of the model with respect to the sediment properties such as settling velocity, critical bed shear stress for erosion and the erodibility parameter. The enabling of sedimentation (with critical bed shear

stress for deposition: $\tau_d = 1000$ N/m^2) implies that deposited sediment causes sedimentation immediately. As a result sediment in the model experiences relatively high sedimentation rates and therefore no build-up of a thin fluid mud layer on bed takes place, which would be the case in reality. The thin layer of fluid mud on the seabed is expected to reduce wave erosion, vertical mixing and sedimentation. It is expected that this configuration induces the concentrations in the model to be lower than measured.

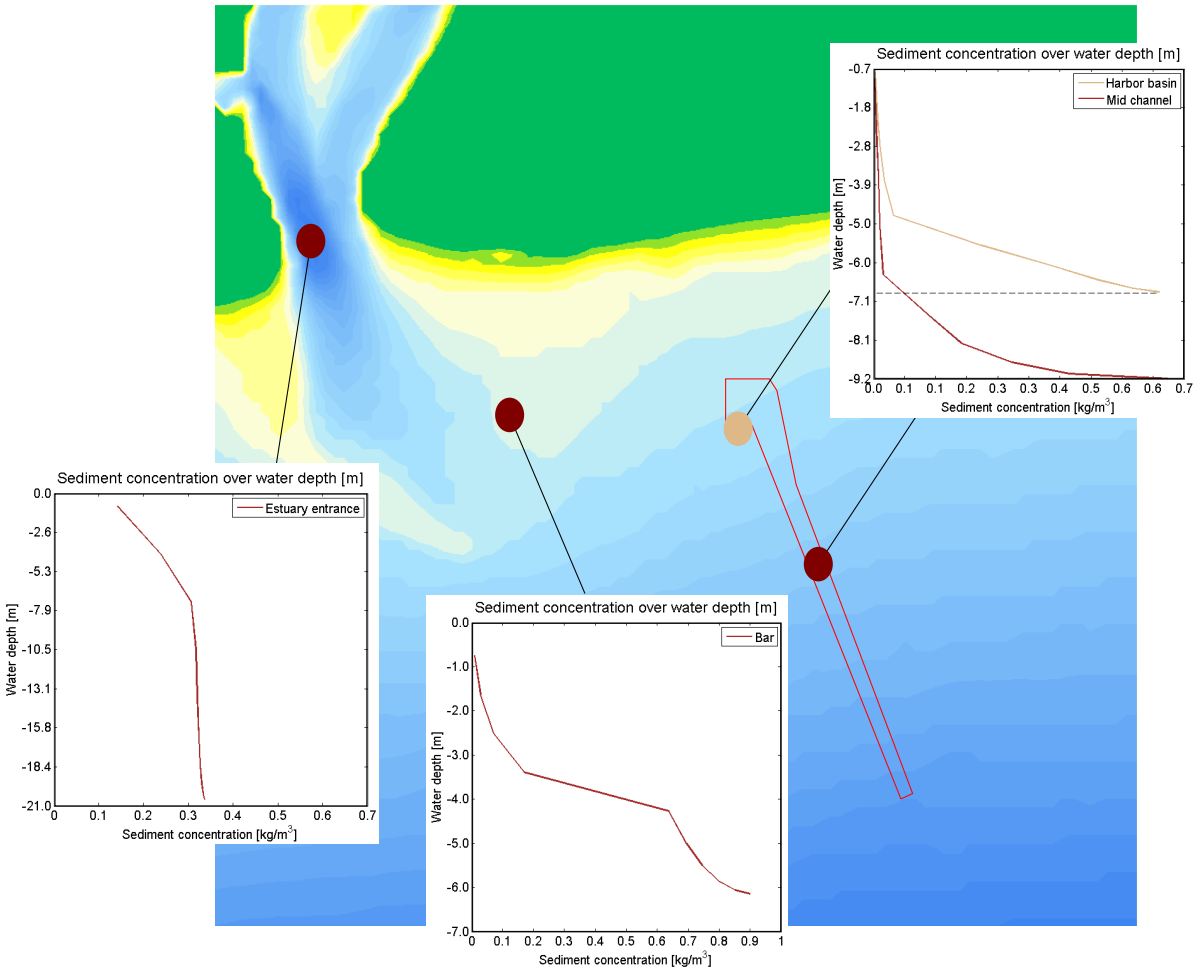

Figure 3.12: Sediment profiles of coast sediment fraction at different locations at max flood velocity

Residual transport It is shown that wave eroded material in the coastal zone is concentrated in the bottom part of the water column in the model, similar to the measured profiles. The residual current due to stratification that was discussed in the previous section causes the residual transport of sediment to take place in the Delft3D model. A transect is drawn along the proposed channel location in the model to calculate the gross sediment flux from the residual transport. The gross sediment fluxes for the wet ($H_s = 1.5$ m) and dry ($H_s = 0.75$ m) season are summarized in Table 3.4:

Table 3.4: Gross residual fluxes in Westward direction from Delft3D model in kg

Season	Daily flux [kg/day]	Monthly flux [kg/month]	Yearly flux [kg/season]
Wet	$1.5 * 10^7$	$4.4 * 10^8$	$3.1 * 10^9$
Dry	$3.2 * 10^6$	$9.5 * 10^7$	$4.8 * 10^8$

The difference in sediment flux between the two seasons is significant and mainly caused by the lower sediment concentrations during the dry season. The total yearly flux is estimated at $3.5 * 10^9$ kg/year or $9 * 10^6$

m^3/year (for 400 kg/m^3).

It is interesting to see that the residual sediment flux from the Delft3D model is close to the calculated fluxes by the use of measured data in the previous section, even though sediment concentrations in the Delft3D model are lower than measured. It is expected that the Delft3D model overestimates the flow velocities near the bed as no thin fluid mud layer is present that would move slower than the surrounding water body. The sediment being suspended higher up into the water column combined with the lower sediment concentrations in the model, compensate for the measured higher concentrations in the lowest meter only.

Estuary transport of coastal sediment Sediment eroded in the coastal area is transported into the Estuary during flood flow. In the Estuary entrance the sediment concentration is mixed over the entire water column which is probably caused by the high flow velocities and accompanying turbulence.

Figure 3.13 shows the time averaged flow velocity over one week in the Estuary entrance. The bottom part of the water column shows a mean flow in flood direction, whereas the top part shows a net flow in ebb direction. This suggests that import of sediment takes place, due to higher sediment concentrations lower in the water column. However, the Delft3D model overestimates the flood discharges in the Estuary entrance, and therefore the net inflow in the lower part of the water column will most probably be lower in reality. Therefore no reliable quantitative estimate on the importing character of the Estuary is possible.

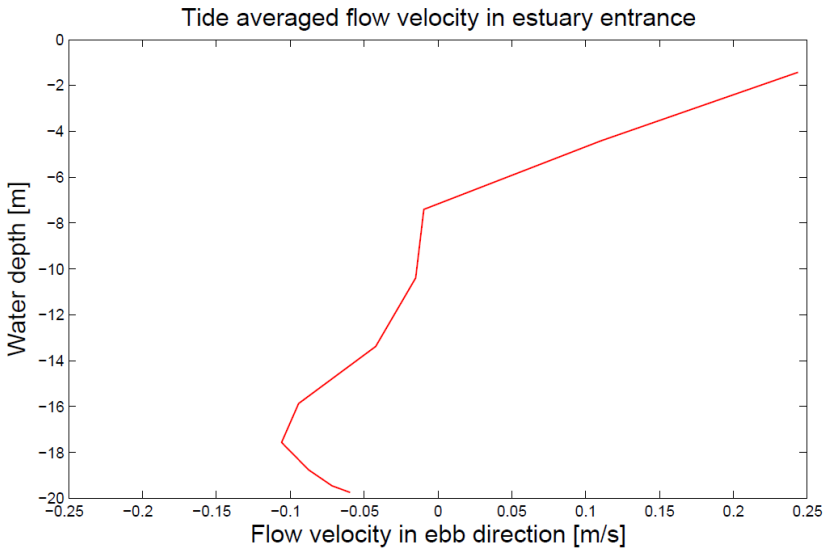

Figure 3.13: Mean flow velocity in Estuary entrance (over 1 week during the wet season)

ESTUARY SEDIMENT TRANSPORT

Tidal discharges from the Estuary could carry suspended sediment from the Estuary as far as the proposed channel dependent on the flow and sediment characteristics. An indication of the sediment transport from the Estuary is obtained from analyzing the sedimentation pattern for different tidal scenarios (spring, mean and neap tides). The flow velocities during the tidal scenarios determine vertical mixing of sediment and the distance the sediment is transported from the Estuary entrance. The wet and dry season are investigated separately as wave heights and salinity influence the sedimentation pattern.

Figure 3.14 shows the sediment concentrations in the Estuary entrance over one tidal cycle. It is observed that the order of magnitude for the sediment concentrations during spring and mean tides are correct, but predicted lower by the Delft3D model in general (except for the sediment concentration during a dry spring tide). It is noted that in the Delft3D model all sediment transported through the Estuary entrance during the ebb tide consist of 'river sediment' with lower settling velocities and critical bed shear stresses than the coastal sediment fraction. Coastal sediment transported into the Estuary is deposited relatively far away from the entrance and is eroded less easily than the river sediment fraction during ebb discharge.

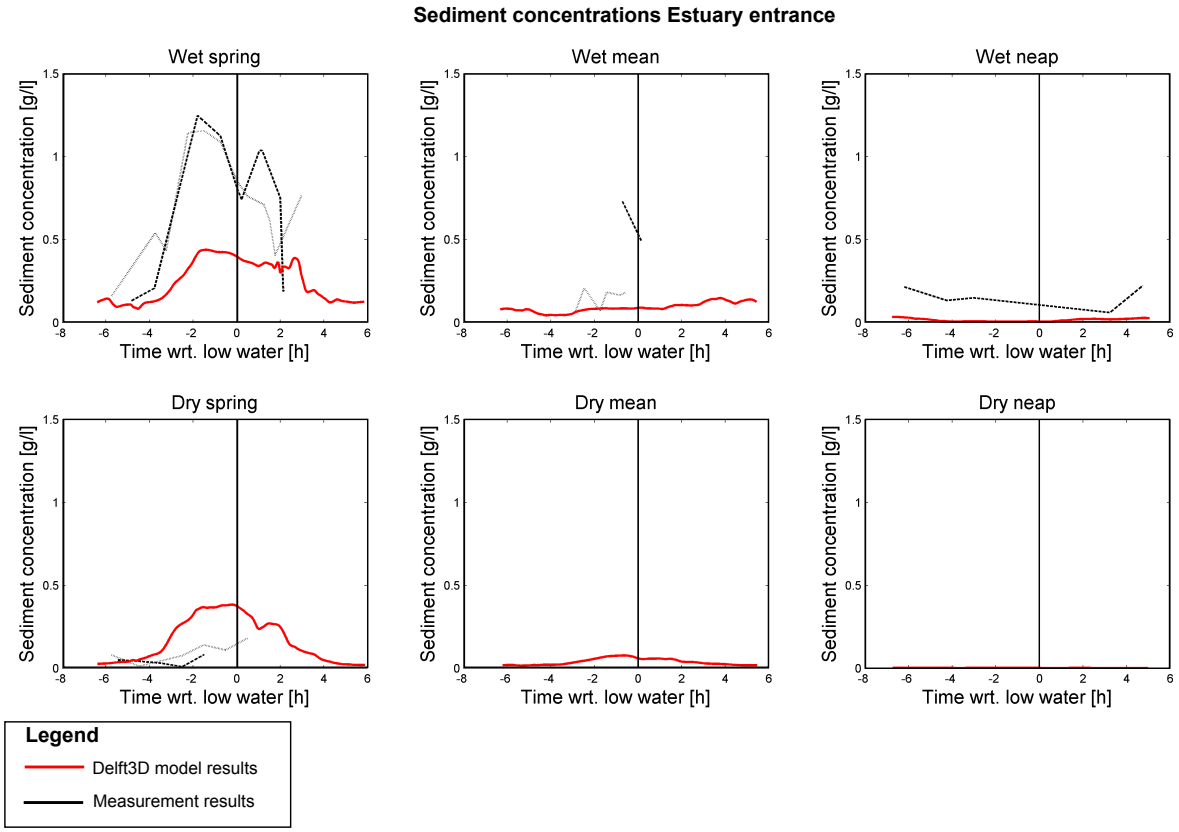

Figure 3.14: Depth averaged (river) sediment concentrations for six tidal scenarios in the Estuary entrance

The difference between the wet and dry season is small. As explained before, the sediment concentrations in the Estuary entrance are expected to be higher during the wet season as a result of higher fluvial discharge from the River and increased offshore suspended sediment concentrations interacting with the Estuary.

SEDIMENT DEPOSITION PATTERN

Figure 3.15 shows the qualitative deposition pattern of sediment supplied by the Estuary for three tidal scenarios in the wet and dry season. The dry season conditions are modeled with waves of $H_s = 0.75$ m and the wet season conditions are modeled with $H_s = 1.5$ m, both from Southern direction.

From Figure 3.15 it is concluded that during spring tides sediment is deposited over a significantly larger area than the other scenarios. During mean and neap tides, sediment is deposited for the largest part on the Estuary side of the ebb tidal bar and does not reach the project area. Additionally, sediment concentrations are lower during mean and neap tides, therefore the quantity of sediment deposited during these tides is

lower as well.

The discharge from the Estuary is pushed towards the East by the ebb tidal bar, causing sediment to be directed towards the location of the proposed channel. The influence of waves cause the deposited sediment to be transported further towards the proposed channel. The difference in wave heights between the wet and dry season cause the largest variation in sedimentation around the approach channel.

The ebb tidal bar forms a barrier between the Estuary and the coastal system. In the model it is shown that a large part of the sediment is deposited on the Estuary side of the ebb tidal bar, while in reality no signs of accretion in this area are found. It is expected that the deposited sediment would not cause sedimentation instantly as it does in the Delft3D model (because of the high τ_d). The freshly deposited sediment layer between the Estuary entrance and the ebb tidal bar would be transported back into the Estuary more easily in reality as it does not consolidate immediately. In longer model simulations it was shown that the accumulation of sediment between the Estuary entrance and the ebb tidal bar is limited compared to the build-up of sediment outside the ebb tidal bar.

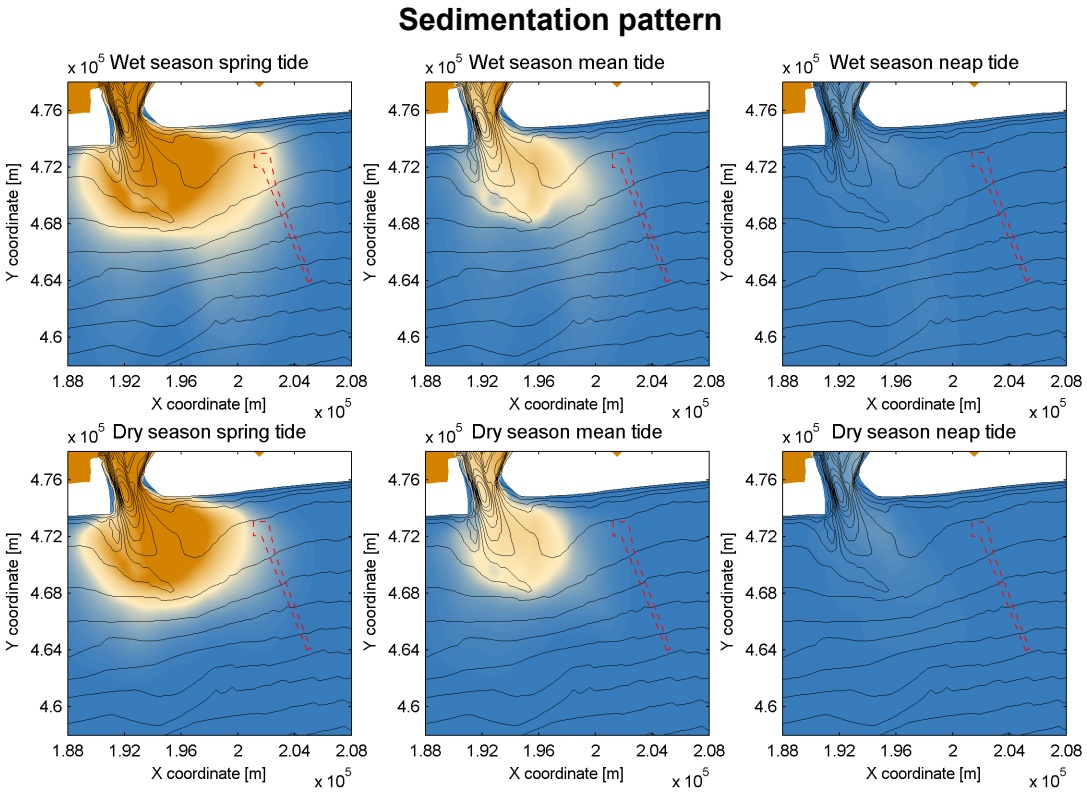

Figure 3.15: Qualitative sedimentation pattern for tidal scenarios, wet season: $H_s = 1.5$ m and dry season: $H_s = 0.75$ m

CONCENTRATION PROFILES

Sediment concentration profiles at maximum ebb velocity during a wet spring tide are shown in Figure 3.16. Sediment concentrations are highest in the top part of the water column at all locations. It is expected that sediment is kept in suspension by the relatively high flow velocities of the fresh water discharge in the higher parts of the water column. The sediment settles slowly, and once it reaches the lower part of the water column the lower flow velocities are less able to keep the sediment in suspension. Additionally, sediment induced buoyancy effects cause damping of turbulence in the lower part of the water column as wave eroded material already exceed the saturation concentration.

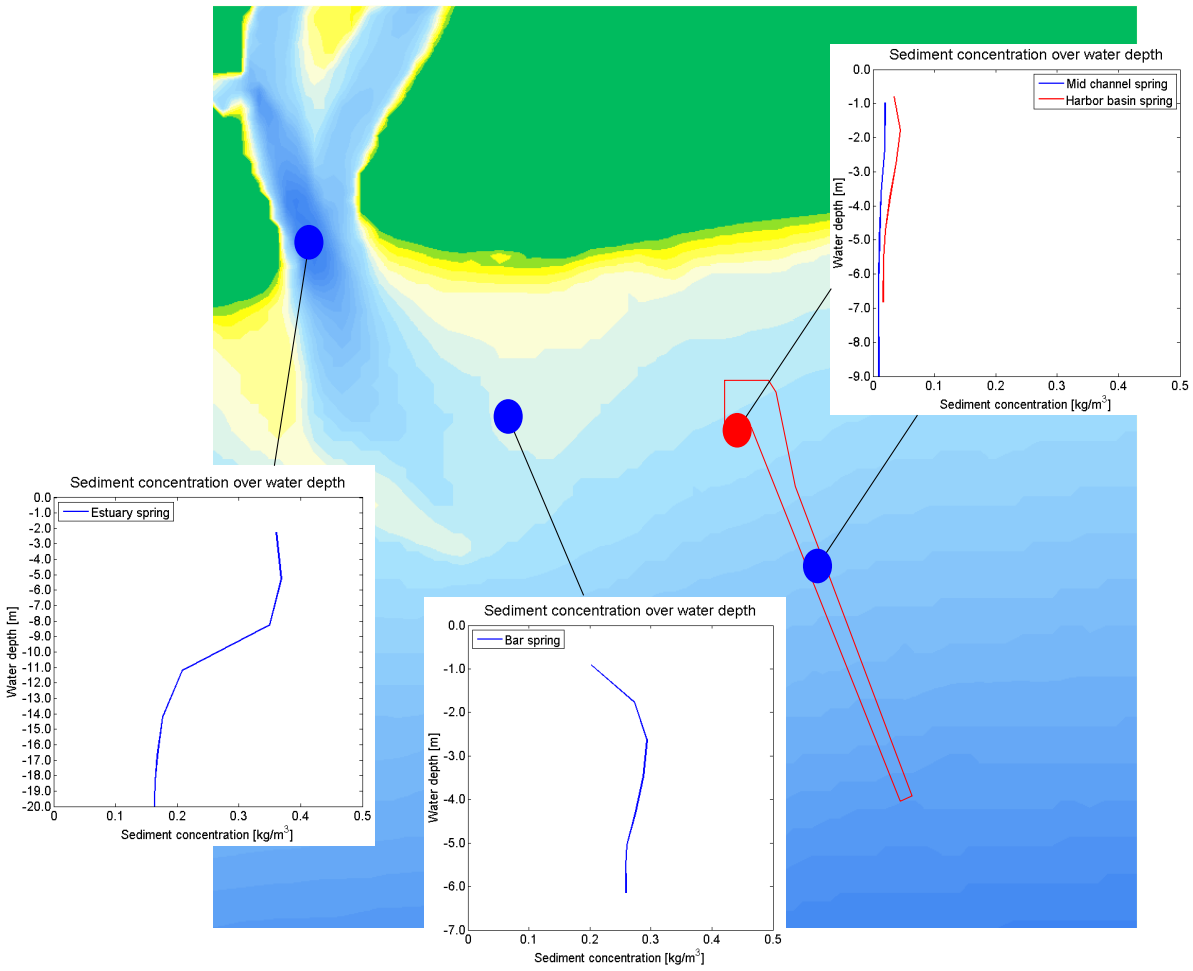

Figure 3.16: Maximum ebb tide sediment concentration profiles at Estuary entrance, ebb tidal bar and at dredged channel location.

ESTUARY SEDIMENT FLUXES

Three transects are used to estimate sediment fluxes from the Estuary. As the model is not calibrated extensively for sediment concentrations and Estuary discharges, quantitative values are rough estimates. Therefore relative amounts of sediment from the Estuary reaching the approach channel is of main interest in this consideration. The transects are shown in Figure 3.17. Each tidal scenario (spring, mean and neap tide for wet and dry season) is run for two tidal cycles from which the sediment fluxes are taken.

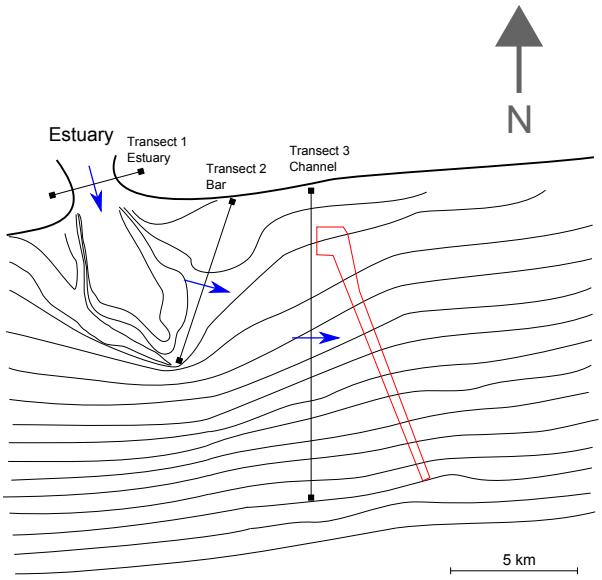

Figure 3.17: Transects used for Estuary sediment fluxes.

The gross sediment fluxes in direction of the arrows in Figure 3.17 are determined. Gross sediment fluxes towards the proposed channel are considered to determine the actual infill (assuming 100 % trapping of sediment in the channel). Figure 3.18 shows the fluxes per scenario through the individual transects. The results for each transect are discussed separately below:

Transect 1: Estuary During spring tides the sediment flux through the Estuary entrance is significantly larger than for the other tidal scenarios. Spring tides occur only twice a month, therefore the mean tides account for the main part of the total yearly flux through the Estuary entrance. The yearly gross flux through transect 1 is approximately $2 * 10^{10}$ kg/year based on multiplication of the scenarios with their yearly frequency of occurrence. This value is used as a reference to calculate the relative fluxes through the other sections and is only a rough indication of the total flux. The sediment concentrations were shown to be underestimated and therefore it is expected that the total flux is probably higher than determined by the Delft3D model. The flux of sediment through the Estuary entrance is taken as 100 %.

Transect 2: Bar In Figure 3.18 it is shown that the sediment transported over the ebb tidal bar as a proportion of the total net sediment flux from the Estuary is small. Approximately 20 - 25 % (ie. $4 * 10^9$ kg/year) of the total flux is transported over the ebb tidal bar. The relative transport over the Estuary is similar for a spring tide and for a mean tide, however in absolute number spring tides account for approximately 5 times the flux compared to a mean tide. The difference between the wet and dry season is small, because the influence of waves behind the ebb tidal bar is relatively low.

Transect 3: Channel The amount of sediment reaching the approach channel from the Estuary entrance is limited. During the wet season around 5 % of the total gross flux from the Estuary reaches the channel transect, whereas this value is only 2 % during the dry season. This difference is mostly caused by the waves that keep sediment in suspension longer and carry sediment further towards the dredged channel in the wet season. The total amount of sediment that is transported through transect 3 is approximately 4 % (ie. $8 * 10^8$ kg/year) of the total gross flux through the Estuary entrance.

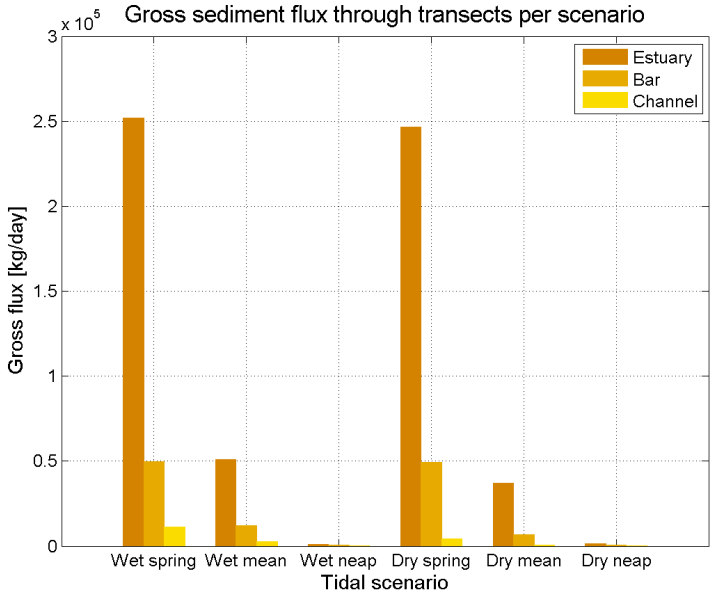

Figure 3.18: Sediment fluxes through transects per tidal scenario.

Table 3.5 shows an overview of the percentages of flux through the three transects.

Table 3.5: Relative gross sediment fluxes through transects

	Wet season			Dry season		
	Spring	Mean	Neap	Spring	Mean	Neap
Estuary	100%	100%	100%	100%	100%	100%
Bar	20%	24%	59%	20%	19%	34%
Channel	4%	5%	13%	2%	2%	3%

Net fluxes In the above consideration gross sediment fluxes from the Estuary are used to estimate direct infill of the proposed channel. It was shown that sediment transported over the ebb tidal bar is partly able to reach the proposed channel. A part of the sediment might settle between the ebb tidal bar and the channel and could cause infill indirectly at a later stage. No long term sediment accumulation occurs in the project area according to LWI and therefore the deposition of sediment between the ebb tidal bar and the channel is expected to be temporary.

The amount of sediment accumulating between the ebb tidal bar and the proposed channel is dependent on the net flux instead of the used gross fluxes. From the Delft3D model a net flux over the ebb tidal bar of around 10% of the gross flux from the Estuary entrance. This sediment could cause infill indirectly, potentially in the form of fluid mud as will be discussed in the following section. Another part might be transported into the Estuary due to the near-bed residual flow.

3.3. FLUID MUD

Grab samples showed the occurrence of fluid mud in the project area and according to the infill studies done by LWI the infill in the dredged channel is for a large part determined by occasional fluid mud events. The measured fluid mud had typical concentrations of 30 – 60 g/l and a layer thickness of around 50 cm. The area where the fluid mud was observed is indicated in Figure 3.20. The fluid mud layers have not been observed to reach further East than measurement location P2, which is the Eastern extent of the brown area in the figure. Therefore it is questioned whether the observed fluid mud layer is able to reach as far as the dredged channel. Figure 3.19 shows how fluid mud formation in the project area was described in earlier studies.

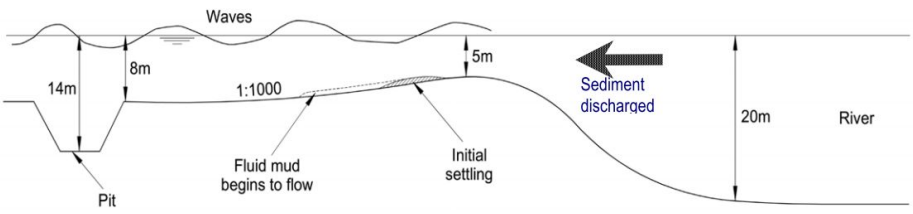

Figure 3.19: Process of fluid mud formation due to waves after initial settling HR Wallingford (2005)

Fluid mud was found to be formed during large wet spring tides and high wave events, however a limited amount of data is available and therefore the frequency and magnitude of the fluid mud layer is highly uncertain. Three processes can cause the formation of fluid mud according to McAnally et al. (2007) and Winterwerp and van Kesteren (2004). These are separately discussed in the following paragraphs in order to determine which mechanism is expected to be responsible for fluid mud formation in the project area:

1. sediment induced buoyancy effects initiate a collapse of the vertical sediment concentration profile;
2. rate of sediment aggregation and settling into the near-bottom layer exceeds the de-watering rate of the suspension;
3. soft sediment beds liquefied by wave agitation.

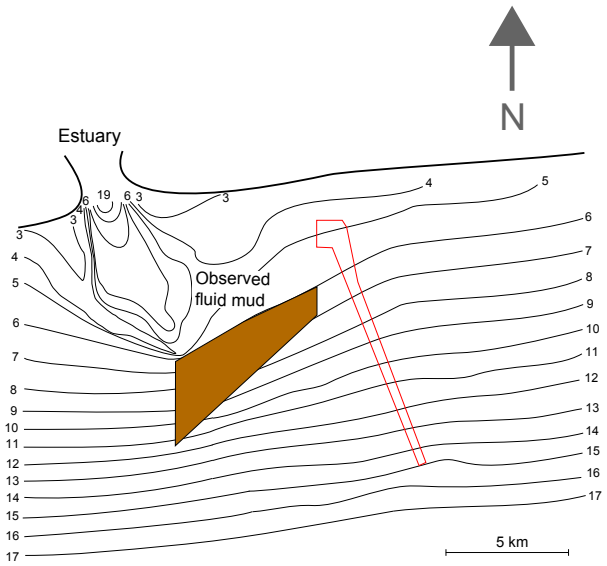

Figure 3.20: Area of observed fluid mud layer by LWI

SEDIMENT INDUCED BUOYANCY EFFECTS

The concept of sediment induced buoyancy effects was treated in Section 2.4.3. In the Estuary depth averaged sediment concentrations during large spring tides are measured up to 1,200 mg/l. During these high flow velocities sediment is rather evenly distributed over the water column. Once the discharge decreases after peak in- or outflow the flow velocity decreases as well and the capacity of the flow to keep sediment in suspension is reduced accordingly. It is plausible that the saturation concentration is met (particularly) outside the ebb tidal bar during large spring tides.

EXCEEDANCE OF DE-WATERING RATE OF SUSPENSION

Fluid mud formation of bed sediments could be caused by rapid settling of suspended material (eg. eroded material by waves) (Winterwerp and van Kesteren, 2004). During a high wave event sediment accumulated outside the ebb tidal bar could be eroded fast. Increased turbulence due to these waves allow sediment to be mixed higher up in the water column than during regular wave heights (as were measured by

the OBS devices). These sediments settle after the initial erosion, however hindered settling effects cause fluid mud to form because the upward flow of water exceeds the settling velocity of particles. The fluid mud de-waters/consolidates slowly and will therefore stay present for some time. This is found to be typically occurring during energetic swell events (Sheremet et al., 2011).

The area where fluid mud is formed, just outside the ebb tidal bar in the near shore zone, was found to consist mainly of sandy material by the grab samples from Fugro (2006). Therefore the sediment eroded during these wave events have to be accumulated over time before it is eroded and formed into fluid mud. It is therefore expected that a high wave event after a period of low waves is the most favorable situation for fluid mud to form.

LIQUEFACTION

Waves can loosen a cohesive sediment bed and generate fluid mud. The bed sediment can start behaving as a fluid when the soil matrix is destroyed by excess pore pressure buildup. A distinction is made between liquefaction and fluidization of soil. Fluidization is considered to be a special case of liquefaction.

Liquefaction is a phenomenon that occurs when saturated sediments are subjected to a stress that causes the loosely packed grain framework to collapse, temporarily suspending the grains in the pore fluid. Rapid settlement follows until a grain-supported structure is re-established. Fluidization occurs when the upwards water velocity exceeds the settling velocity of the grains, the grains become suspended in the stream and the water-sediment mixture starts behaving as a fluid.

Waves in shallow water generate gradients in pore pressure that in turn can cause the pore fluid to flow. Starting with a bed at rest subject to a constant wave action, the wave-averaged water pore pressure increases with time and the wave-averaged effective normal stress in the soil skeleton decreases with time (Mehta et al., 1994). When the wave-averaged effective normal stress is zero, the sediment bottom is fluidized (McAnally et al., 2007). Figure 3.21 shows a schematization of the stress profiles in the bed where u_w = wave-averaged pore pressure [N/m^2]; σ_h = hydrostatic pressure [N/m^2]; Δu = wave-averaged excess pore pressure [N/m^2]; and σ = wave-averaged effective normal stress [N/m^2]. σ decreases with a buildup of excess pore pressure until fluidization occurs, when $\sigma = \sigma_h + \Delta u$.

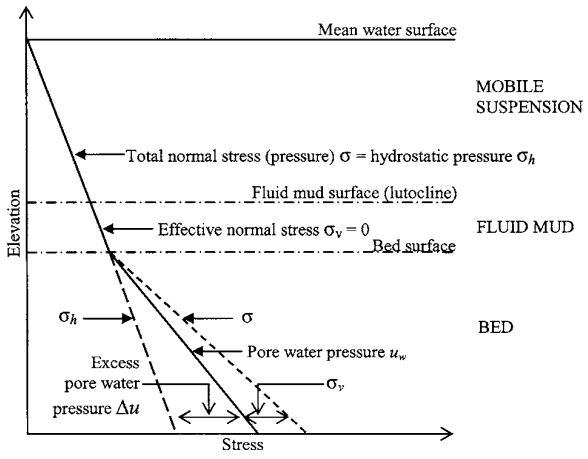

Figure 3.21: Schematic of instantaneous stress profiles in a water-mud system (Mehta et al., 1994)

The bulk density of liquefied material is close to the consolidated bulk density before liquefaction, the measured fluid mud concentrations in the project area are around 30 – 60 g/l and are therefore very low for liquefied material. The exact understanding of mud liquefaction due to waves is limited and recent research conducted by Winterwerp et al. (2012) showed that liquefaction of mud by waves under natural conditions does not occur. Therefore it is not expected that liquefaction is of any influence.

3.3.1. FLUID MUD INFILL

Fluid mud is most likely formed in the project area during high wave events, when accumulated material is eroded in short periods of time. Sediment induced buoyancy effects could cause fluid mud as well, however

it is not expected that this is the main driving mechanism for the mobile fluid mud layer of several tens of centimeters as measured.

The amount of sediment that could cause indirect infill in the form of fluid mud is rather uncertain. Fluid mud was measured during a large wet season spring tide in combination with an extreme wave event. However, even under these 'ideal' circumstances the fluid mud layer did not reach the area of the proposed channel.

In Section 3.2.3 it is stated that sediment is deposited in the area between the Estuary and the proposed channel. If this sediment is mobilized in the form of fluid mud, a portion would most probably reach the channel. The exact quantities of infill this would generate are difficult to estimate and require further research. However, as the near-bed residual current is present in the direction of the Estuary it is expected that a large part of the sediment eroded in this region is transported back towards the Estuary.

3.4. DISCUSSION

Sediment fluxes have been estimated for both the residual current and the Estuary sediment transport. As only a limited amount of data is available for this study, no extensive calibration of the model was conducted. The model was set-up to find qualitative information on the sediment transports, however the order of magnitude of the sediment concentrations and flow velocities showed to be in an acceptable range to provide a rough estimate of the quantitative fluxes.

The Delft3D model showed that the near-bed residual (Westward) current in the project area could be explained by stratification effects. These findings are in contrast to the suggestions by LWI that ocean currents are (entirely) responsible for the residual flow. The relative contribution of the stratification effects on the residual current cannot be assessed with the available data. If stratification is largely responsible for the residual currents, this would mean that West of the entrance an Eastward residual flow should occur. This should be studied in future research.

The extend of the fresh water plume of the Estuary carrying sediment towards the proposed channel and coastal area determines the sedimentation area for a large part and might change for different fresh water discharges from the River. As the fresh water discharges from the River are uncertain, the extent of the fresh water plume and associated sediment plume in reality could deviate from the model results. This leads to uncertainty of the calculated sedimentation pattern and stratification induced currents.

The effect of flocculation of sediment is not taken into account in the model, as the settling velocity of the river sediment fraction is taken constant at $W_s = 0.2$ mm/s. Flocculation could reduce the distance the sediment travels from the Estuary entrance and thereby reduce the sediment transport from the Estuary to the proposed channel.

It was shown that the sediment concentration profile in the water column could collapse due to sediment induced buoyancy effects. In the lower parts of the water column in the coastal area it is shown that sediment concentrations are highest near the bed as a result of buoyancy destruction. The reduction in turbulence higher up in the water column due to this might cause river sediment to settle faster as well.

Roughly 10% of the gross sediment flux from the Estuary is deposited between the ebb tidal bar and the proposed channel according to the model. This sediment could account for additional infill if it is picked up by waves and transported towards the proposed channel by (tidal) flows. It is expected that the net sediment flux is somewhat lower in reality than found by the Delft3D model. Delft3D scales the amount of erosion by the layer thickness of available sediment if it is smaller than a certain height (10 cm). Therefore accretion of several centimeters is required first before erosion can take place. The model is run for two tidal cycles and therefore the required layer thickness of sediment is not available until enough sediment is deposited first.

As sandy material is present along the entire ebb tidal bar, it is expected that long term accretion does not take place. This is a result of the relatively high flow velocities on the ebb tidal bar as well as the relatively strong wave action due to the smaller depth.

The time averaged flow velocity in the Estuary entrance shows that a net flow in the direction of the Estuary is present in the model. This could suggest a net import of sediment into the Estuary. However, the flood discharges in the model are relatively high compared to the ebb discharges, which makes it difficult to confirm this hypothesis by the use of the model. Due to the stratified character and sediment concentrations measured in the Estuary entrance (see Section 2.2.2) it is expected that a net import of sediment occurs during regular tidal ranges and net export occurs during spring tides only.

The infill expected from fluid mud is highly uncertain due to the limited amount of observations and measurements. It is expected that during extreme wave events erosion rates are of such magnitudes that hindered settling of eroded material causes fluid mud to form. Additionally, during wet spring tides, when high sediment concentrations are present in the Estuary entrance, sediment induced buoyancy effects can initiate the development of a fluid mud layer as well. During the observations, fluid mud was not shown to reach the proposed channel location, even though the most favorable conditions were present. Therefore the infill caused by fluid mud is expected to be relatively low compared to the residual transport.

3.5. CONCLUSION OF DOMINANT MORPHOLOGICAL PROCESSES

A list of conclusions drawn from the results presented in this chapter is provided below. This chapter has achieved the second sub-objective by analyzing the dominant morphological processes using simple tools as well as a Delft3D model.

RESIDUAL TRANSPORT

- The residual transport in the coastal region causes a sediment flux in the direction of the approach channel of around $4 * 10^9$ kg/year based on measured flow velocities and sediment concentrations in the project area.
- The largest part of this sediment transport occurs during the wet season, as wave heights and residual currents are strongest in this period. Daily mean fluxes are around 2,500 kg/m/day during the peak months of August, September and October. This is equivalent to approximately 1 m infill per month for a density of 400 kg/m^3.

DELFT3D MODEL

Using a Delft3D model, sediment transports in the project area are simulated. From the model results the following conclusions are drawn:

- Stratification effects from the fresh water Estuary discharge are found to be responsible for a residual current towards the Estuary. The measured residual current in the project area could be a combination of the large scale ocean current and the stratification effects. The relative contribution of these two driving mechanisms to the total residual current requires further research.
- Sediment concentrations in the coastal region show similar profiles as measured, caused by sediment induced buoyancy effects. However, lower absolute concentrations were found and suspensions reached higher up into the water column. This is probably caused by the critical shear stress for deposition used in the model and the lack of bed shear stress reduction from a thin fluid mud layer at the bed. A rough estimate of the residual transport from the Delft3D model is in the same order of magnitude as calculations from measured quantities in the first section, confirming the earlier calculations.
- The sediment transports from the Estuary shows that only a limited amount (~ 4 % of yearly gross flux) of sediment supplied by the Estuary would cause direct infill in the approach channel. Direct infill from the Estuary is highest during large wet spring tides and concentrated in the harbor basin area of the approach channel. The gross flux at the channel is estimated at $8 * 10^8$ kg/year, which is suspended high in the water column.
- Approximately 10 % of the yearly gross flux from the Estuary is net deposited between the ebb tidal bar and the proposed channel. A portion of this sediment could cause indirect infill in the channel.

FLUID MUD

- Fluid mud is most probably formed during high wave events, when sediment accumulated outside the ebb tidal bar is eroded in short amounts of time and hindered settling prevents direct sedimentation.
- Fluid mud is observed during the measurements and is therefore expected to be of influence on the infill of the dredged channel. Due to the limited information and according uncertainty regarding fluid mud infill, it is difficult to provide a quantitative estimate on the expected infill. As during the considered 'ideal' circumstances for fluid mud no fluid mud was observed in the area of the proposed channel, it is expected that infill from fluid mud only occurs occasionally.

OVERALL

- The sediment infill of the dredged channel is expected to be mainly caused by the residual transport and therefore the consideration of mitigation measures will be focused on this infill process, see Figure 3.22.

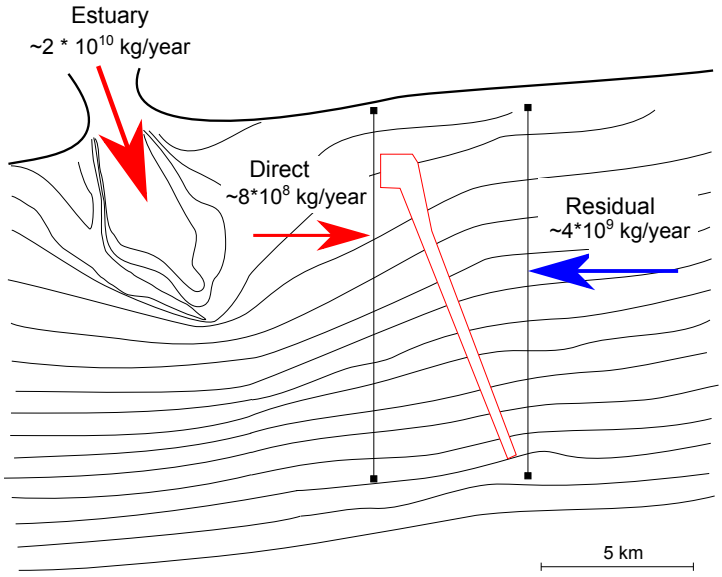

Figure 3.22: Sediment fluxes from Estuary and residual transport towards proposed channel

4

INFILL REDUCTION CONCEPTS

This chapter treats mitigation measures for sediment infill in offshore dredged channels in general, and for the project case in particular. The first goal of this chapter is to provide a list of measures that can be applied in general cases to reduce sedimentation of dredged channels. The second goal is to apply the list of general mitigation measures to the specific case and propose a list of potentially effective measures for this case.

First, the general channel infill process is briefly described in Section 4.1. In Section 4.2 generic infill reductions are presented and discussed, individual measures are described shortly with associated figures to demonstrate the working mechanism. Two categories of measures are distinguished in this section, measures that focus on sediment infill in the dredged channel and measures that focus on maintenance dredging to remove sediment from the channel. In the discussion of this section the measures are elaborated more extensively and a framework is given to estimate the effectiveness of each measure. The conclusion of this section provides a table with an overview of the measures in which the different solutions can be compared. Section 4.3 considers the proposed measures for the specific case. An evaluation is done to propose potentially effective measures to mitigate sediment infill of the proposed channel.

4.1. CHANNEL INFILL PROCESS

This section describes the infill process of a dredged channel, following Rijn (1986). The infill process as described here represents the mechanism causing fine sediment infill of a dredged channel as considered in this chapter. Other channel infill mechanisms such as side slope instability are not considered.

Sediment is eroded by wave action from the bed once the critical shear stress for erosion is exceeded by the wave induced bed shear stress. Advection of eroded sediment by horizontal flow velocities cause the sediment to be transported towards the dredged channel. From continuity, an increase in water depth at the channel reduces the depth averaged flow velocity. This causes the sediment transport capacity to be reduced and sediment settles in the dredged channel. Additionally, due to the increased water depth, wave induced bed shear stresses are lower in the channel. This causes less erosion of material in the dredged channel compared to the surrounding bed.

Fine sediment that is deposited in the channel does not settle directly into a rigid bed as is the case for sand, but slowly consolidates over time. Therefore a high concentrated (fluid) mud suspension is expected to be present initially after infill of the channel.

The amount of infill in the dredged channel relative to the total amount of sediment transported across the channel is defined as the trapping efficiency. The trapping efficiency is determined by the channel layout, flow pattern and sediment characteristics.

Figure 4.1 shows a schematization of the infill process in a dredged channel.

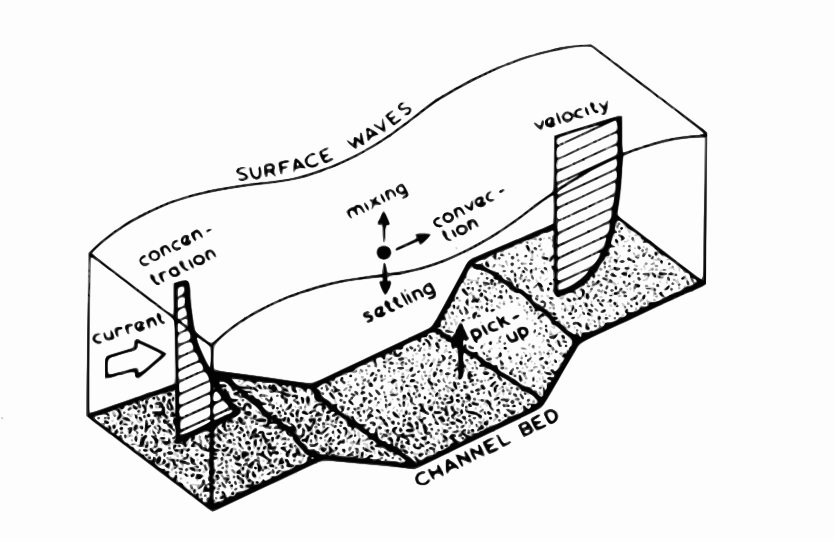

Figure 4.1: Schematic infill process of a dredged channel (Rijn, 1986)

If sediment is mixed over the entire water column (concentrations below the saturation concentration), the trapping efficiency is strongly determined by the settling velocity, horizontal flow velocity and turbulent mixing capacity of the flow. Turbulent mixing causes flocculation and floc break-up which influences the settling velocity. Settling velocities are reduced lower in the water column as a result of hindered settling due to higher concentrations. This type of infill is referred to as **Type 1**.

If very low flow velocities are present in combination with high sediment concentrations (concentrations above the saturation concentration), sediment could be concentrated in a near-bed layer, as a result of insufficient turbulent energy available to mix the sediment over the water column (as discussed in Section 2.4.3). In this case the trapping efficiency is predominantly determined by gravitational effects, as the sediment behaves similar to a density current. This type of infill is referred to as **Type 2**.

Both types of infill are schematized in Figure 4.2.

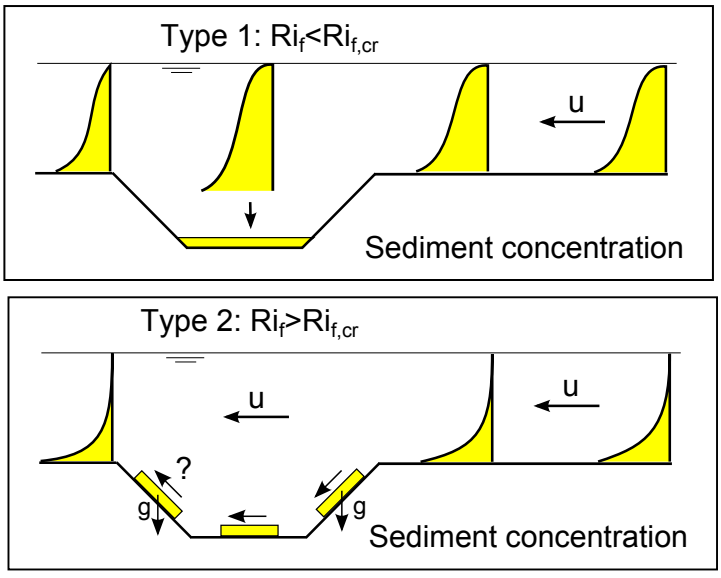

Figure 4.2: Schematic infill process for suspended sediment and concentrated near-bed layer

The sedimentation of a dredged channel is primarily determined by the following characteristics:

- Channel geometry

  Depth, width, side slope angle

- Hydrodynamic regime

  Wave height, flow velocity, flow direction

- Morphologic properties

  Sediment concentration, settling velocity, critical bed shear stress for erosion

4.2. GENERIC INFILL REDUCTION MEASURES

In this section a general approach is taken to introduce reduction measures for fine sediment infill in an offshore dredged channel. The proposed measures are considered for similar circumstances as the project case. As is shown in Chapter 3 the sediment concentration profile in the project area generally shows saturated conditions. In similar environments, where a muddy seabed is present in combination with limited flow velocities and considerable wave energy, it is expected that Type 2 infill mainly occurs. Therefore the proposed measures are focused on mitigating Type 2 infill.

The proposed measures are found from reference literature, personal communication with experts at Boskalis and brainstorm sessions. Most measures from reference literature focus on Type 1 infill and might therefore be less applicable in the case considered here. The measures from reference literature are shown in this section as well, in the discussion the applicability of the measures in the considered situation is treated.

The following list of general circumstances are taken representative for the infill mitigation measures:

- Offshore located approach channel perpendicular to coast;
- Residual flow velocity directed perpendicular/oblique to channel;
- (Cohesive) muddy seabed and gentle bed slope with shore parallel depth contours;
- Max channel depth wrt. local water depth: $\frac{h_{chan}}{h_{seabed}} \approx 3$;
- Swell wave climate with typical wave heights of $H_s \approx 1$ m;
- (Stratification induced currents due to nearby estuary.)

Some measures are specifically focused on one particular condition such as the stratification induced currents due to a nearby estuary. To estimate an order of magnitude for the required materials for each measure, a channel length of 10 km and a width of 250 m is used (similar to the specific case).

An overview of the general system is schematized in Figure 4.3.

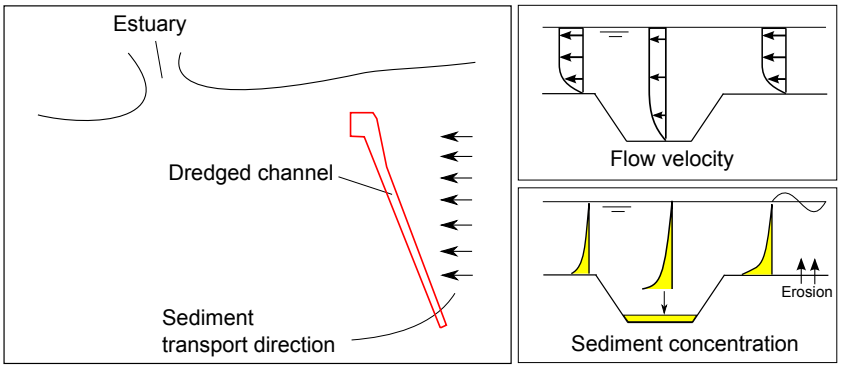

Figure 4.3: Schematic infill process of a dredged channel Rijn (1986)

4.2.1. INFILL REDUCTION MEASURES

A list of measures is presented in this section that could be effective to mitigate sediment infill in a dredged approach channel. The complete list of infill reduction measures is divided into three categories. First all measures are presented that are associated with the channel layout, secondly measures are proposed that are applied adjacent to the channel and finally maintenance dredging measures are presented.

CHANNEL LAYOUT

Measure 1: Channel location

Description: The channel location could be of significant influence to the amount of sediment infill. In shallow areas sediment concentrations are generally higher due to the higher bed shear stresses from wave orbital velocities. By locating the channel further offshore, the sediment infill could be reduced due the lower sediment concentrations. Additionally, the relative channel dredged depth is decreased if it is located in deeper water, reducing the trapping efficiency of the channel PIANC (2008).

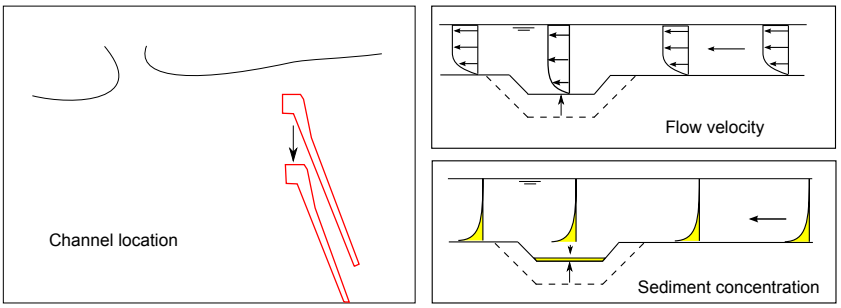

Figure 4.4: Change channel relocation

Measure 2: Channel orientation

Description: The orientation of the channel with respect to the dominant flow direction is of influence to the sediment infill. Channels aligned parallel to the flow direction attract flow due to the larger water depth (and associated lower hydraulic resistance). The increased flow velocity in the channel could reduce sedimentation and cause a self-cleansing effect PIANC (2008).

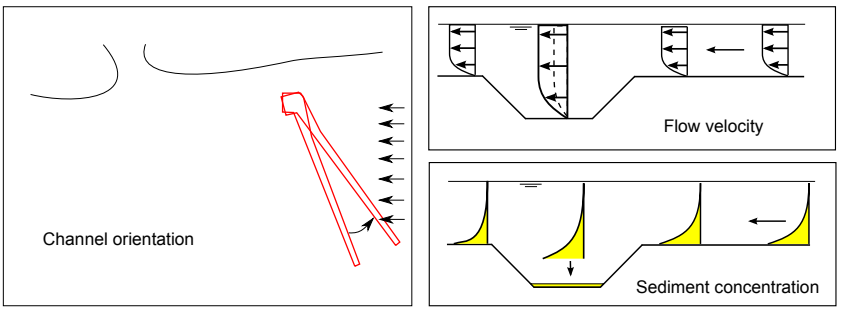

Figure 4.5: Channel orientation

Measure 3: Steep side slopes
Description: Steep channel side slopes could reduce the trapping efficiency of the channel. For the same bottom width of the channel, a smaller width at the top of the channel reduces the available time for sediment to settle.

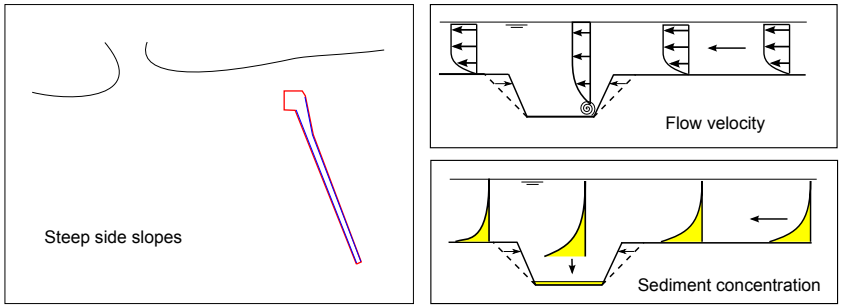

Figure 4.6: Steep side slopes

Measure 4: Channel bed slope
Description: A slope in the channel bed in offshore direction could remove sediment from the channel if a density current is initiated. Fluid mud formed by fine sediment in the channel could (passively) leave the channel under the influence of gravity if a sufficiently steep channel bed slope is constructed and the sediment remains mobile after infill.

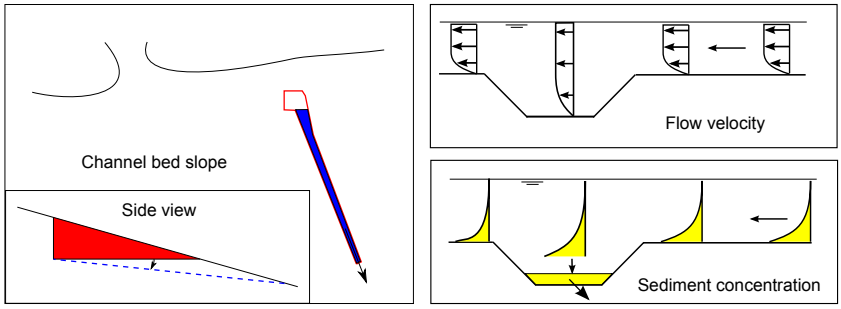

Figure 4.7: Channel bed slope

MEASURES ADJACENT TO CHANNEL

The following list of measures could be applied adjacent to the channel, limiting the amount of sediment transported to it.

Measure 5: Rocks/sand on seabed
Description: An increase in bed friction adjacent to the approach channel could be achieved by applying rocks or (coarse) sand on the seabed. The additional roughness of the seabed might cause the following effects on the sediment transport:

- Reduce flow velocity due to increased friction;
- Wave energy dissipation due to increased friction;
- Increased vertical mixing due to turbulence increase;
- Reduced erosion due to coverage of underlying mud;
- Increased erosion due to higher bed shear stresses.

The specific effects of this measure are treated in the discussion section.

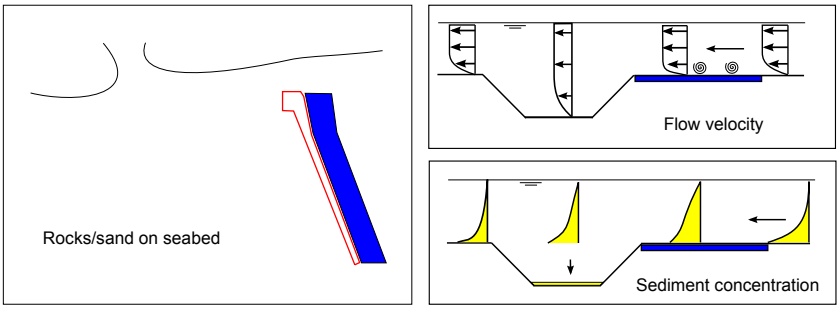

Figure 4.8: Rocks/sand on seabed

Measure 6: Wall along channel

Description: A vertical wall parallel to the channel could obstruct the Westward flow and thereby reduce the sediment transport towards the channel.

A high crested wall could be constructed that reaches above the water level, in this case the flow is entirely blocked and no sediment can be transported towards the channel.

A low crested wall could be constructed to obstruct the near-bed transport of sediment, which could be particularly effective if the mud is concentrated close to the seabed.

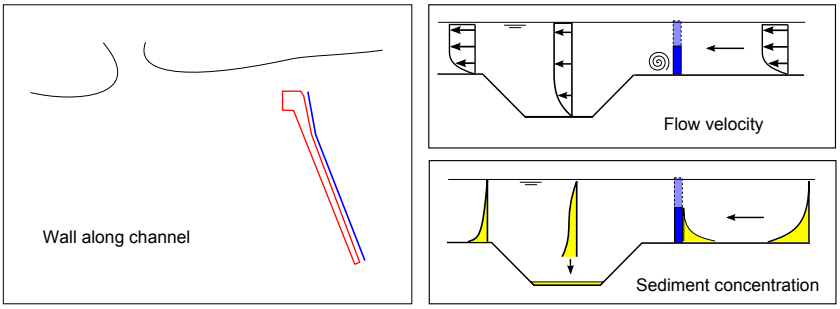

Figure 4.9: Vertical wall along channel

Measure 7: Training walls

Description: Training walls could be constructed to direct the flow more perpendicular to the channel. If the flow is directed perpendicular to the channel, less time is available for sediment to settle in the channel. Flow could also be directed more parallel to the channel to increase the effect of flow refraction and thereby increase flow velocities near the channel bed.

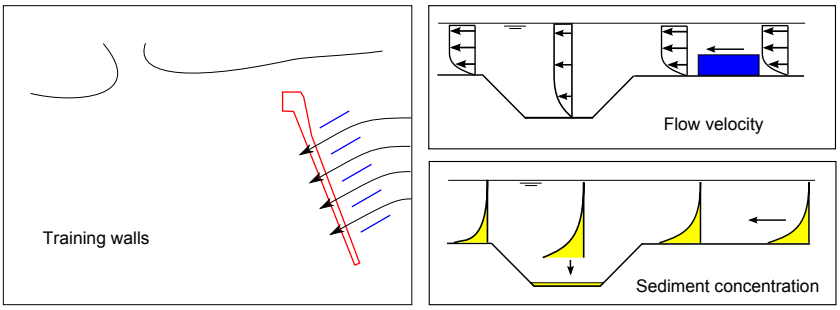

Figure 4.10: Training walls

Measure 8: Sediment trap
Description: A sediment trap adjacent to the dredged channel could reduce the sediment infill in the main channel. As a result, less maintenance dredging is required in the main channel and depending on the capacity of the sediment trap the maintenance dredging can be carried out less frequently. Dredging activity in the sediment trap is not affected by shipping traffic in the main channel, therefore the total down-time is reduced.

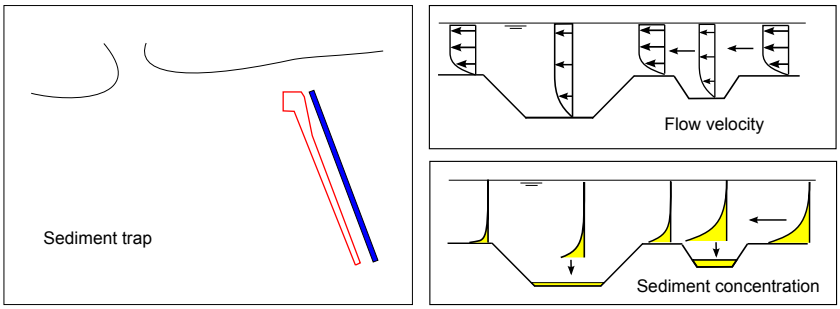

Figure 4.11: Sediment trap

Measure 9: Coast parallel breakwater
Description: A breakwater in parallel direction to the coast reduces wave action behind it. Sediment concentrations reduce due to lower erosion rates. The breakwater could either be constructed submerged or emerged, depending on the local conditions and required wave height reduction.

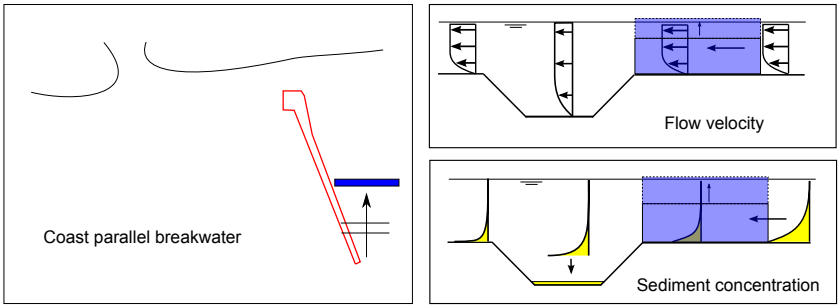

Figure 4.12: Coast parallel breakwater

Measure 10: Remove top layer seabed
Description: If the (weak) top layer of the seabed is removed adjacent to the dredged channel, sediment is eroded less easily by the waves. The bed shear stresses are lower due to the increased depth and the critical shear stress for erosion is higher for the deeper soils.

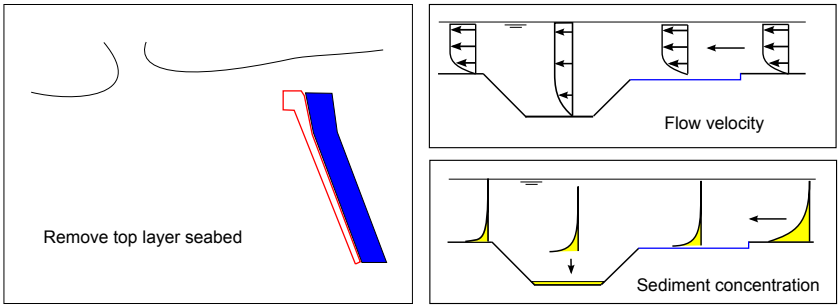

Figure 4.13: Remove top layer seabed

ALTERNATIVE MEASURES

Measure 11: Close estuary

Description: The inflow of fresh water and sediments from the estuary could be stopped by closing off the estuary entirely. This measure results in a reduction of stratification induced currents and no sediment from the estuary reaching the coastal area.

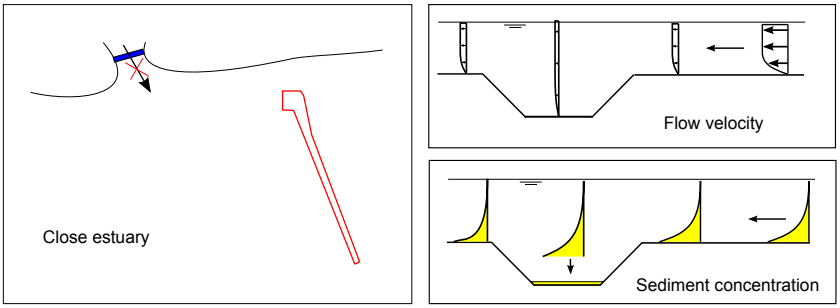

Figure 4.14: Close estuary

Measure 12: Redirect estuary plume

Description: The fresh water plume from the estuary can be redirected in order to reduce horizontal gradients in stratification that cause a coast parallel current near the seabed. The ebb tidal bar in front of the estuary entrance can be locally removed to direct the estuary discharge plume in the desired direction. This could result in lower sediment transport rates towards the channel area.

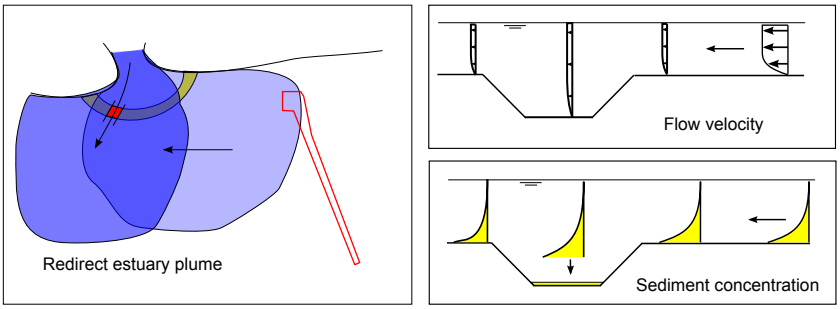

Figure 4.15: Redirect estuary plume

Measure 13: Water jets on channel bed

Description: Water jets in the channel bed can be used as an active system to reduce sedimentation. Sediment is eroded by the flow from the jets and advected by local (tidal) currents (National Research Council, 1987).

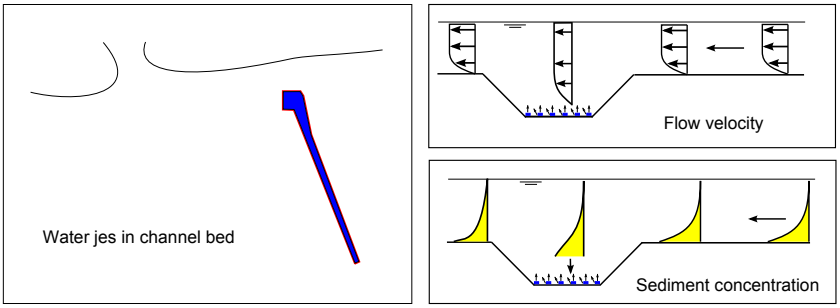

Figure 4.16: Redirect fresh water plume

4.2.2. MAINTENANCE MEASURES

Measure 14: Tidal removal

Description: By the use of agitation in the dredged channel, sediment is mixed over the entire water column. Local (tidal) currents could transport the material away from the dredged channel.

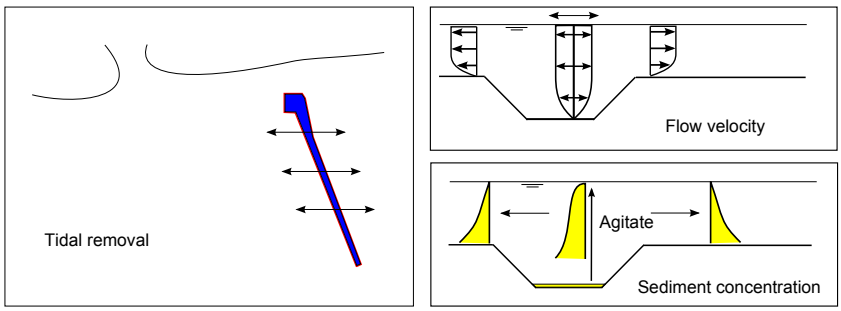

Figure 4.17: Tidal removal

Measure 15: Additional shipping lane

Description: An additional shipping lane could increase the maintenance dredging workability due to lower down-time by hinder from shipping traffic in the channel. Dredging can take place in a separate channel, as passing vessels use the remaining lane(s).

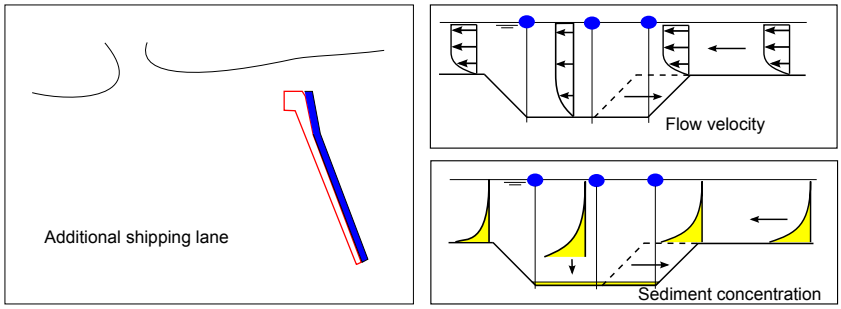

Figure 4.18: Additional shipping lane

Measure 16: Channel over-depth

Description: An over-depth in the channel reduces the required frequency of maintenance dredging. A larger capacity for sediment infill is available before the minimum allowable channel depth is reached and safety for navigation can be guaranteed (National Research Council, 1987).

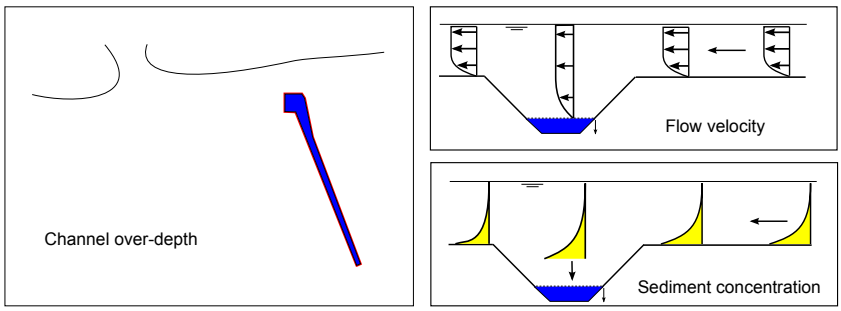

Figure 4.19: Channel over-depth

Measure 17: Sedimentation pits

Description: Local deeper pits could be dredged in the channel bed to concentrate sedimentation at specific locations. Sediment that settles in the dredged channel accumulates in the deeper parts under the influence of gravity. From these pits sediment could be removed with stationary equipment as sediment keeps flowing towards the deep part of the pit.

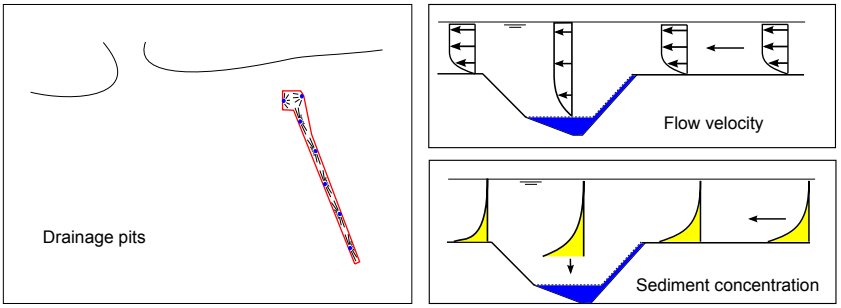

Figure 4.20: Sedimentation pits

Measure 18: Waiting basin

Description: Maintenance dredging activity could be hindered by shipping traffic in the dredged channel. Particularly in the case of long single lane channels significant time is required to clear the channel for cargo vessels to be able to reach the mooring facilities safely. The time required to clear the channel could be reduced by constructing a small refuge type of waiting basin such that cargo vessels can pass without the need to exit the dredged channel completely.

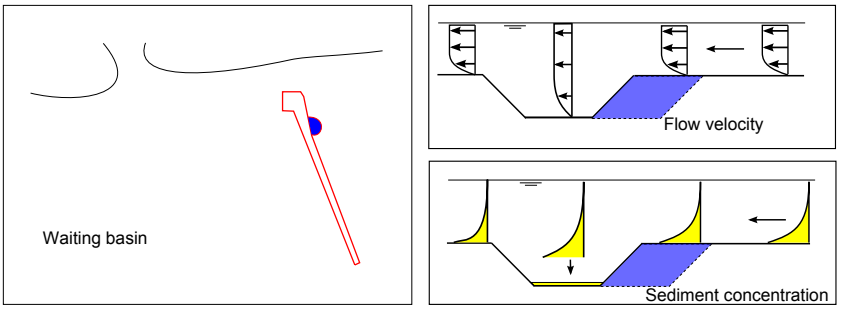

Figure 4.21: Waiting basin

Measure 19: Temporary sediment removal

Description: Sediment could be temporarily deposited just outside the dredged channel to secure safe navigation during high infill rates. The sediment on the sides of the channel should then be removed afterwards separately.

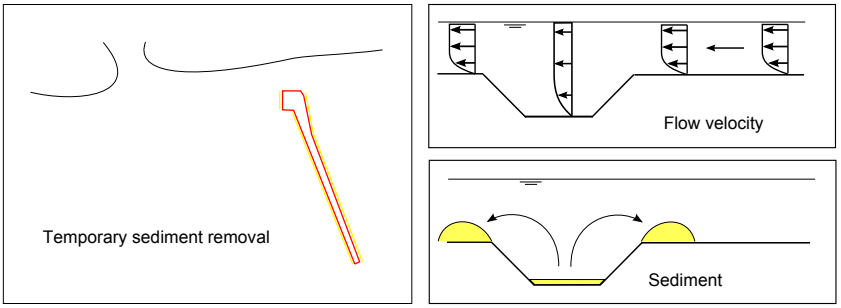

Figure 4.22: Temporary sediment removal

4.2.3. DISCUSSION

The measures proposed in the previous section are discussed here. The potential effectiveness of each measure is described, some with formulas that could be used to quantify the effect of a specific solution. The restrictions or requirements for the effectiveness are discussed as well. Some measures might only work temporarily and therefore an estimation is given on the time scale of the effectiveness. Figure 4.23 shows an overview of all measures.

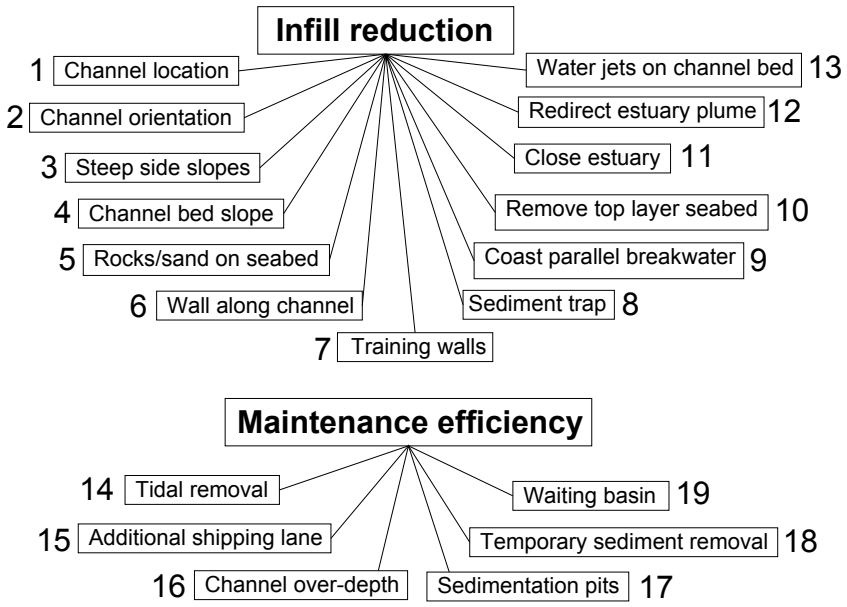

Figure 4.23: Solutions overview

The solutions from Section 4.2 affect different aspects of the infill process. Therefore the solutions are divided into groups based on which infill process is affected by the solution:

1. Trapping efficiency
2. Sediment transport
3. Maintenance efficiency

For each group the associated solutions are discussed separately.

1. TRAPPING EFFICIENCY

The solutions that focus mainly on influencing the trapping efficiency are given in Table 4.1:

Table 4.1: Trapping efficiency measures

#	Measure
1	Channel location
2	Channel orientation
3	Steep side slopes
4	Channel bed slope
13	Water jets on channel bed

Channel location The channel location is often of significant influence on the sediment infill. An offshore shifting of the channel location could imply lower sediment concentrations due to the lower wave induced shear stresses in deeper water. The erosion of mud by waves is proportional to the bed shear stress and therefore a reduction in wave action might be effective in reducing sediment concentrations (ie. transport). As

was shown in Figure A.2 the bed shear stress by waves reduces quadratically with water depth. The sediment concentrations are expected to be reduced due to these lower bed shear stresses and thereby the infill quantities as well. Additionally the trapping of sediment is reduced due to the smaller dredged depth. The offshore current velocities transporting the sediment depend on the driving mechanism of the flow, large scale ocean currents tend to be stronger offshore, whereas local stratification and wind induced currents could be lower at offshore locations.

The location of the dredged channel is often chosen from an economic perspective where a combination of navigation, maintenance and construction costs of the channel and harbor facilities determine the location. In some cases, the location is most probably chosen such that a minimum amount of (capital) dredging is required and other facilities such as a breakwater and jetty do not have to be constructed in deep water. If the reduction in sediment infill is reduced significantly enough by shifting the channel offshore this could be a reasonable argument to choose for the different location and should be taken into account when designing the channel.

Channel orientation The channel orientation with respect to the dominant flow direction determines the trapping efficiency of sediment by its influence on the flow pattern inside the approach channel. Flow refraction could enhance flow velocities near the bottom of the channel and thereby reduce the sedimentation. From continuity it is concluded that the velocity component perpendicular to the channel is reduced due to the increased water depth. However, for the flow component parallel to the channel the velocity could increase. If the channel is small relative to the coastal system characteristic length scale (tidal wave length) it is assumed that the overall water level gradient is not affected by the channel. The flow in parallel direction of the channel experiences less hydraulic drag due to the larger water depth and increases in flow velocity, see Figure 4.24 (PIANC, 2008).

Based on a depth averaged approach, the flow velocity in the channel can be approximated by:

$$u_1 = U_0 \frac{h_0}{h_1} \sqrt{sin^2\alpha_{0,f} + (\frac{h_1}{h_0})^3 cos^2\alpha_{0,f}} \tag{4.1}$$

With u_1= flow velocity in channel [m/s], h_0 = surrounding water depth [m], h_1 = channel water depth [m], $\alpha_{0,f}$ = flow approach angle wrt. channel axis [°], $\alpha_{1,f}$ = flow angle in channel wrt. channel axis [°]. Eq. 4.1 states that the depth averaged flow velocity in the channel depends on the $\frac{h_1}{h_0}$ ratio and $\alpha_{0,f}$ and could increase in magnitude if the right orientation and channel depth is present.

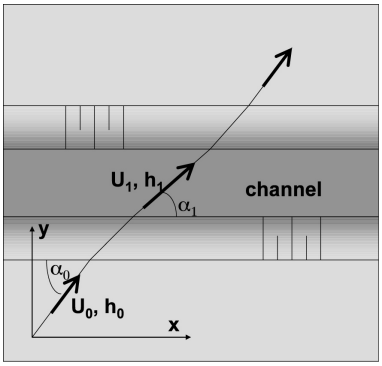

Figure 4.24: Refraction pattern over dredged channel (flow and waves), after PIANC (2008)

Figure 4.25a shows the results of Eq. 4.1 for different approach angles. For approach angles smaller than approximately $\alpha_{0,f} < 60°$, the depth averaged flow velocity increases. However, Jensen et al. (1999) showed with a full 3D model, that flow velocities in the channel only increase for approach angles from around $\alpha_{0,f} <$ 20°and smaller (see Figure 4.25b). This is caused by secondary currents resulting from a non-equilibrium between the pressure gradient and centrifugal forces (PIANC, 2008).

Roos (2004) showed that an adaptation length is required for the flow to accelerate until it reaches its equilibrium velocity $u_{1,e}$ in the channel. The adaptation length is given by $\lambda_a = h_1 C^2/2g$, with C = Chezy roughness [$m^{0.5}/s$], and is generally around a few kilometers.

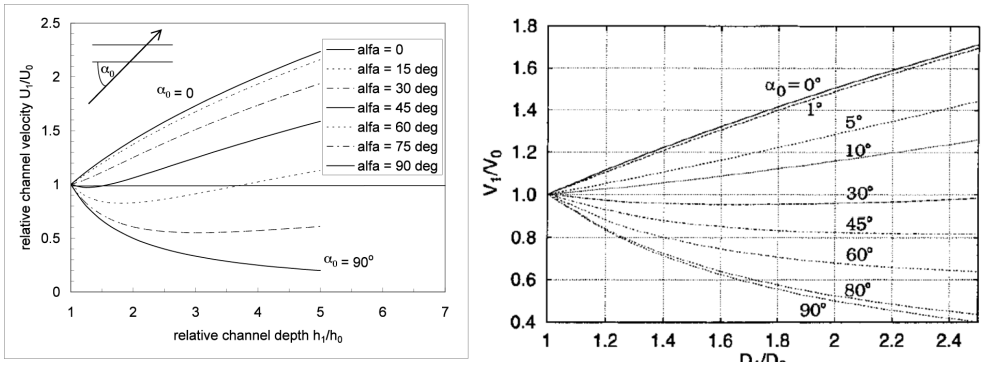

(a) (b)

Figure 4.25: Flow velocity change due to flow refraction $\frac{U_1}{U_0}$ as a function of water depth increase $\frac{h_1}{h_0}$ and approach angle $\alpha_{0,f}$ (a) Depth averaged approach, after PIANC (2008) and (b) 3D approach, after Jensen et al. (1999)

Another effect of the channel orientation is wave refraction, generally wave heights reduce in the channel area due to the larger water depth. However, wave heights could increase up to 30 % for a critical angle ($\alpha_{0,w} \approx 25°$) and thereby increase erosion in the channel. Waves with larger approach angles cross the channel and waves with smaller approach angles tend to refract out of the dredged area. The wave height increase was found by model tests with regular waves, for irregular waves the wave height increase was limited (van Rijn). Additionally, increased wave heights in the dredged channel might be undesirable for shipping safety.

Infill in the dredged channel could be reduced if the sediment carrying capacity of the flow is increased wrt. to the original layout. Based on the given argumentation on the effects of the channel orientation, the effectiveness of this measure is most significant if small approach angles for the flow can be obtained ($\alpha_{0,f} < 20°$). Depending on the specific location it might be possible to adjust the channel orientation. For a dominant flow direction parallel to the coast the dredged channel should be orientated almost parallel to the coast as well, which requires the channel to be very long in order to cover the required depth increase from offshore to near shore. This could lead to a significant increase in capital dredging and might not be economically feasible. Another aspect regarding the orientation of the channel is the direction of the waves, the orientation is commonly determined based on vessel navigation wrt. the dominant wave direction. Therefore the channel orientation cannot always be chosen based on the flow or wave refraction effects.

Increasing the sediment carrying capacity of the flow in the channel could be particularly effective for Type 1 infill as the infill and sediment concentration near the bed are more dependent on the flow velocity. In the case of saturated concentrations (Type 2 infill), sediment will most probably be transported along the bed into the channel. The amount of sediment settling in the channel is probably not reduced by an increase in channel parallel flow velocity. Additionally, the flow needs significant increase to suspend the sediment over the entire water column, which is not expected to be achieved by this measure. However, as long as the sediment remains mobile in the channel, the increased flow velocity could increase the transport of the sediment suspension out of the channel in parallel direction.

Channel side slopes The channel side slopes decrease the overall width of the channel and could thereby reduce the trapping efficiency. In the case of very steep slopes (steeper than 1:5) flow separation occurs causing the flow pattern to become more complicated, this is illustrated in Figure 4.26. An increase of trapping of sediment could be caused due to the recirculation zone.

Side slopes of a dredged channel are usually constructed as steep as possible to reduce the capital maintenance dredging volume. In muddy systems such as discussed in this report, slopes are usually gentle as fine sediments have relatively small angles of internal friction. Often additional infill is expected as a result of slope instability. Constructing steeper slopes is therefore not practical in many situations. Steeper side slopes can only be constructed by the use of rock or quay wall type of structures, which do require additional construction materials and are not further considered in this report.

Type 2 infill is characterized by saturated conditions, with sediment concentrated close to the bed. The trapping is therefore not influenced by the time available for the suspension to settle, but more by the amount of sediment able to be transported out of the channel.

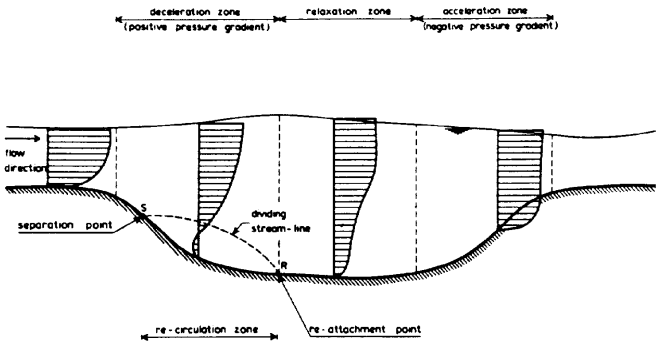

Figure 4.26: Flow over channel in the case of steep side slopes, after National Research Council (1987)

Channel bed slope The channel bed slope could be constructed such that sediment is able to flow out of the channel under the influence of gravity. The required slope is predominantly determined by the characteristics of the mud suspension, such as the layer thickness and sediment concentration. Figure 4.27 shows the mean flow velocity of a fluid mud layer (u_m) as a function of the mud layer thickness (d_m) for different bed slopes (β). On the left side of the 'dewatering' line the fluid mud layer will consolidate and reduce in speed. On the right side of the 'entrainment' line, sediment will disperse vertically due to instability of the density current.

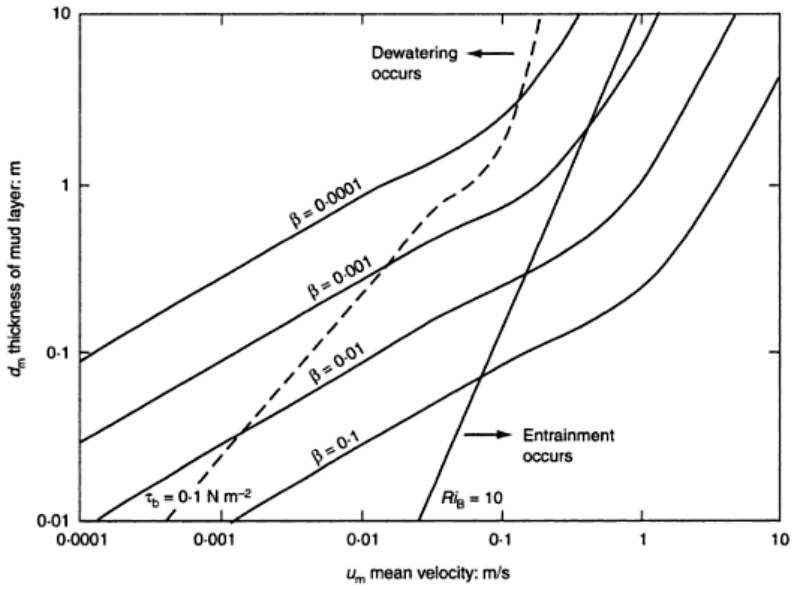

Figure 4.27: Mean flow velocity u_m of fluid mud layer with thickness d_m on a sloping bed for different bed slopes (Whitehouse et al., 2000). Note: The fluid mud dry density used in the graph is 1075 kg/m^3 and the dynamic viscosity is uniform (0.7 Ns/m^2) according to Whitehouse et al. (2000). However a dry density of 1075 kg/m^3 would represent a stationary layer (Winterwerp and van Kesteren, 2004), therefore it is assumed that the given density represents the bulk density instead of the dry density.

Following from Figure 4.27, a slope in the order of 1:1000 is required to have a stable density current for a mud layer thickness of 1 m, thinner mud layers require steeper slopes. A mud layer of 1 m will probably not occur instantly, it is expected that the mud layer thickness in the channel grows gradually by accumulating infill. Depending on the consolidation rate a mobile mud layer could remain present in the channel until a thickness is reached that is able to move under the influence of gravity. For specific cases, consolidation behavior is required as well as more sophisticated density flow modeling to estimate the flow of the fluid mud layer more precisely.

The required bed slope to cause a density current in the approach channel could be steeper than the surrounding bed slope. That would imply that the dredged depth increases in offshore direction, and could result in a deep pit at the end of the channel where sediment accumulates. Therefore it is not practical to

apply this measure if steeper slopes are required than the surrounding seabed.

The amount of additional capital dredging is estimated based on a required bed slope of 1:1000 to initiate a density current. A channel length of 10,000 m and width of 250 m result in an amount of sediment removal in the order of $1 * 10^7$ m^3. The time scale of the measure is expected to be influenced by sedimentation on the bed despite the bed slope. The time scale of effectiveness is difficult to determine as for a perfect effective bed slope the sedimentation should be zero. However, it is not expected that the channel bed slope would prevent all sedimentation and maintenance dredging would still be required.

Water jets on channel bed The working mechanism of water jets in the channel bed is such that sediment is resuspended continuously or periodically by the jets and carried away by local currents.

This measure is most commonly applied at berthing facilities to keep the area in front of the quay wall or jetty up to depth. It is most effective for eroding beds parallel to the dominant current direction, once sediment is brought in suspension it is carried away by the local currents. Water jets are considered less practical in larger areas due to the limited areal influence of the jets (PIANC, 2008). The jets create a teardrop shaped scour hole with the maximum width of around one-third of the scour distance, at around 2/3 of the scour distance see Figure 4.28. Jenkins et al. (1993) developed relations for the jet-induced shear stresses as a function of jet discharge velocity, jet diameter, sediment density and the maximum range of jet shear stress contours:

$$X_m = d[\frac{\tau(u_{0,j} d_j/\upsilon)^{0.4}}{120\rho_m u_0^2}]^{-0.417} \tag{4.2}$$

With u_0, j= jet discharge velocity [m/s], d_j= jet diameter [m], ρ_m= bulk density mud mixture [kg/m^3], υ = kinematic viscosity of water [m^2/s] and τ= applied jet shear stress [dynes/cm^2]. The graphs in Figure 4.29 show results from Eq. 4.2. The stresses are used in dynes/cm^2, 1 dynes/cm^2 is equal to 0.1 Pa.

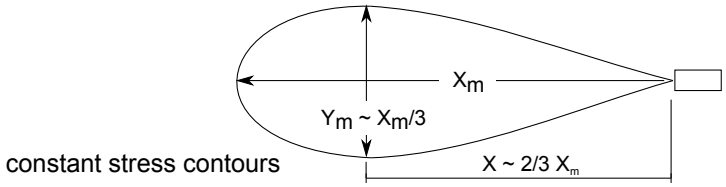

Figure 4.28: Constant stress contour from jet flow, $x \approx 2/3 X_m$ (Jenkins et al., 1993)

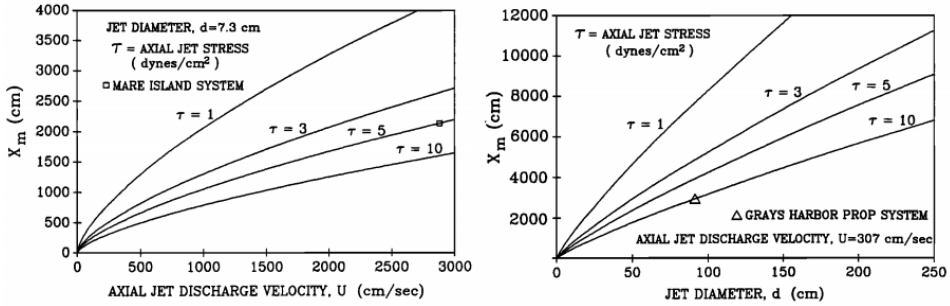

Figure 4.29: Maximum range (x_m) of jet shear stress (τ) depending on axial discharge velocity (U) (left graph) and jet diameter (d) (right graph), (1 dyne/cm^2 = 0.1 Pa) Jenkins et al. (1993)

Depending on the local critical shear stress for erosion of the mud (τ_e) the area of influence of a jet can be estimated. Assuming a critical shear stress for erosion $\tau_e = 0.5$ N/m^2, the maximum range of the jet shear stress (X_m) as tested by Jenkins et al. (1993) would be around 20 m. For a channel of 250 m wide, and assuming entire coverage of the channel bed by the jet induced shear stress, 1250 water jets would be required for 1 km of channel length.

2. SEDIMENT TRANSPORT

The solutions that focus on reducing sediment transport towards the dredged channel are:

Table 4.2: Sediment transport measures

#	Measure
5	Rocks/sand on seabed
6	Wall along channel
7	Training walls
8	Sediment trap
9	Coast parallel breakwater
10	Remove top layer seabed
11	Close estuary
12	Redirect estuary plume

Rocks/sand on seabed Rocks or sand on the seabed could be able to reduce sediment transport towards the dredged channel by multiple mechanisms, as presented at page 59. The solution could be constructed such that only the bed roughness is increased, or that erosion from bed sediments is reduced as well. The latter requires a significantly larger height of the layer of rocks or sand. The measure is highly depending on the local conditions and requires significant further consideration for each of the effects. The effects of the measures are discussed shortly.

Reduce sediment transport

- Reduce flow velocity
- Wave energy dissipation
- Reduced erosion due to coverage of underlying mud

Reduce trapping efficiency

- Vertical mixing of sediment

Time scale

- Coverage of rocks/sand by mud

Reduced flow velocity - The flow velocity could be reduced by increasing the bed friction by applying sand or rocks on the seabed. If the flow over the seabed experiences higher bed friction, its depth averaged velocity decreases. The increase in roughness could change the flow velocity profile from smooth (in the case of smooth mud beds) to rough (once rocks or (coarse) sand are applied on the bed) if the roughness length (z_0) is increased sufficiently. The flow velocities in the lower region could increase by the turbulent flow profile, as is shown in Figure 4.30. The associated change in sediment transport is dependent on the sediment concentration profile.

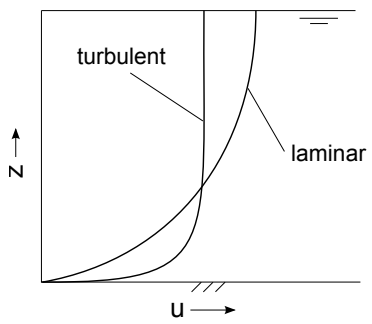

Figure 4.30: Flow velocity profile for turbulent and laminar flow

Sediment concentration profile - If sediment is mixed evenly over the entire water column the total transport would be reduced due to the lower depth averaged velocity. However, sediment is commonly not evenly distributed over the water column and an increase in flow velocity near the bed enhances sediment transport.

The Rouse profile for fine sediment gives a suspended sediment concentration profile from the balance between the settling flux and turbulent mixing flux of sediment for equilibrium conditions, (see Section 2.4.3). Based on the assumption of a logarithmic velocity profile (hence a parabolic diffusivity profile). The increased roughness could effect the vertical turbulent mixing through increased production of turbulence at the bed.

The turbulent mixing of sediment can be determined by the instantaneous sediment flux in vertical direction. This is given by the following equation (Winterwerp and van Kesteren, 2004):

$$\overline{w'c'} = -\varepsilon_{T,z} * \frac{\partial \bar{c}}{\partial z} \tag{4.3}$$

With $\overline{w'c'}$ = vertical turbulent fluctuations in transport of sediment averaged over the turbulent timescale [kg/m^2/s], $\varepsilon_{T,z}$ = vertical turbulent eddy diffusivity [m^2/s], $\frac{\partial \bar{c}}{\partial z}$ = vertical gradient in turbulent timescale-averaged sediment concentration [kg/m^2].

The settling flux of sediment $F_{settling}$ [kg/m^2/s] is given by:

$$F_{settling} = W_s * c \tag{4.4}$$

With W_s= median settling velocity [m/s] and c = sediment concentration [kg/m^3].

With higher roughness the shear velocity u_* increases and therefore the turbulent mixing is enhanced. However, whether vertical mixing is effective depends on the capacity of the flow to keep the sediment in suspension. For Type 1 infill this measure is probably

The flux Richardson number (Ri_f) gives a relation between the buoyancy production and destruction, and can be used to determine the stability of the sediment concentration profile. If Ri_f exceeds a critical value $Ri_{f,crit}$ the sediment concentration collapses and a high concentrated layer near the bottom is established as was seen in Section 2.4.3. A formula for the depth averaged saturation concentration (C_s) is Winterwerp (2001):

$$C_s = K_s \frac{\rho}{\Delta g} \frac{u_*^3}{hW_s} \tag{4.5}$$

Where $K_s \approx 0.7[-]$, ρ= water density [kg/m^3], Δ= relative density difference between solids and water [-], u_* = shear velocity [m/s], h = water depth [m] and W_s= reference settling velocity [mm/s]. It can be seen that an increase in shear velocity could increase the saturation concentration as well. It should be determined whether the increase in shear velocity is sufficient to mix sediment.

Wave dissipation - Wave dissipation due to increased roughness could occur as well,the dissipation of wave energy for rough beds is given by:

$$D_f = \frac{1}{2\sqrt{\pi}\rho_0 f_w u_{orb}^3} \tag{4.6}$$

Where f_w = friction factor given by $f_w = min 0.3, 1.39(\frac{A}{z_0})^{-0.52}$, $A = \frac{u_{orb}}{\omega}$ by Soulsby et al., 1993b.

For smooth beds the friction factor is:

$$f_w = 0.0251 Re_w^{-0.187} for Re_w > 5 * 10^5 \tag{4.7}$$

The increased roughness might reduce wave heights. However, the increased friction causes additional shear stress and therefore erosion could be enhanced depending on the application of the solution.

Time scale - The sediment supplied towards the area where the measure is applied remains unchanged. If sediment transport is reduced over the rough bed, sedimentation takes place and the measure is covered in mud over time. If sediment transport is not reduced, vertical mixing is the most important mechanism in reducing infill of the dredged channel. Even in the case of increased vertical mixing, the rocks or sand are expected to sink into the weak soil and be covered in mud eventually by sedimentation during periods of low wave energy.

The required materials are estimated for an area of 1 km wide and the full length of the dredged channel of 10 km. A layer thickness of 0.5 m should be sufficient to increase the roughness, however if erosion of mud underneath the layer is to be prevented a layer thickness of 1.5 m is assumed to be required. The amount of required materials is in the order of $1 * 10^7$ m^2 of sand or $1 * 10^{10}$ t of rocks.

Summary - Considering the large range of effects from this measure, not all possible effects are elaborated extensively. The separate measures require more extensive research to be quantified. If sediment is mixed over the water column by increasing the saturation concentration, the reduction in infill could be considerable. However, it is not expected that an increase in roughness is capable of increasing the saturation concentration sufficiently. Particularly due to the fact that sediment is transported towards the considered area in saturated state it is expected that coverage of the solution by mud will occur. Therefore this measure is not expected to be effective.

Block sediment transport Blocking the sediment transport (for example by a vertical wall parallel to the channel) could be effective in reducing sediment transport towards the dredged channel as sediment can physically not reach the channel due to the obstruction.

High crested wall A high crested vertical wall could be constructed to block the entire transport of sediment in lateral direction. The flow and wave pattern is probably significantly changed if a structure of this magnitude is constructed. The change in flow pattern is difficult to assess without numerical modeling. However, it is plausible that the flow is contracted around the edges of the structure, creating high flow velocities around the structure that are unfavorable for shipping. The zone behind the breakwater could be low energetic and enables fines to settle, see Figure 4.31.

In circumstances as considered here, where a muddy seabed is present, the subsoil is generally weak. Constructing such a large structure just to reduce sediment infill is therefore often not practical. Depending on the availability of rock the measure could be relatively costly for the potential reduction in sediment transport.

If the structure is constructed over the total length of the channel (~ 10 km), the amount of rocks is in the order of $1 * 10^9$ t for a 1:2 slope and average water depth of 10 m. A time scale for the effectiveness is difficult to assess due to the complexity of the effects on the flow regime. Bypassing of sediment is expected to occur and thereby reduce the effectiveness of this measure over time.

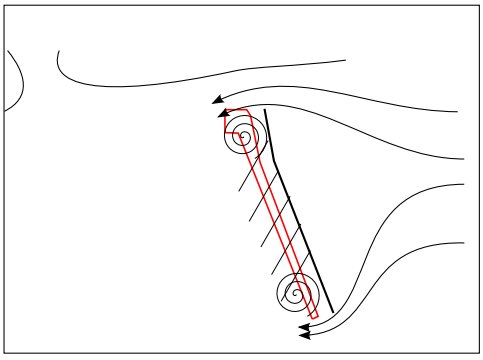

Figure 4.31: Flow contraction around vertical wall

Low crested wall A low crested wall has been applied in Japan and investigated by Tsuruya et al. (1990). Here a reduction of 30 % of infill was obtained. The effectiveness of this measure is highly determined by the flow profile, as flow perpendicular to the walls is contracted over the walls and thereby increases in flow velocity (thus sediment transport capacity). If the flow is directed more oblique to the walls, the flow can be somewhat redirected and steer the sediment transport in offshore direction. Sediment would probably accumulate in front of the vertical wall and thereby reduce the time scale of the effectiveness. Once sediment is accumulated enough to bypass the vertical wall, the effect is reduced significantly. If the wall is constructed at a height of 2 m, the required amount of rock is in the order of $1 * 10^8$ t. The timescale before bypass will start is probably in the order of months, depending on the sediment transport rate.

The effectiveness of blocking sediment transport is difficult to assess quantitatively with a simple analysis.

Hydronamic modeling should be carried out in order to find the exact effects of the walls on the flow pattern at a specific situation. Due to the expected timescale and large amount of required rocks, different alternatives to mitigate infill should be considered before this measure is analyzed fully. Changing the flow pattern over such a large scale is often not practical and leads to additional (often unforeseen) problems in sedimentation. Therefore this measure is not expected to be effective.

Redirect flow A solution was proposed to redirect the flow using training walls. The effectiveness of this measure could be compared to changing the channel orientation and induce a self-cleansing effect in the channel.

Training walls are used in harbor basins along rivers to increase the flow circulation and thereby reduce sedimentation PIANC (2008). In order to achieve a considerable change in the hydrodynamics, the flow should be changed over a large part of the dredged channel. The possibility to redirect flow along the entire channel length of the order of 10 km is difficult to assess quantitatively with simple tools. Additionally, in river systems the flow has a constant direction and the effects of training walls are more easily to assess. For Type 1 infill, an increase in flow velocity could reduce the amount of sediment settling in the channel due to the larger capacity of the flow to keep sediment in suspension. For Type 2 infill the increase in flow velocity would probably decrease the amount of sediment settling in the channel to a lesser extend, because the sedimentation is less determined by vertical mixing processes that are enhanced by the higher flow velocities.

If it is assumed that the training walls need to be in the order of 5 m high and 3 km long and placed around 250 m apart, 40 walls are required over the 10 km channel length. The walls could be constructed by rocks as sill-like structures. The amount of required rock is in the order of $1 * 10^{10}$ t.

Influence on sediment transport due to scour and turbulence as a result of wave and current action around these structures should be taken into account. Hydrodynamic modeling is required to find the potential effectiveness in changing the flow pattern by the training walls. Similar to the previous measure, changing the flow over such a large area by solid structures is often not practical and could lead to additional (often unforeseen) problems. Therefore this measure is not expected to be effective.

Trap sediment A sediment trap could be used to prevent sediment from causing infill in the dredged channel. The total amount of dredged material is probably not reduced by the sediment trap, because the infill takes place in the trap instead of the main channel. Therefore the benefit from a sediment trap is such that a buffer is created to reduce the frequency of maintenance dredging and reduce the hinder by dredging to shipping traffic in the dredged channel.

The effectiveness of a sediment trap is determined by its capacity to reduce sediment transport towards the main channel. For Type 1 infill the sediment trap is expected to be less effective than for Type 2 infill, as the trapping efficiency is probably higher for Type 2. The trapping efficiency could be estimated by dredging a trial pit and/or sediment transport modeling. The dimensions of the sediment trap should be chosen based on the desired capacity and maximum trapping efficiency. The amount of dredged material for the sediment trap is in the order of $1 * 10^6$ m^3.

Coast parallel breakwater A coast parallel breakwater was proposed to reduce sediment transport behind the structure as bed erosion by waves is reduced. The breakwater could either be constructed high crested or submerged as long as waves are dissipated significantly.

The following aspects are of influence on the dimensions of the breakwater:

- Offshore distance;
- Wave diffraction behind the breakwater;
- Sediment settling distance.

The breakwater should be long enough to limit waves over a significant area to prevent sediment already in suspension from reaching the dredged channel as well as limit the effect of diffraction behind the breakwater.

Waves are commonly able to erode fine sediments at quite a large depth if the top bed layer is weak. Therefore it is assumed that the breakwater should be located at a water depth of at least 10 m. The cross shore length of the dredged channel over which sediment transport is reduced is around 5 km. Due to this large distance, the length of the breakwater is assumed to be in the same order of magnitude because of

diffraction effects. It is assumed that sediment is able to settle over this distance, which leads to accumulation behind the breakwater. The required amount of rock is estimated based on a breakwater with a height of 10 m, a slope of 1:2 and a length of 5 km. The amount of rock would then be in the order of $1 * 10^9$ t.

There are additional effects that affect the feasibility of this measure and should be taken into account:

- Stability of accumulated sediment behind structure;
- Change in hydrodynamics;
- Locally generated (wind) waves behind breakwater.

The exact effects of this measure are difficult to assess analytically and require more sophisticated analysis. However, as is the case for the previous two measures, the availability of material (rocks) as well as the soil characteristics play an important role in the feasibility of this solution.

Remove top layer of sediment If the top layer of sediment is removed, the sediment transport could be reduced due to lower erosion rates. The increase in water depth and stronger subsoil could reduce erosion of the bed.

The erosion of sediment is governed by wave action, which is reduced in case of increased water depth. Generally, hydrodynamic energy to mobilize sediment is greater than the energy to keep fines in suspension (Winterwerp, 2014) (Type 1 infill). Therefore, a small reduction in wave induced shear stresses is probably not effective in reducing the amount of sediment transport. The soil strength and critical shear stress for erosion determine the depth to which the bed should be lowered.

Assuming this measure would significantly reduce erosion, sediment supply could cause infill in the area with the lowered bed level and only a temporary sediment transport reduction is achieved. This measure is then similar to the sediment trap, however a larger surface area should be removed.

The shore parallel distance is determined by the distance required for sediments to settle, again based on the sediment concentration profile and (hindered) settling velocity. Assuming 2 m of soil should be removed to reach a stronger subsoil and a shore parallel length of 500 m is required, the dredged volume is in the order of $1 * 10^7$ m^3.

The time scale is directly linked to the sediment supply and assuming 100 % trapping, the dredged volume is divided by the sediment transport rate. The timescale would then be in the order of months (depending on local conditions). This measure can be seen as an alternative of the sediment trap, which increases the capital dredging costs and reduces the maintenance dredging temporarily. Compared to the sediment trap this measure is expected to have a lower trapping efficiency due to the smaller depth. Waves are more capable to keep sediment suspended for this case compared to the sediment trap. Therefore this measure is not expected to be effective.

Reduce estuary influence In cases where an estuary is present close to the dredged channel, such as discussed in this report, measures could be taken to reduce the effects of the estuary on the sediment transport. Before looking at measures to alter the interaction of the coastal system to the estuary, the influence of the estuary should be investigated.

One option is to close off the estuary, however this implies significant additional measures and permits in most cases. The fresh water discharge from the estuary should be redirected to another estuary or river and the ecological effects in the estuary basin should be considered before such a severe change in the system is executed.

Residual transport is assumed to be (partly) determined by stratification induced currents. Reducing the stratification could therefore be effective in reducing sediment transport. Redirecting the fresh water plume away from the dredged channel could lower the horizontal gradients in stratification and thereby the flow velocity of the near bed current in the area of the dredged channel, see Figure 4.32.

Redirection of the fresh water discharge from the estuary could be achieved by changing the ebb tidal bar in front of the estuary entrance and cause the flow to move away from the dredged channel. The effect of this measure is case specific due to the characteristics of the specific estuary. Hydrodynamic modeling should be undertaken to estimate the effectiveness of this measure for specific sites. The amount to be dredged from the river bar would be in the order of $1 * 10^7$ m^3. The breach in the ebb tidal bar could experience infill if the flow is not strong enough to keep it open. This depends on the initial design, however an estimate of the timescale is years.

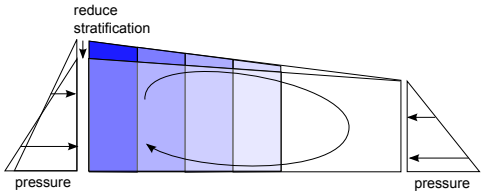

Figure 4.32: Reduction in horizontal stratification, thereby reducing the near bed flow

3. MAINTENANCE EFFICIENCY

The maintenance measures are discussed in this section. The measures that increase maintenance efficiency that were provided in the previous section are given in the table below:

Table 4.3: Maintenance efficiency measures

#	Measure
14	Tidal removal
15	Additional shipping lane
16	Channel over-depth
17	Sedimentation pits
18	Waiting basin
19	Temporary sediment removal

Tidal removal Tidal removal of sediment from the dredged channel could be an efficient way of maintaining the (nautical) depth of the channel. Sediment is mixed over the water column by agitation and should then be carried away by (tidal) currents. The actual removal of sediment by this process is determined by the sediment settling properties and flow pattern. Sediment with a high settling velocity is most probably not able to be transported out of the channel by the tidal currents, especially if the currents are only weak. Low settling velocities cause the sediment to be transported over larger areas by the local currents.

The sediment transport distance could be determined by the settling time or by the residual currents. The mean settling time is given by:

$$T_{m,set} = \frac{z_{max}}{w_{s,50}} \tag{4.8}$$

With $T_{m,set}$= mean settling time, z_{max}= maximum water depth above surrounding bed where sediment is brought to by agitation and $w_{s,50}$= mean settling velocity. The distance where the sediment is carried to is found by integrating the tidal flow velocity over the settling time.

$$X_{disp} = \int_{t=0}^{t=T_{m,set}} u_{tide}(t)dt \tag{4.9}$$

Where X_{disp}= displacement in shore parallel direction, u_{tide}= (depth averaged) tidal flow velocity in shore parallel direction. The same could be done for sediment displacement in cross shore direction.

If $T_{m,set}$ is larger than the tidal ebb/flood duration ($T_{flood/ebb}$), sediment will be suspended longer than half a tidal cycle and the net displacement of sediment away from the channel could be limited. Figure 4.33 shows the sediment displacement by the tidal currents for different $T_{m,set}$ relative to the period of a flood tide T_{flood} for high settling velocities. The flood flow is assumed to be directed towards the left in the figure. Figure 4.34 shows the sediment displacement for relatively low settling velocities, where on the left side a residual current is present over the total water depth and on the right side stratification is present with larger residual current in the upper part of the water column than in the lower part resulting in a net displacement in ebb direction.

Ebb flow is assumed to be opposing the mean residual current. Sediment that is carried away by the ebb flow in shore parallel direction will most probably cause infill in the dredged channel eventually by the

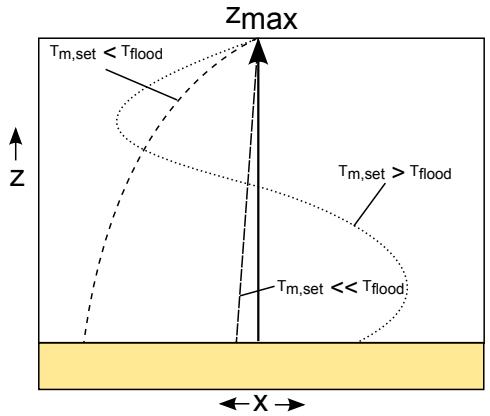

Figure 4.33: Sediment displacement for different (relatively high) settling velocities

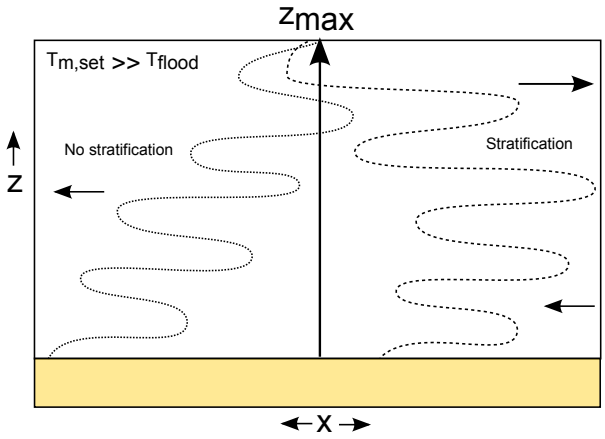

Figure 4.34: Sediment displacement for relatively low settling velocities by residual currents with and without stratification

residual flood directed current. Therefore sediment transported on the ebb tide could only be effective in reducing infill if the tidal flow is directed Southwards as well. This way sediment is eventually transported offshore and passes the channel at the deeper parts.

During the flood tide, sediment is transported in the direction of the residual current that is responsible for the dominant transport mechanism. Therefore sediment removed from the channel during the flood tide is less likely to return and cause infill later on. However, if sediment has a very low settling velocity, the flow alters direction while the sediment is still in the upper part of the water column. Thereby transporting sediment back towards the dredged channel.

Based on the above explanation this measure is determined by the local flow pattern and should be considered for each specific case. Assuming a (low) mean settling velocity of 0.1 mm/s and a z_{max} of 10 m the $T_{m,set} = 10,000$s $\approx$ 3hr and therefore sediment should be able to settle for a large part during one flood or ebb cycle.

Additional shipping lane An additional shipping lane could be constructed if the infill in the dredged channel is of such quantity that maintaining the depth is not possible due to the hinder of shipping. The sediment trap was proposed to be useful in such cases and requires significantly less dredging compared to a entire second shipping lane. The additional shipping lane could be used if the trapping efficiency of the sediment trap (and thus probably of the main dredged channel) is low. If only a limited amount of sediment is captured by the sediment trap, the main dredged channel will experience almost the same amount of infill as without the sediment trap. The sediment infill should then still be of such high quantity that maintenance dredging is not economically feasible.

However, it is expected that if the trapping efficiency of the sediment is low, the trapping efficiency of the

main dredged channel will probably low as well. If this is the case sediment infill rates would in many cases not be of such high quantities that additional measures for maintenance efficiency are required. This does depend on the dimensions of the sediment trap and dredged channel of course.

The additional amount of capital dredging for an additional shipping lane is in the order of $1 * 10^7$ m^3.

Channel over-depth An over-depth in the channel could reduce the required maintenance dredging frequency due to a larger buffer for sediment infill before the minimum navigational depth is reached (Rijn, 1986). This measure is often applied and is particularly useful in cases with episodic infill events. Large infill quantities in a short period of time could decrease the channel depth significantly while maintenance dredging capacity is not able to meet the increased supply. The over-depth should therefore be determined based on the expected peak infill rates and the maximum maintenance dredging capacity. The additional amount of capital dredging is in the order of $1 * 10^6$ m^3, depending on the expected amount of peak infill.

Sedimentation pits The measure that proposed sedimentation pits to be constructed in the channel is based on the assumption that sediment deposits in a fluid layer in the channel that is able to move under the influence of gravity. Therefore stationary dredging equipment could be used to remove sediment from the sedimentation pits. The pits are located such that half can be emptied during the ebb tide and half during the flood tide, using the agitation process as discussed above. The emptying process of the sedimentation pits is therefore not practical in all situations and the use of stationary equipment should be considered for each specific site.

Another possibility is to dredge two trenches on each side of the channel bed, such that sediment infill is concentrated in these areas and can be removed more easily compared to a flat channel bed. The advantage of this additional possibility is not treated in detail and should be considered in further research.

A bed slope in the order of 1:100 is assumed to be required to initiate a density current by a thin fluid mud layer. The amount of dredged material to construct the sedimentation pits is dependent on the depth of the pits and the number of required pits. If the bed slope over the width of the channel (250 m) is taken at $1:100$, the depth of a pit should be around 2.5 m. The area covered by each pit is assumed to be a half circle with a surface area of approximately 0.1 km^2 (for a slope of 1:100). For a channel of 10 km long and 250 m wide, 25 sedimentation pits would be required. This would result in an increase in capital dredge in the order of $1 * 10^6$ m^3. The initial dredging of the sedimentation pits is relatively complex, particularly due to the large number of required pits.

Waiting basin A waiting basin could be constructed for dredging vessels to be able to wait for shipping traffic to pass the dredging vessel before continuing the dredging cycle. This feasibility of this measure is dependent on the down-time for maintenance dredging by the hinder of shipping traffic and the costs associated with the waiting basin. If waiting times due to single ships is low, the waiting basin would not increase the maintenance efficiency much as dredging vessels have to move in and out the waiting basin often. If single vessels cause significant down-time due to long sailing/mooring times the measure could be more effective. Dredging vessels should be able to wait in the basin safely and be able to sail back to the channel easily to continue work. Therefore the geometry of the waiting basin should be determined. If dredging vessels need to be moored in the waiting basin, time is lost due to the mooring process and additional costs are associated with the mooring facilities. The capital dredging for the waiting basin is estimated to be around $1 * 10^6$ m^3 if the basin requires a surface area of 0.25 km^2 and water depth of 10 m.

Temporary sediment removal During peak infill periods, sediment could be deposited just outside the shipping lane if the capacity of (regular) maintenance dredging is insufficient. As the infill is assumed to consist of mud, the deposited material is more likely to flow back into the dredged channel compared to coarse sediment. Depending on the rheological behavior of the deposited material, an estimate can be made on the amount of sediment that is expected to flow back into the channel within a short period of time and thereby cause additional infill. The sediment deposition is only required to remain stable for a short period of time and should later be removed. However, during peak infill periods, the sediment transport capacity is high, which is caused by high waves and high flow velocities. Therefore, sediment deposited outside the channel is more likely to be eroded and transported back into the channel during these peak infill periods.

The sediment should not be deposited on the side slopes of the dredged channel due to the possibility to initiate a sediment flow towards the dredged channel, therefore a minimum distance of a few to several hundreds of meters is required, depending on the slope steepness.

4.2.4. CONCLUSION

In the previous section, 19 measures were established and discussed. Table 4.4 shows an overview of these measures with a separate list for measures that focus on maintenance dredging. An indication of the most important properties of the measures are determined from the discussion section. The columns 'Type 1' and 'Type 2' show an indication whether the measure is expected to be effective for that kind of infill. Type 2 infill is considered to be the dominant infill mechanism for the given circumstances, therefore Type 1 infill is treated to a lesser extend.

Three types of mitigation measures are identified that focus on separate aspects of the infill process:

1. Reduce sediment transport towards the channel
2. Reduce trapping efficiency of the channel
3. Increase maintenance efficiency to remove sediment from the channel

The first two types focus on the prevention of infill, whereas the third improves the process of removal of sediment from the channel. The measures shown in Table 4.4 have different practical applications and effective timescales.

Different types of measures are also found based on the construction method. Some measures require the use of rocks or other heavy materials, whereas other measures require additional dredging. The channel location and orientation can only be applied if the channel is not yet constructed, as these measures should already be implemented in the initial design phase. Solutions that apply measures adjacent to the channel can be applied later, for example if it is found that infill rates are higher than expected originally.

Effective time scales The time scale of the effect of the measures indicate how often the measure should be maintained in order to uphold its effectiveness. A short time scale results in frequent maintenance (dredging) and therefore lower feasibility of the solution. Measures that do not have specified times scales are assumed to have permanent effects, such as a different channel layout or closure of the estuary. A consideration based on the additional costs for the measure and the effective time scale should be carried out to find the most feasible option.

Practical aspects Many considered measures require rocks to construct ('hard') solid structures. Due to the required dimensions these measures are associated with relatively high costs in comparison to regular maintenance dredging. Additionally, some measures have limited time scales of effectiveness and are therefore less economically feasible. Muddy systems are often found in deltaïc regions, where rivers carry fine sediment towards the coasts. Due to the geological properties of deltaïc regions, the availability of rocks in these regions is generally low. Additionally, the subsoil in muddy areas is commonly weak which is unfavorable for the foundation of heavy structures. Therefore measures that require rocks are often not attractive from a costs point of view. Solutions 2, 3, 5, 7, 9 and 11 are not expected to be feasible to mitigate Type 2 infill based on their effectiveness, costs and effective time scale.

The other measures are concluded to have higher feasibility, however the actual effectiveness is site specific. Measures that do not require significant amounts of rock are found to have relatively high feasibility due to lower initial costs. Yet, the effectiveness of the different measures is only an indication and based on the assumption that the solution would work as proposed (particularly in the case of the channel bed slope).

The measures that increase maintenance efficiency should be considered for each specific case, based on the availability of dredging equipment, down-time due to shipping and infill quantity. All solutions are found to be effective, however dependent on the local conditions. A combination of the maintenance efficiency measures is considered to be the most effective, as the measures focus on different aspects of the maintenance dredging program.

Overall Due to the complexity of fine sediment infill and the variability in local conditions, it is difficult to find generally applicable measures. A single solution that mitigates the total sediment infill significantly on a long term is not expected to exist. Influencing the hydrodynamic and morphologic conditions of a large (muddy) system is generally challenging and requires detailed knowledge of the specific site. Based on the analysis, generic solutions that reduce sediment transport to a proposed channel on a long term were not found. Measures that focus on removing sediment from the channel efficiently are expected to have the highest feasibility in general terms.

An aspect of the main objective of this thesis is to find measures that use preferably natural processes. As is seen in this section, the solutions that use the most ('non-natural') rigid structures are expected to have lower potential due to the costs and additional effects.

Table 4.4: Generic solutions overview

#	Name	Type 1	Type 2	Required material	Time scale	Main effects	Main restrictions
1	Channel location	+	+	-	-	Reduced transport and trapping	Economy of design
2	Channel orientation	+	+/-	-	-	Self-cleansing	Flow direction/navigation
3	Steep side slopes	+	-	-	-	Reduced trapping	Soil characteristics
4	Channel bed slope	+/-	+(?)	$1 * 10^7$ m^3 dredging	Months/years	Self-cleansing	Density current requirements
5	Rocks/sand on seabed	+/-	-	$1 * 10^{10}$ t rocks or $1 * 10^7$ m^3 sand	Weeks/months	Decrease transport and increased vertical mixing	Material availability
6	Wall along channel	+/-	+	$1 * 10^8 - 1 * 10^9$ t rocks	Months/years	Block sediment transport	Material and soil
7	Training walls	+	+/-	$1 * 10^{10}$ t rocks	-	Reduced trapping	Hydrodynamic scale
8	Sediment trap	+/-	+	$1 * 10^6$ m^3 dredging	Weeks/months	Reduce maintenance intensity	Trapping and capacity
9	Coast parallel breakwater	+/-	+/-	$1 * 10^9$ t rocks	Years	Reduced transport	Material and soil
10	Remove top layer seabed	+/-	+	$1 * 10^7$ m^3 dredging	Months	Reduced transport	Time scale
11	Close estuary	+	+	$1 * 10^{10}$ t rocks	-	Reduced flow velocities	Permit and river system
12	Redirect estuary plume	+	+	$1 * 10^7$ m^3 dredging	Years	Reduced flow velocities	Estuary hydrodynamics
13	Water jets on channel bed	+	+	1250 jets/km	-	Reduce sedimentation	Local currents and material
	Maintenance measures						
14	Tidal removal			-	-	Reduce maintenance intensity	Local currents and sediment
15	Additional shipping lane			$1 * 10^7$ m^3 dredging	-	Increase maintenance workability	Required material
16	Channel over-depth			$1 * 10^6$ m^3 dredging	-	Peak infill buffer	Peak infill quantity
17	Sedimentation pits			$1 * 10^6$ m^3 dredging	-	Reduce maintenance intensity	Dredging equipment
18	Waiting basin			$1 * 10^6$ m^3 dredging	-	Increase maintenance workability	Down time reduction
19	Temp. sediment removal			-	-	Peak infill buffer	Sediment characteristics

4.3. SITE SPECIFIC INFILL MEASURES

In this section the specific project case is considered. The measures presented in the previous section are evaluated for this specific case and a number of solutions that are expected to be effective are proposed. A further analyses of the potential measures is suggested, and a number of measures are selected for more extensive evaluation.

The site specific conditions for the project case are listed below:

1. Channel location

   Offshore dredged channel perpendicular to open coast;

   Muddy surrounding seabed with gentle slope: 1:1000;

   Surrounding water depth: 5 - 15 m (LAT);

   Estuary entrance West of channel.

2. Hydrodynamics

   Waves with small angle to channel ~ 30°;

   Currents predominantly perpendicular/oblique to channel;

   Stratification due to salinity differences causing residual currents.

3. Infill mechanism

   Sediment concentration profile with high concentrations near the bed caused by sediment induced buoyancy effects;

   Residual flow in Westward direction

   Peak infill significantly larger than mean infill and concentrated over a few months during the wet season.

4. Channel geometry

   Length: 10 km;

   Width: 250 m;

   Depth: 14 m LAT;

   Side slope: 1:10-25.

Two external restrictions apply to the specific case and an initial list is made of solutions that are practically possible due to these restrictions. The following restrictions are taken into account:

1. Channel location and orientation is fixed, following earlier considerations on the channel location by LWI (2006a);

2. Vessel safety regulations for interaction between these ships and dredging vessels.

The current maintenance dredging plan as proposed by LWI is shortly described in the following paragraph. This plan could be used as a reference for the consideration.

4.3.1. MAINTENANCE DREDGING PLAN

The current maintenance plan as proposed by LWI is shortly described here. The navigation channel and harbor basin should be kept at a depth of −14 m LAT for a bulk density lower than 1,200 kg/m^3 (corresponding to a sediment concentration of 300 g/l). A combination of a trailer suction hopper dredger(TSHD) and a water injection dredger (WID) is used, (a description of these equipment types is given in Appendix D). The TSHD is used to dredge the approach channel and the WID to remove sediment around the berths in the harbor area. As a result of safety regulations for vessel movements in the dredged area the workability is restricted to times when no vessels are moving in the dredged area.

Dangerous cargo safety regulations for dredging activity
In the current maintenance dredging plan the following regulations are applied, LWI (2012a):
Vessel arrival: A dredging ship should have left the approach channel before a cargo vessel enters the channel. The dredging ship can commence work in the channel on a safe distance astern the cargo vessel (~500 m). Dredging work in the harbor basin area can commence after berthing of the vessel. Down-time: up to ≈ 3 h.
Vessel loading: During loading of the cargo vessel, dredging is not allowed within 200 - 250 m of the cargo vessel. As two berths are present, the dredging could be managed such that no effective additional down-time is caused.
Vessel departure: The dredging ship should have left the approach channel before departure of the cargo vessel and is able to commence work after the cargo vessel has completely left the channel. Down-time: up to ≈ 3 h.

A yearly total of 440 movements of vessels is expected to take place. The down-time caused by safety regulations is roughly 30 % of the year as determined by LWI (2012a). In combination with operational efficiency and weather conditions the workability of the TSHD is 50 % and of the WID 35 % of the year. During the wet season the sediment infill rates are significantly larger and therefore maintenance dredging demand is higher in this time of the year. In the dry season it is proposed to dredge an over depth of approximately 1 m in the approach channel such that a buffer is created for infill during the wet season. A TSHD is deployed for approximately 7 months a year and a WID for 12 months a year to remove the expected infill of 10 million m^3/year, estimated by LWI.

Some additional measures are suggested that are potentially useful for reducing maintenance costs:

1. Dredging of sediment traps adjacent to the dredged areas, so that maintenance dredging can be carried out in the traps without disruptions due to vessel movements;

2. Placement of sediment adjacent to the channel during high infill rates instead of disposing it at distant disposal sites. Higher levels of productivity are then achieved, however care should be taken that sediment is not reintroduced into the dredged area;

3. Increase the use of bed slope and WID to enable fluidized sediment to flow out of the channel;

4. Refinements in interaction between dredger and vessels that use the terminal so that workability is improved.

4.3.2. EVALUATION

The measures proposed in the Section 4.2 are considered for the specific case individually, taken into account the restrictions and local conditions. The restrictions and availability of material determine that a number of measures are not (economically) feasible. The remaining solutions are evaluated individually. Following this evaluation an overview is given of potential measures that could be feasible for the project case specifically.

EXTERNALLY RESTRICTED MEASURES

Some measures are not applicable for this project due to external restrictions. The restricted measures and associated type of restriction are presented in the table below:

Table 4.5: Restricted measures

#	Name	Restriction
1	Channel location	Predetermined location
2	Channel orientation	Predetermined location
11	Close estuary	Permit

LOCATION RESTRICTED

Due to the location of the project in the Niger Delta, Nigeria, the availability of rock is limited and the muddy subsoil makes foundation of heavy structures costly. Therefore solutions that require large amounts of rock are considered less economically feasible. It is recommended to consider these measures once the remaining solutions are found to be ineffective. Additionally, the main objective of this thesis is to find measures that use mostly natural processes, however these

The solutions that are restricted due to the project location are listed below:

Table 4.6: Measures dependent on availability of rock

#	Name
3	Steep side slopes
5	Rocks on seabed
6	Wall along channel
7	Training walls
9	Coast parallel breakwater

POTENTIAL EFFECTIVE MEASURES

The measures above are excluded from the consideration based on local restrictions, the remaining measures are evaluated separately in this section.

4. Channel bed slope In the case of (expected) low consolidation rate of the mud infill, a mud layer is present that is expected to remain fluid for some time. Depending on the mud layer characteristics a density current could be initiated if the bed is constructed under an angle. The dredged depth becomes larger towards the end of the channel if the slope is steeper than 1:1000, which prevents the sediment flowing down the slope to exit the dredged channel. The surrounding bed consists of a slope of 1:1000, therefore the bed in the channel should not be constructed steeper. According to Figure 4.27 a narrow band is found for stable density currents on a slope of 1:1000 and larger. The fact that the width of the density current is only restricted to the channel could increase its stability as no spreading in lateral direction occurs. The layer thickness and concentration are of significant influence and a clear understanding of the infill and consolidation process is required to determine the effectiveness of this measure.

5. Sand on seabed As the application of rocks on the seabed is not feasible due to the availability of rock in the Niger Delta, sand could be used instead. The sediment concentration profile in the region of the dredged channel consists of a high concentration layer near the bed and negligible sediment suspended higher in the water column. This is a result of the sediment induced buoyancy effects caused by the low flow velocities. It is expected that the sand layer is not capable of increasing the turbulent mixing of sediment sufficiently in order to prevent sedimentation on the sand layer. This measure is therefore not expected to be effective in this specific case.

8. Sediment trap The sediment trap was also proposed by LWI (2012a) as a potential measure to reduce sediment infill in the dredged area. As the sediment is concentrated low in the water column, the trapping efficiency is expected to be relatively high. The dimensions of the sediment trap might be important for the effectiveness of the measure and should be based on the expected peak infill and trapping efficiency.

10. Remove top layer seabed The removal of the top layer of the seabed is expected to be effective for temporary infill reduction as was shown in the previous section. For the longer period the removal of sediment over a large area is similar to a sediment trap as frequent maintenance dredging should be performed to prevent infill in the channel. In the specific case, the sediment trap would provide a more practical solution due to the more convenient maintenance dredging in a straight narrow channel.

12. Redirect estuary plume The residual current responsible for the sediment transport towards the proposed channel is found to be (partly) driven by stratification effects from the Estuary. Therefore reducing the horizontal salinity gradient East of the Estuary entrance, sediment transport in Westward direction could be significantly reduced.

13. Water jets on channel bed The water jets should be able to suspend the sediment high into the water column such that the higher (surface) flow velocities are able to carry enough sediment away from the dredged channel. Due to the local humid environment and offshore location of the terminal, practical effects with respect to maintenance of the jet system are important to consider as well.

14. Tidal removal The effectiveness of tidal removal of sediment from the dredged channel is dependent on the local sediment properties and tidal velocities. The stratification in the project region causes a net Eastward flow in the upper part of the water column and a net Westward flow in the lower part. Agitation during the ebb tide is therefore significantly less effective than during the flood tide, as sediment is directed back towards the channel by the Westward flow in the lower part of the water column. Agitation during the flood tide is probably effective, however depending on the sediment settling velocities (which are currently not known).

15. Additional shipping lane The strict safety regulations cause significant down-time to the maintenance dredging. Therefore a second shipping lane could decrease the maintenance down-time. In the specific case a high trapping efficiency is expected, therefore the effectiveness of the sediment trap was predicted to be high. A sediment trap requires less dredging and is expected to improve the maintenance efficiency to an equal extent. Therefore the sediment trap would be the preferred solution compared to an additional shipping lane.

16. Channel over-depth The over-depth of the proposed channel could be effective during times of high infill. This measure was proposed by LWI as well. The trapping efficiency of the channel might be increased by this measure, however for limited additional depths this effect is expected to be small. The over-depth is considered to be useful as an additional measure to improve the infill capacity during peak infill periods.

17. Sedimentation pits The effectiveness of sedimentation pits are dependent on the required slope for density currents and the available equipment for the initial dredging. TSHD's are not able to construct these pits, whereas a Cutter Suction Dredger (CSD) is capable of dredging this geometry. The equipment available for the maintenance dredging should be able to dredge from the pits. More research is required to find the effectiveness of these pits before this solution can be applied in practice.

18. Waiting basin The effectiveness of a waiting basin is dependent on the used equipment for the maintenance dredging. If equipment is used with small draughts, the vessels are able to exit the dredged channel half way without the requirements for a dredged basin. Additional dredging is required and the increased workability is lower than for a sediment trap, therefore a sediment trap would be the preferred option.

19. Temporary sediment removal This measure is highly determined by the sediment characteristics, it is expected that the side slopes of the dredged channel become 1:25 due to the soil characteristics. The deposited fine material causes a fluid layer that could flow back into the channel. Therefore this solution is not expected to be effective at this particular project.

4.3.3. CONCLUSION

The mitigation measures for sediment infill from the previous section are considered for the specific case. The main objective of this thesis is to find mitigation measures that reduce sediment infill in the proposed channel. The solutions that focus on maintenance efficiency are therefore not considered extensively in this report as these are outside the main scope.

Due to the relatively low additional dredging effort and effectiveness for fine sediment infill during high infill rates, three maintenance measures are particularly effective for the project case, shown in Table 4.7. An additional shipping lane requires significant additional dredging while the advantage compared to a sediment trap is only marginal. The waiting basin is not expected to increase the workability sufficiently as time is lost for navigation and mooring inside the basin as well. Temporary sediment removal would cause sediment to be transported back to the channel quickly, which makes this measure less effective.

Table 4.7: Suggested maintenance measures specific project

#	Name
14	Tidal removal
16	Channel over-depth
17	Sedimentation pits

From the discussion of this chapter the following measures are considered to have the highest potential for reducing the infill in the proposed channel:

Table 4.8: Project specific infill reduction measures

#	Name
4	Channel bed slope
8	Sediment trap
12	Redirect estuary plume

These three solutions have relatively low initial costs and are expected to provide significant reduction in sediment infill of the proposed channel compared to the other considered measures.

Channel bed slope It is assumed that the channel bed slope is able to initiate a density current due to the relatively low consolidation rate of the local mud. As a result the required maintenance dredging is significantly reduced as a large quantity can be transported out of the channel under the influence of gravity. In order to estimate the actual effectiveness of the channel bed slope in reducing sedimentation requires clear understanding of the channel infill process and consolidation behavior of the mud. It is not expected that the infill due to the residual transport generates a layer thick enough to initiate a density current immediately. As the information on the characteristics of the local bed material is limited, the consolidation behavior cannot be estimated besides what was found from the trial pit.

Sediment trap Based on the assumption that trapping of a large portion of the entire sediment flux is achieved by the sediment trap, the solution is found effective. Additionally, the initial effort for the sediment trap is relatively low and the maintenance down-time is significantly increased by the measure which makes the measure economically attractive. The actual feasibility of the sediment trap on reducing sedimentation in the dredged channel is dependent on the trapping efficiency and the required dimensions during peak infill. A clear understanding of the trapping efficiency of the sediment trap is required for further assessment of this solution.

As both the measures 4 and 8 require clear understanding of the channel infill process, it is concluded that a local model to simulate the channel infill could be useful. The Delft3D model from Chapter 3 is not capable of simulating the infill of a dredged channel due to the coarse computational grid. In the following chapter a small model is used to determine the trapping efficiency of the channel. This model is not capable of simulating a density current in the channel, however in future research, results from this model could be useful to assess the effectiveness of a slope in the channel bed.

Redirect estuary plume The estuary (fresh water) plume is expected to be redirected by dredging a channel in the ebb tidal bar in front of the estuary entrance. This measure can be assessed by hydrodynamic modeling with the Delft3D model used in Chapter 3. This is further treated in the following chapter.

5

SOLUTIONS ANALYSIS

The solutions proposed in the previous chapter are considered in the following sections. This chapter aims to achieve the fourth and fifth sub-objectives formulated in Chapter 1. The three solutions that were selected for further consideration are:

1. Channel bed slope;
2. Sediment trap;
3. Redirect estuary plume.

The channel bed slope option is treated in the first section. The sediment trap is the second solution that is analyzed in this chapter. A separate 2-DV model is set-up to simulate the infill of the proposed channel which is referred to as the 'trapping model'. The set-up of the trapping model is described, followed by the model results and discussion. A trapping efficiency of the channel and sediment trap is estimated based on this model.

The third section of this chapter describes the redirection of the estuary plume by a channel in the ebb tidal bar. The channel should attract more flow in Southern direction and reduce the horizontal salinity gradients driving the residual near-bed current.

This chapter finalizes with a conclusion on the findings of the investigated solutions.

5.1. CHANNEL BED SLOPE

The channel bed slope is suggested as one of the potential mitigation measures to reduce sedimentation in the proposed channel. The measure should be able to initiate a density current and thereby result in a self-cleansing channel.

5.1.1. CHANNEL GEOMETRY

The surrounding bed slope is 1:1000, which persists until the edge of the continental shelf. Therefore a slope of 1:1000 or steeper would cause an increasing depth of the channel and associated significant increase in capital dredging volume. If the channel would not be extended further offshore than the existing layout, a deep pit is located at the offshore end of the channel. A density current carrying sediment down the slope, would accumulate in the deep offshore end of the channel and eventually fill the channel from below.

A more gentle slope than 1:1000 could prevent a deep pit at the offshore end. With continuous bed slope of 1:2000 the total length of the channel would increase with 10 km, as can be seen in Figure 5.1. The cross-sectional surface area of the measure with a channel bed slope of 1:2000 is double the surface area of a channel without the slope. However, as the channel width is not required to have the same width as the requirement for the ships the additional dredged volume is in the order of half the initial capital dredging volume.

5.1.2. REQUIRED SLOPE

In the previous chapter, Figure 4.27 showed a diagram with stability requirements for fluid mud flow. From this graph it is found that for slopes gentler than 1:1000 ($\beta < 0.001$) only a narrow band of properties of the fluid mud layer would result in a stable fluid mud layer.

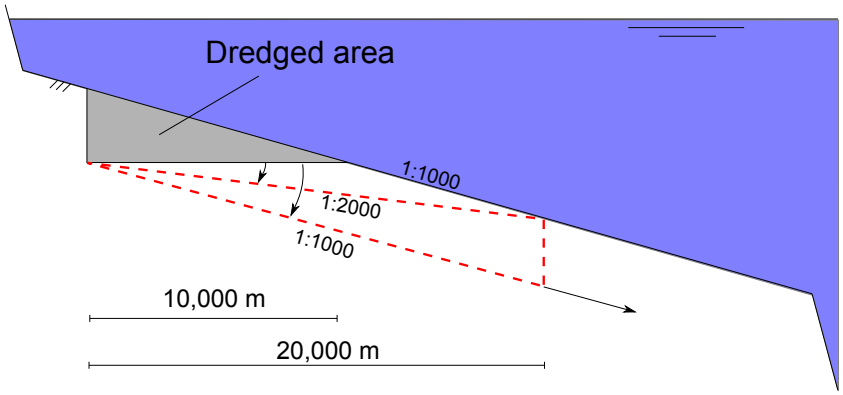

Figure 5.1: Schematization of side view of proposed channel and different bed slopes

Whether the sediment deposited in the channel would generate a density current is determined partly by the infill process. If sediment is deposited in small quantities at a time it is expected that consolidation rates are relatively high and the small layer thickness would not be able to flow down the slope. If high sediment infill rates occur and the layer remains mobile, a density current is more likely to be formed.

The channel parallel component of the (stratification driven) near-bed residual current is directed in shoreward direction and would therefore oppose the density current. This could reduce the flow of the density current.

5.1.3. CONCLUSION

The maximum (practical) channel bed slope of 1:2000 is not expected to be able to initiate a stable mud flow due to the narrow band of stability requirements for this process. The consolidation behavior and infill process determine the effectiveness to a large extent. By the use of more sophisticated tools such as fluid mud flow models this measure can be assessed for different scenarios of the infill. Due to time limitations and lack of the required data and tools this measure is not further treated.

The use of a water injection dredger in combination with the channel bed slope could be effective to initiate a density current and should be further studied.

5.2. TRAPPING EFFICIENCY AND SEDIMENT TRAP MODELING

In this section the trapping efficiency of the approach channel and sediment trap are modeled using a 2-DV trapping model. First the trapping model is described in detail, followed by modeling of the trapping efficiency of the approach channel. Subsequently the effectiveness of the sediment trap on reducing infill in the dredged channel is estimated.

5.2.1. TRAPPING MODEL

A 2-DV trapping model is set-up with the Delft3D software package. The trapping model is used to estimate the trapping efficiency of the proposed channel by the residual (fine) sediment transport identified as the main source of infill in Chapter 3. Existing trapping models are available, such as the sutrench model by Rijn (1985), however these do not deal with fine sediment and the concept of sediment induced buoyancy effects. The Delft3D software is chosen because the concept of buoyancy destruction and cohesive sediment transport are well integrated.

The residual current responsible for the sediment transport is only found in the bottom half of the water column (see Chapter 3 and LWI (2012b)). The trapping model is not set-up to simulate the stratification effects correctly but rather to represent the sediment infill from a residual current in the bottom part of the water column. The sediment is assumed to be exclusively present near the bed, therefore the flow pattern in the upper part of the water column is not of particular interest to this study. Depth averaged tidal velocities from the large Delft3D model are used as input for the trapping model in combination with a residual current over the entire water depth.

The sediment concentration profile measured in the vicinity of the dredged channel showed high concentrations near the bed, with practically no sediment suspended above 1 m from the seabed under normal wave conditions ($H_s \approx 1.5$ m during the wet season). The capacity of waves to bring sediment in suspension is higher than the capacity of the flow to keep the sediment suspended. Due to the sediment induced buoyancy effects a thin layer of fluid mud is formed on the bed. It is expected that this fluid mud layer limits the influence of wave induced shear stresses on the bed and thereby reduce erosion over time.

GOVERNING EQUATIONS

The Delft3D model solves the Navier-Stokes equations for incompressible fluid, under shallow water and Boussinesq assumptions. In the vertical momentum equation the vertical accelerations are neglected, the vertical velocities are computed from the continuity equation. The 2-DV model only takes one horizontal direction (x) into account as well as the vertical direction (z). The momentum balance in horizontal direction is given by equation 5.1. No terms with y direction components are considered (Deltares, 2014).

$$\frac{\delta u}{\delta t} + \frac{u\delta u}{\delta x} + \frac{w}{h}\frac{\delta u}{\delta z} = \frac{1}{\rho_0}P_x + F_x + \frac{1}{h^2}\frac{\delta}{\delta z}(\upsilon_V \frac{\delta u}{\delta z}) + M_x \tag{5.1}$$

With: u = velocity component in x-direction [m/s], w = velocity component in z-direction [m/s], h = total water depth [m] = $d + \zeta$, d = mean water depth [m] and ζ = water level variation [m]. P_x = pressure gradient [N/m], F_x = unbalance of horizontal Reynolds stresses [m/s^2], υ_V = vertical eddy viscosity [m^2/s]and M_x = external sources of momentum such as wave stresses [Nm].

The vertical velocity w is computed from the continuity equation:

$$\frac{\delta \zeta}{\delta t} + \frac{\delta (hu)}{\delta x} + \frac{\delta w}{\delta z} = h(q_{in} - q_{out}) \tag{5.2}$$

With: $q_{in/out}$ = local source or sink per unit volume [1/s].

The vertical momentum equation is reduced to a hydrostatic pressure equation as a result of the shallow water assumption:

$$\frac{\delta P}{\delta z} = -\rho g h \tag{5.3}$$

This means that vertical accelerations due to buoyancy effects and sudden variations in bottom topography are not taken into account.

The $k-\varepsilon$ turbulence closure model is used in the trapping model. As buoyancy destruction is considered to be of importance, a constant eddy viscosity is not able to represent the correct behavior. The $k-\varepsilon$ model gives transport equations for turbulent kinetic energy k and energy dissipation ε. In this model it is assumed that production, buoyancy and dissipation are the dominating terms. Horizontal length scales are assumed

to be larger than vertical length scales (shallow water, boundary layer type flows). The vertical eddy viscosity is given by:

$$v_{3D} = c_\mu \frac{k^2}{\varepsilon} \tag{5.4}$$

With $c_\mu = c_D c'_\mu$ where c_D = constant relating mixing length ≈ 0.1925 [-] and c'_μ = constant in Kolomogorov-Prandtl's eddy viscosity formulation = 0.09 [-],

The sediment concentration profile is dependent on the settling velocity and vertical mixing. The vertical mixing of sediment is given by the vertical fluid mixing coefficient from the turbulence closure model (ε_f). Turbulent mixing of cohesive sediment due to waves is not incorporated in the Delft3D model, which is a limitation of the model.

The mean settling velocity of sediment is defined in the model configuration, hindered settling could reduce the settling velocity if sediment concentrations are high enough. Hindered settling is incorporated in the model by the following equation:

$$w_s = \left(1 - \frac{c_s}{C_{soil}}\right)^5 w_{s,0} \tag{5.5}$$

With: w_s = settling velocity [m/s], c_s = mass concentration of suspended sediment [kg/m^3], C_{soil} = reference density for hindered settling [kg/m^3] and $w_{s,0}$ = defined mean settling velocity [m/s].

Wave streaming in the wave boundary layer has been neglected for this study.

MODEL SET-UP

The trapping model is a single row model ($1x250$ cells of $20x20$ m) that represents a 5 km section of the project area intersecting the dredged channel. Figure 5.2 shows the represented section of the trapping model in the large Delft3D model, the angle of the trapping model with respect to the dredged channel is 25°. Due to the oblique intersection the channel will be 600 m wide in the trapping model instead of 250 m for a perpendicular cross section. The intersection is at the mid of the dredged channel at a surrounding water depth of $h = 9.2$ m.

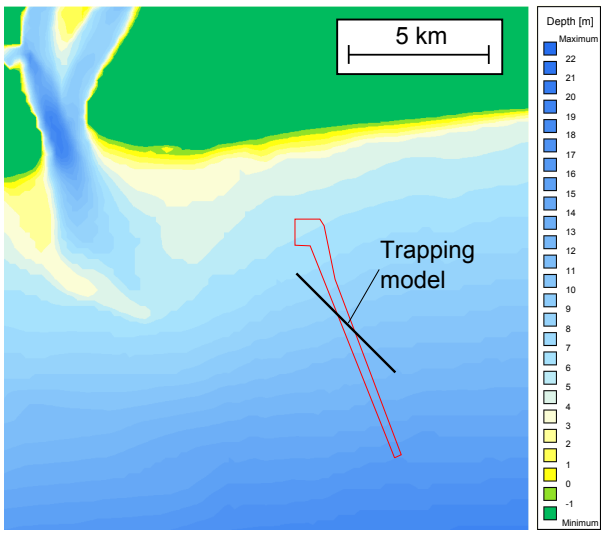

Figure 5.2: Location of trapping model

In vertical direction 20 layers are used in the model with the distribution of the layer heights as shown in Table 5.1. To simulate the near bed processes in detail a high resolution is used near the bed. The computational grid of the model without (left) and with (right) the channel is shown in Figure 5.3.

Table 5.1: Model layer height distribution

Layer	Height [%]	Layer	Height [%]
1	8	11	3
2	9.4	12	2
3	10.5	13	1.5
4	12	14	1
5	12	15	0.7
6	12	16	0.5
7	9.5	17	0.3
8	7.5	18	0.25
9	5.5	19	0.2
10	4	20	0.15

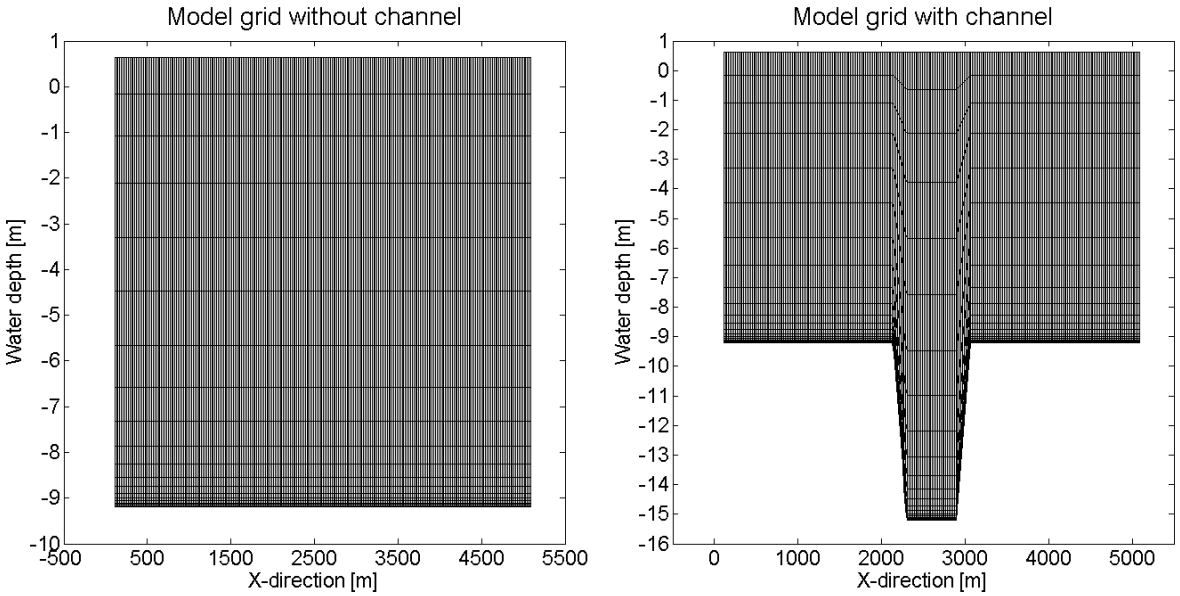

Figure 5.3: Computational grid without channel (left) and with channel (right)

BOUNDARY CONDITIONS

The model boundary conditions for flow are taken from the large Delft3D model. The depth averaged tidal flow velocities are used in the direction of the near bed residual current. From Figure 3.7 in Chapter 3 it was shown that the near bed residual current has an angle of 45°to North, which results in an angle of 25°to the channel.

The North-Western (NW) boundary of the trapping model consists of a water level boundary for a mean tidal range of $\hat{\zeta}$ = 0.63 m with a period of T = 12h = 43200 s. The South-Eastern (SE) boundary consists of a total discharge boundary that represents the tidal velocities and residual current, with $\hat{Q}_{tide}$ = 27.6 m^3/s equivalent to a fluctuating tidal velocity of u_{tide} = 0.15 m/s and Q_{res} = 9.2 m^3/s equivalent to a residual current of u_{res} = 0.05 m/s. Both velocities are logarithmically distributed in the vertical on the boundary. Flow in the direction of the NW or left model boundary is associated with flood flow and directed in negative x-direction in the model. The residual component on the SE boundary is therefore applied as a negative total discharge value.

A Neumann boundary condition for sediment transport into the model is used, which sets the sediment concentrations at the boundary equal to those just inside the model domain.

The phase difference between the water level and flow velocity in the large Delft3D model showed a near-standing wave pattern with a phase difference of approximately ϕ = 105°. The phase difference between

the water level and discharge is optimized in the trapping model to obtain minimum horizontal velocity gradients. Due to the complex flow profile over the vertical in the large Delft3D model, the small trapping model cannot represent the flow pattern correctly. A phase difference of $\phi = 175°$was found to show the least horizontal gradients in flow velocity. The phase difference of $\phi = 175°$means that the highest flow velocities in flood and ebb directions occur during high and low water level respectively.

Figure 5.4 shows the depth averaged flow velocity for the North-Western and South-Eastern boundaries for a phase difference of 175°.

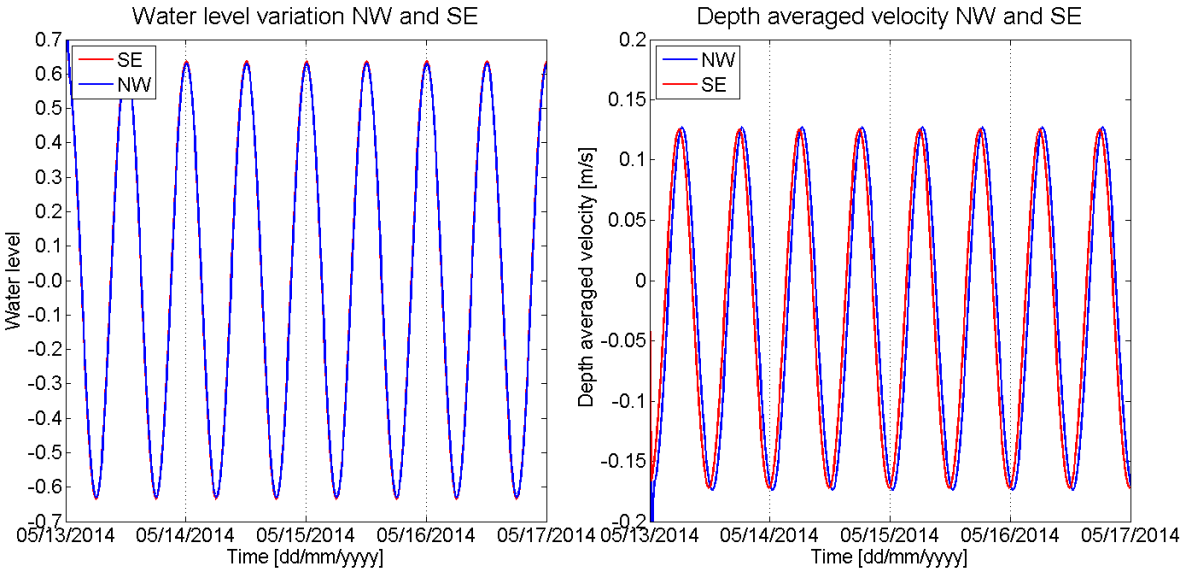

Figure 5.4: Water level variation (left) and depth averaged velocity at NW(blue) and SE(red) boundaries for $\phi = 175°$. Positive values are in SE direction.

MODEL CONFIGURATION

The sediment properties that are used in the model are shown in Table 5.2.

Table 5.2: Sediment parameters

Parameter	Symbol	Value	Unit
Settling velocity	W_s	0.5	mm/s
Reference density for hindered settling	C_{soil}	100	kg/m^3
Specific density	ρ_s	2650	kg/m^3
Critical shear stress for deposition	τ_d	0 and 1000	N/m^2
Critical shear stress for erosion	τ_c	0.5	N/m^2
Erosion parameter	M_e	0.0003	kg/m^2/s

Additional parameters used in the trapping model are provided in Table 5.3.

Flow velocity First the model was run without sediment to analyze the hydrodynamic behavior. The phase difference of 175°showed the smallest horizontal gradients, however some horizontal gradients are still present. Figure 5.5 shows the horizontal flow velocity at flow reversal and maximum flood flow. The horizontal velocity gradients are larges during flow reversal and smallest at maximum ebb or flood flow. Horizontal gradients are approximately equal for both flow directions which causes minimal additional residual flow. Figure 5.5 shows the horizontal flow velocities with the proposed channel. The flow velocities in the channel area are clearly lower, as can be explained by continuity.

Table 5.3: Additional parameters trapping model

Additional parameters	Symbol	Value	Unit
Computational cell width (x,y)	dx,dy	20	m
Time step	dt	6	s
Gravity	g	9.81	m/s^2
Water density	ρ_w	1021	kg/m^3
Bed roughness	C	80	$m^{0.5}/s$
Background horizontal eddy viscosity	v_H^{back}	1	m^2/s
Background horizontal eddy diffusivity	D_H^{back}	1	m^2/s
Background vertical eddy viscosity	v_V^{back}	1e-6	m^2/s
Background vertical eddy diffusivity	D_V^{back}	1e-6	m^2/s
Prandtl-Schmidt number (sediment)	σ	1.0	-

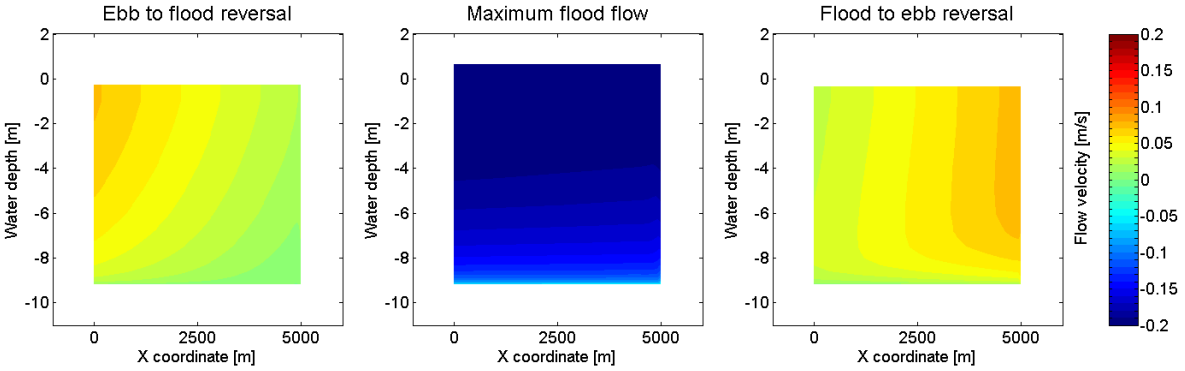

Figure 5.5: Horizontal velocity profile at flow reversal from ebb to flood reversal (left), maximum flood (mid) and flood to ebb reversal (right).

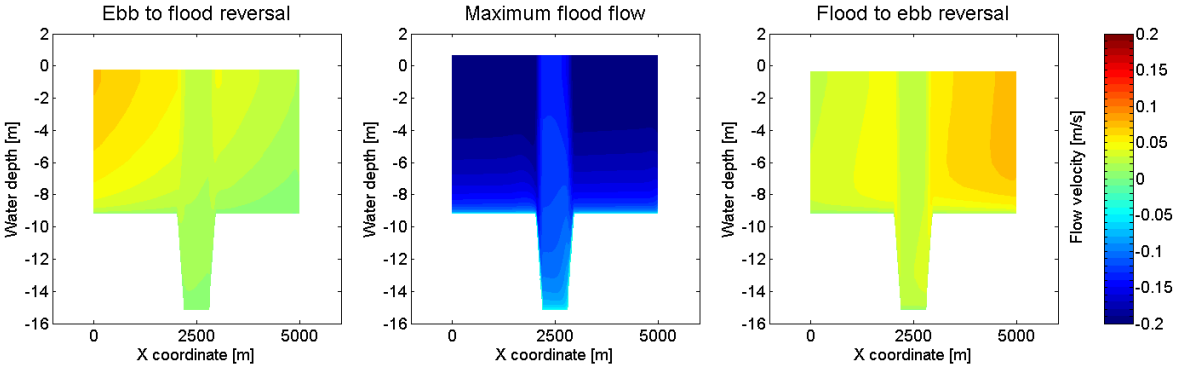

Figure 5.6: Horizontal velocity profile with channel at flow reversal from ebb to flood reversal (left), maximum flood (mid) and flood to ebb reversal (right).

Wave heights A constant wave height of H_s = 1.5 m is used, equal to the mean wave height during the wet season. Due to the constant wave height of H_s = 1.5 m the bed shear stress exceeds the critical bed shear stress for erosion along the entire domain, even at the channel bed. The bed shear stress fluctuations are only caused by the water level variation. The bed shear stress caused by the flow is relatively very small due to the low flow velocities. Because of the small fluctuations in bed shear stress the critical shear stress for deposition is only changed between 1000 N/m^2 and 0 N/m^2, enabling or disabling sedimentation onto the bed respectively.

Viscosity From the model results it is shown that at flow reversal, peaks in vertical eddy viscosity are generated. This is probably caused by sharp vertical velocity gradients ($\frac{\delta u}{\delta z}$) near the bed. Figure 5.7 shows the velocity profile over depth and the vertical eddy viscosity in the bottom 5 layers. With different phase velocities and discharge values the peaks could not be removed from the eddy viscosity profiles. As the peaks are in the same order of magnitude as the vertical eddy viscosity due to the regular flow velocities it is assumed that the impact of the peaks is not of major influence on the behavior of the sediment and trapping efficiency.

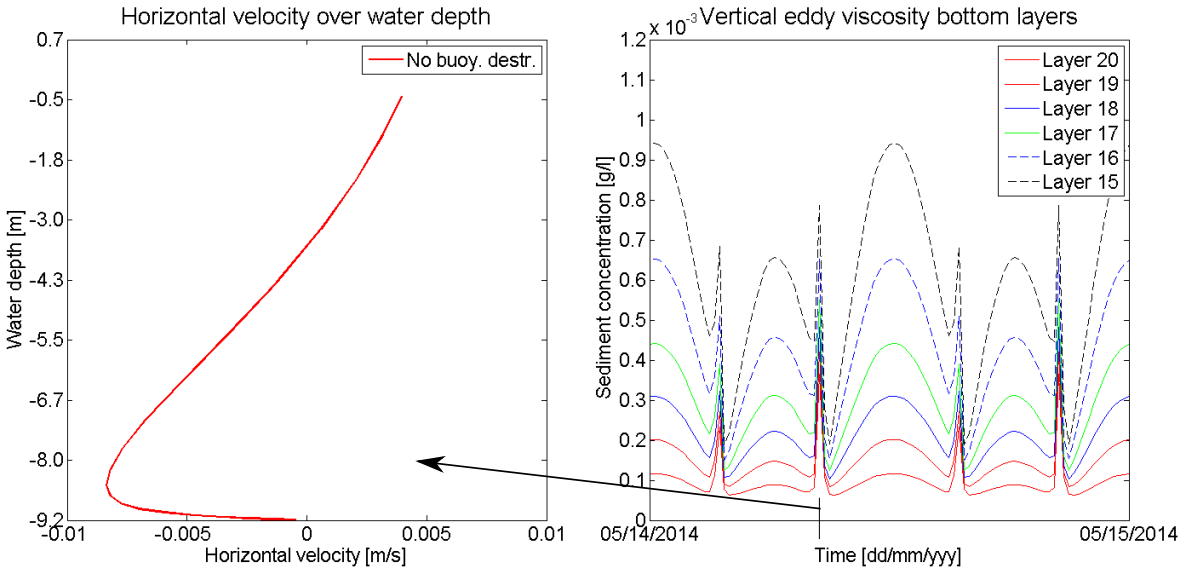

Figure 5.7: Horizontal velocity profile at flow reversal (left) and vertical eddy viscosity of bottom layers over 2 tidal cycles (right).

SEDIMENT CONCENTRATION

The sediment concentration profile is dependent on the erosion/deposition rate and the vertical mixing. The model is run with and without the effect of sediment on the fluid density to see the influence of sediment induced buoyancy effects (or buoyancy destruction) on the sediment concentration. Additionally, runs are executed without deposition of sediment to allow a build-up of a fluid mud layer on the bed. The fluid mud layer should reduce further erosion of the underlying bed and obtain a stable layer thickness. All simulations are done for a 4 day period.

The model is initially executed for the following scenarios:

- No buoyancy destruction, $\tau_d = 1000$ N/m^2
- Buoyancy destruction, $\tau_d = 1000$ N/m^2
- Buoyancy destruction, $\tau_d = 0$ N/m^2

No buoyancy destruction The results of the model without buoyancy destruction show that the sediment concentration is mixed over the entire water column with higher sediment concentrations in the lower part of the water column, see Figure 5.8 (left). The sediment concentration in the bottom layer is shown on the right in Figure 5.8. The fluctuations are mostly caused by the difference in vertical mixing and partly by the difference in wave induced bed shear stresses during low and high water. The peaks that were shown for the vertical eddy viscosity are shown in the sediment concentration, small downward peaks in the concentration profile are present when vertical mixing is increased. It is shown that the sediment concentration is not increasing over time and a dynamic equilibrium in deposition and erosion occurs. The sediment concentrations fluctuates around 1.4 g/l in the bottom layer.

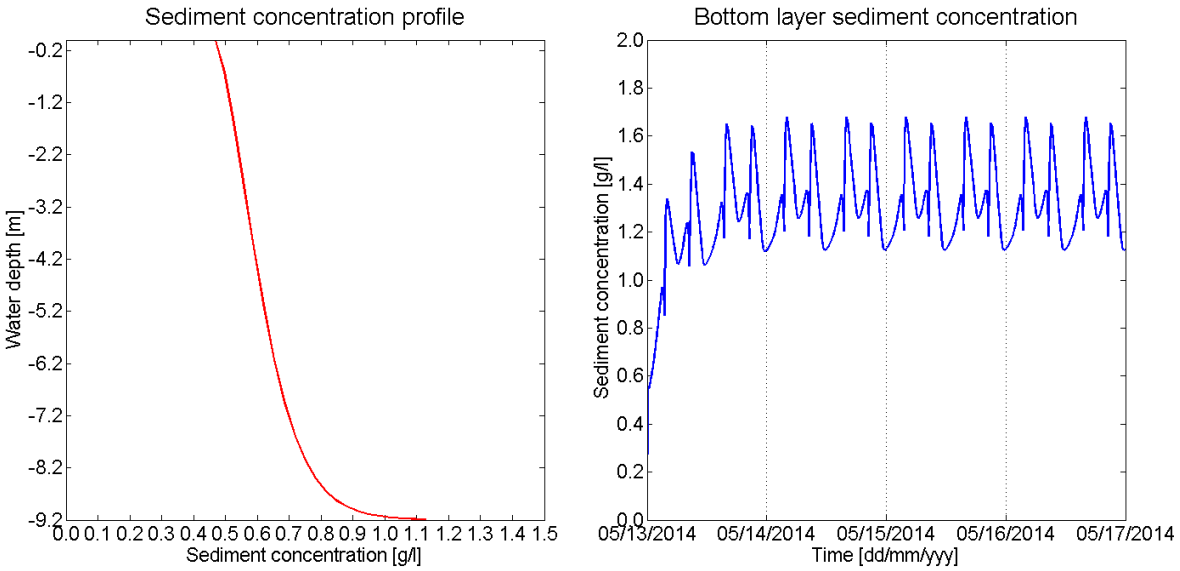

Figure 5.8: Sediment concentration without buoyancy destruction, with deposition. Left figure shows the sediment concentration profile, right figure shows the sediment concentration in the bottom layer.

Buoyancy destruction, with sedimentation If the influence of sediment on the fluid density is taken into account, the sediment concentration profile shows a different pattern, see Figure 5.9. As expected a collapse in the sediment concentration profile occurs and the sediment is concentrated near the bed. Sedimentation is allowed in this simulation, which causes the sediment concentration to be relatively low as most of the suspended sediment is able to deposit immediately due to the limited vertical mixing. The sediment concentration in the bottom layer shows a dynamic equilibrium with a mean value of 1.3 g/l. The peaks in the sediment concentration are again a result of the vertical viscosity fluctuations during flow reversal, but are shown to be insignificant to the overall behavior. The sediment concentration is mostly determined by the difference in water level that causes fluctuations in wave induced bed shear stresses.

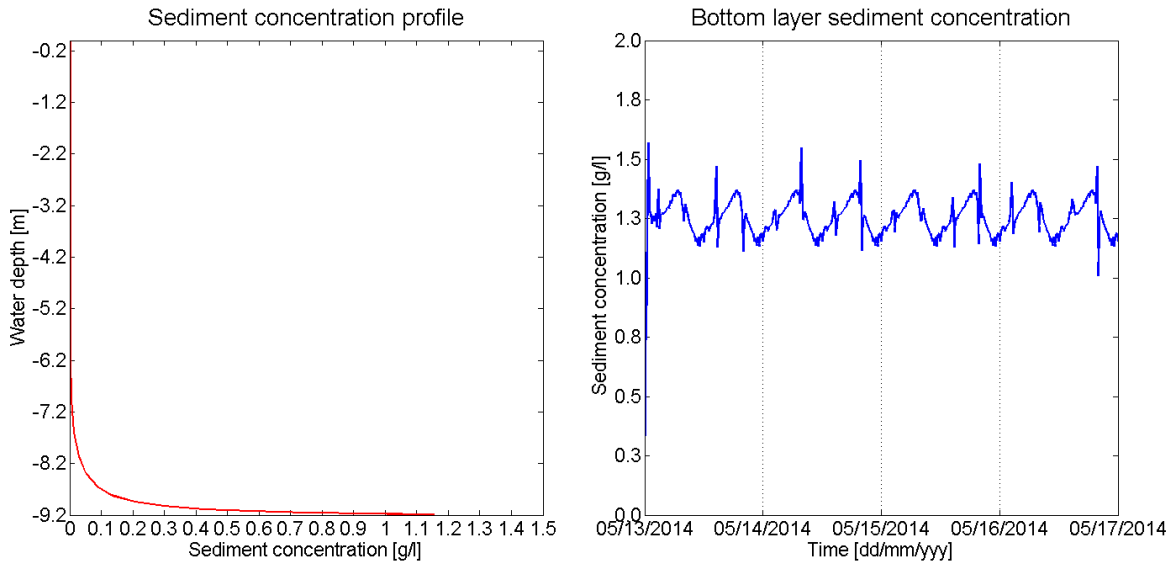

Figure 5.9: Sediment concentration without buoyancy destruction, with deposition. Left figure shows the sediment concentration profile, right figure shows the sediment concentration in the bottom layer.

Buoyancy destruction, without sedimentation If sedimentation is not allowed, all sediment suspended by waves is kept in the system and can only leave through the open boundaries. The erosion rate and vertical mixing are the only factors that determine the sediment concentration. Figure 5.10 shows the sediment concentration over the vertical at the end of the simulation (left) and the sediment concentration in the bottom layer (right). It was expected that wave induced bed shear stresses would reduce as a result of the fluid mud layer on the bed. However, as can be seen in Figure 5.10 (right) the sediment concentration increases continuously. This shows that a reduction in wave erosion does not occur as was expected. The sediment concentration reaches up to 150 g/l near the bed and continues to increase.

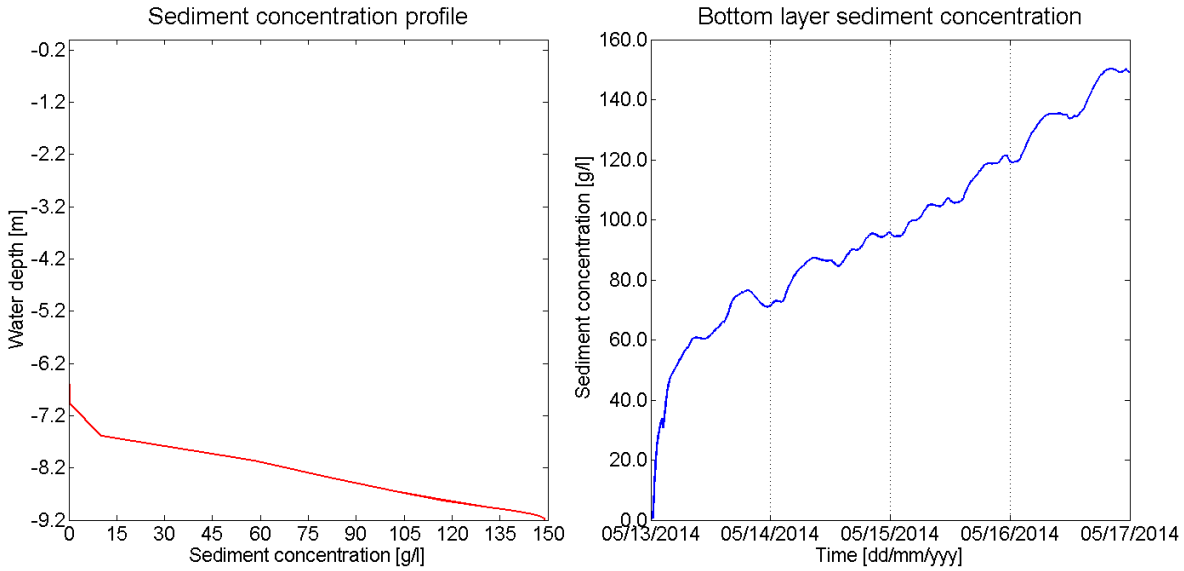

Figure 5.10: Sediment concentration without buoyancy destruction, without deposition. Left figure shows the sediment concentration profile, right figure shows the sediment concentration in the bottom layer.

SEDIMENT TRANSPORT

The sediment transport rates for the different scenarios are shown in Figure 5.11. It is shown that all sediment transport rates are negative, which is caused by the residual flow directed in negative X-direction. The sediment transport for the buoyancy destruction scenario (blue) with sedimentation over the entire domain shows small transport rates compared to the other scenarios (order of $1 * 10^{-6}$ $m^3/s/m$), this is caused by the fact that continuous deposition and sedimentation takes place and the sediment concentration is located close to the bed. The gross of the sediment is only suspended for a short period as most of it deposits immediately after it is eroded. A gradient in sediment transport is particularly strong for the buoyancy destruction case without sedimentation. This is caused by a high inflow of sediment on the SE boundary as a result of the Neumann boundary condition for sediment transport. The higher flow velocities in negative X-direction cause high transport rates into the model on the SE boundary. These high sediment concentrations propagate slowly through the rest of the domain, causing higher transport rates on the SE side of the model.

Eddy viscosity The eddy viscosity for the different model scenarios is shown in Figure 5.12. It is shown that without buoyancy destruction a clear parabolic eddy viscosity profile (as expected) is present. For buoyancy destruction without sedimentation the vertical eddy viscosity is zero for the part where sediment is present in the water column. This is caused by the turbulence damping of the fluid mud layer. For the case with buoyancy destruction and sedimentation the eddy viscosity profile is somewhat different. Some vertical mixing is present in the bottom part of the water column as a result of the continuous erosion and deposition of sediment. The mixing is zero at the interface between the bottom part where sediment is present and the top part without suspended material.

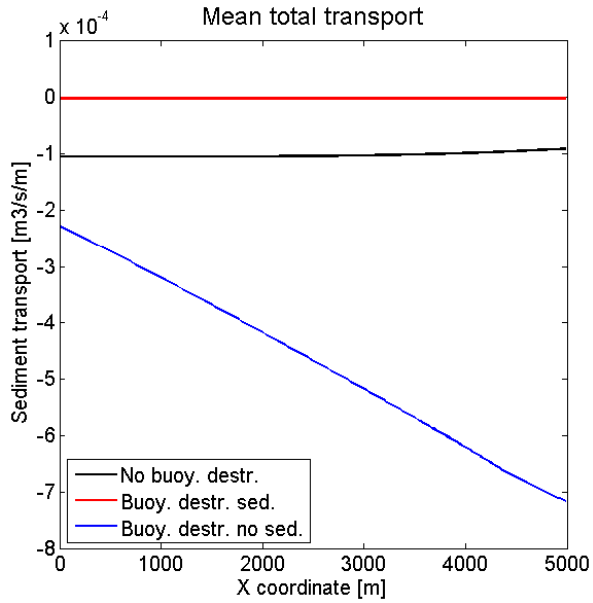

Figure 5.11: Mean total sediment transport over model domain, no buoyancy destruction (black), buoyancy destruction without sedimentation (red) and buoyancy destruction with sedimentation (blue). The units are in $m^3/s/m$ solid material.

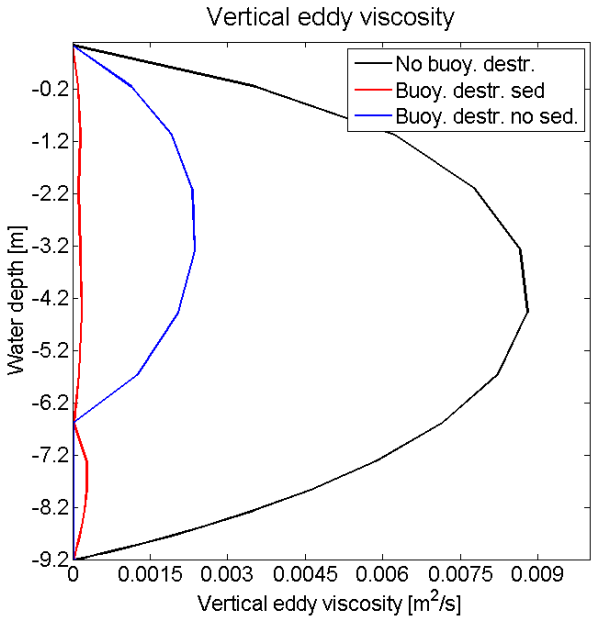

Figure 5.12: Vertical eddy viscosity for the three scenarios

5.2.2. MODEL RESULTS WITH CHANNEL

The model is run with the dredged channel in order to estimate the trapping efficiency for the different scenarios. The channel bed is assumed to consist of stronger soil than the surrounding bed and no initial erodible sediment layer is applied in the model.

No buoyancy destruction In this scenario no buoyancy destruction takes place and sedimentation is enabled. Sediment is shown to be suspended over the entire water column, therefore it is expected that the trapping efficiency of the channel is relatively low compared to the case when sediment is concentrated close to the bed. The mean total transport of sediment without buoyancy destruction and sedimentation allowed in the entire domain is shown in Figure 5.13. The sediment transport reduces significantly as a result of trapping by the channel. A gradient in sediment transport in the surrounding area is visible as well. On the left side of the channel sediment transport increases towards the model boundary whereas on the right side of the channel the sediment transport decreases towards the model boundary. This gradient is caused by the trapping of the channel, a relatively larger part of the sediment transport in positive x-direction is not transported back in negative x-direction on the left side of the channel due to the trapping. On the right side of the channel the same occurs, which causes that a larger part of the sediment transport in negative x-direction is not transported back out of the channel during transport in positive x-direction. The trapping efficiency of the channel is taken as the relative difference in sediment transport between both sides of the channel, which is approximately 55 %.

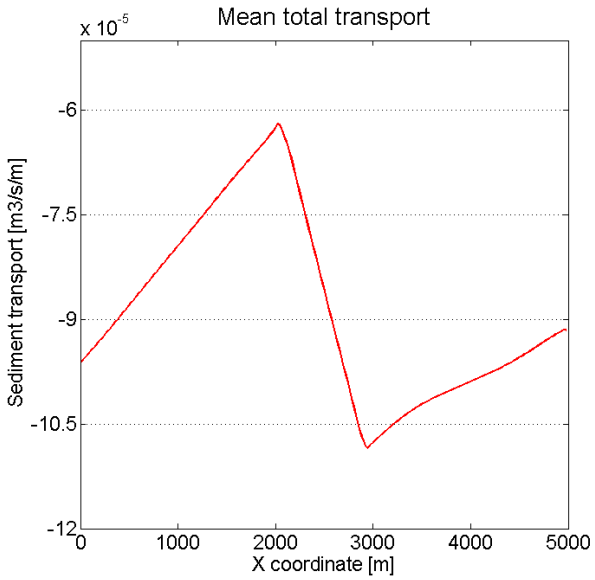

Figure 5.13: Mean total sediment transport over channel in the case of no buoyancy destruction and sedimentation allowed over entire bed.

BUOYANCY DESTRUCTION

The trapping of the channel is modeled for different scenarios with buoyancy destruction.

- Sedimentation in entire domain.
- Sedimentation in channel;
- No sedimentation in entire domain;

Sedimentation in entire domain As was stated before, the gross of the eroded sediment is suspended only shortly if sedimentation is allowed in the entire domain. The sediment transport rate in the model (around 350 kg/m/day) is relatively low compared to the measurements (around 2,500 kg/m/day) because of this effect. Instantaneous buoyancy destruction occurs due to the high erosion rate. The mean total transport

throughout the domain for this case is shown in Figure 5.14. As the mean total sediment transport reaches 0, the trapping of the channel is 100 % in this case.

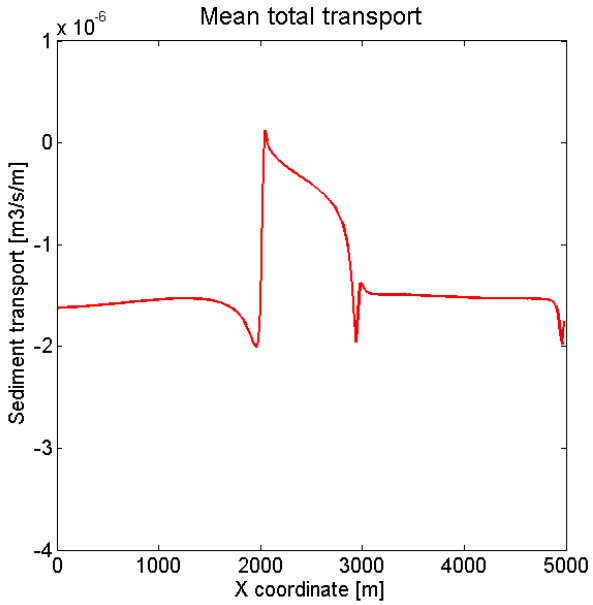

Figure 5.14: Mean total sediment transport over channel in the case of buoyancy destruction and sedimentation allowed over entire bed.

Sedimentation in channel If sedimentation is enabled in the channel only, the channel functions as a sediment sink. Figure 5.15 shows the mean total transport for this scenario. The transport in the channel changes sign, which means that sediment transport is directed in positive x-direction in the left part of the channel and in negative x-direction in the right part of the channel. This suggests that sediment infill is directed from both sides,this is explained by the tidal varying flow velocity direction and the high trapping efficiency of the channel.

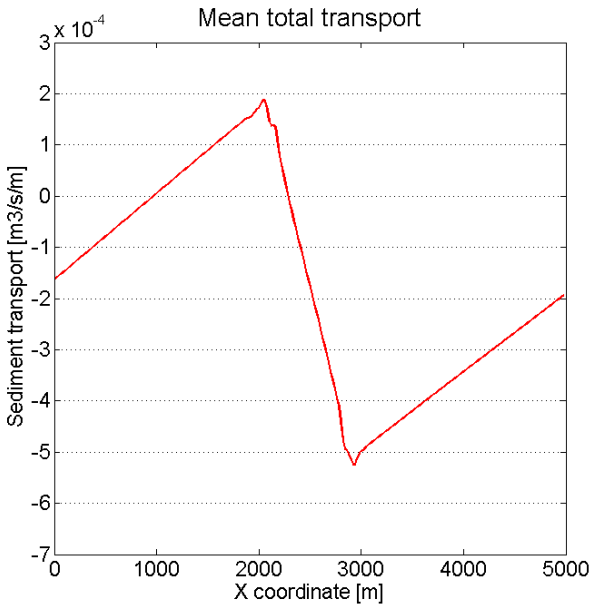

Figure 5.15: Mean total sediment transport over channel in the case of buoyancy destruction and sedimentation allowed on the channel bed only.

The high sediment transport rate causes high sediment concentrations in the channel and associated hindered settling. The sedimentation rate is lower than the rate of accumulation of sediment and therefore the sediment concentration in the channel increases. At some point the settling velocity reaches 0 mm/s, once the sediment concentration reaches the reference density for hindered settling. No further sedimentation occurs and the channel bed only experiences erosion of earlier deposited material as a result of the wave induced bed shear stresses. Figure 5.16 shows the sediment concentration profile in the channel at different moments in time. In the first 48 hours the sediment concentration is relatively low and the sedimentation is large compared to the amount of infill. After 60 hours it is shown that the sediment concentration has increased rapidly in the channel and concentrations rise even above the surrounding bed level. Sediment that reaches above the surrounding bed levels is transported towards the sides by horizontal density gradients and tidal flow velocities. This results in lower trapping efficiency and sediment bypassing the channel.

Hindered settling causes low consolidation rates and therefore the suspended sediment concentration starts to increase in higher parts of the water column as well. Once the height of the sediment suspension reaches the top of the pit, sediment is able to be transported out of the channel and the trapping efficiency is reduced, see Figure 5.16.

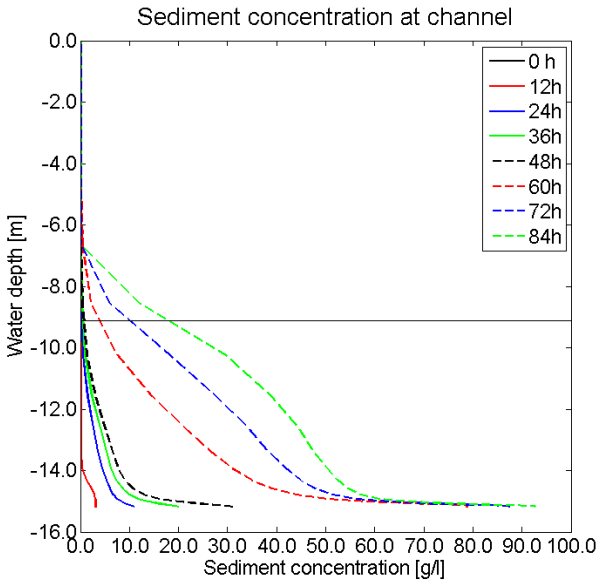

Figure 5.16: Sediment concentration in channel over water depth at different moments in time. The black horizontal line shows the surrounding bed level (9.2 m)

No sedimentation in entire domain The previous paragraph showed that if sedimentation is allowed in the channel, the infill rate becomes larger than the sedimentation rate as a result of hindered settling. Therefore the previous case becomes similar to the case of no sedimentation in the channel at all. Figure 5.17 shows the mean total transport over the model domain for the case without sedimentation. It is shown that the sediment transport reduces over the channel. A trapping efficiency of 31 % is achieved with this. However, initially when no sediment is present in the channel the trapping efficiency is significantly higher and decreases over time as sediment starts to bypass the channel.

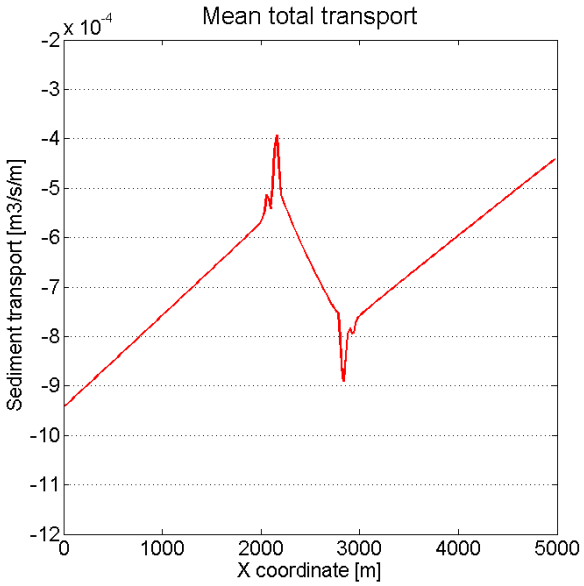

Figure 5.17: Mean total sediment transport over channel in the case of buoyancy destruction and no sedimentation in the entire domain.

Conclusions The previous analysis showed the following results:

- The trapping efficiency of the channel without buoyancy destruction is around 55 %.
- The trapping efficiency of the channel with buoyancy destruction and sedimentation enabled in the entire domain is 100 %.
- If sedimentation is only permitted in the channel, high sediment concentrations develop and a thick fluid mud layer is formed. The low consolidation rate as a result of hindered settling causes the sediment concentration to increase higher up in the channel as well.
- Due to overflow as a result of high sediment concentrations, sediment bypasses the channel if no sedimentation is enabled adjacent to the channel.
- Sediment concentration profiles measured by LWI in the vicinity of the dredged channel for transport by the residual current are most similar to the case with sedimentation allowed. The transport rates in the trapping model are lower than in reality, but the concentration profile is concluded to be the most similar.
- Wave induced bed shear stresses are not shown to decrease due to the fluid mud layer, therefore the sediment concentration increases continuously.
- Sediment concentration profile for sedimentation in the entire domain is closest to the measured sediment concentration profile, therefore this case is taken as representative for the sediment infill from the residual transport. If sedimentation is allowed, the consolidation time of the sediment is very low due to the low concentrations and limited hindered settling. In reality the effect of hindered settling is more pronounced and immediate consolidation does not occur as it does in the Delft3D model. In order to achieve this effect sedimentation is not allowed in the channel to simulate the infill for not consolidating material.

SEDIMENT TRAP MODELING

The sediment trap was proposed in the previous chapter as an effective solution to limit infill from the residual Westward transport. The previous paragraph showed that sediment concentrations for the case with sedimentation in the entire domain represents the measured sediment concentration profile in the vicinity of the channel the most accurately. The sediment concentration in the Delft3D model is lower than measured in the field, however the behavior as a result of the buoyancy destruction is shown to be similar. This model configuration is used to model the effect of a sediment trap on the sediment infill in the dredged channel.

If sedimentation is allowed in the channel, rapid consolidation in the channel occurs due to the low concentrations and associated limited hindered settling. In reality the effect of hindered settling is expected to be more pronounced due to the higher concentrations near the bed and sedimentation is expected to occur slower than modeled in the trapping model.

In order to model the effectiveness of a sediment trap in reducing sediment infill from the Westward transport two scenarios are compared to account for the consolidation behavior:

1. Sedimentation allowed in entire domain;

2. Sedimentation allowed adjacent to dredged channels only.

The first scenario is used as an upper estimate and the second scenario as a lower estimate for the trapping efficiency of the sediment trap.

The sediment trap dimensions used in the model are: 60 m wide and 5 m deep with side slopes of 1 : 12. At the top of the channel the width is thus 180 m. The sediment trap is assumed to be dredged parallel to the approach channel and therefore intersected under the same angle by the trapping model.

Sedimentation allowed in entire domain In the previous section it was shown that the channel achieves 100 % trapping of sediment if sedimentation is enabled in the entire domain. The amount of sediment captured by the sediment trap is modeled with the above dimensions, assuming that sedimentation takes place in the trap and in the channel. Figure 5.18 shows the sediment concentrations at the end of the simulation with only the approach channel (left) and with the sediment trap (right). Sediment concentrations show to be lower in the channel if the sediment trap is applied.

Figure 5.19 shows the mean total sediment transport with and without the sediment trap. The sediment trap reduces the sediment transport towards the channel with approximately 55 %. This is seen as an upper limit of the trapping efficiency of the sediment trap with these dimensions.

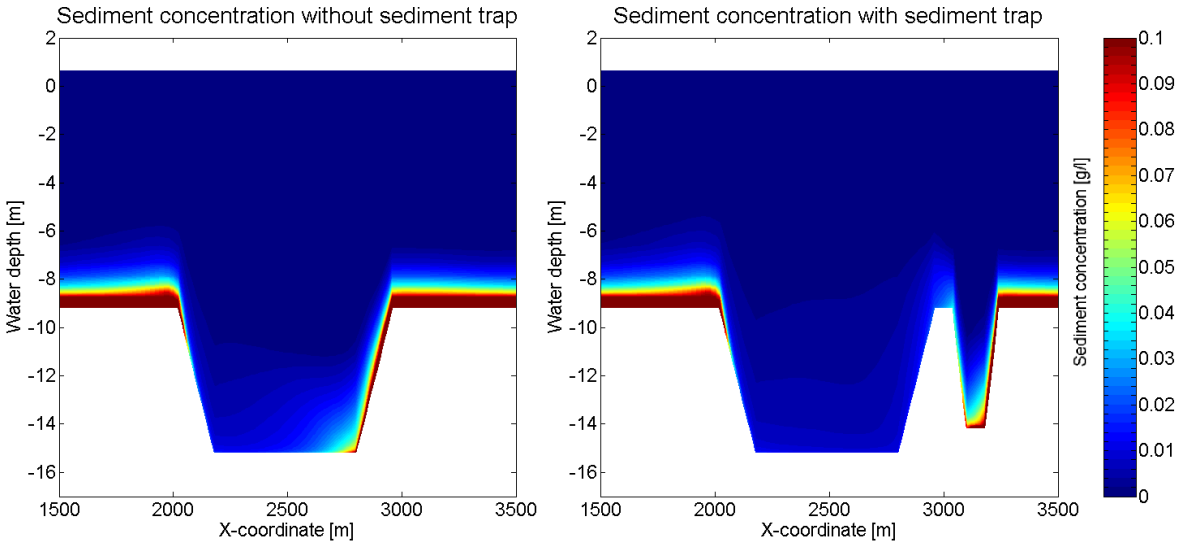

Figure 5.18: Sediment concentration at end of model simulation without sediment trap (left) and with sediment trap (right).

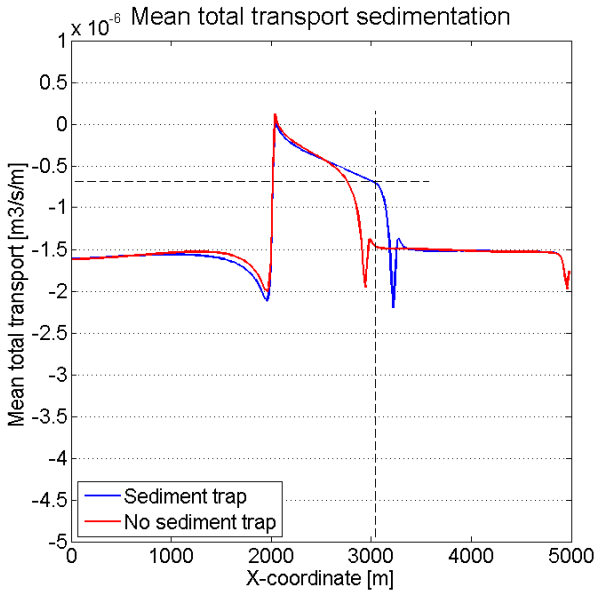

Figure 5.19: Total sediment transport without sediment trap (red) and with sediment trap (blue). The dashed lines show the edge of the sediment trap and the sediment transport at that location.

Sedimentation adjacent to dredged channels only If sedimentation is enabled in the area adjacent to the dredged channels only, sediment remains suspended in the channel and the sediment trap. Figure 5.20 shows the sediment concentrations without the sediment trap (left) and with the sediment trap (right). It is shown that sediment concentrations are (as expected) reduced significantly less in the channel compared to the previous scenario.

The total transport over the model domain is shown in Figure 5.21, the sediment transport is reduced by approximately 20 % by the sediment trap. From the figure it is concluded that the trapping efficiency of the main channel is in the order of 45 % only. The sediment trap increases the total amount of trapping of sediment only slightly (a few %).

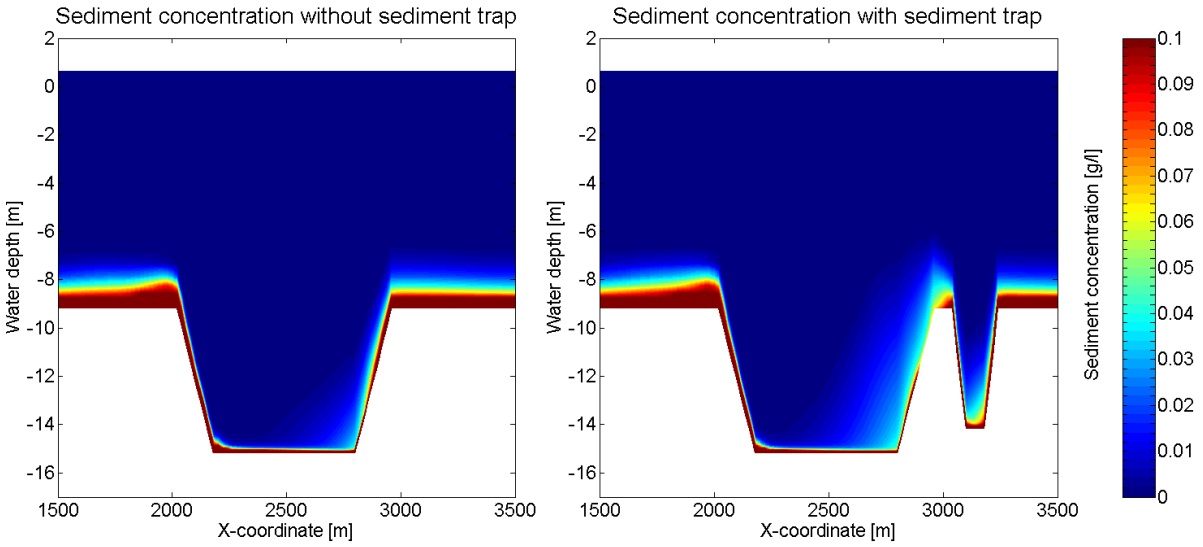

Figure 5.20: Sediment concentration at end of model simulation without sediment trap (left) and with sediment trap (right).

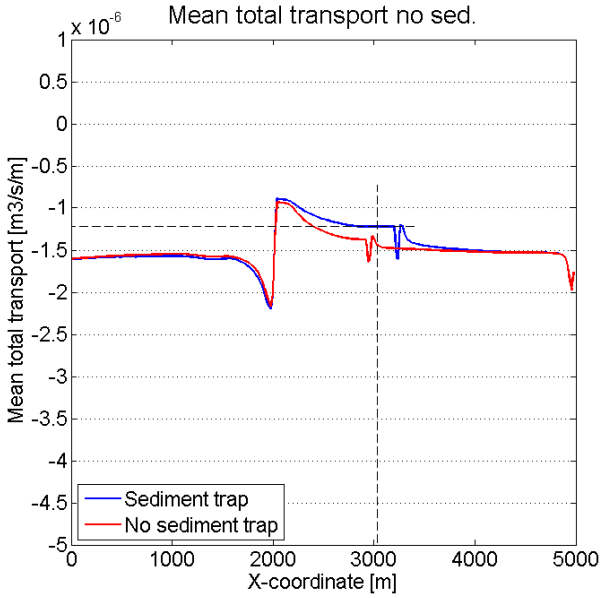

Figure 5.21: Total sediment transport without sediment trap (red) and with sediment trap (blue). The dashed lines show the edge of the sediment trap and the sediment transport at that location.

The sediment trap is found to achieve a trapping efficiency between 20 % - 55 % from the model simulations. The upper limit is found for the scenario where sedimentation is enabled in the entire domain and the lower limit is found by disabling sedimentation in the dredged channels.

The trapping efficiency is expected to be closer to the scenario with sedimentation, as in reality consolidation takes place relatively quickly for low infill rates. Additionally wave induced bed shear stresses are reduced by the fluid mud layer on the seabed causing less erosion of bed material in the channel.

It is expected that the trapping efficiency of the sediment trap could be higher if the dimensions are increased. This is not further studied in this research.

Fluid mud layer sediment trap Even though modeling of the infill due to fluid mud was not the aim of this chapter, the results from modeling the sediment infill in the channel without sedimentation enabled are found to be interesting. The sediment concentration in the channel resulting from infill from a fluid mud layer is shown in Figure 5.22 (left). Suspended sediment concentrations over 10 g/l are found above the adjacent bed level. As a result, sediment is transported to the sides of the channel. In Figure 5.22 (right) the flow velocity field is shown for this event. Here it is observed that flow velocities are directed away from the channel due to horizontal gradients in density from the sediment in the channel.

It is expected that a sediment trap is not very effective against fluid mud infill as it is shown that bypassing of sediment takes place once suspended sediment in the channel reach above the adjacent bed surface. Once this happens sediment is transported towards the sides of the channel due to the horizontal density gradients, thus causing infill in the approach channel. Earlier it was concluded that a high trapping efficiency is expected for the fluid mud infill, however these model results show that bypassing of sediment due to overflowing of the pit occurs. Therefore the trapping efficiency of fluid might only be high for a short period, until the infill reaches the top of the trap.

The formation of fluid mud is expected to be caused by a significantly larger erosion rate than sedimentation rate, as is the case in the model for no sedimentation.

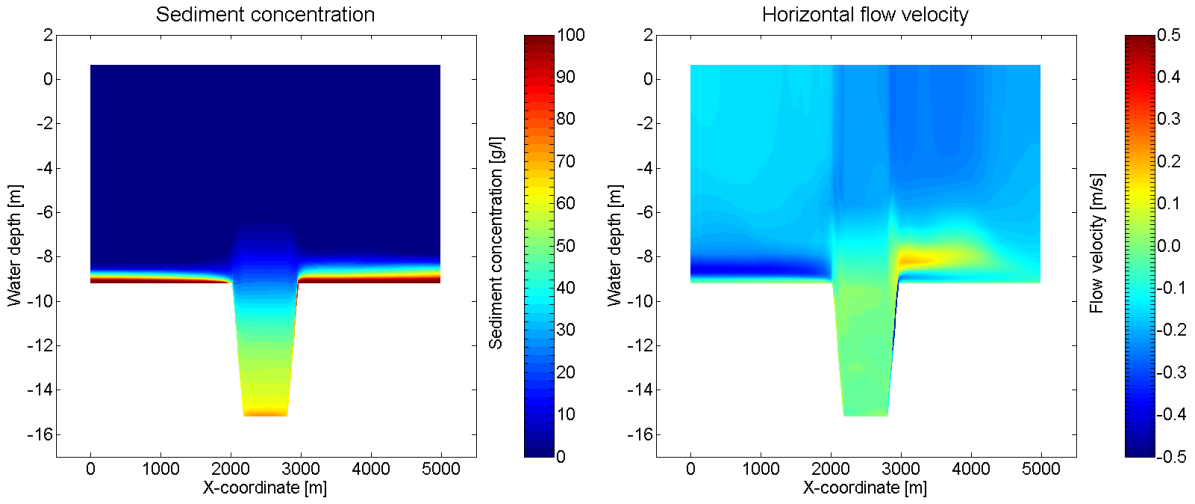

Figure 5.22: Sediment concentration for fluid mud infill (left) and flow velocity as a result of horizontal density gradients due to sediment from channel (right)

5.2.3. DISCUSSION

The sediment trap has shown to reduce the sediment transport by the residual current for 20 - 55 %. Whether this reduction is enough to conclude that the sediment trap should be constructed is discussed in this section.

TRAPPING TIME SCALE

The perpendicular cross-sectional area of the sediment trap is 160 m^2. For a mean daily flux of 2,500 kg/m/day in the wet season and a trapping efficiency of 20 - 55 % the trap would be filled within 1 to 3 months for a sediment density of 300 kg/m^3. This assumes that the trapping efficiency is constant and the sediment has enough time to consolidate.

It is expected that the trapping efficiency of the sediment trap reduces over time after infill has taken place and the depth of the trap is decreased. Additionally, if consolidation rates are relatively low, sediment bypasses the trap more easily. Therefore, the sediment trap needs to be maintained more frequently than the calculated 1 to 3 months in order to uphold the trapping efficiency.

The lower and upper estimates for the trapping efficiency of the channel alone are 45 - 100 %. The associated trapping efficiency of the sediment traps are 20 - 55 % respectively. Hence, the sediment trap captures around 50 % of the total trapped sediment. In the case of 100 % trapping by the channel alone, the sediment trap does not cause additional total infill as trapping of the entire flux already takes place. The model results for no sedimentation in the channel have shown that the sediment trap increased the total trapping only slightly. It is expected that a sediment trap increases the total amount of trapping as the total cross sectional dredged area is larger and the trapping efficiency of the channel is 100 % for the upper estimate only. Additionally, the bed surface between the sediment trap and the main channel will most probably erode and cause additional infill in the main channel and could reduce the trapping efficiency of the sediment trap eventually.

The sediment concentrations in the model are lower than measured, this could be of influence on the trapping efficiency due to different hindered settling effects and difference in flow behavior of the more dense suspension in reality.

In this study only one geometry of the sediment trip is tested, it is expected that a larger trap could increase the trapping and does not have to be maintained as often. Wave induced motions are expected to prevent the consolidation of mud in the sediment trap. Therefore a relatively deep trap would probably be effective to obtain higher consolidation rates.

ASSUMPTIONS

The trapping model is based on a number of assumptions that are of influence on the reliability and applicability of the outcomes. The following assumptions are of particular interest:

- The parallel flow component in the channel is not taken into account. Due to the relatively small angle of the flow with respect to the proposed channel and sediment trap the trapping efficiency and resulting infill is likely to be influenced by the parallel flow component.

- Only fine sediment is considered in the model. In reality a combination of cohesive and non-cohesive material is expected to be part of the infill which could lead to different consolidation behavior.
- Wave streaming in the wave boundary layer is not taken into account in the model because the wave angle is large compared to the residual flow direction. In reality wave streaming could cause additional transport, however, it is uncertain what the influence is of the mud layer on the wave streaming velocity.
- 3D effects of stratification and salinity are not taken into account and the residual flow is assumed to occupy the entire water depth with a constant velocity. The top part of the water column was found to have an opposing residual current to the bottom part of the water column, therefore the flow profile is different and expected to be more variable than simulated in the model.
- Only one cross section in the middle of the proposed channel is considered. The trapping efficiency and sediment transport rates might be different for other cross sections of the channel.

ALTERNATIVES

In order to assess the practical applicability of the sediment trap, the base case without sediment trap is compared to the alternative with sediment trap.

Alternative 1: No sediment trap If no sediment trap is constructed, the capital dredging volume is the same as the base value (estimated by LWI around 30 Mm^3, neglecting clean-up and side slope degradation). The infill in the main channel is in the order of 10 Mm^3/year and should be removed by maintenance dredging. The shipping related downtime was estimated by LWI to be around 30 % of the time. Therefore the total amount of infill should be removed in 70 % of the available time. The proposed maintenance dredging plan states that a WID is deployed for 12 months per year and a TSHD (with 16,000 m^3 storage) for 7 months per year in order to keep the channel navigable.

Alternative 2: Sediment trap If a sediment trap is constructed of the size as used in this chapter, the capital dredging volume is approximately increased with an additional 1 Mm^3. The shipping related downtime in the sediment trap is 0 %, which results in an increase in dredging capacity. If 20 - 55 % is trapped in the sediment trap, the workability downtime of 30 % is compensated for by the trapping of the sediment trap. Continuous maintenance dredging is still expected to be required during the wet season with the construction of the sediment trap, however, the production capacity of the TSHD could possibly be lower. Besides, outside the peak months the sediment trap is most probably more effective due to lower infill rates and associated increased consolidation of the mud infill. Therefore the total deployment of maintenance equipment could be reduced by the construction of the sediment trap.

5.2.4. CONCLUSION

A sediment trap is concluded to be effective to reduce infill in the approach channel, which is particularly beneficial during peak infill rates in the wet season. The sediment trap requires frequent maintenance dredging if the trapping efficiency is to be secured. During the down-time from shipping the sediment trap could be maintained such that the generally unused down-time can be used effectively. During the dry season infill rates are significantly lower and it is expected that consolidation rates in the trap are higher.

During high infill rates the trapping efficiency of the trap is expected to decrease. Therefore a larger sediment trap than modeled here might be required to increase the time scale of effective trapping. The exact geometry should be considered with further studies based on a cost/benefit analysis.

5.3. REDUCTION OF HORIZONTAL SALINITY GRADIENTS

The large Delft3D model is used to simulate the second solution to reduce sediment infill in the dredged channel. A dredged channel in the ebb tidal bar should reduce the horizontal salinity gradients in the area of the approach channel. Thereby limiting the residual flow caused by this stratification. The channel should attract more flow in offshore direction and redirect the fresh water plume from the estuary away from the project area.

Additionally, sediment originated from the Estuary might be deposited more offshore, reducing the sediment supply towards the dredged channel.

In the original project proposal, a channel is required through the ebb tidal bar to allow ships to sail into the Estuary. This channel is designed to be dredged to a depth of 8 m LAT and to a width of 150 m. The channel through the ebb tidal bar is implemented for the same depth (9.2 m MSL) and a larger width to allow more flow through the channel. The width in the Delft3D model is approximately 400 m.

The bathymetry of the Delft3D model with the channel in the ebb tidal bar is shown in Figure 5.23.

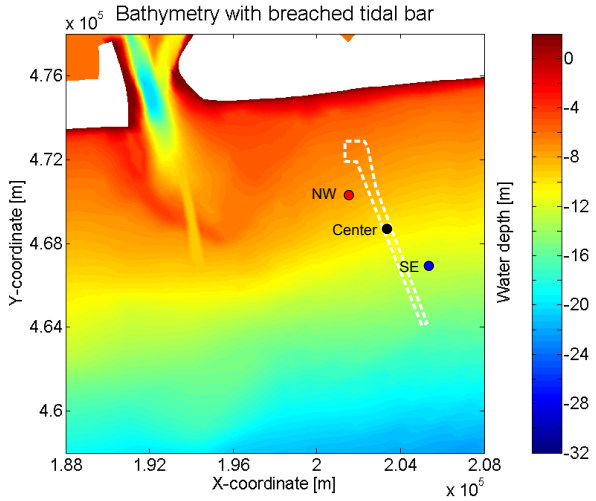

Figure 5.23: Bathymetry Delft3D model with channel in tidal bar.

5.3.1. RESIDUAL FLOW VELOCITY

The tide averaged flow velocity for a mean tide during the wet season shows no significant effect on the near-bed residual flow velocity if the channel in the ebb tidal bar is implemented. Figure 5.24 shows the tide averaged flow velocity for the scenarios with and without a channel in the ebb tidal bar for the same locations used in Chapter 3. The flow velocity in the higher part of the water column does show a larger difference than the bottom flow velocities. The following section shows the salinity profiles for both cases.

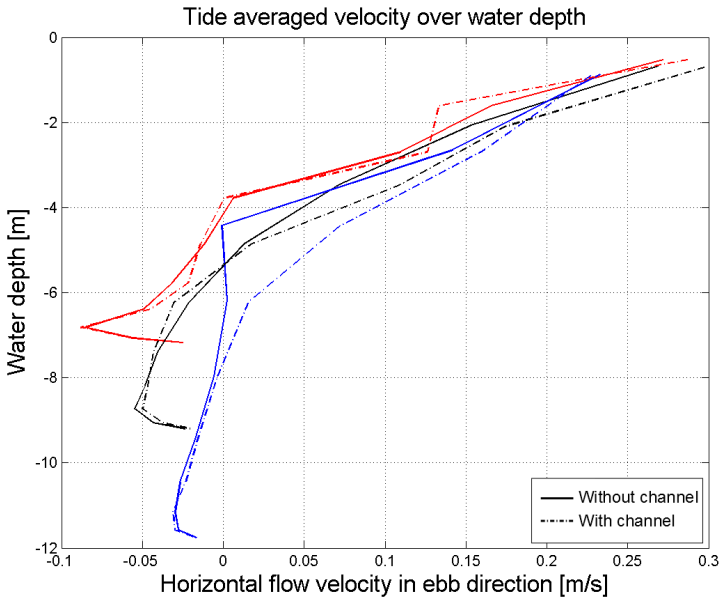

Figure 5.24: Tide averaged velocity in positive ebb direction with channel (solid) and without channel (dashed)

5.3.2. SALINITY

The salinity profiles in the top layer are shown in Figure 5.25 and the salinity in the bottom layer in Figure 5.26. It can be seen that the shape of the fresh water plume in the top layer is significantly changed by the channel in the ebb tidal bar. The salinity in the bottom layer does not show a distinct different at the location of the approach channel. This confirms the difference in top and bottom flow velocities shown in Figure 5.24.

Around the estuary entrance, the salt water inflow is predominantly originated from the deepest part of the ebb tidal bar on the Eastern side. With the channel in the ebb tidal bar salt water can more easily be transported into the estuary and a small increase in bottom salinity is found in the estuary entrance.

From the salinity profiles it is concluded that the residual current is most probably caused by the vertical stratification. The flood flow directed towards the estuary is originated from the bottom part of the water column, whereas the (less saline) ebb discharge is mostly present in the top part of the water column. The salt water inflow of the estuary is of such large quantities that the channel is not capable of reducing the flow velocities in the area of the dredged channel significantly.

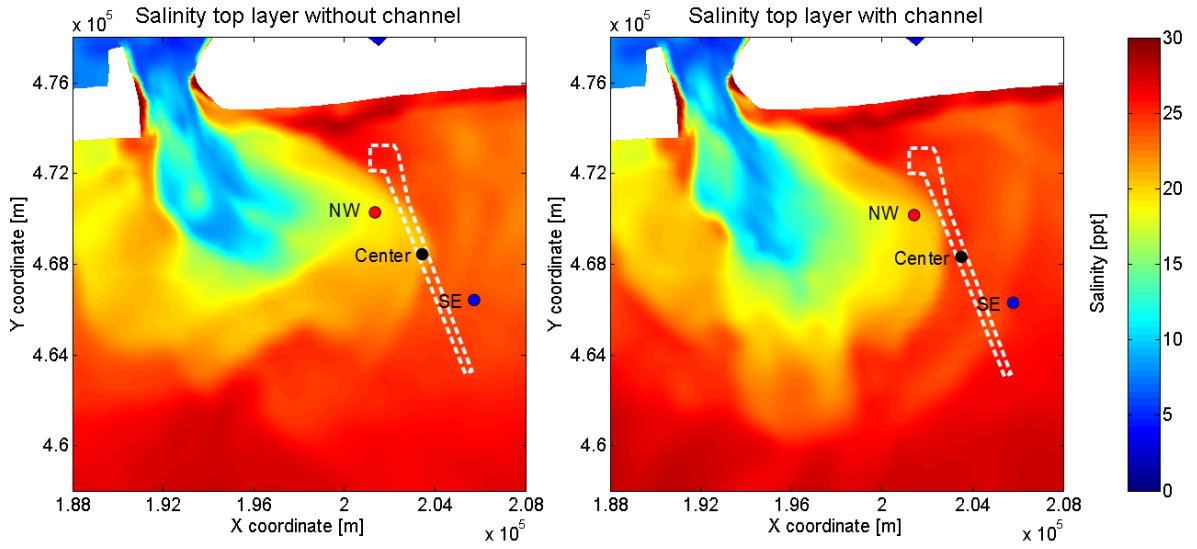

Figure 5.25: Salinity in top layer at maximum flood flow with (left) and without (right) channel in the ebb tidal bar

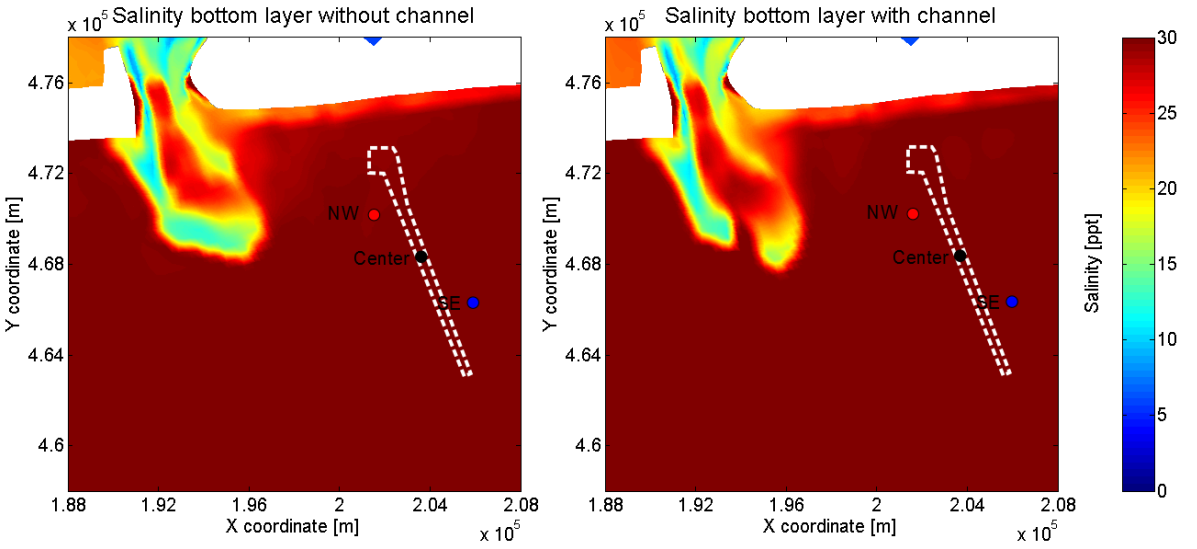

Figure 5.26: Salinity in bottom layer at maximum flood flow with (left) and without (right) channel in the ebb tidal bar

5.3.3. SEDIMENTATION

The sedimentation pattern during a wet spring tide with waves of H_s = 1.5 m is modeled with and without the channel in the ebb tidal bar. The sedimentation pattern for the scenarios with and without the channel is shown in Figure 5.27. No scale bar is present in the figure as the sedimentation pattern is analyzed only qualitatively. It is observed that only a very small difference in sedimentation is caused by the channel in the ebb tidal bar. Therefore no significant reduction in sediment supply to the dredged channel is to be expected.

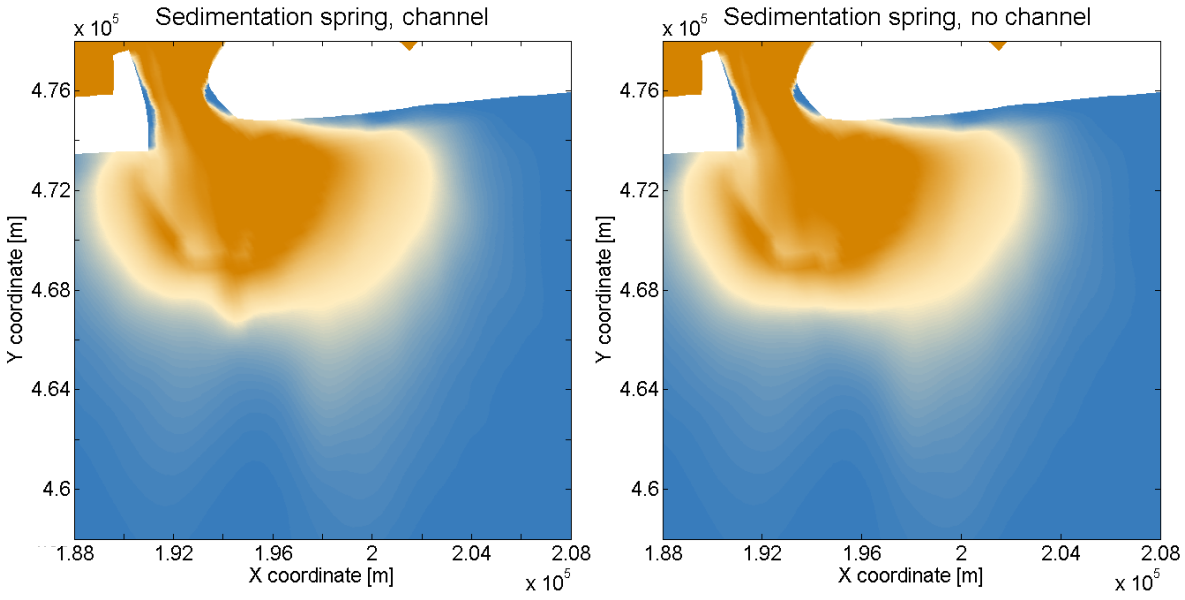

Figure 5.27: Sedimentation pattern after a wet spring tide with waves of H_s = 1.5 m.

5.3.4. CONCLUSION

From the model results it is shown that dredging a channel in the ebb tidal bar is not effective in reducing the residual currents, nor in reducing the sediment supply from the Estuary significantly.

The vertical flow profile is found to be changed only significantly in the top part of the water column. The bottom salinity experiences no noticeable change in the area of the proposed channel. The channel in the ebb tidal bar is concluded to be too small to cause a significant change in the bottom flow profile at the project site.

5.4. CONCLUSIONS

In this chapter three solutions for reducing the sediment infill in the approach channel were analyzed. The first solution is considered only briefly as a simple analysis showed the solutions has relatively low potential and more data and sophisticated tools are required to assess the solution in detail. The second considered solution is the sediment trap adjacent to the approach channel to limit sediment infill from the residual near bed transport. By the use of a small scale 2-DV model the sediment infill was analyzed. The sediment trap is considered to be effective in reducing sediment infill in the dredged channel between 20 - 55 %. Additionally, qualitative sediment infill from a fluid mud layer was observed in the 2-DV model as well. It was shown that during high infill rates during fluid mud events, the consolidation rate of the sediment in the channel is lower than the infill rate and sediment bypasses the channel once the infill reaches the surrounding bed level.

The third solution that is analyzed in this chapter is a dredged channel in the ebb tidal bar. This measure was proposed to reduce the stratification induced residual current in the project area. However, by the use of the Delft3D model from Chapter 3, it was shown that the residual current does not decrease in flow velocity. Furthermore, sediment supplied by the Estuary did not show to be affected significantly by the change in ebb tidal bar bathymetry.

6

CONCLUSIONS AND RECOMMENDATIONS

6.1. CONCLUSIONS

The conclusions from this research are separated in three categories in order to distinguish the different aspects of the objectives of this report. First the conclusions from the system analysis are shown, followed by the conclusions on general mitigation measures for fine sediment infill. Finally, the conclusions on the proposed site specific mitigation measures are presented.

It is noted that the amount of data available for this study was limited, and additional monitoring is required for further studies.

6.1.1. SYSTEM ANALYSIS

The following conclusions are drawn from the system analysis conducted in Chapter 2 and 3:

- The project area is located in a complex hydrodynamic and morphologic system with strong seasonal variations. High waves and river discharge conditions during the wet season cause significantly larger sediment transport rates compared to dry season conditions.
- Sediment transported by currents from the estuary and sediment transported by the residual Westward current are the two main sources for infill of the proposed channel.
- The Delft3D model was used to estimate suspended sediment transport from the estuary towards the proposed channel. It was found that only a limited amount (4 %) of the gross sediment transport through the estuary entrance reaches the proposed channel. Approximately 10 % of the gross sediment transport from the estuary is deposited between the ebb tidal bar and the proposed channel. A portion of this sediment will be transported back towards the estuary, whereas another part causes potential infill in the proposed channel indirectly. This indirect infill is likely to take place in the form of fluid mud. During extreme wave events sediment accumulated between the estuary and the channel erodes rapidly, causing a fluid mud layer to develop. The expected infill from this mechanism is uncertain due to the limited amount of observations. During 'ideal' circumstances the fluid mud layer was not found to reach as far as the proposed channel, which suggests that infill of this type occurs infrequently.
- Sediment induced buoyancy effects cause high near-bed concentrations that are transported by a residual Westward current in the coastal zone. The Delft3D model showed that the residual near-bed current is partially caused by local stratification effects, which is in contrast to suggestions by earlier studies that state large scale ocean currents are entirely responsible for the residual current.
- The residual transport is concluded to be the main overall contributor for sediment infill in the proposed channel by comparing the sediment fluxes of the different sediment transport mechanisms.

6.1.2. GENERAL MITIGATION MEASURES

This section provides conclusions on mitigating sediment infill for similar (general) circumstances as the considered specific case.

- The main sediment transport mechanisms for should be identified first, as the sediment concentration profile and (transport driving) flow regime are determinative for the sediment infill. The capacity of waves to erode sediment is generally higher than the capacity of the flow to keep sediment in suspension in such environments. Therefore, it is likely that sediment induced buoyancy effects take place and cause the sediment concentration to be concentrated close to the seabed.
- Three types of measures are identified to reduce sedimentation of approach channels. The three types focus on the following aspects of the infill process: sediment transport towards the channel, trapping efficiency of the channel and efficient removal of sediment from the channel.
- Achieving long term reduction of sediment transport towards the channel is generally difficult because of the high complexity of fine sediment transport and high sediment availability. Additionally, solutions that require the use of rocks or fixed structures are generally not practically or economically feasible in muddy deltaïc regions due to the weak subsoil and low availability of rocks.
- Due to the complexity of reducing sediment transport and detailed required knowledge of the local site, measures that focus on trapping reduction and efficient removal of sediment from the channel are expected to be the two types of measures with the most potential. In the initial design phase, the channel location and layout should be designed to reduce sedimentation as much as possible in order to minimize maintenance dredging.

6.1.3. LOCAL MITIGATION MEASURES

Conclusions drawn on mitigation measures considered for the specific case are treated in this section. Three measures to mitigate sediment infill in the specific case were found potentially effective by initial evaluation of the proposed options and were further analyzed.

- Two of the considered measures were concluded to have only limited potential effectiveness after further analysis:
  - Channel bed slope

    A downward sloping channel bed could cause mud infill to be transported towards the offshore end of the channel under the influence of gravity. The consolidation rate of the mud determines whether the sediment remains mobile long enough to generate a stable fluid mud layer. A stable fluid mud flow for the maximum possible steepness of the bed slope is only achieved for a narrow band of properties of the mud layer. Therefore, it is expected to be unlikely to achieve the right circumstances for a stable mud flow in this specific case. Due to a lack of detailed knowledge of the local material and lack of required modeling tools this option is not discussed in detail. A combination of a slope in the channel bed and the use of water injection dredging may improve the effectiveness and should be considered in further research.
  - Redirect estuary plume

    By constructing a channel through the ebb tidal bar in front of the estuary entrance the (fresh water) estuary plume could be redirected causing the residual flow to decrease in the project area. By the use of the Delft3D model this measure is simulated. A reduction in the near-bed residual flow is not achieved by this measure according to the model outcomes. No significant change in the spatial distribution of sediment deposition from the estuary was found in the model, which could have been an additional advantage of this measure. If the channel in the ebb tidal bar is increased in dimensions a positive effect might be found, however this would probably lead to unrealistically high required dredging volumes.

  The preferred option to mitigate sediment infill in the proposed channel is elaborated more extensively:

  - Sediment trap

    A 2-DV trapping model showed that the proposed main channel traps 55 - 100 % of the total sediment transport. The lower limit is found for unconsolidated material, whereas the upper limit

is found for quickly consolidating material. A sediment trap of 25 m wide and 5 m deep applied parallel to the main channel traps 20 - 55 % of the total sediment transport according to the model.

- For a constant trapping efficiency, the sediment trap would be filled during the peak wet season period in approximately 1 - 3 months for a sediment density of 300 kg/m^3. If the trap is partially filled, the trapping efficiency is likely to be lower, depending on the consolidation rate of the mud infill. Due to wave action sediment is expected to be kept in suspension in the trap and causing the consolidation rate to remain low. A relatively deep sediment trap is therefore expected to be beneficial for the consolidation rate.

- Down-time due to shipping traffic was estimated to reduce the workability of the maintenance dredging vessels by approximately 30 %. A sediment trap of the considered geometry requires approximately 1 million m^3 initial dredging which is a relatively small amount compared to the 30 million m^3 required for the main channel. Maintenance dredging (and possibly the initial dredging) of the sediment trap could take place during maintenance down-time of the main channel. Particularly during the wet season when infill rates are high, a sediment trap is concluded to increase maintenance efficiency. Dredging equipment with lower production capacity is expected to be sufficient to keep the channel navigable as more time is available to dredge the same amount of material. The increased storage for sediment infill by the sediment trap may allow for less frequent maintenance dredging as well.

6.2. RECOMMENDATIONS

The following recommendations follow from this research:

- Additional field data on sediment properties, the occurrence of fluid mud and flow velocities in the project area would improve the quantitative accuracy of this study. However, significant additional data is required to increase the accuracy considerably due to the high variability of the system. Acquiring this data is expected to be costly and requires a long period of observations. Therefore, obtaining enough additional data might not be economically feasible. Hence, improving the accuracy of the outcomes without additional data is preferred. This could be achieved by conducting a sensitivity analysis or probabilistic approach of the calculations and thereby find a range of outcomes with an associated reliability interval.

- Improvements of the used Delft3D model will increase the (quantitative) understanding of the system. The model can be improved by enabling flocculation, incorporation of non-cohesive sediment and using different critical shear stress for deposition. By the use of additional data, further calibration could be performed. The effect of a mud layer near the seabed does not reduce the erosion of underlying sediment in the model, which does occur in reality. This is a limitation of the Delft3D software package and is therefore recommended to integrate for future development of the model.

- Further research in the optimum use of a nautical depth for the vessels using the approach channel is recommended. It should be considered to what extent sediment infill is a problem. The low consolidation rate of the sediment and propeller wash from vessels keep sediment concentrations low in the approach channel, potentially causing no substantial hinder to navigation.

- The 2-DV trapping model suggests that the trapping efficiency of a dredged channel may be significantly reduced if some infill has taken place. Due to hindered settling, the sediment concentration in the channel remains low and reaches to the surrounding bed level relatively quickly for only low concentrations. Further infill (ie. trapping efficiency) of the channel seemed to decrease as a result of this low concentrated infill already. This suggests that the amount of maintenance dredging might be significantly lower due to a reduction in trapping efficiency and should be considered in further studies.

- The sediment trap is found to be effective in trapping a portion of the sediment transport towards the main channel. The geometry should be optimized for the trapping efficiency and sediment capacity. The consolidation rate of sediment infill from the residual current determines the trapping efficiency for a large part and should be monitored in the field. Wave action is likely to reduce the consolidation rate and therefore a relatively deep sediment trap is thought to be beneficial for the trapping efficiency.

BIBLIOGRAPHY

Allen, J.R.L. The nigerian continental margin: Bottom sediments, submarine morphology and geological evolution. *Marine Geology*, 1:289–332, 1964.

Allen, J.R.L. Late quaternary niger delta and adjacent areas: Sedimentary environments and lithofacies. *Bulletin of the American Association of Petroleum Geologists*, 49(5):547–600, 1965.

Allen, J.R.L. and Wells, J.W. Holocene coral banks and subsidence in the niger delta. *The Journal of Geology*, 70(4):381–397, 1962.

Bakker, S.A. Uncertainty analysis of the mud infill prediction of the olokola lng approach channel. Master's thesis, Delft University of Technology, 2009.

Boskalis, . Soil investigation. Project documents, 2012a.

Boskalis, . Geotechnical design parameters for the soil conditions. internal memo, 2012b.

Deltares, . *Delft3D-FLOW User Manual*. Deltares, 3.15.33641 edition, 2014.

EGSi, . Metocean investigation. Data Interpretation and Modelling, 2004.

EGSi, . Project sedimentation study. Infill predictions for base case, 2006.

Fischer, H.B.; List, E.J., and Koh, R.C.Y. *Mixing in Inland and Coastal Waters*. Academic Press, 1979.

Fugro, . Project onshore sand winning project. Hydrology Study, 2006.

Google, . Google maps. internet source. visited at 16/10/2013.

Houwman, K.T. and Hoekstra, P. Tidal ellipses in the near-shore zone (-3 to -10 m; modelling and observations. *Coastal Engineering*, 1998.

HR Wallingford, . Prediction of infill. Model refinements following October 2004 to January 2005 field measurements, 2005.

Jenkins, S. A.; Aijaz, S., and Wasyl, J. Transport of fine sediments by hydrostatic jets. In *Nearshore and Estuarine Cohesive Sediment transport*, pages 331–347. 1993.

Jensen, J.H.; Madsen, E.Ø., and FredsØe, J. Oblique flow over dredged channels - i: Flow description. *ASCE, Journal of Hydraulic Engineering*, 125(11):1181–1189, 1999.

Louisiana State University, . The world delta database, the niger delta. Internet source. http://www.geol.lsu.edu/WDD/AFRICAN/Niger/niger.htm, Visited on 09/05/2014.

LWI, . Sediment infill for reduced trestle length. Project documents, 2006a.

LWI, . Metocean dataset. Reissued 2012, 2006b.

LWI, . Outline capital and maintenance dredging execution plan. Project documents, 2012a.

LWI, . Dredging and offshore sand winning data book. Project documents, 8 2012b.

Manning, A.J.; Baugh, J.V.; Soulsby, R.L.; Spearman, J.R., and Whitehouse, R.J.S. *Cohesive Sediment Flocculation and the Application to Settling Flux Modelling*.

McAnally, W.H.; Friedrichs, C.; Hamilton, E.; Shrestha, P.; Rodriguez, H.; Sheremet, A., and Teeter, A. Management of fluid mud in estuaries, bays and lakes. i: Present state of understanding on character and behavior. *Journal of Hydraulic Engineering*, pages 9–22, 2007.

Mehta, A.; Lee, S-C., and Li, Y. Fluid mud and water waves: a brief review of interactive processes and simple modeling approaches. Technical report, U.S. Army Corps of Engineers Waterways Experiment Station, Vicksburg, Miss., 1994. WES Contract Rep. No. DRP-94-4.

Milliman, J.D.; Rutkowski, C., and Meybeck, M. River discharge to the sea, a global river index. In *International Geosphere Biosphere Programme: A Study of Global Change*. 1995. Land-Ocean interactions in the Coastal Zone.

Mitchener, H.J.; Whitehouse, R.J.S.; Soulsby, R.L., and Lawford, V.A. Estuarine morphodynamics. Technical Report 17, HR Wallingford, 1996. Development of SedErode - instrument for in-situ mud erosion measurements.

Mofjeld, H.O. and Lavelle, J.W. Formulas for velocity, sediment concentration and sediment flux for steady uni-directional pressure-driven flow. Technical report, NOAA, Pacific Marine Environmental Laboratory, 1988.

National Research Council, . *Sedimentation control to reduce maintenance dredging of navigational facilities in estuaries*. National academy press, 1987. Marine Board, Commission on Engineering and Technical Systems.

NEDECO, . *The Waters of The Niger Delta*. S.R.O. The Hague, 1961.

Park, K.; Wang, H.V., and Kim, S. A model study of the estuarine turbidity maximum along the main channel of the upper chesapeake bay. *Estuaries and Coasts*, (31):115–133, 2008.

PIANC, . Minimizing harbour siltation. Technical Report 102, Maritime Navigation Commission, 2008.

Pietrzak, J. Cie5302 stratified flows lecture notes, 2013. Draft version.

Porrenga, D.H. Clay minerals in recent sediments of the niger delta. In *Fourteenth National Conference on Clays and Clay Minerals*, pages 221 – 233, 1966.

Rider, K.E. Shelf circulation patterns off nigeria. Master's thesis, Texas A & M University, May 2004.

Rijn, L.C. van. *sutrench-model two-dimensional vertical mathematical model for sedimentation in dredged channels and trenches by currents and waves*. Rijkswaterstaat, 1985.

Rijn, L.C. van. Sedimentation of dredged channels by currents and waves. In *Int. Conf. on Numerical and Hydraulic Modelling of Ports and Harbours*, 1986.

Roos, P.C. *Seabed pattern dynamics and offshore sand extraction*. PhD thesis, Twente University, The Netherlands, 2004.

Sexton, W. and Murday, M. The morphology and sediment character of the coastline of nigeria - the niger delta. *Journal of Coastal Research*, 10(4):959–977, 1994.

Sheremet, A.; Jaramillo, S.; Su, S.F.; Allison, M.A., and Holland, K.T. Wave-mud interaction over the muddy atchafalaya subaqueous clinoform, louisiana, united states: Wave processes. *Journal of Geophysical Research*, 116, 2011.

Tsuruya, H.; Murakami, K, and Irie, I. Numerical simulations of mud transport by a multi-layered nested grid model. In *Coastal Engineering Proceedings 1990*, number 22, pages 2998–3011. ICCE, 1990.

University of Miami, . Guinea current. internet source. visited at 24/10/2013.

University of Washington, . Etm: The estuarine turbidity maximum, puget sound oceanography 2011. Lecture slides, 2011. url: http://faculty.washington.edu/pmacc/Classes/Est2011/Estuaries2011.html.

van Rijn, L.C. Basics of channel deposition/sedimentation. note.

Whitehouse, R.; Soulsby, R.; Roberts, W., and Mitchener, H. *Dynamics of Estuarine Muds*. Thomas Telford Publishing, 2000. HR Wallingford.

Winterwerp, J.C. Stratification effects by cohesive and noncohesive sediment. *Journal of Geophysical Research*, 106(C10):22,559–22.574, October 2001.

Winterwerp, J.C. Stratification effects by fine suspended sediment at low, medium, and very high concentrations. *Journal of geophysical research*, 111, 2005.

Winterwerp, J.C. Sediment dynamics. Lecture slides, 2014.

Winterwerp, J.C. and van Kesteren, G.M. *Introduction to the physics of cohesive sediment in the marine environment*. Elsevier, 2004. Developments in Sedimentology 56.

Winterwerp, J.C.; de Boer, G.J.; Greeuw, G., and van Maren, D.S. Mud-induced wave damping and wave-induced liquefaction. *Coastal Engineering*, 64, 2012.

A

CRITICAL BED SHEAR STRESS

Multiple relations are found in literature to estimate the critical bed shear stress for erosion (τ_e) of cohesive sediments, however all of these relations are highly empirical (Winterwerp and van Kesteren, 2004). A critical bed shear stress for deposition(τ_c, d) is often used as well, which gives a maximum bed shear stress that allows for sedimentation (Manning et al.). This value is practical in use for modeling, however in reality simultaneous deposition and erosion occurs (Winterwerp and van Kesteren, 2004).

The first two relations for $black\tau_e$ are based on the bulk density of the bed. An increase in (dry) bed density generally increases the number of bonds between the particles (flocs), hence increases bed strength. The two correlations read (Whitehouse et al., 2000):

$$\tau_e = E1C_M^{E2} \tag{A.1}$$

$$\tau_e = E3\left(\rho_B - 1000\right)^{E4} \tag{A.2}$$

With C_M being the solids concentration in kg/m^3 and ρ_B being the bulk density in kg/m^3. E1-E4 are empirical constants, $E1 = 0.0012$, $E2 = 1.2$, $E3 = 0.015$ $E4 = 0.73$ (Mitchener et al., 1996)

Smerdon and Beasley (1959) found a relation between the plasticity index PI of the mud to τ_e. During their laboratory experiments the undrained shear strength of the material varied between 0.1 kPa to 10 kPa, because of these high strengths, this relation gives relatively reliable estimates (Whitehouse et al., 2000).

$$\tau_e = 0.163PI^{0.84} \qquad PI \ in \ \% \tag{A.3}$$

The plasticity index PI is determined by the plastic limit PL and the liquid limit LL of the soil. These parameters are empirically found by standardized soil mechanical tests. The plasticity index PI is the difference between the liquid limit and the plastic limit ($PI = LL - PL$). It is a measure of the amount of water bounded within the sediment at specific stress or strength levels. The plasticity index and liquid limit can be used to classify the soil with respect to its level of plasticity and cohesive behavior. If the soil's cohesive behavior is determined by clay particles, a relation between the clay content and plasticity index is found which can be used to estimate the type of clay particles that bind water.

The critical bed shear stresses depend on the rate of consolidation of the clay sample, as the bulk density increases over time due to consolidation and the same will be valid for the plasticity index. Sediment that has just been deposited has a lower density and will therefore be eroded more easily. the critical bed shear stress for consolidated and unconsolidated bed material are treated separately.

A.1. CONSOLIDATED BED

Properties of the bed material have been determined for the dredging works by Boskalis Boskalis (2012b) based on soil data from Fugro (2006). The bed properties of the approach channel change with depth and are specified as shown in Table A.1.

The critical bed shear stresses associated with Table A.1 are calculated for equations A.2 and A.3. Equation A.1 is not applicable for bulk densities > 400 kg/m^3, therefore this relation is only used for unconsolidated deposits.

Table A.1: Soil parameters along approach channel

Depth below bed [m]	Bulk density [kN/m³]	Shear strength [kPa]	PI [%]	LL [%]
0 - 2	17	5	20	40
2 - 4	17	15	30	50
4 - 10	16	25	50	80

$$\tau_e = E3\left(\rho_B - 1000\right)^{E4} = 0.015\left(1700 - 1000\right)^{0.73} = 1.79 \text{ N/m}^3 \tag{A.4}$$

$$\tau_e = 0.163 PI^{0.84} = 0.163\left(20\right)^{0.84} = 2.02 \text{ N/m}^2 \tag{A.5}$$

The critical bed shear stress for erosion of the consolidated bed is in the order of 2 N/m^2 for both relations.

A.2. UNCONSOLIDATED DEPOSITS

For unconsolidated deposits the soil characteristics are not known, however they can be assumed to represent certain densities. EGSi (2004) assumed sediment concentrations of $100 - 200 kg/m^3$ for freshly deposited sediments. The relations of equations A.1 and A.2 are used to estimate the critical shear stress for erosion of freshly deposited sediments using a density of 100 and 200 kg/m^3.

$$\begin{aligned} \tau_e &= E1 C_M^{E2} = 0.0012(100)^{1.2} = 0.30 \text{ N/m}^2 \\ \tau_e &= E1 C_M^{E2} = 0.0012(200)^{1.2} = 0.69 \text{ N/m}^2 \end{aligned} \tag{A.6}$$

$$\begin{aligned} \tau_e &= E3\left(\rho_B - 1000\right)^{E4} = 0.015\left(1100 - 1000\right)^{0.73} = 0.43 \text{ N/m}^2 \\ \tau_e &= E3\left(\rho_B - 1000\right)^{E4} = 0.015\left(1200 - 1000\right)^{0.73} = 0.72 \text{ N/m}^2 \end{aligned} \tag{A.7}$$

For freshly deposited material the critical bed shear stress is higher with equation A.2. An average value for the bed shear stress of freshly deposited material is estimated to be around 0.5 N/m^2.

WAVE INDUCED BED SHEAR STRESS

The maximum shear stress that is generated by waves (τ_b) is used to determine whether erosion will occur. In order to assess the possibility and magnitude of erosion of the bed due to waves at the project location, characteristic waves are determined. Using wave data from LWI LWI (2012b) and Boskalis typical wave heights with associated periods for the project area are determined. A distinction is made between wind waves and swell waves, see Table A.2.

Table A.2: Characteristic waves

Wind		Swell	
Hs [m]	Tp [s]	Hs [m]	Tp [s]
0.5	5	0.5	11
1	5	1	12
1.5	5	1.5	13
2	7	2	14
		2.5	14
		3	16

An important aspect of the local wave climate is the variability over the year. During the wet season wave heights are significantly higher and have a larger probability of occurrence. Therefore, if waves are capable of eroding the bed this will happen more during the wet season than during the dry season. A graph of the average (single) wave energy per month is shown in Figure A.1. It can be seen that the average wave energy is highest in July and August and lowest in December and January.

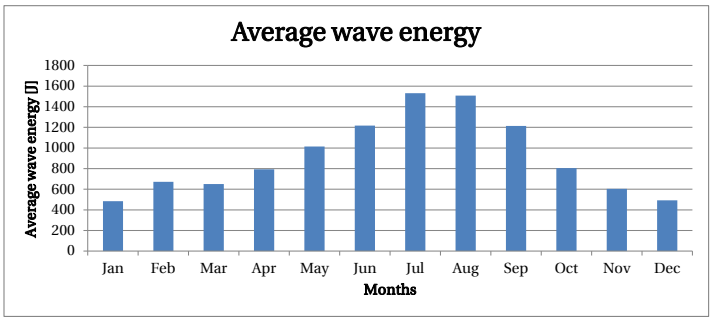

Figure A.1: Average wave energy per month

The bed shear stresses induced by the characteristic waves are calculated for various depths. The rms instantaneous maximum bed shear stress is used for wave induced erosion rates, the equations are obtained from Winterwerp and van Kesteren (2004) and Whitehouse et al. (2000). The maximum instantaneous bed shear stress ($\tilde{\tau}_w$) due to waves is given by:

$$\tilde{\tau}_w = \frac{1}{2}\rho f_w u_{orb}^2 \tag{A.8}$$

With ρ=water density = 1021 [kg/m°3] (30ppt and 20 °C), f_w= bed friction factor [-] which is dependent on the wave Reynolds number R_w:

$$R_w = \frac{U_w A}{\upsilon} \tag{A.9}$$

Where U_w= bottom orbital velocity amplitude [m/s], $A = U_w T/2\pi$= semi orbital excursion [m], T = wave period [s], υ= kinematic viscosity [m^2/s], $U_w or\, u_{orb}$ is given by:

$$U_w = u_{orb} = \frac{\pi H_{rms}}{T_p \sinh(kh)} \tag{A.10}$$

Here $H_{rms} = H_s/\sqrt{2}$, T_p = peak wave period (s) and k = wave number [$1/m$]. f_{ws} = smooth bed friction factor and is given by:

$$f_{ws} = BR_w^{-N} \tag{A.11}$$

Where:

$$\begin{aligned} &B = 2, \quad N = 0.5 \\ &for\ R_w \leq 5 * 10^5 (laminar) \\ &B = 2, \quad N = 0.5 \\ &for\ R_w > 5 * 10^5 (smooth\ turbulent) \end{aligned} \tag{A.12}$$

The depth is varied from 5 to 15 m for all characteristic waves, as the area around the dredged approach channel and harbor basin covers this depth range. Figures A.2 and A.3 show the results for the bed shear stress induced by the characteristic waves. Some graphs are not smooth due to a transition between smooth turbulent and laminar behavior of the flow as is calculated in Eq. A.12. The critical bed shear stress for erosion of consolidated bed ($\tau_b = 2$ N/m^2) and unconsolidated deposits ($\tau_b = 0.5$ N/m^2) are shown as dashed lines in the graphs.

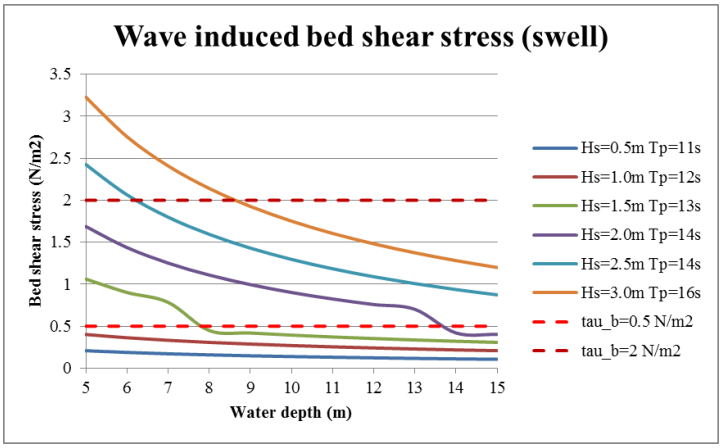

Figure A.2: Characteristic swell wave induced bed shear stress

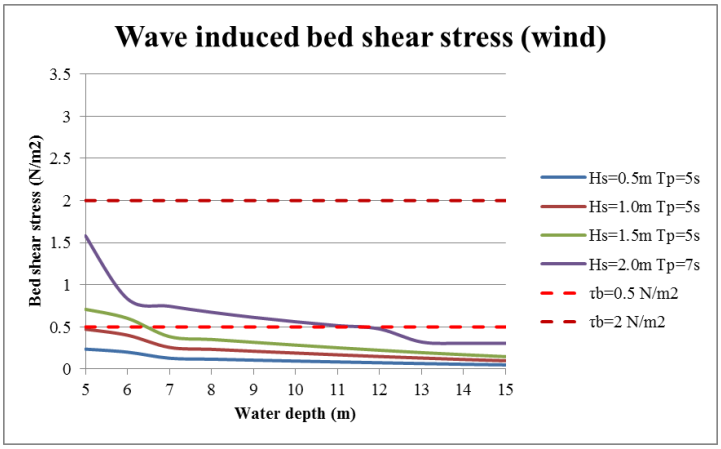

Figure A.3: Characteristic wind wave induced bed shear stress

The graphs show that large swell waves are capable of eroding consolidated bed material in the shallower regions of the coastal zone. Wind waves are not capable of eroding the consolidated bed material as the bed shear stresses do not exceed 2 N/m^2. Unconsolidated deposits are eroded relatively easily by swell waves, above H_s = 1.5 m freshly deposited sediments are eroded for depths smaller than 10 m. Wind waves of H_s = 2.0 m erode freshly deposited sediments for water depths smaller than approximately 10 m.

B

EARLIER INFILL CALCULATIONS

In earlier research to the infill of the dredged area EGSi and LWI have conducted numerical modeling tests to simulate the concentrations and extend of the sediment plume from the Estuary. The models were executed to assess the infill of the dredged area by the Estuary and the influence of the location of the dredged area on the amount of infill. The earlier ('Base Case') layout for the terminal had the maneuvering area located at 8 km offshore. To reduce costs of the pipeline trestle the possibilities for reducing the offshore distance were investigated.

The sediment and water discharge of the Estuary were measured during different tides and seasons by LWI. These data were presented in Chapter 2. EGSi used a 3D mud transport model (SUBIEF-3D) to predict the movement of suspended sediment under the action of hydrodynamic forcing for the 'Base Case' scenario of the terminal layout. The model includes the effect of the damping of turbulence by vertical gradients in density but does not include the effect of gradients in buoyancy caused by sediment. Additional processes were added to the model for the studies: drag reduction, wave stirring, non-linear interaction of bed shear stress from waves and currents, wave-driven currents, settling velocity as a function of turbulence and concentration, simultaneous deposition and erosion and hindered settling (EGSi, 2006). For the model calculations a few assumptions were made:

1. The bar and area between the bar and estuary mouth are mainly sandy and offshore of the bar and inside the estuary are muddy.
2. The inside of the estuary was treated as a boundary condition for generating sediment.
3. Offshore of the bar wave action is sufficient to fluidize the bed at all times, no deposition possible except within dredged areas.

This means that all sediment discharged by the Estuary is deposited as fluid mud and will distribute itself likewise. The amount of sediment that reaches the dredged area is considered to be equal to the total amount of infill, as sediment will stay in the dredged area. The model was calibrated using measured through-depth suspended sediment concentrations at the estuary mouth. The extend of the ebb tide plume of sediment calculated by the model represents the observed ebb tide plume during a large spring tide when a sedimentologist from LWI was present. The predicted annual infill resulting from the Estuary only was calculated based on the infill generated by 600 dry season mean tides, 85 wet season mean tides and 15 wet season large spring tides. Table B.1 shows the results of the modeling.

The results from this model show that the annual infill by the Estuary alone, accounts for $1.4 * 10^6$ m^3/year which is only a small proportion of the total calculated infill ($10 * 10^6$ m^3/year). However, this is calculated for the 'Base Case' terminal layout and is therefore not representative for the current terminal layout.

LWI used the same 3D mud transport model (SUBIEF-3D) to predict sediment infill from the Estuary for different terminal layouts. The 4 km offshore distance option is the most similar to the current proposed layout of the terminal. The model was run for multiple tidal ranges, dry and wet season and different wave heights. Figure B.1 shows the sediment concentrations near the bed and at mid-depth determined by the SUBIEF model for a wet spring tide without waves just after low water. It can be seen that high concentrations (multiple 1,000 mg/l) are present near the bed mostly just behind the ebb tidal bar.

Table B.1: Infill of dredged area generated by the Estuary

Tide type	No tides/yr	Net Flux per tide (tonnes/tide)	Total flux (tonnes/tide)
Dry mean	600	600	360,000
Wet mean	85	1,200	102,000
Wet large spring tide	15	5,400	81,000
Annual infill (tonnes/yr)			543,000
Annual infill (m^3/yr)*			~1,400,000*

** Calculated assuming sediment is dredged at a dry density of 400kg/m^3*

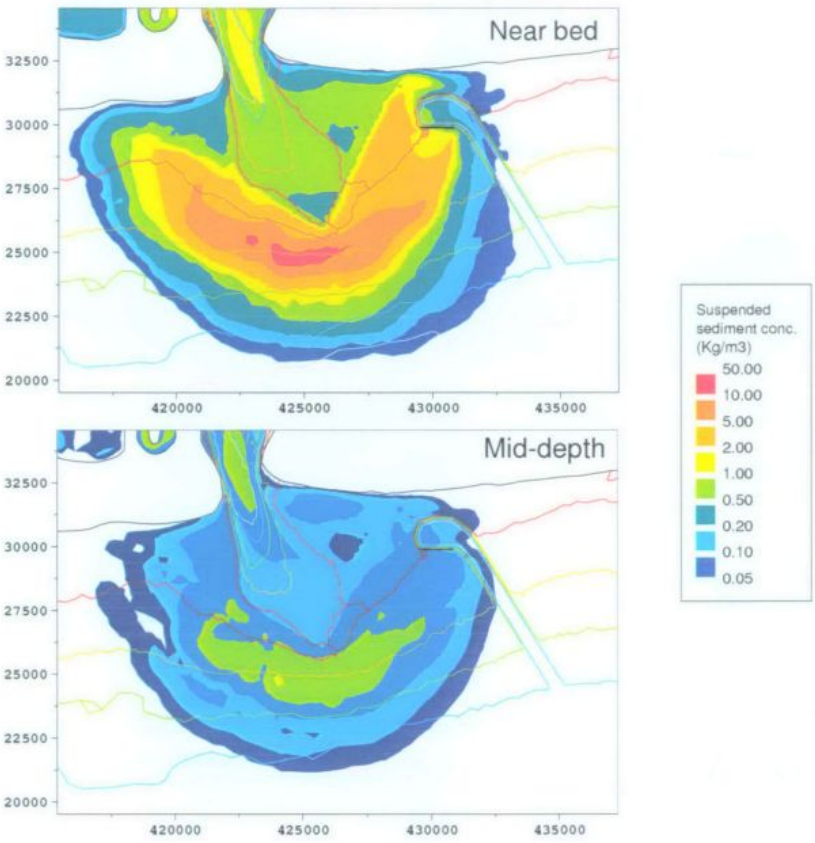

Figure B.1: Estuary sediment plume for wet spring tide just after low water LWI (2006a)

The results for the 4km trestle length were extrapolated to obtain infill rates for the current proposed terminal layout. Here, the infill caused by the Estuary is estimated to be 6 M m^3/year and due to Westward fluvial transport 4 M m^3/year. The infill rates due to the Estuary cannot directly be related to the total amount of sediment supplied to the coastal system. One of the remarks made by LWI is that the dredged channel acts as a sink of sediment and sediment discharged by Estuary might reduce because less sediment is transported back into the estuary at flood tide.

B.1. EARLIER INFILL STUDIES

For previous studies on infill rates of the dredged areas significant local measurements have been conducted to gain insight in sediment transport processes. Numerical modeling of sediment transport has been carried out by LWI and EGSi to obtain quantitative infill rates. First measured sediment concentrations and infill rates are discussed, followed by a paragraph on infill modelling. Finally suggested dominant processes for infill are examined.

LOCAL MEASUREMENT DATA

A lot of measurement data are available on sediment transport. The most relevant data is summarized here. In 2004 a trial dredge pit has been dredged to assess infill rates in this area. The results from the trial dredge pit case are discussed in a separate appendix due to the confidentiality of this information.

Table B.2 shows measured values of river discharge and sediment concentrations at spring tides during a wet season. A peak concentration of 1,200 mg/l is found during a 'big' wet spring tide. These relatively high sediment concentrations can account for high sediment transport rates, this is discussed in the next section. The highest sediment concentration during the big wet spring tides occurs during ebb tide, which indicates that the sediment in concentration is originated from within the estuary.

Table B.2: Summary of spring tide measured discharges and depth-averaged concentrations at the estuary entrance LWI (2012b)

Date	Average discharge (1000's m³/s)		Peak discharge (1000's m³/s)		Average depth-averaged concentration (mg/l)		Peak depth-averaged concentration (mg/l)	
	Ebb	Flood	Ebb	Flood	Ebb	Flood	Ebb	Flood
During infill of pit and observations of fluid mud								
15/16/17 October 2004	~20	~16	-35	~22	~820	~650	~1200	-
2 weeks later when the pit infill seems to have slowed (transition period)								
30/31 October/1 November 2004	-	-	27-30	17-19	~220	-	~500	-
Dry season								
17/18 December 2004	-	-	~25	-	-	-	~350	-

Sediment concentrations: Sediment concentrations were measured during multiple measurement campaigns by LWI, however not all data was reliable enough to use. Bottom mounted OBS sensors before August 2005 were used at 0.20 m and 0.40 m above the bed and after August 2005 at 4 levels above the bed between 0.20 m and 1.00 m to measure sediment concentrations at multiple locations. The OBS data was synchronized with ADCP current and wave data in order to assess the sediment flux and wave effects on sediment concentrations. OBS data was extrapolated to find near bed concentrations. During very high concentration events the lower OBS devices become saturated, it was assumed that saturated OBS responses are representative for a concentration of 30 g/l (30 kg/m^3). Extra attention was paid to the occurrence of very high concentrated layers (or fluid mud). In October 2004 and 2006, fluid mud was observed in the project area. The fluid mud was measured using grab samples, these samples were analyzed in a laboratory to estimate their concentrations.

Suspended sediment concentrations in the offshore area can be of the order of hundreds to thousands of mg/l in the bottom meter of the water column but are generally very low in the surface waters (LWI, 2012b). The near bed suspended sediment concentrations are influenced by wave action and the seasonal discharge

of fine sediments from the Niger Delta. In the mouth of the Estuary there is a strong seasonal variation in suspended sediment concentrations and a strong tidal dependency. In the wet season on the largest spring tides depth averaged suspended sediment concentrations can exceed 1,000 mg/l during the dry season the average concentrations can be an order of magnitude lower.

On the seaward side of the bar grab samples and cores indicate that the bed is soft and muddy. Sediment discharged from the estuary on the ebb tide can escape from the bar, forming a high concentration layer near the bed in the area just outside and to the South-East of the bar. Offshore there is a general near bed flux of fine sediment from East to West driven by the near bed residual flow. The high concentration layer formed outside the river bar joins the prevailing westward flux of sediment (LWI, 2012b).

The observations made during the trial dredge pit showed that the majority of the offshore sediment is present in the bottom meter of the water column. The following studies estimated the near bed sediment flux that were used to calculate infill rates of the dredged channel. From the measurement data synchronized flow velocity and turbidity information were used to estimate monthly average sediment fluxes and daily peak fluxes presented in Figure B.2. The bed frames that were used to measure the velocity and concentrations consisted of an Aquadopp and four OBS sensors (i.e. post-August 2005). Velocity data at 1 m was extrapolated linearly from the 0.8 m reading using the mean gradient of the measured velocities between 0.6 and 0.8 m (i.e. the first 3 bins of Aquadopp data). Velocities below 0.2 m were assumed to decrease linearly to zero at the bed. The sediment concentrations were estimated as described above.

Concentrations in the near bed layer associated with episodic discharge from the river mouth have been observed at up to about 50,000 mg/l and the thickness of such layers has been estimated at up to 0.3 m. The highest concentration layers are also likely to be influenced by gravitational forces causing them to flow down slope. If the movement of the high concentration layers is intercepted by the dredged areas of the Marine Facility the near bed layer will simply flow down slope into the dredged area. The layer will continue to flow under the influence of currents, bed slopes and its own weight within the dredged area. Over time any intercepted layer will gradually consolidate increasing in concentration and forming fluid mud and denser underlying deposits. Once the dry density of the infill exceeds about 300kg/m 3 the layer will form an impediment to navigation. The presence of a thick layer of fluid mud in the operational areas also represents a risk of rapid loss of depth if such a layer is able to dewater over a short time to form a denser deposit. Fluid mud, if present in abundance, in the dredged areas will tend to flow seawards down the channel under its own self weight LWI (2012a).

The monthly mean suspended concentration data averaged over the bottom meter of the water column are shown in Figure B.2 (a). The sediment concentrations for April, June and July are zero because of a lack of data for these months. The gross daily fluxes have been averaged on a monthly basis and plotted as bar graphs showing the North/South (b) components and the East/West (c) components separately. The maximum daily fluxes for each month have also been plotted in these figures. Individual events are clearly much larger than the monthly average, but these tend to be short lived (of the order of a few tidal cycles) during periods when a high concentration layer is present. The seasonality of the fluxes is clearly evident, with a strong westerly flux during the wet season as a result of the westerly near bed residual current and high suspended sediment concentrations.

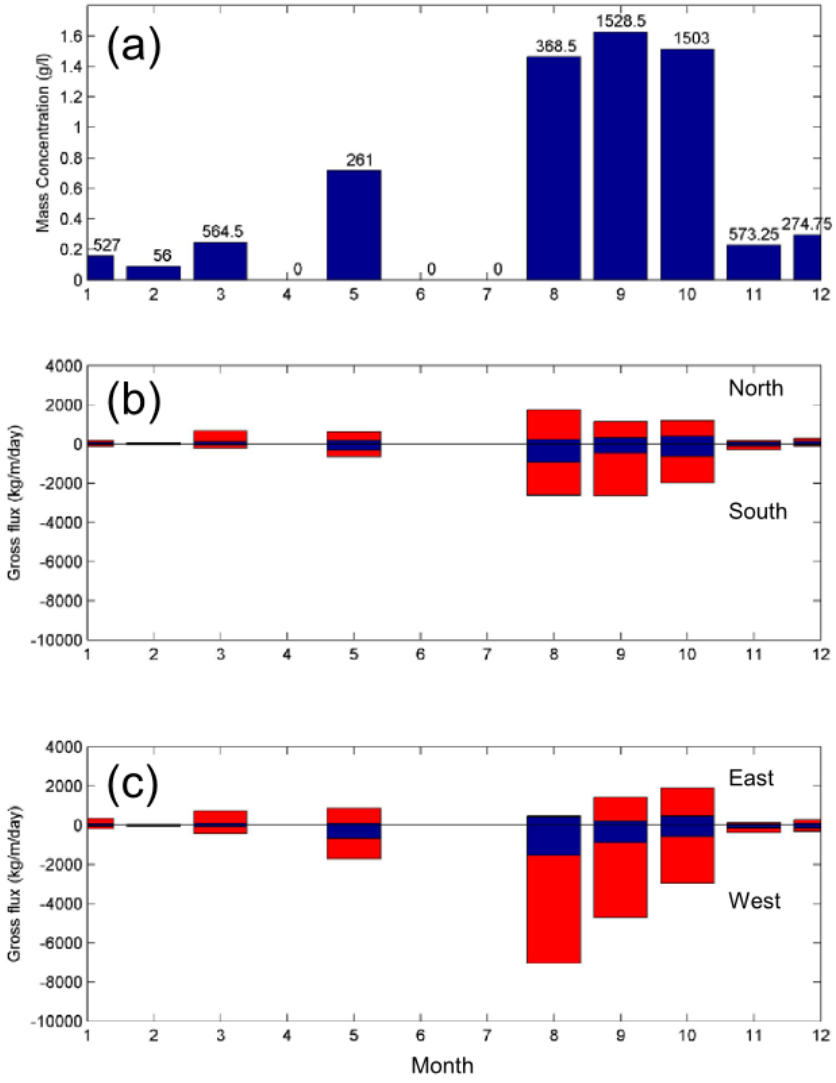

Figure B.2: Monthly average sediment concentrations in bottom meter (a) and sediment flux rates in North/South (b) and East/West (c) direction. Red bars indicate daily maximums and blue bars indicate monthly means LWI (2012b)

C

DELFT3D MODEL

This appendix presents the set-up of the used Delft3D model. The Delft3D model is set-up to model the hydrodynamics and sediment transport of the project area. The processes that are incorporated in the model are salinity, sediments and (in some model runs) waves. As is discussed in Chapter 1, only cohesive sediment is considered and therefore no sand is present in the model. A limited amount of measurements is available which did not allow for extensive calibration of the model. The model is set-up in a more qualitative way such that the processes are modeled in the right order of magnitude.

The model set-up is treated first, followed by calibration results.

C.1. MODEL SET-UP

First the domain and grid are explained, followed by the bathymetry, boundary conditions and physical parameters.

C.1.1. DOMAIN AND GRID

As modeling of the project area has been carried out by LWI and EGSi in the past, the model layout is chosen similar to the previous models. However, the earlier studies used a flexible mesh grid opposed to a curvilinear grid as it is used in this study. A curvilinear grid is chosen because a rectangular grid would be less able to represent the complex topography of the area without having many 'staircase' borders and the lack of ability to increase the resolution at specific model sections. A flexible mesh is not chosen due to its complexity in set-up and the sufficient adequacy of the curvilinear grid. The model has 10 layers in the vertical with different layer heights, see C.1.

Table C.1: Layer heights

Layer	1	2	3	4	5	6	7	8	9	10	Total
% of depth	15	15	15	15	15	10	7	5	2	1	100

The model domain contains the coastal area around the project area and stretches from the first estuary West of the main Estuary to the first estuary East of it, however the coastal bathymetry of these estuaries is not taken into account in the Delft3D model in order to have straight parallel depth contours at the boundaries. Offshore the model extends to the 30 m depth contour. In order to model the estuarine dynamics, the Estuary is included in the model to approximately 30 km upstream. Additional storage areas are introduced to the model grid to account for the large wetland area that is under the influence of tide in the real situation. This extra storage was also applied in the previous models and the approximate equal size of the areas are applied in this study.

The left image in Figure C.1 shows the model grid (blue) and open boundaries (red). It can be seen that the highest resolution is obtained in the estuary mouth and East of the mouth offshore, this is chosen because these areas are important for this study, as the estuary entrance is highly dynamic and the area East of the mouth is where the dredged works are located. The boundaries will be discussed in section C.1.3.

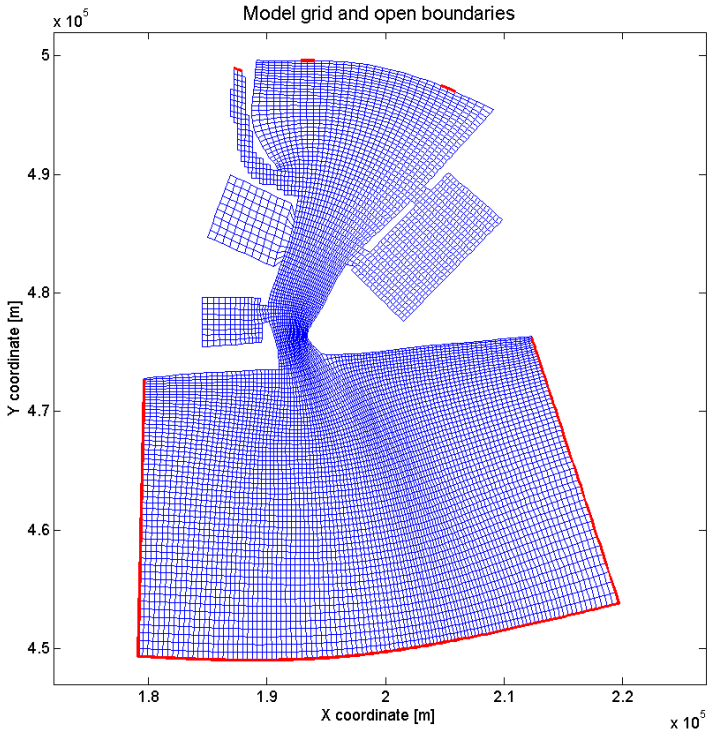

Figure C.1: Model grid with open boundaries (red)

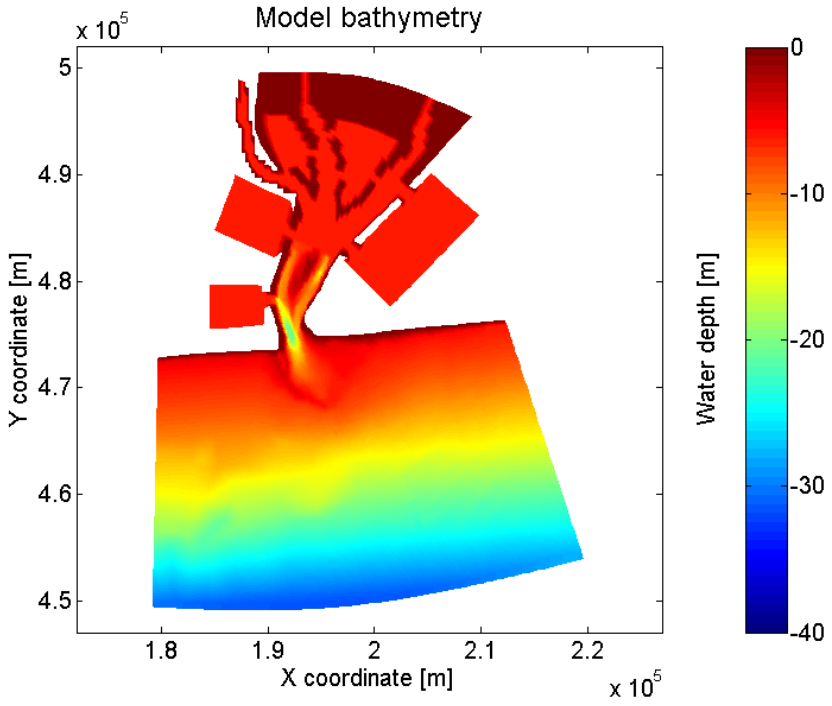

Figure C.2: Model bathymetry

C.1.2. BATHYMETRY

The bathymetry of the model is based on surveys executed for earlier studies (provided relative to LAT). The depth is relative to mean sea level (MSL), which is located at 1.19 m above LAT LWI (2012b). As the Western

and Eastern boundaries are located at the adjacent estuaries the measured depths show ebb tidal deltas of these estuaries. For this study it is not required to model the interaction between the different estuaries and therefore the bathymetry is smoothed in order to obtain shore parallel depth contours and thereby reduce unwanted boundary effects. Figure C.2 shows the bathymetry of the model. The survey data does not cover the entire estuary, therefore a constant depth of 6 m is applied in the estuary and the additional storage areas (which is used by LWI as well).

C.1.3. BOUNDARY CONDITIONS

The model contains multiple open boundaries as can be seen in Figure **??** in red. The offshore boundaries are divided in West, South and East and the upstream (North) boundaries are the three branches of the River entering the estuary. The boundary conditions consist of flow conditions and transport conditions. The flow conditions determine the hydrodynamic characteristics of the boundary and the transport conditions determine the exchange of salinity and sediment at the boundary. The following boundary conditions are applied to the different borders:

Table C.2: Boundary conditions

	North	East	South	West
Flow conditions				
Type	Total discharge	Water level	Water level	Water level
Value	600/1800 m^3/s	Neumann = 0	Astronomic	Neumann = 0
Transport conditions				
Salinity	0	30 ppt	30 ppt	30 ppt
Sediment_coast	0 (Neumann)	0 (Neumann)	0 (Neumann)	0 (Neumann)
Sediment_river	0 (Neumann)	0 (Neumann)	0 (Neumann)	0 (Neumann)

The astronomic water level boundary condition of the Southern boundary is generated by Delft Dashboard (Deltares), which used the TOPEX/POSEIDON global tide model.

The transport conditions for the sediment fractions are set to zero as no set concentration should enter the model. An additional parameter is used to obtain correct sediment concentrations at the boundaries which is called: Neubcmud. This parameter sets a Neumann boundary condition for the sediment concentrations at the model boundaries.

C.1.4. PHYSICAL PARAMETERS

The physical parameters that are used in the model are discussed here. First the constants and roughness is presented, followed by the sediment and morphology.

CONSTANTS AND ROUGHNESS

The constants that are used in the model are gravity (9.81 m/s^2), water density (1021 kg/m^3, average local water density based on temperature and salinity Rider (2004)) and temperature (24 °Rider (2004)).

A uniform Chézy roughness of C = 65 $m^{0.5}/s$ is used in the model. Multiple calibration runs have been executed to obtain the correct hydrodynamic system in the estuary where the roughness was used to decrease resonance and inertia of the system. Due to a lack of data on the water levels and associated discharges this could not be calibrated extensively.

SEDIMENT AND MORPHOLOGY

The two sediment fractions 'Sediment river' and 'Sediment coast' have been used to account for the flocculated state of sediment in saline water and unflocculated state of sediment in fresh water. An initial layer of both sediments is present in the model from the start, which is redistributed by the hydrodynamic forces. River sediment is present in the estuary from 5 km upstream of the estuary entrance Northwards. Around the estuary entrance no sediment is present as the bed is sandy in this area until the ebb tidal bar offshore of the entrance. From outside the ebb tidal bar coast sediment is present in the rest of the domain.

In Appendix A it was concluded that the consolidated mud bed along the coast does not erode due to the presence waves. The only transported material in the system is sediment that has been deposited recently and has not consolidated significantly. Therefore the critical bed shear stresses and dry bed densities of the

eroded mud are relatively low. Table C.3 shows the default values of the sediment properties. This is further discussed in the model results.

Table C.3: Default sediment properties

	River sediment	Coast sediment	Dimension
Reference density for hindered settling	100	100	kg/m^3
Specific density	2650	2650	kg/m^3
Dry bed density	200	200	kg/m^3
Settling velocity	0.2	0.75	mm/s
Bed shear stress for sedimentation	1000	1000	N/m^2
Critical bed shear stress for erosion	0.3	0.5	N/m^2
Erosion parameter (Partheniades)	0.0001	0.0001	-

The morphology settings of the model are set to include the effect of sediment on fluid density and a spin-up interval before morphological changes of 0. The morphological scale factor is 1 by default and the bathymetry is not updated during the simulations.

C.2. MODEL OUTPUT

C.2.1. SCENARIOS

The model as it is described above is used to simulate multiple scenarios. These scenarios are chosen based on literature and availability of measurement data. As is discussed in previous chapters, a significant influence of the season acts on the system. The dry and wet season have different characteristics and according to LWI the wet season is the most significant in terms of sediment transport. The Delft3D model is set-up for both the dry and wet season in order to investigate the differences and calibrate the model to different scenarios.

WET AND DRY SEASON

Initially the model is run separately for the wet and the dry season in order to account for the difference in salinity. For both the seasons two months is run with different fresh water inflow from the River. For the dry season the fresh water inflow is 600 m^3/s in total and for the wet season the fresh water inflow is three times larger, namely 1,800 m^3/s (these values were used by LWI as well LWI (2012b)). Figure C.3 shows the differences in surface salinity at low water slack tide for a spring tide in the wet and the dry season. In the default runs the salinity is the only difference between the wet and the dry season because waves and shore parallel currents are not applied in this model.

SPRING, MEAN AND NEAP TIDE

For every season different tidal cycles are modeled in order to find their relative influence on the sediment transport and to be able to compare the model results with local observations. The different tides that are compared are spring, mean and neap tides, either for wet and dry season.

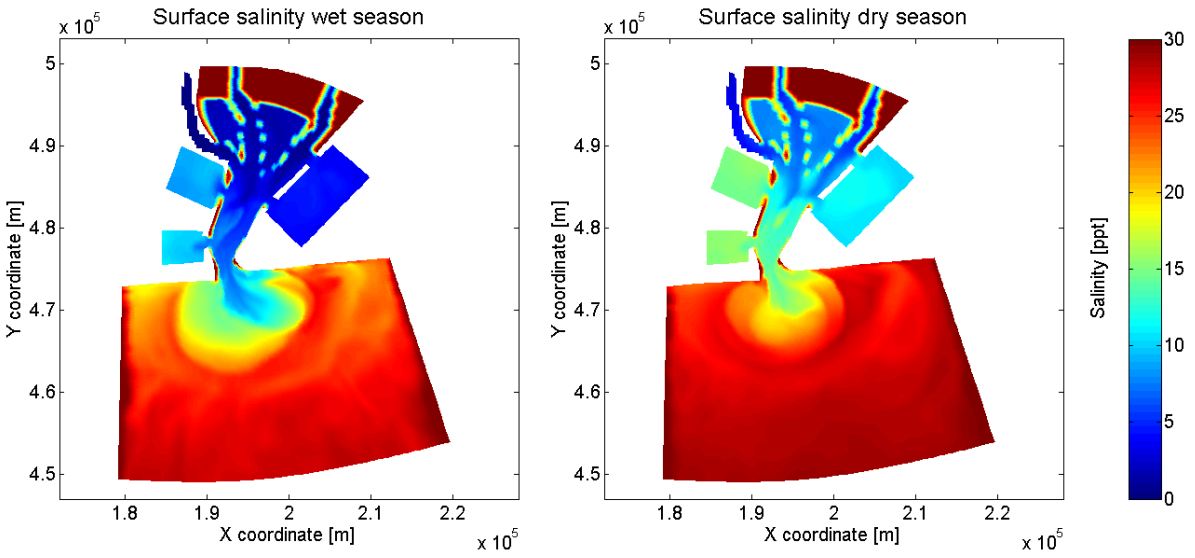

Figure C.3: Surface salinity at low water slack for a spring tide during the wet (left) and dry (right) season

C.2.2. HYDRODYNAMIC PROCESSES

The hydrodynamic processes of the model should be modeled correctly in order to obtain the right sediment transport patterns. Again, the goal is to obtain the right order of magnitude of the processes. First the water levels are discussed, followed by the

WATER LEVELS

Table C.4 shows the tidal levels as obtained from the harmonic analysis of the tidal record taken from the Estuary entrance tide gauge (LWI, 2012b). These water levels are with respect to LAT, whereas the Delft3D model water levels are with respect to mean sea level (MSL). Therefore the tidal ranges are used to compare the model results with the measurements. The mean measured spring and neap tidal ranges are: 1.55 m and 0.71 m respectively.

Table C.4: Tidal levels from harmonic analysis

Tidal level	Short	Height
Highest Astronomical Tide	HAT	2.25 m
Mean High Water Spring Tide	MHWS	1.89 m
Mean High Water Neap Tide	MHWN	1.54 m
Mean Sea Level	MSL	1.19 m
Mean Low Water Neap Tide	MLWN	0.83 m
Mean Low Water Spring Tide	MLWS	0.34 m
Lowest Astronomical Tide	LAT	0.0 m

The water levels for the six scenarios (dry/wet season and spring/mean/neap tide) are shown in Figure C.4. The red stars indicate the mean tidal levels as found by LWI LWI (2012b). The spring and mean tide is somewhat larger than a mean spring tide, however most of the available measurement data is taken during large spring tides with ranges up to 2.2 m. Therefore a larger than mean spring tide is chosen representative in the Delft3D model to be able to compare the measured data better to the model data. Additionally, two inequalities are found in the tidal signal, therefore a single tide is likely to deviate from the mean ranges measured by the tide gauge.

The water levels in the estuary mouth from 01/03/14 to 10/04/14 (after the initial 2 month run to let the salinity become in equilibrium) are shown in Figure C.5. The tidal ranges fluctuate between approximately 0.5 m and 1.8 m, which is in agreement with the measurements (see section 2.6). From this tidal signal the three tidal scenarios are picked, see Table C.5.

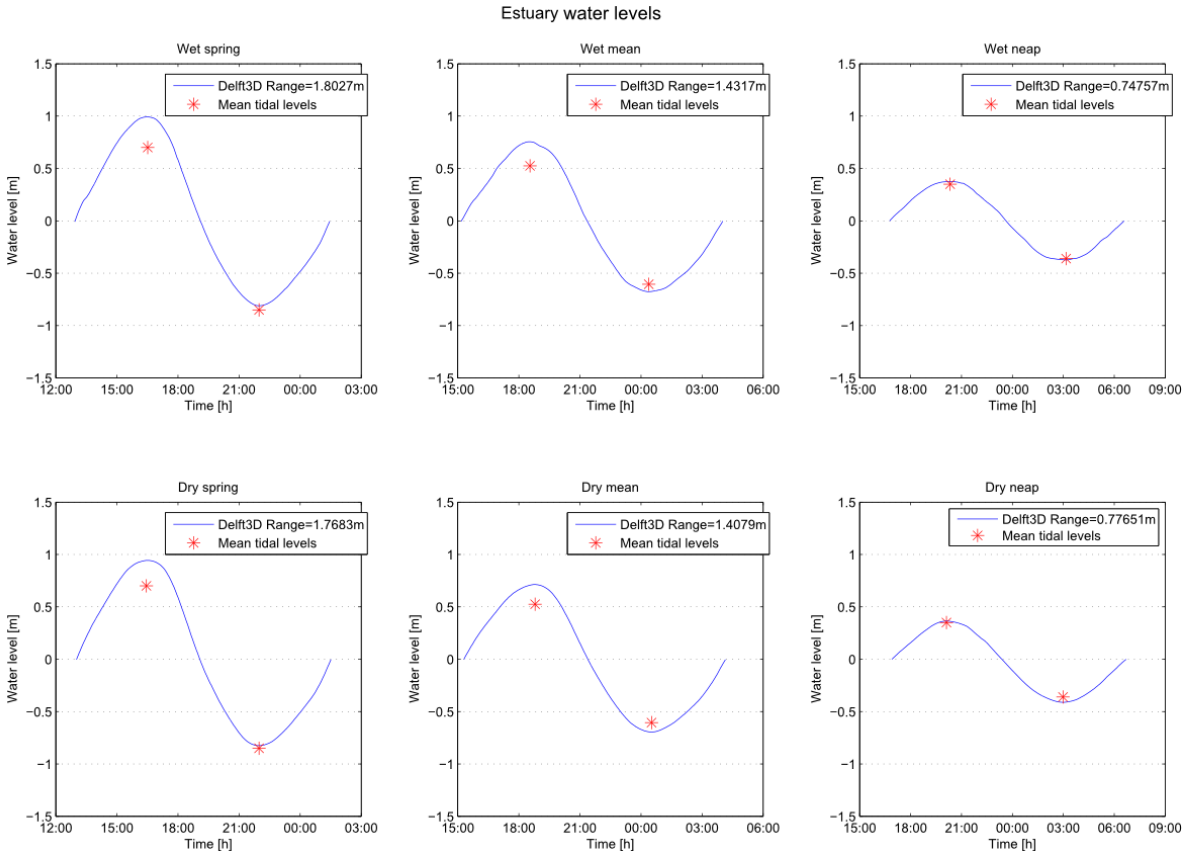

Figure C.4: Water levels for all scenarios, with mean tidal levels indicated with a red '*'

Table C.5: Tidal scenario dates

	Date
Spring	31/03/14
Mean	04/04/14
Neap	07/04/14

Due to the geometry of the estuary in the model, some resonance occurs and water levels increase due to a standing wave. This has been checked by increasing the roughness in the estuary and thereby reducing resonance. Increasing the roughness has other implications, and due to the time this is not optimized as the implications are considered to be limited. It is not clear whether resonance occurs in reality in the estuary and therefore it is not possible to check this further.

LWI observations During multiple measurement campaigns spread over two years by LWI transects were taken in the estuary mouth for discharge, sediment concentrations and flow velocities. Tidal ranges were measured during these campaigns as well. All the measurements show tidal ranges larger than the ranges calculated from the harmonic analysis. Both during the dry and wet season ranges are larger and a spring range of 2.2 m is observed multiple times, while the maximum astronomical tidal range is 2.25 m (difference HAT and LAT). This is a strange phenomenon as the measurements were taken at different times throughout the year in 2004 and 2005 and do therefore not seem to be a coincidence.

The following possible explanations to the differing water levels during the observations are given:

1. The observations were taken during larger tides than mean tides, even though they seem random.

2. The measurements are done inaccurately.

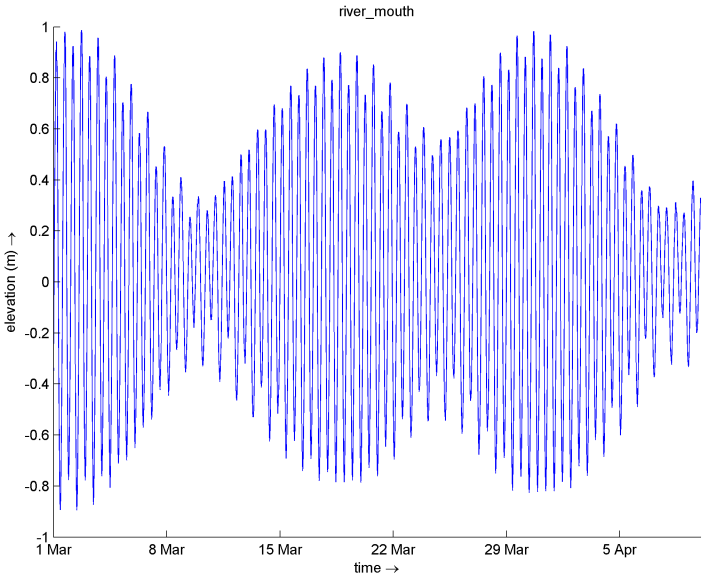

Figure C.5: Tidal signal in estuary mouth

3. During the measurements other processes interacted with the water levels and therefore larger ranges were obtained.

4. Resonance occurs in the estuary.

5. Tidal inequalities cause the mean ranges in the harmonic analysis to be smaller than single measured tidal ranges.

Due to time restricted and limited data this is not further treated in this report.

ESTUARY DISCHARGES AND VELOCITIES

The estuary discharges for the six scenarios are shown in Figure C.6. The measured discharges are taken from Figure 2.8 provided by LWI, in the graph it is shown that the discharge is zero at low water. However, it is not confirmed by any other data whether a phase difference of 90°is present between the water levels and discharges. Therefore the measured discharges are used for the magnitudes and not for the calibration of the phase differences. It is expected that the phase difference does not differ significantly from 90°, as the measurements do show that the tidal discharge is zero around low water.

In Figure C.6 can be observed that the discharges from the Delft3D model show differences with the measurement results. The most important differences are the peak discharge values and the phase differences. As explained, the horizontally phase difference is not further treated. The peak ebb discharge is larger in the model but does not differ as much as the peak flood discharge. The difference in peak ebb discharge is within 15 %, which is assumed to be acceptable. The flood discharge peak is significantly larger in the Delft3D model than measured. It is not known what causes the difference in ebb and flood discharge, as the difference is significantly larger than the fresh water inflow of the River.

As is discussed the priority is that the processes are modeled correctly and the order of magnitude should be correct. The infill of the proposed channel caused by the estuary is dependent on where the sediment is transported to and over which area it is distributed. Therefore the flood discharge is less important and the global flow pattern is of more importance on the sedimentation in the coastal area.

The following remarks are made on the estuary tidal discharges:

1. The model contains additional storage area to account for the large area that is influenced by the tide in the real world. Thereby increasing ebb and flood discharges. The exact area of the storage spaces is not optimized.

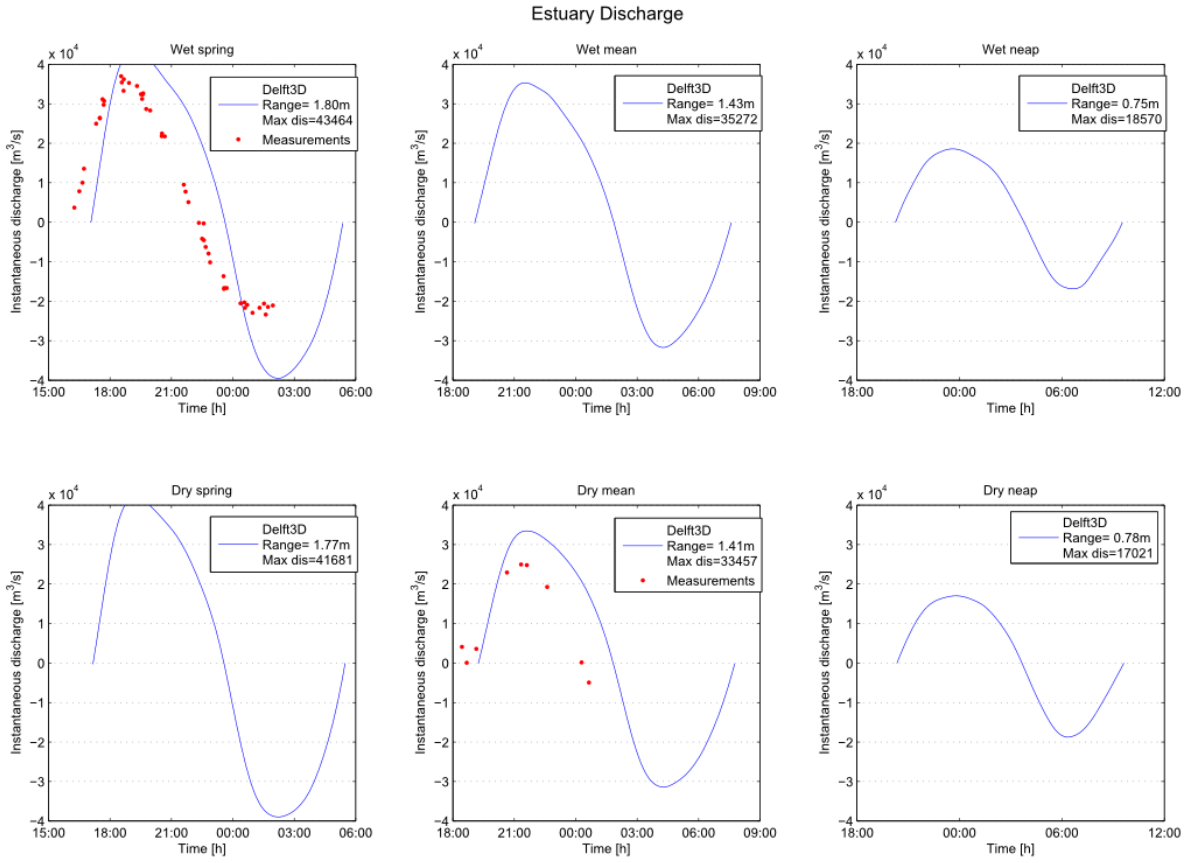

Figure C.6: Estuary discharges for all scenarios, red dots indicate measurement data

2. NEDECO NEDECO (1961) gives an estimation of the River discharge which was also used by LWI, this is based on a simple relation where 8 % of the Niger River discharge flows through the River. During the wet season this percentage might be higher than during the dry season as smaller rivers have relatively higher resistance during high discharges than the larger rivers. The River might attract more water during high discharge events than during lower discharge events. Therefore a smaller flood discharge peak is only present during the wet season, as no appropriate measurements are available for the dry season this cannot be checked. Further research is required to obtain the right understanding of the Estuary discharge.

3. LWI managed to obtain a correct discharge profile in their model with the same fresh water discharge values as are used in this Delft3D model. In order to accommodate the smaller flood discharges they applied higher roughness in the area of the ebb tidal bar during flood tide. It is not known how LWI managed to obtain the correct discharges exactly as a detailed description of their model is not available. The boundary condition of the rivers in the upstream part might be different than a fixed fresh water discharge, however the boundary conditions are specified as fresh water discharge in their report.

SALINITY PROFILES

Salinity profiles have been measured by LWI and can be compared to the model results in order to calibrate the fresh water run-off from the River and the boundary conditions for salinity. Figure C.7 shows the modeled and measured salinity profiles. Not all measurements are taken at high and low tide, the maximum and minimum measured salinity profiles are therefore taken from the measurement data and the model data. It can be seen that qualitatively the salinity profiles are correct.

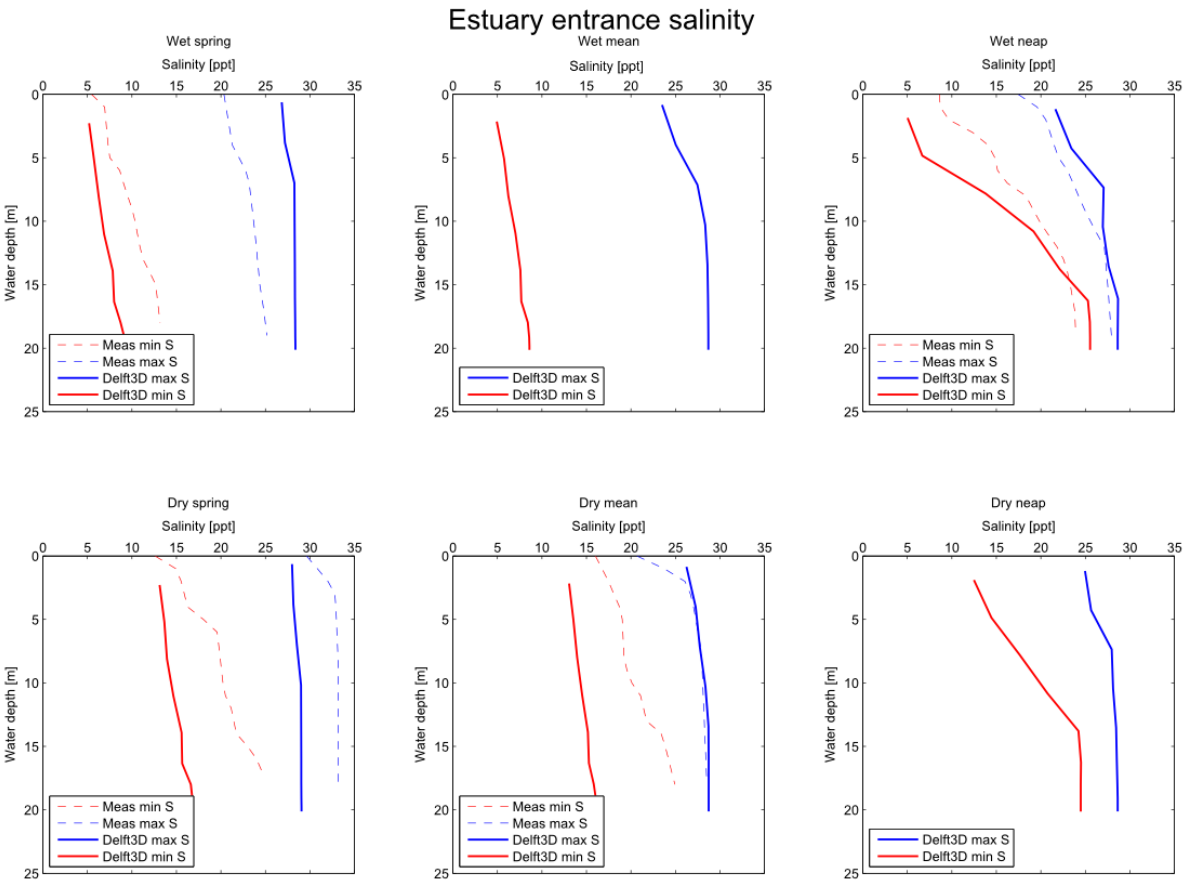

Figure C.7: Estuary entrance salinity for all scenarios, red and blue lines are minimum salinity profiles respectively and solid and dashed lines are model data and observations respectively

SEDIMENT PLUME

The salinity is an important output parameter of the Delft3D model for estimating the residual current and the sediment transport from the estuary. As the model is not calibrated extensively additional uncertainty is introduced. A satellite image is available from the dry season where a clear sediment plume is visible from the Estuary. The sediment plume is expected to be equivalent to the extent of the fresh water plume.

It is not known which tidal range is associated with the satellite image, therefore the image is compared to the model output for a spring and mean tidal range in Figure C.8. The sediment plume extent in the satellite image is indicated by a thick red line, the thin line indicates an observed difference in sediment concentration.

The figure shows that the extent of the sediment plume in the satellite image is comparable to the extent of the sediment plume from the Delft3D model. The dry season conditions show a smaller extent and therefore the model seems to calculate the estuary plume to an acceptable accuracy.

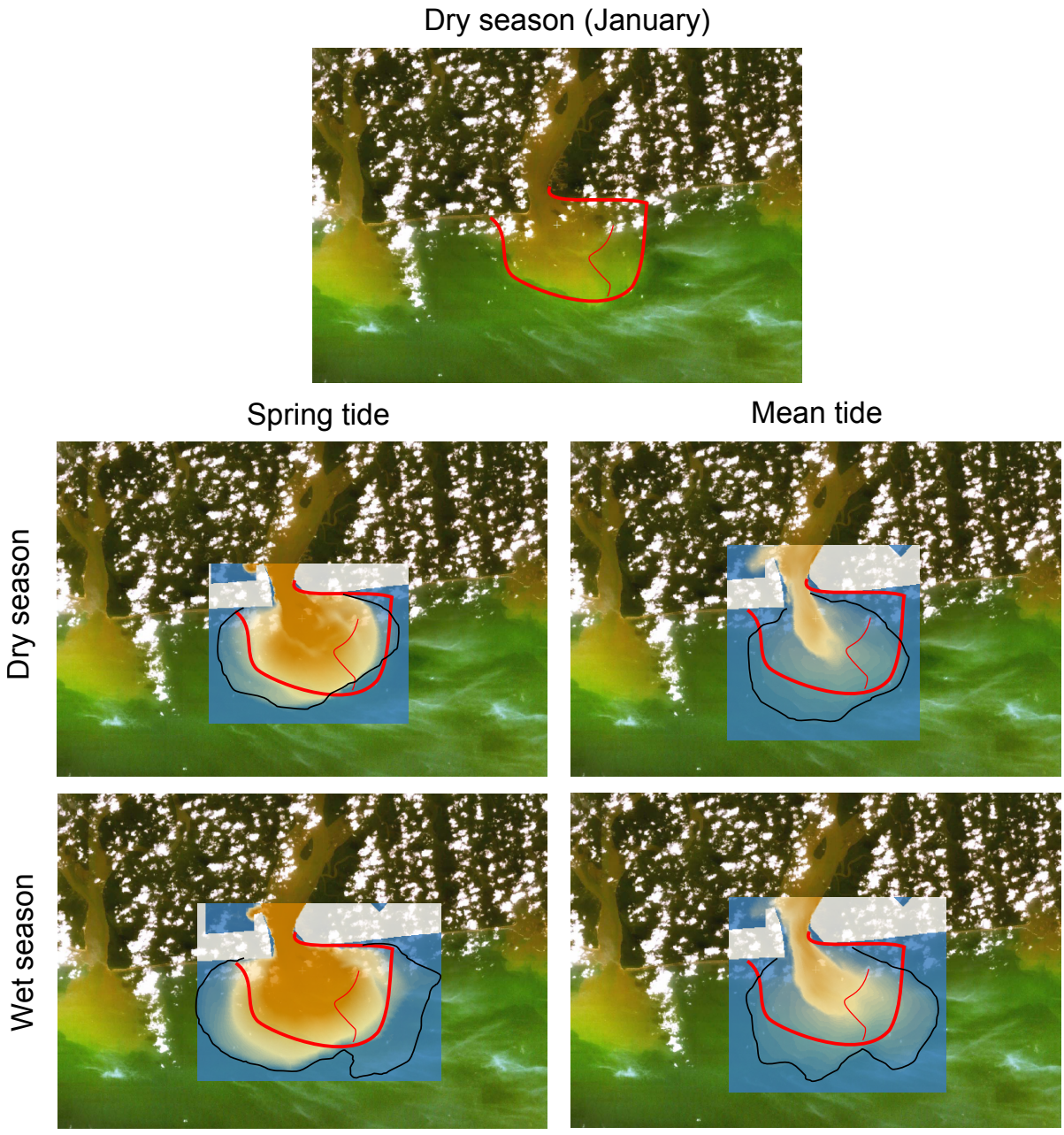

Figure C.8: Comparison of sediment plume extent of satellite image (top) indicated in red to wet and dry season top layer salinity concentration, of which the extent is indicated with a black line

D

DREDGING EQUIPMENT TYPES

Two types of equipment are considered to be practical in use for maintaining the approach channel's depth. These are listed and shortly explained below:

Equipment 1: Trailing Suction Hopper Dredger (TSHD)

Description: The TSHD is able to pick up sediment from the sea bed by sweeping drag heads over the soil surface where a strong suction pump pulls the soil/water mixture into the ship's storage (hopper). Once the hopper is fully loaded the ship sails out to a disposal area and removes the sediment from the hopper by either using doors/valves in the bottom of the ship, pumping the sediment through a pipeline or rainbowing the sediments. Agitation is carried out by omitting the hopper and depositing sediment high into the water column immediately after picking it up from the bed.

(a) TSHD

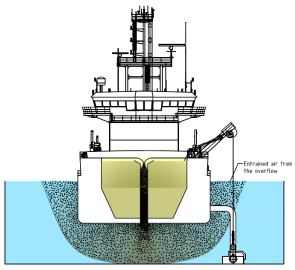

(b) Agitation

Pros	Cons
+ High production rates	- Relatively expensive for physical relocation of sediment
+ Different ship capacities available	- Low hopper filling efficiency for mud
+ Agitation efficient for mud beds	

Equipment 2: Water Injection Dredger (WID)

Description: The WID is a self sailing vessel or pushed barge. The WID is fitted with a water pumping installation and a beam with jet nozzles that can be lowered to the sea bed. The WID injects large volumes of water into the top soil layer, thereby initiating a gravity driven density current. The presence of a bed gradient (e.g. a slope or trench) and currents may significantly improve the transport capacity.

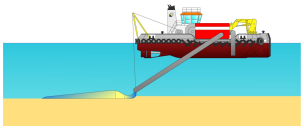

Figure D.1: Schematic representation of WID

Pros	Cons
+ Cost efficient	- Limited bed slope reduces effectiveness
+ Effective for mud beds	- Limited production capacity